PLACE IN RETURN BOX to remove this checkout from your record.
TO AVOID FINES return on or before date due.
MAY BE RECALLED with earlier due date if requested.

DATE DUE	DATE DUE	DATE DUE

5/08 K:/Proj/Acc&Pres/CIRC/DateDue.indd

COORDINATION OF DIVISION COMPLEXES ACROSS THE PLASTID ENVELOPE MEMBRANES

By

Jonathan Matthew Glynn

A DISSERTATION

Submitted to
Michigan State University
in partial fulfillment of the requirements
for the degree of

DOCTOR OF PHILOSOPHY

Genetics

2009

ABSTRACT

COORDINATION OF DIVISION COMPLEXES ACROSS THE PLASTID ENVELOPE MEMBRANES

By

Jonathan Matthew Glynn

Chloroplasts are cellular organelles descended from a cyanobacterial endosymbiont and house the photochemical machinery which powers synthesis of reduced carbon compounds from carbon dioxide and water. In higher plants, the chloroplast is also the site of synthesis for a select group of lipids, amino acids, and plant hormones. This set of organelle-specific functions make the chloroplast essential to survival of land plants, the most prominent group of terrestrial primary producers. The replication and segregation of plastids within land plants occurs through binary fission and is an important part of plant cell biology, as chloroplast size and number may impact the efficiency of photosynthesis and the partitioning of chloroplasts to daughter cells during plant cell division.

The apparatus that facilitates the scission of a single chloroplast into two daughter chloroplasts is a complex macromolecular machine, partly composed of a host-derived dynamin ring on the outside of the organelle and an endosymbiont-derived FtsZ ring (Z-ring) inside the organelle. The activities of these two rings must be tightly coordinated across the two envelope membranes of the chloroplast to ensure the timely progression and completion of division.

Here, I show that ARC6, a known FtsZ assembly factor that promotes formation of FtsZ filaments, also specifies the mid-plastid positioning of the paralogous outer envelope proteins PDV1 and PDV2, which have parallel functions in dynamin recruitment. PDV2 positioning requires a direct interaction between ARC6 and PDV2 that may be regulated by post-translational modification of ARC6 within the intermembrane space. I also show that PARC6 (Paralog of ARC6), like ARC6, is a multifunctional inner envelope chloroplast division protein. PARC6 acts downstream of ARC6 to position PDV1 at the division site, but is not required for PDV2 or ARC5 localization. *Arabidopsis parc6* mutants exhibit compound chloroplast division phenotypes and FtsZ filament morphology defects suggesting that PARC6 acts antagonistically to ARC6 within the chloroplast stroma as an inhibitor of FtsZ assembly. This FtsZ assembly-inhibiting activity of PARC6 may occur through interaction with ARC3, a protein with functional similarity to bacterial MinC. PARC6-GFP localization is dynamic, consistent with its complex role in division. Our findings indicate that PARC6 and ARC6 play related but distinct roles in coordinating the internal and external components of the chloroplast division complex.

DEDICATION

This work is dedicated to my mother and father, both of whom instilled the values and ideals that are a critical component of any scientist's success.

This work is dedicated to my grandfather, Elmer E. Lehman, whose patience, thoughtfulness, and pragmatic approach to life were an inspiration to all who knew him.

This work is dedicated to Van McWilliams and Helmut Bertrand, two teachers who kept me interested in science at times when I might have followed another path.

This work is dedicated to my family, whose understanding and encouragement over the years have been irreplaceable.

Most importantly, this work is dedicated to Angie. Your attitude, patience, kindness, understanding, support, and smile have helped make this possible. You are the love of my life and I am thankful for every day we have together.

ACKNOWLEDGEMENTS

I wish to acknowledge my advisor, Katherine W. Osteryoung, for her support and approach to mentoring that fosters independent critical thinking.

I wish to thank the members of my guidance committee for their encouragement and useful commentary:

Dr. Jianping Hu

Dr. Robert Last

Dr. Beronda Mongomery-Kaguri

Dr. Andreas Weber

I wish to thank Aaron Schmitz, Deena Kadirjan-Kalbach, Shin-ya Miyagishima, Qiang Wang, and Yue Yang for helpful scientific discussions and friendship over the past several years.

I wish to thank John Froehlich for insightful experimental advice, useful scientific discussions, and technical support throughout this project.

TABLE OF CONTENTS

LIST OF FIGURES

Images in this dissertation are presented in color.

ABBREVIATIONS

Δ	Deletion
35S	Cauliflower Mosaic Virus 35S promoter
AA	Amino acid
ABRC	Arabidopsis Biological Resource Center
AD	Activation domain
ARC	Accumulation and Replication of Chloroplasts
ATP	Adenosine-5'-Triphosphate
BD	DNA binding domain
BiFC	Bimolecular Fluorescence Complementation
BLAST	Basic Local Alignment Search Tool
C	Celcius
CD	Circular dichroism
CFP	Cyan fluorescent protein
Chl	Chlorophyll
Col	Columbia
CT	C-terminus or C-terminal
C-terminal	Carboxy terminal
DIC	Differential interference contrast
EMPTY	Empty vector
EMS	Ethane methyl sulfonate
Fts	Filamentation temperature sensitive

FZL	FZO-like
FZO	Fuzzy onions
GC	Giant chloroplast
GDP	Guanosine-5'-diphosphate
GFP	Green fluorescent protein
GST	Glutathione-S-transferase
GTP	Guanosine-5'-triphosphate
His	Histidine
His_8	8X Histidine tag
IEM	Inner envelope membrane
IMS	Intermembrane space
INT	Intermediate
IP	Immunoprecipitation
IPTG	Isopropyl-beta-D-thiogalactopyranoside
L*er*	Landsberg *erecta*
MORN	Membrane occupation and recognition nexus
NADPH	Nicotinamide adenine dinucleotide phosphate (reduced)
NMR	Nuclear magnetic resonance spectroscopy
N-terminal	Amino terminal
OEM	Outer envelope membrane
PARC	Paralog of ARC
PBD	PDV2 binding domain
PBS	Phosphate-buffered saline

PD	Plastid dividing
PDB	Protein Data Bank
PDV	Plastid division
pro	Proline or promoter (subscript)
SD	Synthetic dropout
SD/-ULT	Synthetic dropout media lacking uracil, leucine, and tryptophan
SD/-ULTH	SD media lacking uracil, leucine, tryptophan, and histidine
SOE-PCR	Site overlap extension polymerase chain reaction
TBS	Tris-buffered saline
THM	Thylakoid membrane
TM	Transmembrane domain
TP	Transit peptide
Ws	Wassilewskija
YFP	Yellow fluorescent protein
ZBD	FtsZ (or FtsZ2) binding domain
Zip	FtsZ-interacting protein

Chapter 1

Evolution and Operation of the Chloroplast Division Machinery

Plastid Biology and Analysis of Chloroplast Division

Chloroplasts are cellular organelles in land plants, responsible for photosynthesis and a number of other life-supporting functions, such as amino acid biosynthesis and lipid metabolism (Pyke 2009). In land plants like *Arabidopsis thaliana*, each mature leaf mesophyll cell contains 60-120 chloroplasts (Figure 1.1), depending on the accession and growth conditions (Aldridge, Maple, *et al.* 2005, Pyke 1999, Pyke 2009, Pyke and Leech 1994). Chloroplasts within *Arabidopsis* are typically ovoid-shaped structures, 5-7 microns (μm) in length, and harbor three distinct compartments: the thylakoid lumen, the stroma, and the intermembrane space (Figure 1.1). Each of these compartments is bounded by a biological membrane: the thylakoid lumen is surrounded by the thylakoid membrane, the stroma by the inner envelope membrane, and the entire organelle is bounded by the outer envelope membrane; the space between the inner and outer envelopes is called the intermembrane space (IMS). The thylakoid membrane is the site of photocollection and electron transport that drives photosynthesis, while the thylakoid lumen stores hydrogen ions generated during the photolysis of water molecules. These hydrogen ions are transferred to the stroma through an ATP synthase embedded within the thylakoid membrane to generate ATP within the stroma. The transport of electrons through the electron transport chain results in the reduction of NADPH. Within the stroma, ATP is consumed during operation of the Calvin cycle, which generates reduced carbon (triose phosphate) from carbon dioxide and NADPH. The inner and outer envelope membranes separate the chloroplast stroma from the surrounding cytosol and other organelles. These two membranes contain a variety of metabolite transporters

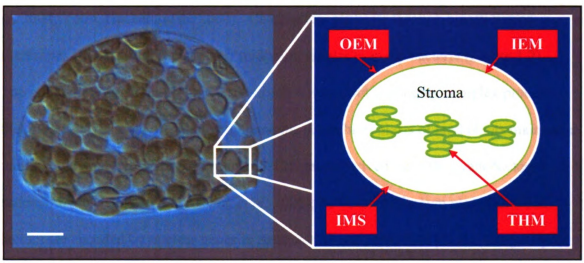

Figure 1.1. Overview of chloroplast morphology and features of a typical chloroplast. The left panel shows a typical mesophyll cell from an expanded leaf of *Arabidopsis thaliana* accession *Col-0*. Using DIC microscopy, wild type chloroplasts typically appear as greenish spherical or ovoid bodies, approximately 5-7 μm in diameter. The right panel is a schematic detailing the compartments and membranes that make up a typical chloroplast. Outer Envelope Membrane (OEM); Intermembrane Space (IMS); Inner Envelope Membrane (IEM); Thylakoid Membrane (THM); and Stromal compartment (Stroma). Scale bar = 10μm.

and protein translocators that allow the plastid to efficiently interface with the rest of the cell (Pyke 2009).

The chloroplasts of land plants are decendants of a cyanobacterial endosymbiont that first inhabited a primitive protozoan about 1.2-1.8 billion years ago (Dyall, Brown, *et al.* 2004, Yoon, Hackett, *et al.* 2004). Chloroplasts replicate through binary fission (Schimper 1883), dividing near their midpoint, similar to many bacteria (Figure 1.2). The process of division may appear relatively simple, but is a highly complex process that involves a number of protein components. The chloroplasts of land plants maintain a minimal genome, typically harboring 110-120 genes derived from the cyanobacterial endosymbiont (Cui, Veeraraghavan, *et al.* 2006); however, all known plastid division factors are encoded by nuclear genes in *Arabidopsis* and other land plants (Yang, Glynn, *et al.* 2008). Some of the genes encoding plastid division factors are inventions of the host organism and arose after a stable endosymbiotic relationship was established, while others are descendants of cyanobacterial genes that were transferred to the nucleus from the endosymbiont genome during the evolution of photosynthetic eukaryotes.

Because of their common origin, several components of the chloroplast divisome share a high degree of sequence similarity with cyanobacterial division proteins from extant species (Yang, Glynn, *et al.* 2008). Due to the evolutionary history of the chloroplast, the study of chloroplast division has benefited greatly from the study of bacterial cell division. Surprisingly, genetic screens for cyanobacterial cell division

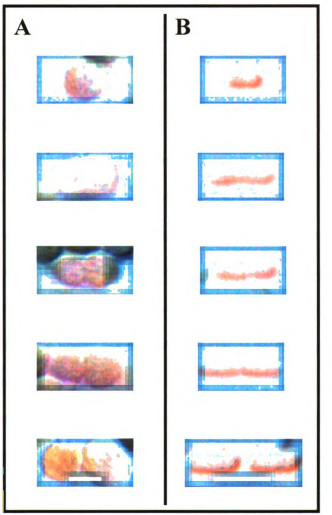

Figure 1.2. Comparison of dividing chloroplasts and cyanobacteria. (A) Micrographs of chloroplasts from *Arabidopsis thaliana Col-0* and (B) cells of the cyanobacterium *Synechococcus elongatus* PCC7942 as they progress from single individuals (upper panels) to two new entities (lowest panel). Scale bars = 5μm.

components have uncovered only a few novel division genes (Koksharova and Wolk 2002, Miyagishima, Wolk, *et al.* 2005), but the division of cyanobacteria has been understudied in comparison to that of *Escherichia coli* (Lutkenhaus 2007, Margolin 2003, Margolin 2005, Rothfield, Taghbalout, *et al.* 2005). Consequently, models of plastid division at a molecular level are often compared to *E. coli* cell division models. Many of the components that make up the divisome of *E. coli* are also utilized by cyanobacteria (Miyagishima 2005), but cyanobacteria possess division factors that are unique to photosynthetic prokaryotes (Koksharova and Wolk 2002, Miyagishima, Wolk, *et al.* 2005) and are probably the most relevant prokaryotic system for comparative analysis with regard to the chloroplast. Regardless, the first known component of the plastid divisome was identified by a reverse genetic approach, parsing sequences of translated expressed sequence tags (ESTs) from *Arabidopsis thaliana* for similarity to the amino acid sequence of the *E. coli* cell division protein FtsZ (Osteryoung and Vierling 1995). Later studies identified more components of the chloroplast divisome by reverse genetics, with the initial query sequences being *E. coli* cell division proteins (Colletti, Tattersall, *et al.* 2000, Itoh, Fujiwara, *et al.* 2001, Maple, Fujiwara, *et al.* 2004).

While reverse genetic screens have been useful in identifying broadly-conserved division proteins common to bacteria and plastids, they fall short in their ability to identify plastid division factors of host origin, as these factors are generally products of genes that emerged after the intial endosymbiotic event (Gao, Kadirjan-Kalbach, *et al.* 2003, Miyagishima, Froehlich, *et al.* 2006, Miyagishima, Nishida, *et al.* 2003a). The discovery of these host-derived components has benefited from forward genetic analysis,

where the leaf cells of mutagenized lines are analyzed for aberrations in chloroplast number and/or morphology by simple light microscopy (Miyagishima, Froehlich, *et al.* 2006, Pyke and Leech 1992, Pyke and Leech 1994) and the causative mutation mapped by routine molecular methods (Jander, Norris, *et al.* 2002). Forward genetic studies have been instrumental to the discovery of plant-specific genes involved in plastid division, uncovering factors that act both inside and outside the organelle. Surprisingly, forward genetic approaches have only recently uncovered high-level regulators of plastid division, such as transcription factors and/or hormone responsive factors (Okazaki, Kabeya, *et al.* 2009), whose existence and involvement in plastid division and differentiation has been postulated for some time. However, the elucidation of the complete inventory of plastid division genes will not come through one mode of analysis, but through a comprehensive approach that incorporates both forward and reverse genetics, comparative genomics, transcriptome/network analysis, proteomics/interactomics, and integrative approaches that utilize all of these strategies in multiple experimental systems.

A Survey of the Molecular Biology of Plastid Division

FtsZ

FtsZ is a conserved division protein found in most bacteria and is a structural homolog of eukaryotic tubulins (Erickson, Taylor, *et al.* 1996). In *E. coli*, FtsZ forms a ring (Z-ring) at the mid-cell which demarcates the site of cell division (Bi and Lutkenhaus 1991), probably serving as a scaffold for other division proteins and providing nominal contractile force during membrane constriction (Ghosh and Sain 2008,

Lan, Daniels, *et al.* 2009, Lan, Wolgemuth, *et al.* 2007, Osawa, Anderson, *et al.* 2008). The biochemistry of the cyanobacterial FtsZ has yet to be rigorously examined and most of what we know of FtsZ assembly and biochemistry come from several detailed studies of FtsZ from *E. coli*, though the similarity between these two proteins (Stokes and Osteryoung 2003) would suggest that they behave similarly *in vitro*. *In vitro*, *E. coli* FtsZ assembles into a simple linear polymer (protofilament) with a diameter of about 5 nm in the presence of GTP, but can form mini-rings or other higher-order structures under certain conditions (Erickson, Taylor, *et al.* 1996). Hydrolysis of GTP to GDP can lead to curvature of the FtsZ polymer, and this induced curvature is thought to be one source of contractile force during cell division (Lu, Reedy, *et al.* 2000). The addition of calcium or low pH conditions facilitates lateral association of FtsZ protofilaments into bundles or sheets approximately 30 nm or more in diameter (Erickson, Taylor, *et al.* 1996). It is thought that the protofilaments serve as building blocks for the cytosolic Z-ring *in vivo*, undergoing further lateral association and organization in the presence of accessory factors such as FtsA (Jensen, Thompson, *et al.* 2005, Pichoff and Lutkenhaus 2002) and ZipA (Hale, Rhee, *et al.* 2000, RayChaudhuri 1999), proteins that enhance polymer bundling and anchor the developing Z-ring to the inner leaflet of the cell membrane (Osawa, Anderson, *et al.* 2008, Pichoff and Lutkenhaus 2005). In addition to the polymer curvature associated with GTP hydrolysis, the sliding of adjacent protofilaments has also been proposed as an alternative or additional source of contractile force during bacterial cell division (Lan, Daniels, *et al.* 2009, Li, Trimble, *et al.* 2007), but is energetically unfavorable (Erickson 2009) and has yet to be experimentally proven.

In contrast to most bacteria, all plant genomes encode at least two phylogenetically-distinct families of FtsZ proteins, termed FtsZ1 and FtsZ2 (Miyagishima, Nozaki, *et al.* 2004, Stokes and Osteryoung 2003). Consistent with their divergent sequences, FtsZ1 and FtsZ2 have distinct roles in plastid division (Schmitz, Glynn, *et al.* 2009, Stokes and Osteryoung 2003, Vitha, McAndrew, *et al.* 2001). Both FtsZ1 and FtsZ2 have been shown to be part of the Z-ring, but the exact arrangement of the polymer is unclear. FtsZ1-FtsZ2 mixed polymers are able to form large protofilament bundles similar to the large protofilament bundles observed using bacterial FtsZ, suggesting that the plastidic Z-ring is probably a heteropolymer rather than several closely-associated FtsZ1 and FtsZ2 homopolymers (Olson 2008). While bundling is probably not critical for contractile activity (Erickson 2009), it is probably required for the formation of a functional and stable Z-ring (Hale, Rhee, *et al.* 2000, Low, Moncrieffe, *et al.* 2004, Margolin 2003). The factors that contribute to FtsZ bundling and stability in plastids are discussed later.

Determining the site of FtsZ protofilament and ring assembly: The Min System

Mid-cell positioning of the Z-ring in bacteria is important for symmetrical division and ensures equal partitioning of cellular contents, including chromosomes and plasmids, during fission. In *E. coli*, two major mechanisms drive placement of the Z-ring at the mid-cell: the Min system and the Nucleoid occlusion (Noc) system (Rothfield, Taghbalout, *et al.* 2005). The Min system of *E. coli* is composed of three proteins: MinC, MinD, and MinE (Lutkenhaus 2007). MinC binds FtsZ and inhibits Z-ring assembly by preventing lateral associations (Hu, Mukherjee, *et al.* 1999, Scheffers 2008, Shen and

Lutkenhaus 2009). However, the FtsZ polymer-inhibiting activity of MinC is regulated by MinD, which is tethered to the membrane and promotes MinC activity only in the polar zones of the cell (Hu and Lutkenhaus 1999, Raskin and de Boer 1999a, Szeto, Rowland, *et al.* 2002). MinD is regulated by MinE, through a mechanism in which MinE binds to MinD and causes it to be released from the membrane (Hu and Lutkenhaus 2001). The maximum concentration of MinE occurs near the midcell adjacent to the membrane, thereby causing the concentration of active MinC and MinD to be highest at the poles (Hale, Meinhardt, *et al.* 2001). While the determinants for MinE localization are unknown, the midcell zone created by MinE activity allows for FtsZ protofilament assembly along the inner leaflet of the plasma membrane at the midcell (Rothfield, Taghbalout, *et al.* 2005). In some bacteria that lack MinE, DivIVA tethers MinD at the cell poles and inhibits FtsZ polymerization within the polar zone by maintaining a higher concentration of active MinCD at the poles (Marston and Errington 1999).

In general, it has long been thought that the functions of the *Arabidopsis* orthologs of MinD (AtMinD) and MinE (AtMinE) are similar to their bacterial counterparts with respect to their functions during chloroplast division. However, recent studies have shown that AtMinD is able to rescue the cell division defects of an *E. coli minD minE* double mutant, indicating that AtMinD has probably acquired additional functions, relative to its bacterial counterpart (Zhang, Hu, *et al.* 2009a). Additionally, the localization patterns of AtMinD and AtMinE vary slightly from those of their bacterial homologs. AtMinD localizes to polar spots and equatorial structures in *Arabidopsis* (Nakanishi, Suzuki, *et al.* 2009), while AtMinE localizes to polar regions in tobacco

chloroplasts (Maple, Chua, *et al.* 2002). Intriguingly, orthologs of MinC have been lost from the genomes of vascular plants (Yang, Glynn, *et al.* 2008) and recent work shows that plants have acquired at least two additional factors to fine-tune the operation of the Min system: ARC3 and MCD1 (Glynn, Miyagishima, *et al.* 2007, Maple, Vojta, *et al.* 2007, Nakanishi, Suzuki, *et al.* 2009).

ARC3 is a chimeric protein, consisting of an FtsZ-like N-terminal domain, a C-terminal PIP5K-like domain, and a conserved middle domain of unknown function (Shimada, Koizumi, *et al.* 2004). ARC3 is proposed as a functional replacement for MinC in plastids (Maple, Vojta, *et al.* 2007), as *arc3* mutants possess chloroplast morphologies of varying size (Marrison, Rutherford, *et al.* 1999, Pyke and Leech 1992, Pyke and Leech 1994), with the enlarged plastids containing multiple FtsZ rings (Glynn, Miyagishima, *et al.* 2007) reminiscent of those observed within bacterial *minC* mutants (Levin, Shim, *et al.* 1998). ARC3 exhibits both polar and equatorial localization within the chloroplast (Maple, Vojta, *et al.* 2007, Shimada, Koizumi, *et al.* 2004). Furthermore, ARC3 has been shown to interact with FtsZ1, MinD, and MinE (Maple, Vojta, *et al.* 2007), suggesting that it acts as a critical interface between the Z-ring and the plastidic Min system. Based on these data, ARC3 has been hypothesized to inhibit FtsZ assembly, but it is not yet known if ARC3 is sufficient to inhibit FtsZ assembly *in vitro*, similar to bacterial MinC (Hu, Mukherjee, *et al.* 1999, Scheffers 2008).

MCD1 is a plant-specific inner envelope protein that regulates division site placement within the chloroplast (Nakanishi, Suzuki, *et al.* 2009). Like ARC3 (Maple,

Vojta, *et al.* 2007, Shimada, Koizumi, *et al.* 2004) and AtMinD (Nakanishi, Suzuki, *et al.* 2009), MCD1 localizes to polar zones and to equatorial structures within the chloroplast (Nakanishi, Suzuki, *et al.* 2009). MCD1 binds AtMinD and is required for AtMinD localization *in vivo*, and thereby directs the position of the Z-ring and division site (Nakanishi, Suzuki, *et al.* 2009). However, it is unclear what pathways lie upstream of MCD1 to direct its localization and activity within the chloroplast.

Orthologs of characterized nucleoid occlusion factors are not encoded in cyanobacterial or plant genomes, suggesting that chloroplasts do not utilize a Noc-like mechanism to prevent scission of the plastid chromosome during fission (Glynn, Miyagishima, *et al.* 2007). Moreover, Z-rings can form around nucleoids in cyanobacteria, indicating that a Noc-like mechanism is probably absent from this lineage (Miyagishima, Wolk, *et al.* 2005). Both plastids and cyanobacteria maintain multiple copies of their chromosome (Falkow, Dworkin, *et al.* 2006, Pyke 2009), consistent with chromosomal preservation during division being accomplished by maintaining multiple chromosomal copies (Scott and Possingham 1980). Notably, plastids and cyanobacteria possess an additional membrane system, the thylakoid membrane, that is not found in *E. coli* or other bacteria (Falkow, Dworkin, *et al.* 2006). It has been proposed that some mechanism of thylakoid partitioning might occur in plants, as the thylakoid membranes might be an impediment to the contractile apparatus and thylakoids appear to be actively redistributed during plastid fission (Boffey and Lloyd 1988, Leech, Thomson, *et al.* 1981, Possingham and Lawrence 1983). It is possible that a thylakoid segregation mechanism

might be integrated into the plastidic Min system, but work on this aspect of plastid division remains to be explored.

Assembly and stabilization of the Z-ring: ARC6

The plastidic Min system only creates a zone conducive to FtsZ polymer assembly, but mounting evidence suggests that additional factors are required to: (1) stabilize the Z-ring by promoting protofilament bundling and (2) anchor FtsZ polymers to the membrane. In *E. coli*, two proteins serve this purpose: ZipA and FtsA. Both ZipA and FtsA proteins elicit their effect upon the Z-ring by binding to a short conserved motif near the C-terminus of FtsZ called the core motif or core domain (Pichoff and Lutkenhaus 2002). ZipA is a bitopic membrane protein of the plasma membrane thought to enhance bundling of FtsZ filaments near the membrane (Hale, Rhee, *et al.* 2000, RayChaudhuri 1999). FtsA is a peripheral membrane protein that has been shown to anchor the Z-ring to membranes both *in vivo* and *in vitro* (Jensen, Thompson, *et al.* 2005, Osawa, Anderson, *et al.* 2008, Pichoff and Lutkenhaus 2005). FtsA may also be involved in protofilament bundling, as some functional redundancy between FtsA and ZipA is evident in *E. coli* (Geissler, Elraheb, *et al.* 2003). Two other division factors are known to bind the core motif in some gram positive organisms, EzrA (Singh, Makde, *et al.* 2007) and ZapA (Low, Moncrieffe, *et al.* 2004); these proteins bind the C-terminus of FtsZ and somehow modulate FtsZ dynamics, but their precise effects upon FtsZ polymerization are still under investigation. Interestingly, engineering the short membrane-tethering amphipathic helix of FtsA onto the C-terminus of FtsZ is sufficient to drive Z-ring formation along artificial membranes *in vitro* (Osawa, Anderson, *et al.*

2008). Cyanobacteria, green algae, and land plants do not encode orthologs of ZipA or FtsA, but do encode FtsZ molecules that bear the conserved C-terminal core motif (Miyagishima, Nishida, *et al.* 2003b). This suggests that other factors, possibly with an amino acid sequence dissimilar from FtsA and ZipA, might provide a similar FtsZ tethering and/or bundling function within plastids.

ARC6 was discovered by a forward genetic approach and encodes a protein product that stabilizes the plastidic Z-ring, possibly by promoting FtsZ filament formation (Vitha, Froehlich, *et al.* 2003). ARC6 may also provide both FtsZ bundling and tethering functions, despite the divergence of its sequence from ZipA or FtsA; *ARC6* overexpressors have elongated FtsZ filaments and *arc6* mutants have short, disorganized FtsZ filaments (Figure 1.3) (Vitha, Froehlich, *et al.* 2003).

ARC6 is a nuclear-encoded bitopic inner envelope protein of cyanobacterial origin (Vitha, Froehlich, *et al.* 2003); the cyanobacterial ortholog of ARC6 is called Ftn2 (Koksharova and Wolk 2002). The *Arabidopsis* ARC6 protein is 801 amino acids in length (Figure 1.4), bears an N-terminal transit peptide that directs the protein to the chloroplast, and a putative J-domain that may facilitate interaction with Hsp70/DnaK-type chaperones. ARC6 family members also harbor a single transmembrane domain that anchors the protein in the inner envelope membrane (Vitha, Froehlich, *et al.* 2003). Like the FtsZ proteins, ARC6 forms a continuous (non-punctate) ring at the division site (Yang, Glynn, *et al.* 2008); this ring co-localizes with the plastidic Z-ring (Figure 1.5).

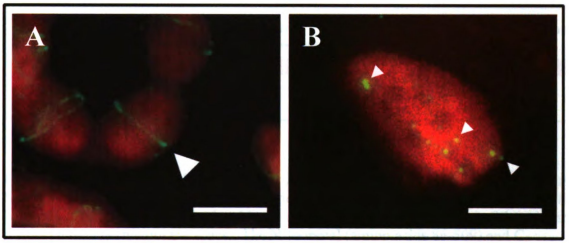

Figure 1.3. FtsZ2-1 immunolocalization in wild type *Arabidopsis* chloroplasts and in *arc6* mutants. (A) FtsZ forms equatorial rings (large arrowhead) in wild type chloroplasts and (B) forms short fragments or spots (small arrowheads) in *arc6* mutants, suggesting that ARC6 stabilizes the Z-ring *in vivo*. Chlorophyll autofluorescence is indicated in red. Scale bar = 5μm.

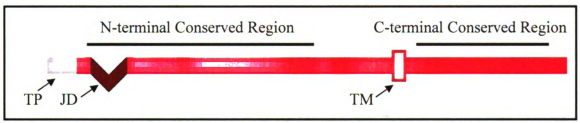

Figure 1.4. Schematic of the *Arabidopsis* ARC6 protein. The above panel highlights the known features of ARC6 based on previous data (Vitha, Froehlich, *et al.* 2003). The N-terminus of ARC6 resides in the chloroplast stroma and the C-terminus of the protein resides in the intermembrane space. The N-terminal (amino acids 86-509) and C-terminal (amino acids 683-793) conserved regions show very high similarity to other ARC6/Ftn2 family members. Transit peptide (TP, amino acids 1-67); Predicted J-domain (JD, amino acids 89-153); and Transmembrane Domain (TM, amino acids 615-635).

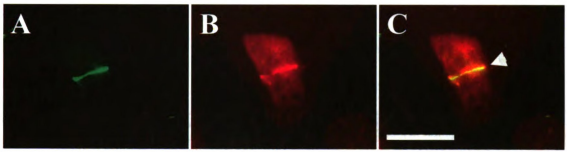

Figure 1.5. FtsZ and ARC6 colocalize to continuous rings within the chloroplast. Immunolabeling of FtsZ2-1 (A, green) and ARC6 (B, bright red color) is shown. Chlorophyll autofluorescence (B, dull red color) roughly marks the boundaries of the chloroplast. Colocalization of the two proteins (arrowhead) is indicated in panel (C) using an overlaid image from panels (A) and (B). Scale bar = 5 μm.

The N-terminus of ARC6 resides within the stroma, where it interacts with FtsZ2 family members; this interaction requires the C-terminus of FtsZ2 (Maple, Aldridge, *et al.* 2005, Schmitz, Glynn, *et al.* 2009). Presumably, the ARC6-FtsZ2 interaction is analogous to that observed for FtsA-FtsZ and/or ZipA-FtsZ in *E. coli* (Pichoff and Lutkenhaus 2002), but an FtsZ-tethering or FtsZ-bundling activity for ARC6 has yet to be shown. In chapter 2 of this work, I describe refinement of the boundaries of the stromal domain of ARC6 responsible for binding FtsZ2, show that the C-terminus of FtsZ2 is both necessary and sufficient for binding ARC6, attempt to discern the effect of ARC6-FtsZ2 interaction *in vivo*, and provide a homology model of ARC6 that points toward structural and functional similarities between ARC6 and ZipA, despite their divergent amino acid sequence.

The function of the IMS-localized C-terminal region of ARC6 was completely unknown until a recent study that showed the C-terminus of ARC6 binds to PDV2 and is responsible for positioning both PDV1 and PDV2 (described below) at the division site (Glynn, Froehlich, *et al.* 2008). In chapter 3, I present these results and some additional data in support of this function for the C-terminus of ARC6. Chapter 4 builds on these findings, where I present approximation of the boundaries of the PDV2-binding domain of ARC6 ($ARC6_{PBD}$), characterize a predicted site of post-translational modification within this domain, and introduce a new hypothesis on the regulation of division by $ARC6_{PBD}$ phosphorylation and dephosphorylation.

ARC6/Ftn2 family members are present as single-copy genes in cyanobacteria, algae, and moss. In tracheophytes, *ARC6* has undergone at least one gene duplication event, resulting in a novel plastid division gene we have termed *PARC6* (*P*aralog of *ARC6*). Like ARC6, PARC6 is a multifunctional division protein that resides within the inner envelope membrane, acting downstream of ARC6 to position PDV1 and possibly regulating FtsZ assembly through ARC3 — implicating PARC6 in the operation of the plastidic Min system (Glynn, Yang, *et al.* 2009, Zhang, Hu, *et al.* 2009b). In chapter 5, I summarize this work and provide further insights into the role of ARC6, PARC6, PDV1, and PDV2 during plastid division in vascular plants.

While it is unknown if ARC6 and PARC6 definitively interact with each other or how they precisely influence each other's activity *in vivo*, it is suspected that some functional connection between these two paralogous proteins exists due to their high degree of sequence similarity. In chapter 6, I highlight preliminary analysis of a novel *ARC6* allele, $arc6_{D205N}$, that exhibits division defects reminiscent of *Arabidopsis min* mutants and propose a hypothesis that the $arc6_{D205N}$ division defect results from aberrations in the ability of ARC6 to interact with a Min-system component.

Facilitating outer envelope constriction during division: ARC5, PDV1, and PDV2

In addition to the division factors inherited from the ancestor of the chloroplast, a few factors were invented by the host following symbiosis. Notably, three of these host-derived factors operate within or upon the outer envelope membrane. ARC5 is a dynamin-like protein that localizes to both cytosolic patches and an equatorial ring on the

outside of the plastid. Unlike the continuous ARC6 ring (Glynn, Froehlich, *et al.* 2008, Vitha, Froehlich, *et al.* 2003, Yang, Glynn, *et al.* 2008), the ARC5 ring has a discontinuous, or punctate, appearance in *Arabidopsis* and other photosynthetic eukaryotes (Gao, Kadirjan-Kalbach, *et al.* 2003, Miyagishima, Froehlich, *et al.* 2006, Miyagishima, Nishida, *et al.* 2003a, Yang, Glynn, *et al.* 2008). The significance of this punctate pattern is still unclear. It is anticipated that these foci represent discrete sites of membrane remodeling rather than a bounding contractile spiral (which would likely appear as a continuous ring *in vivo*), which suggests that initial constriction of the outer membrane might invove membrane removal from discrete foci rather than direct mechanical constriction of the outer envelope by ARC5. Notably, the late stages of dynamin constriction activity involve a significant change in the organization of ARC5 topology relative to the outer envelope membrane, in which ARC5 polymers come into direct contact with the cytosolic face of the outer envelope (Yoshida, Kuroiwa, *et al.* 2006). This end-stage change in orientation may reflect a simultaneous change in the pinchase activity of ARC5 polymers, but further investigation is required to confirm this hypothesis.

ARC5 can be recruited to the division site by either PDV1 or PDV2, two coiled-coil proteins that arose during land plant evolution (Miyagishima, Froehlich, *et al.* 2006). Like ARC5, PDV1 localizes to a punctate ring (Miyagishima, Froehlich, *et al.* 2006). PDV2 localizes to a continuous ring similar to that observed for ARC6 (see chapter 3). Interestingly, full ARC5 contractile activity requires both PDV1 and PDV2, as *pdv1* and *pdv2* mutants possess a large proportion of dumbbell-shaped chloroplasts, similar to the

dynamin activity defect observed in *arc5* mutants (Miyagishima, Froehlich, *et al.* 2006). Overexpression of PDV1 and/or PDV2 leads to an increase in the rate of chloroplast division *in vivo* (Okazaki, Kabeya, *et al.* 2009). Taken together, these observations indicate that the PDV proteins probably affect the rate of plastid division through modulating ARC5 contractile activity, although the PDV proteins probably influence the operation of other division components as well. It is still unclear if either of the PDV proteins interacts directly with ARC5 to mediate its recruitment and/or activity along the cytosolic surface of the chloroplast outer envelope.

Other factors with notable roles in maintaining chloroplast morphology and/or division.

A number of other factors have been discovered through genetic and cytological analyses. The precise role of these proteins in the process of chloroplast division remains unclear, but we will provide a brief treatment of each of these here.

GC1 (Giant Chloroplast 1) is distantly related to *E. coli* SulA and was identified by a reverse genetic approach (Maple, Fujiwara, *et al.* 2004). In proteobacteria, SulA expression is part of the SOS response to DNA damage (Huisman, D'Ari, *et al.* 1984) and delays cell division by directly binding FtsZ and inhibiting FtsZ assembly (Trusca, Scott, *et al.* 1998). For *Arabidopsis*, it is unclear if GC1 binds FtsZ1 or FtsZ2 *in vivo*; overexpression of *GC1* bypasses plastid division defects observed in *AtFtsZ* overexpressors (Raynaud, Cassier-Chauvat, *et al.* 2004), but strangely GC1 does not bind FtsZ1 or FtsZ2 in two-hybrid assays (Maple, Fujiwara, *et al.* 2004). However, GC1 can self-associate (Maple, Fujiwara, *et al.* 2004), similar to SulA (Cordell, Robinson, *et al.*

2003). GC1 is localized to the chloroplast periphery and has not been shown to interact with any other division components (Maple, Fujiwara, *et al.* 2004). While GC1 deficiency results in enlarged chloroplasts, similar to *arc6* mutants, it is unclear if GC1 overexpression inhibits chloroplast division (Maple, Fujiwara, *et al.* 2004, Raynaud, Cassier-Chauvat, *et al.* 2004) in the same way that SulA overexpression leads to division arrest in cyanobacteria (Sakr, Jeanjean, *et al.* 2006). Further work is required to understand the inputs that lead to GC1 activity and the precise mechanism by which GC1 affects plastid morphology *in vivo*.

MSL2 and MSL3 belong to a family of mechanosensitive ion channels that reside in the chloroplast (Haswell and Meyerowitz 2006). *MSL2* and *MSL3* appear to be redundant genes with respect to chloroplast morphology, as only *msl2 msl3* double mutants exhibit plastid morphology defects (Haswell and Meyerowitz 2006). MSL3 has been shown to colocalize with AtMinE in transient expression assays conducted using tobacco leaf cells, but the significance of this finding remains unclear (Haswell and Meyerowitz 2006). It has been suggested that mechanosensitive ion channels, like MSL2 and MSL3, are a means by which chloroplasts sense volume, thereby influencing the decision to continue expanding or to initiate division (Pyke 2006). This seems reasonable, since chloroplast volume is only slightly reduced in division-impaired backgrounds like *arc6* (Pyke 1998, Robertson, Pyke, *et al.* 1995). However, the precise mechanism by which MSL2 and MSL3 influence plastid morphology, and presumably division, remains to be elucidated.

FZL (FZO-Like) was discovered based on its similarity to FZO (Gao, Sage, *et al.* 2006), a protein known to mediate mitochondrial membrane fusion in animals and fungi (Hales and Fuller 1997). FZL is chloroplast-targeted protein that localizes to the envelope and thylakoid membranes (Gao, Sage, *et al.* 2006). Unlike the other characterized members of the dynamin superfamily within plants, FZL is suspected to be a membrane remodeling GTPase that regulates organization of the thylakoid membranes, as *fzl* mutants have thylakoid morphology defects and possess aberrant vesicular inclusions within the stroma (Gao, Sage, *et al.* 2006). *fzl* mutants also show defects in chloroplast morphology — possibly implicating the organization or position of the thylakoid membranes in division (Gao, Sage, *et al.* 2006). Curiously, FZL-GFP localizes to spots or vesicles around the periphery of the chloroplast, which seems inconsistent with its role in thylakoid biogenesis. However, it has recently been shown that *tgd4 act1* double mutants have enlarged plastids with thylakoid defects similar to *fzl* mutants, perhaps as a result of the loss of both sources of membrane material that partly compose the thylakoid membrane in plants (Xu, Fan, *et al.* 2008). Based on its mutant phenotype and localization, we suspect that FZL might be part of a vesicular transport system that aids trafficking of membrane material from outside the chloroplast (i.e. the TGD4 pathway) to the thylakoid membrane (Xu, Fan, *et al.* 2008), which suggests that the chloroplast morphology phenotype observed within *fzl* mutants is a pleiotropic effect, but further work is required to rigorously test this hypothesis. Regardless, the impact of thylakoid morphology upon the process of chloroplast division is interesting and should be investigated further.

Some factors that make up the chloroplast divisome remain to be identified. The Plastid Dividing (PD) rings are electron-dense structures that appear after the Z-ring is established; these structures are dynamic and may be involved in mediating constriction (Miyagishima, Kuroiwa, *et al.* 2001). While the consituitve parts of the PD rings are unknown, the Kuroiwa laboratory is in the process of dissecting these rings and identifying their constituent parts using a synchronizable red algae, *Cyanidioschyzon merolae* (Yoshida, Kuroiwa, *et al.* 2006). It is thought that land plants will possess the same components, as the timing, size, and dynamics of the PD rings in land plants are similar to those observed in the red algae (Kuroiwa, Kuroiwa, *et al.* 1998).

While several factors have been introduced here, much work is still required to identify the complete function of each component and the pathways that feed into their expression and activity. Furthermore, several factors are likely to be uncovered in the coming years using comparative genomics, biochemical, and genetic approaches. Throughout this text, I will attempt to overtly indicate where pieces are missing to reiterate this idea, as a final model must account for all the components.

Regulating Plastid Fission: *Why Do Plastids Divide in Land Plants?*

It is currently theorized that at least four major inputs feed into the regulation of plastid fission in higher plants: photosynthetic and photoprotective activity, metabolite transport, cellular division, and cellular differentiation. Presumably, each of these inputs

contributes to the fitness of a particular organism. We will briefly review each of these here.

Photocollection and Photoprotection

The viability of chloroplast division mutants with large chloroplasts raises the question of why plant cells evolved to have multiple chloroplasts. The answer may have to do partly with the ability of multiple small chloroplasts to redistribute more effectively than fewer large chloroplasts inside the cell. Unlike motile unicellular algae with single chloroplasts, land plants are sessile and cannot relocate in response to sudden changes in light intensity. Chloroplasts in land plants avoid potentially damaging high light by moving to the cell periphery and orienting in columns parallel to the plane of incoming light; under low-light conditions, chloroplasts gather in periclinal layers to maximize light absorption (Kasahara, Kagawa, *et al.* 2002). This movement is believed to be largely performed through actin reorganization and myosin motor activity (Paves and Truve 2007, Schmidt von Braun and Schleiff 2008). Consistent with the importance of plastid division for efficient plastid movement, a mutant allele of *Arabidopsis* FtsZ1 shows diminished plastid movement in response to high light (Yoder, Kadirjan-Kalbach, *et al.* 2007). Interestingly, the thylakoid morphology of big-plastid mutants is reminiscent of that in high light-adapted plants (Austin II and Webber 2005), and probably arises due to the impaired movement ability of the enlarged chloroplasts within division-defective backgrounds (Jeong, Park, *et al.* 2002). As discussed earlier, mutations in genes influencing thylakoid organization also impair chloroplast division (Gao, Sage, *et al.* 2006, Xu, Fan, *et al.* 2008). The regulation of thylakoid morphology

and chloroplast movement is probably incorporated into a larger system that maximizes photosynthetic output and minimizes light-induced damage in response to changing environmental stimuli (Suetsugu and Wada 2007, Wada, Kagawa, *et al.* 2003).

Metabolic Exchange: The Possible Effect of Organelle Area-to-Volume Ratio

In addition to the potential role of photosynthesis in regulating plastid division, the shuttling of reduced carbon and metabolites between the plastid and the cytosol might also influence the division process. Presumably, an optimal ratio of organelle surface area to internal volume is maintained in chloroplasts. A larger plastid, such as those in the *arc6* background, has a disproportionate surface to volume ratio relative to smaller plastids (Pyke and Leech 1992, Pyke and Leech 1994, Pyke, Rutherford, *et al.* 1994), and as a result may have insufficient transporter capabilities. Maintaining large numbers of small plastids may allow for greater membrane surface area and prevent bottlenecks of metabolic flux between the plastid and the cytosol or between the plastid and other organelles. However, investigation of this potential regulatory input into the division process has not been explored.

Cell Division and Cell Expansion

Chloroplast division is intimately coupled to cell expansion and cellular division in algae, and to some degree in plants. In dividing meristematic cells and juvenile leaf cells, the pace of plastid division must keep pace with cellular division to ensure that each resulting cell has one of these essential organelles (Boffey and Lloyd 1988, Possingham

and Lawrence 1983), though aplastidic cells can reside within the leaves of plants (Chen, Asano, *et al.* 2009, Forth and Pyke 2006, Pyke, Rutherford, *et al.* 1994). At least one factor, CDT1, has been implicated in coordinating cell division with plastid division in plant cells (Raynaud, Perennes, *et al.* 2005). CDT1 proteins are known to be part of the pre-replication complex, required for origin licensing during nuclear DNA replication in eukaryotes (DePamphilis 2003, Thomer, May, *et al.* 2004), including *Arabidopsis* (Castellano, Boniotti, *et al.* 2004, Masuda, Ramos, *et al.* 2004). However, in *Arabidopsis*, RNAi knockdown lines that diminish expression of CDT1 paralogs have profound defects in chloroplast morphology and CDT1 has been shown to interact with ARC6 (Raynaud, Perennes, *et al.* 2005). The precise details of how CDT1 impacts chloroplast division are unknown, but the dual function of CDT1 proteins in nuclear DNA replication and plastid division should be examined further.

As cells expand, the number and/or volume of chloroplasts increases proportionately in mesophyll cells, so that ~70% of the cell volume is consistently occupied by chloroplasts, even in division-impaired mutants (Pyke 1998, Robertson, Pyke, *et al.* 1995). Cell expansion is part of leaf cell development in plants and is influenced by brassinosteroids (Hu, Poh, *et al.* 2006, Nakaya, Tsukaya, *et al.* 2002), auxin (Chen, Shimomura, *et al.* 2001, Jones, Im, *et al.* 1998), and cytokinin (Baskin, Cork, *et al.* 1995, Beemster and Baskin 2000). Of these, only cytokinins have been shown to influence plastid differentiation (Reski, Wehe, *et al.* 1991) and plastid division (Okazaki, Kabeya, *et al.* 2009). In *Arabidopsis*, application of exogenous cytokinin or overexpression of *CRF2* (Cytokinin-Responsive Factor 2) leads to an increased rate of

plastid division as a result of increased expression of PDV1 and PDV2 (Okazaki, Kabeya, *et al.* 2009), two factors involved in modulating dynamin (ARC5) recruitment and activity (Miyagishima, Froehlich, *et al.* 2006). Strangely, while cytokinin does upregulate the rate of chloroplast division through the PDV proteins, expression levels of other division factors such as FtsZ or ARC6 are unchanged in response to cytokinin (Okazaki, Kabeya, *et al.* 2009) — suggesting that the protein level of PDV1 and PDV2 can stimulate the activity of both cytosolic and stromal division factors from their position within the outer envelope membrane (Okazaki, Kabeya, *et al.* 2009). While it is clear that cell expansion and cytokinin certainly influence plastid differentiation and division, the full scope of the gene regulatory network that controls plastid fission remains to be determined.

Controls on Division During Cellular Development and Differentiation

In addition to binary fission of chloroplasts within leaf cells, plastids can undergo developmentally-regulated division and differentiation during plant development. For example, plastid differentiation during fruit development in tomato occurs through a unique budding/fragmentation mechanism where even enlarged chloroplasts are capable of differentiating into normal chromoplasts during fruit ripening (Forth and Pyke 2006). The bypass of the block in plastid division within *suffulta* mutants that occurs during tomato fruit development is not observed with the enlarged chloroplasts of *ftsZ*, *arc6*, or *arc12* mutants (although *Arabidopsis* itself does not possess chromoplasts); once an oversized chloroplast is generated, it is presumed to have lost its polarity and can no longer divide using an FtsZ-based mechanism (Schmitz, Glynn, *et al.* 2009). It is

possible that the pathway that produces stromules, stroma-containing extrusions of the plastid, might be involved in these fission events, as stromules are generated even in the absence of a functional Z-ring (Holzinger, Kwok, *et al.* 2008). The molecular identification of *suffulta* and the study of plastid fission in the big-plastid backgrounds (i.e. *arc6*, *arc12*, and others) will likely provide critical insights into FtsZ-independent pathways of plastid partitioning.

Perspectives and Acknowledgements

Previous to this body of work, several issues in the field of plastid division were unclear. Within the following chapters, I attempt to address at least three major questions: (1) what discrete region of ARC6 binds FtsZ2 family members and what is the purpose of this interaction *in vivo*? (2) How does ARC6 participate in the coordination of the stromal and cytosolic plastid division machineries? (3) What is the function of *Arabidopsis* ARC6 paralog (PARC6) and how might PARC6 and ARC6 link into the plastidic Min system? I follow these chapters with some general conclusions and suggested future directions for research. Additionally, this volume contains two appendices that highlight peripheral projects undertaken during the last few years. I hope it is a clear and fascinating read. Please note that portions of this chapter are reproduced from (Glynn, Miyagishima, *et al.* 2007) (http://www.traffic.dk/) and is Copyright Blackwell Publishing. Blackwell grants authors the freedom to reuse their own articles in new publications, provided that they are the editor of the new publication.

Chapter 2

Identification and Modeling of an FtsZ2-Binding Domain within ARC6

Abstract

The plastidic Z-ring is not a static structure, but probably undergoes remodeling in response to various input signals. The regulation of FtsZ filament dynamics is an important part of remodeling the Z-ring during its assembly and constriction. *ARC6* has been shown to be required for assembly and/or stabilization of the Z-ring *in vivo*. This stabilizing activity has been proposed to occur through FtsZ2 family members, as ARC6 has been shown to bind FtsZ2, but not FtsZ1. However, the precise effect of ARC6 upon Z-ring assembly through its interaction with FtsZ2 has not been demonstrated experimentally, nor have the exact boundaries of the FtsZ2-binding domain (ZBD) of ARC6 been identified. To provide insight into the function of $ARC6_{ZBD}$, we fine-mapped the boundaries of this domain using two hybrid assays and used this information to guide analysis of the *in vivo* function of $ARC6_{ZBD}$. Our results indicate that $ARC6_{ZBD}$ occupies amino acids 351-503. This domain is conserved amongst the Chlorophytes and cyanobacteria, but bears no sequence similarity to other characterized protein sequences. We generated a homology model of $ARC6_{ZBD}$ based on the crystal structure of the FtsZ-binding domain of *E. coli* ZipA, an FtsZ-bundling protein. $ARC6_{ZBD}$ was fit onto the known structure of $ZipA_{ZBD}$, despite the large degree of sequence divergence between $ARC6_{ZBD}$ and $ZipA_{ZBD}$, suggesting that $ARC6_{ZBD}$ might aid bundling of FtsZ filaments through a ZipA-like mechanism, but rigorous *in vivo* analysis and structural data is still needed to validate this model.

Introduction

Plastids are essential organelles. In plant cells, binary fission is a mechanism by which each cell receives its required complement of plastids and likely is influenced by development, environmental cues, and cellular metabolism (Boffey and Lloyd 1988, Leech, Thomson, *et al.* 1981, Possingham and Lawrence 1983). Plastids evolved from a cyanobacterium that took up residence within a primitive protozoan (Cavalier-Smith 2000). Like many free-living cyanobacteria and proteobacteria, chloroplasts divide by binary fission in a process that requires FtsZ (Osteryoung, Stokes, *et al.* 1998, Strepp, Scholz, *et al.* 1998, Vitha, McAndrew, *et al.* 2001).

FtsZ is a filament-forming GTPase with structural similarity to tubulin (Erickson, Taylor, *et al.* 1996, Mukherjee, Dai, *et al.* 1993). *E. coli* FtsZ forms protofilaments that undergo organized assembly into a structure at the mid-cell called the Z-ring, which acts as a dynamic scaffold for other division components (Margolin 2005) and probably generates the force that contributes to cellular constriction (Erickson 2009, Li, Trimble, *et al.* 2007, Osawa, Anderson, *et al.* 2008).

Several systems contribute to controlling both FtsZ protofilament assembly and Z-ring assembly. The Min system, composed of MinCDE, prevents protofilament assembly at the poles, but allows bulk protofilament assembly to occur at the mid-cell, ensuring that the cell divides near its midpoint (Lutkenhaus 2007). ZipA is a bitopic membrane protein that binds a conserved C-terminal segment of FtsZ in *E. coli* and is

thought to be important for protofilament bundling and organization adjacent to the inner leaflet of the cell membrane at the midcell (Hale, Rhee, *et al.* 2000, Mosyak, Zhang, *et al.* 2000, RayChaudhuri 1999). The conserved C-terminal motif of bacterial FtsZ consists of ~12 amino acids and is required for FtsZ function (Ma and Margolin 1999). Besides ZipA, the conserved C-terminus of FtsZ is a target for FtsA, another protein involved in cell division (Pichoff and Lutkenhaus 2002, Pichoff and Lutkenhaus 2005, Pichoff and Lutkenhaus 2007, Ricard and Hirota 1973). FtsA is a membrane-associated protein that acts as a membrane anchor for the Z-ring (Osawa, Anderson, *et al.* 2008, Pichoff and Lutkenhaus 2005) and binds the C-terminal tail of FtsZ through a domain that is structurally distinct from the FtsZ-binding domain of ZipA (Mosyak, Zhang, *et al.* 2000, van den Ent and Lowe 2000). While the coordinated action of MinCDE, ZipA, and FtsA contribute to FtsZ ring formation in proteobacteria, the precise roles of proteins influencing assembly and dynamics of the Z-ring in plastids is still somewhat unclear.

In chloroplasts, FtsZ assembles into ring-shaped structures near the middle of the organelle, analogous to the bacterial protein (Vitha, McAndrew, *et al.* 2001). In the case of plants, however, FtsZ gene duplication and divergence have generated two distinct families of FtsZ protein (termed FtsZ1 and FtsZ2), both of which are required for chloroplast division (Osteryoung, Stokes, *et al.* 1998, Schmitz, Glynn, *et al.* 2009). The most notable difference between these two families occurs at their C-termini, where FtsZ2 family members possess a C-terminal motif similar to the ZipA- and FtsA- binding motif of bacterial FtsZ proteins; this motif is absent from plant FtsZ1 family members (Miyagishima, Nishida, *et al.* 2003b, Stokes and Osteryoung 2003).

While ZipA is an essential gene in some bacteria, orthologs of ZipA are absent from cyanobacteria and plants (Miyagishima, Nishida, *et al.* 2003b). However, we have hypothesized the existence of an FtsA-like or ZipA-like protein in these lineages because FtsZ2 family members have retained the conserved C-terminal extension present in most bacterial FtsZ proteins. Despite the inability to identify a ZipA-like protein in plants by BLAST (Altschul, Madden, *et al.* 1997), analysis of ARC6 suggests that it may fulfill a similar functional role within the plastid. ARC6 promotes Z-ring assembly, possibly by bundling FtsZ filaments within the plastid since loss-of-function *arc6* mutants have short FtsZ filaments distributed throughout the stroma and transgenic lines overexpressing ARC6 have elongated FtsZ filaments, some of which are spiraled or branched (Vitha, Froehlich, *et al.* 2003). A previous report revealed an interaction between ARC6 and FtsZ2-1 that requires the conserved C-terminal extension of FtsZ2-1 and proposed a functional role analogous to that of ZipA or FtsA in *E. coli*; although the precise boundaries for the FtsZ2 binding domain were not identified in this study (Maple, Aldridge, *et al.* 2005).

The results we show here define the FtsZ2 binding domain (ZBD) of *Arabidopsis* ARC6 and show that the $ARC6_{ZBD}$ shares features with the FtsZ-binding domain of *E. coli* ZipA (Mosyak, Zhang, *et al.* 2000). We then used site-directed mutagenesis to identify critical residues within the $ARC6_{ZBD}$ that are probably sites of intermolecular contact between ARC6 and FtsZ2 based on our structural model. Further, we introduced transgenes into *Arabidopsis* that are predicted $ARC6_{ZBD}$ loss-of-function or gain-of-

function alleles based on our protein interaction analyses in yeast. Unfortunately, these transgenes were uninformative with regard to $ARC6_{ZBD}$ function *in vivo* and further analysis will be required to validate the boundaries of $ARC6_{ZBD}$ and provide insight into its structure and function *in vivo*.

Results

The FtsZ2-binding domain of ARC6 ($ARC6_{ZBD}$) occupies amino acids 351-503.

Previously, our colleagues discovered that a portion of the conserved stromal region of ARC6 (AA 154-509) specifically bound FtsZ2-1 in two-hybrid experiments (Maple, Aldridge, *et al.* 2005, Maple and Moller 2006). Recently, our laboratory showed that both *Arabidopsis* FtsZ2 isoforms (FtsZ2-1 and FtsZ2-2) bind the same region of ARC6 with similar affinity and are functionally redundant (Schmitz, Glynn, *et al.* 2009); therefore, we used only FtsZ2-1 (hereforth FtsZ2) in our analyses for simplicity.

To delineate the precise boundaries of the $ARC6_{ZBD}$, we used a two-hybrid-based domain-mapping approach, using exon junctions as the boundaries for our initial constructs (Figure 2.1) since critical domains might be less likely to be interrupted by introns during genome evolution (de Souza, Long, *et al.* 1996, Fodor and Aldrich 2009). The conserved stromal region of ARC6 is encoded within four exons. We generated 9 constructs representing different portions of ARC6 and assayed these for interaction with FtsZ2. The results of these assays indicate that $ARC6_{ZBD}$ is contained within AA 351-

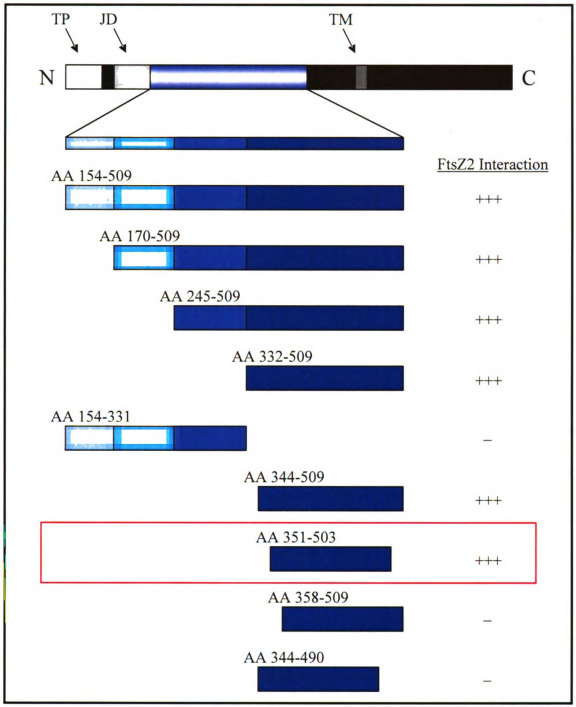

Figure 2.1. Mapping the FtsZ2-binding domain of ARC6 by yeast two-hybrid assay. Constructs shown are GAL4-AD fusions of ARC6, with FtsZ2-1 present as a GAL4-BD fusion. Interaction strength is reported as the ratio of growth (-HIS : +HIS) of a transformant on supplemented synthetic dropout media (+++ growth ratio is greater than or equal to 0.67; - growth ratio is less than or equal to negative control). The minimal portion of ARC6 required for interaction with FtsZ2 is boxed. Transit peptide (TP); J-domain (JD); transmembrane domain (TM); N-terminus (N); and C-terminus (C).

503 (Figure 2.1); the degree of reporter activation from AA 351-503 was similar to that of the original boundaries described previously (Maple, Aldridge, *et al.* 2005).

The C-terminus of FtsZ2 is sufficient for ARC6-FtsZ2 interaction.

Previously it was shown that the C-terminus of FtsZ2 is necessary for ARC6-FtsZ2 interaction (Maple, Aldridge, *et al.* 2005), but it was unclear if this short C-terminal motif was sufficient for ARC6-FtsZ2 interaction, or if other features within FtsZ2 might be required for ARC6-FtsZ2 interaction. To address this question, we generated two-hybrid constructs encoding the C-terminal 19 amino acids of *Arabidopsis* FtsZ2 as a GAL4 fusion and transformed them into yeast carrying plasmids encoding either $ARC6_{154\text{-}509}$ or $ARC6_{ZBD}$. Our results indicate that the C-terminus of FtsZ2 is sufficient for ARC6-FtsZ2 interaction, as GAL4 fusions to both the mature FtsZ2 protein and 19 amino acid motif at the C-terminus of FtsZ2 ($FtsZ2_{459\text{-}478}$) generated comparably high levels of reporter activation (Figure 2.2), though the presence of the full-length FtsZ2 protein was associated with slightly higher levels of *HIS3* reporter activation.

To gain insight into the structure and function of the $ARC6_{ZBD}$, we wanted to generate a testable structural model of this protein domain. There is currently no experimentally-tested structural data available for ARC6, so our initial approaches involved the use of BLAST-based sequence queries (Altschul, Madden, *et al.* 1997) to identify similar domains with solved crystal or NMR structures. Using this approach, we were unable to identify similar sequences with solved three-dimensional structures.

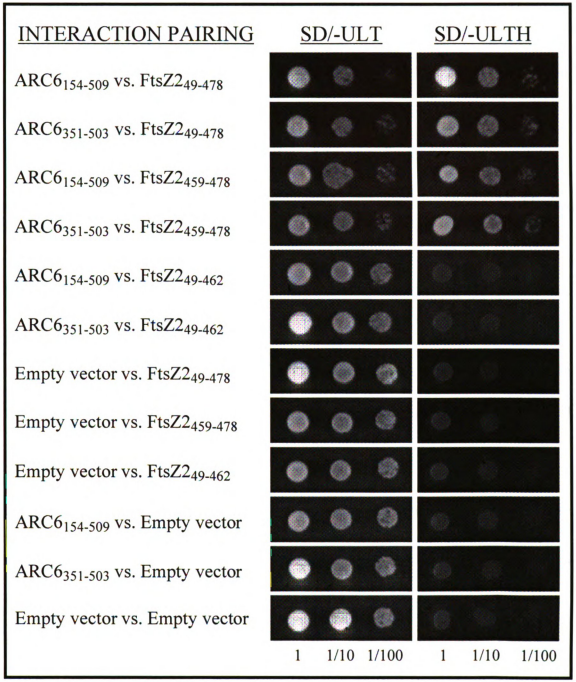

Figure 2.2. Two-hybrid *HIS* reporter assays showing ARC6-FtsZ2 interaction. Yeast harboring pairings of AD-ARC6 and BD-FtsZ2 are shown following 48 hours of growth on the synthetic dropout (SD) media indicated. ARC6-FtsZ2 interaction requires only $ARC6_{351\text{-}503}$ ($ARC6_{ZBD}$) and $FtsZ2_{459\text{-}478}$. Removal of the C-terminus (AA463-478) of FtsZ2 abolishes ARC6-FtsZ2 interaction. Dilutions from a stationary phase culture at OD_{600} = 1.0 are indicated 1, 1/10, and 1/100.

$ARC6_{ZBD}$ can be modeled onto the crystal structure of $ZipA_{ZBD}$.

Because $ARC6_{ZBD}$ binds the short conserved C-terminal motif of FtsZ2 family members and this motif shares conservation with an analogous motif found at the C-terminus of bacterial FtsZ sequences (hereforth referred to $FtsZ_{CT}$), we compared the $ARC6_{ZBD}$ amino acid sequence to sequences of bacterial proteins known to bind $FtsZ_{CT}$, as some of these have solved crystal structures. At least three proteins bind bacterial $FtsZ_{CT}$: FtsA (Pichoff and Lutkenhaus 2007), ZipA (Hale, Rhee, *et al.* 2000), and EzrA (Singh, Makde, *et al.* 2007). The FtsZ-binding domain of FtsA is at least 288 amino acids in length (Pichoff and Lutkenhaus 2007) and there is no crystal structure available for EzrA. The FtsZ-binding domain of ZipA ($ZipA_{ZBD}$) has a solved structure (Mosyak, Zhang, *et al.* 2000) and is similar in length (144 amino acids) to the $ARC6_{ZBD}$ (153 amino acids) and was chosen to generate a structural model of $ARC6_{ZBD}$. We generated a sequence alignment between $ARC6_{ZBD}$ and $ZipA_{ZBD}$ to identify regions of similarity between these two domains (Figure 2.3). The homology-modeling server at http://proteins.msu.edu/ was then used to superimpose the amino acid sequence of $ARC6_{ZBD}$ onto the main chain structure of $ZipA_{ZBD}$ (Protein Data Bank Identification Number 1F47) (Mosyak, Zhang, *et al.* 2000), using the identical residues (Figure 2.3) between the two sequences as anchor points. Following this, we modeled the sidechains of $ARC6_{ZBD}$ using SCWRL (Wang, Canutescu, *et al.* 2008) to get the lowest energy conformation of $ARC6_{ZBD}$ with minimal conflict.

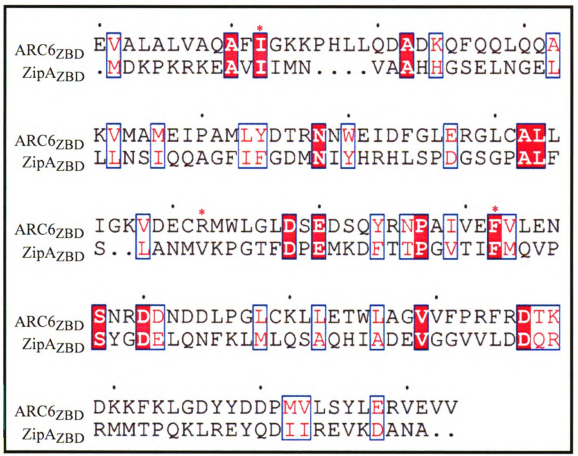

Figure 2.3. Alignment of ARC6$_{ZBD}$ (AA 351-503) with ZipA$_{ZBD}$ (AA185-328).

ARC6$_{ZBD}$ was aligned with ZipA$_{ZBD}$ using a BLOSUM62 scoring matrix with CLUSTALW2 (http://www.ebi.ac.uk/Tools/clustalw2/). Identical residues are shown boxed with shading; similar residues are indicated with boxed lettering. The asterisks (*) above the ARC6$_{ZBD}$ sequence indicate residues that are hypothesized to be critical for intermolecular contact between ARC6 and FtsZ2, based on comparison with *E.coli* ZipA-FtsZ interaction (Moreira, Fernandes, *et al.* 2006).

A comparison of $ARC6_{ZBD}$ and $ZipA_{ZBD}$ is shown in Figure 2.4 and illustrates the prospective structural similarity of these two functionally-similar protein domains, despite their significant differences in amino acid sequence. If this model is correct, it indicates that $ARC6_{ZBD}$ is a domain made up of both alpha helices and beta sheet structures. Curiously, this model conflicts with the mostly helical secondary structure predictions made for $ARC6_{ZBD}$ (Figure 2.5) by three EVA-rated prediction algorithms (http://cubic.bioc.columbia.edu/eva/): PSI-PRED, PROFsec, and SABLE (Rost and Eyrich 2001). However, these programs are not trained to predict secondary structure at physiological pH of the stroma, which is approximately 8.0 under optimal light conditions (McDonald 2003). This difference may explain the discrepancy between the $ARC6_{ZBD}$ secondary structure inferred by comparison with $ZipA_{ZBD}$ and those predicted by PSI-PRED, PROFsec, and SABLE — as the pH of the surrounding medium can significantly affect protein folding by altering the charge or polarity of amino acid side chains (Cramer, Engelman, *et al.* 1992, Dobson 2003, Pagel and Koksch 2008). In any event, these predictions and models need to be carefully and rigorously validated with experimental data (X-ray or NMR-solved structures).

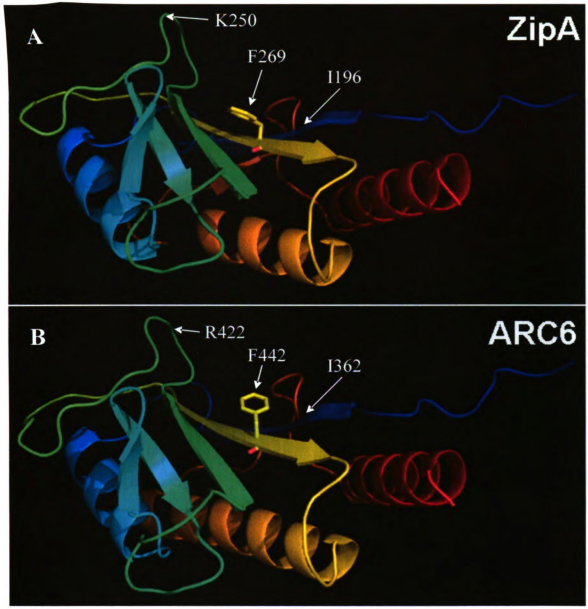

Figure 2.4. Comparison of the *E. coli* ZipA$_{ZBD}$ crystal structure and the *A. thaliana* ARC6$_{ZBD}$ homology model. Cartoon representations of (A) the crystal structure of ZipA (AA 185-328) and (B) the homology model of ARC6 (AA 351-503). Labels and arrows in (A) indicate residues shown to be important for intermolecular contact with the C-terminus of *E. coli* FtsZ (Moreira, Fernandes, *et al.* 2006); the analogous residues in ARC6 are indicated in panel (B). In panel (A), the side chain of the central phenylalanine residue (F269) that stabilizes the ZipA-FtsZ interaction is shown projecting into the hydrophobic pocket that is occupied by the C-terminus of FtsZ; the modeled side chain of the corresponding phenylalanine in ARC6 (F442) is shown for comparison in (B). Amino termini are shown in blue and carboxy termini are shown in red.

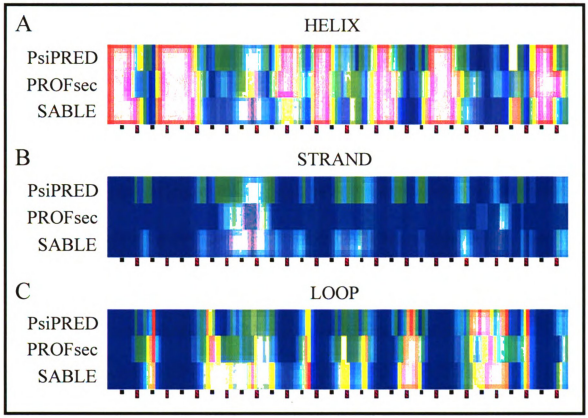

Figure 2.5. Secondary structure predictions of ARC6$_{ZBD}$. Predictions for (A) helical, (B) strand, and (C) loop secondary structures using three top-rated secondary structure prediction algorithms. Red indicates a high propensity for the secondary structure indicated and blue indicates low probablility for structure indicated. Large tick marks = 10 AA and small tick marks = 5 AA.

Mutations that influence ZipA-FtsZ interactions influence ARC6-FtsZ2 interaction.

To test the validity of our model, I made mutations in $ARC6_{ZBD}$ using SOE-PCR and then tested for interaction of $ARC6_{ZBD}$ with FtsZ2 using yeast two-hybrid assays. A previous study had shown that mutations in the following residues of $ZipA_{ZBD}$ affect binding of FtsZ: I196, K250, and F269; of these $ZipA_{F269}$ has the most significant impact upon the strength of the ZipA-FtsZ interaction (Moreira, Fernandes, *et al.* 2006). I hypothesized that if $ARC6_{ZBD}$ and $ZipA_{ZBD}$ do share a common structure and binding scheme for FtsZ, then the analogous positions within $ARC6_{ZBD}$ should be similar to those in $ZipA_{ZBD}$. Therefore, mutagenesis of those same residues within $ARC6_{ZBD}$ should result in varied binding of FtsZ2, in a manner similar to that observed for $ZipA_{ZBD}$. In comparing the two structures (Figure 2.4), I found residues in $ARC6_{ZBD}$ analogous to $FtsZ_{CT}$ contact-critical regions in $ZipA_{ZBD}$. I generated mutations in $ARC6_{ZBD}$, focusing on $ARC6_{F442}$, as this residue occupies a position analogous to $ZipA_{F269}$. The following $ARC6_{ZBD}$ mutations were tested for interaction with FtsZ2: F442Y, F442A, F442K, and F442D (Figure 2.6). Site-directed mutation of F442 had varying effects upon ARC6-FtsZ2 binding, with charged residues causing major disruption of the interaction between the two proteins (Figure 2.6). These results are consistent with the effect of analogous mutations on ZipA

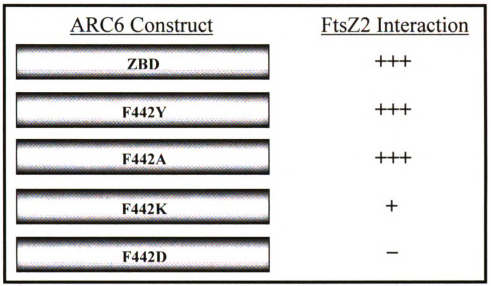

Figure 2.6. $ARC6_{ZBD\ (F442)}$ site-directed mutants. GAL4-$ARC6_{ZBD}$ fusions carrying site-directed mutations for phenylalanine 442 (F442) were tested for their ability to interact with GAL4-FtsZ2-1 in yeast using a *HIS* reporter assay. Hydrophobic substitutions (F442Y and F442A) do not affect interaction strength between ARC6 and FtsZ2, but charged substitutions (F442K and F442D) disrupt ARC6-FtsZ2 interaction consistent with $ARC6_{F442}$ residing within a hydrophobic pocket, similar to $ZipA_{F269}$ (Mosyak, Zhang, *et al.* 2000). Interaction strength is shown as the ratio of yeast growth on –HIS/+HIS synthetic dropout media. Growth ratio $\geq$ 0.67 (+++); 0.66 $\geq$ growth ratio $\geq$ 0.33 (++); 0.32 $\geq$ growth ratio > vector-only negative control (+); and growth ratio < negative control (-).

(Moreira, Fernandes, *et al.* 2006) and suggest that FtsZ2 might bind $ARC6_{ZBD}$ within a hydrophobic pocket, similar to ZipA-FtsZ interaction (Moreira, Fernandes, *et al.* 2006, Mosyak, Zhang, *et al.* 2000). From this analysis, I conclude that the structures of the $ARC6_{ZBD}$ and $ZipA_{ZBD}$ might be similar, with the C-terminus of FtsZ2 binding to $ARC6_{ZBD}$ within a hydrophobic pocket, but further analysis of $ARC6_{ZBD}$ site-directed mutants and real structural analyses (i.e. X-ray crystallography or NMR) are required to fully test this structural model.

Analysis of the $ARC6_{ZBD}$-FtsZ2 Interaction by Pulldown Assay.

To confirm our two-hybrid results, I attempted to use a pulldown approach to compare the FtsZ2-binding abilities of $ARC6_{ZBD}$ and $ARC6_{ZBD\ (F442D)}$. I expressed the C-terminus of FtsZ2 (AA 459-478) as a C-terminal fusion to GST ($GST\text{-}FtsZ2_{CT}$). Both $ARC6_{ZBD}$ and $ARC6_{ZBD\ (F442D)}$ were expressed with a polyhistidine tag at their N-termini ($His_8\text{-}ARC6_{ZBD}$ and $His_8\text{-}ARC6_{ZBD\ (F442D)}$, respectively). All fusions were expressed under control of an IPTG-inducible promoter in *E.coli*. After immobilizing and purifying the polyhistidine-ARC6 fusion proteins using Ni-sepharose beads, I treated $His_8\text{-}ARC6_{ZBD}$ or $His_8\text{-}ARC6_{ZBD\ (F442D)}$ with clarified cell extracts from lines expressing $GST\text{-}FtsZ2_{CT}$. After a series of washes, bound protein was eluted from the beads using concentrated imidazole the eluates were probed for $GST\text{-}FtsZ2_{CT}$. In preliminary results, I observed similar $GST\text{-}FtsZ2_{CT}$ binding characteristics for both

His_8-$ARC6_{ZBD}$ and His_8-$ARC6_{ZBD\ (F442D)}$ (Figure 2.7A). I repeated this protocol with more stringent wash conditions and observed that neither ARC6 fusion was able to retain GST-$Z2_{CT}$ (not shown). To gain insight into the root cause of this result, I performed a pulldown between His_8-$ARC6_{ZBD}$ and either GST-$FtsZ2_{CT}$ or GST-$FtsZ2_{CT\ (F466A)}$; the $FtsZ2_{F466A}$ mutation was previously shown to abolish interaction between ARC6 and FtsZ2 using a two-hybrid based approach (Maple, Aldridge, *et al.* 2005). Surprisingly, both $FtsZ2_{CT}$ and $FtsZ2_{CT(F466A)}$ interact with $ARC6_{ZBD}$ using pulldowns (Figure 2.7B). Curiously, the results of the *in vitro* pulldowns between site-directed mutants of ARC6 and FtsZ2 (Figure 2.7) are inconsistent with two-hybrid assays (Maple, Aldridge, *et al.* 2005) (Figure 2.6), leading us to question the overall importance of $ARC6_{F442}$ and $FtsZ2_{F466}$ *in vivo*.

In vivo analysis of the $ARC6_{F442D}$ site-directed mutation.

Because $ARC6_{F442}$ was shown to be critical for ARC6-FtsZ2 interaction in yeast, but not for *in vitro* interaction, I aimed to test one of these results *in vivo* and clarify the role of $ARC6_{ZBD}$ by analyzing a prospective ZBD loss-of-function mutant. To do this, I generated transgenes encoding the native ARC6 protein and an $ARC6_{F442D}$ mutant protein. Both of these transgenes were placed under control of the native *ARC6* promoter (Vitha, Froehlich, *et al.* 2003). Constructs were introduced into *Col-0* and *arc6* (SAIL_693_G04) backgrounds by *Agrobacterium*-mediated

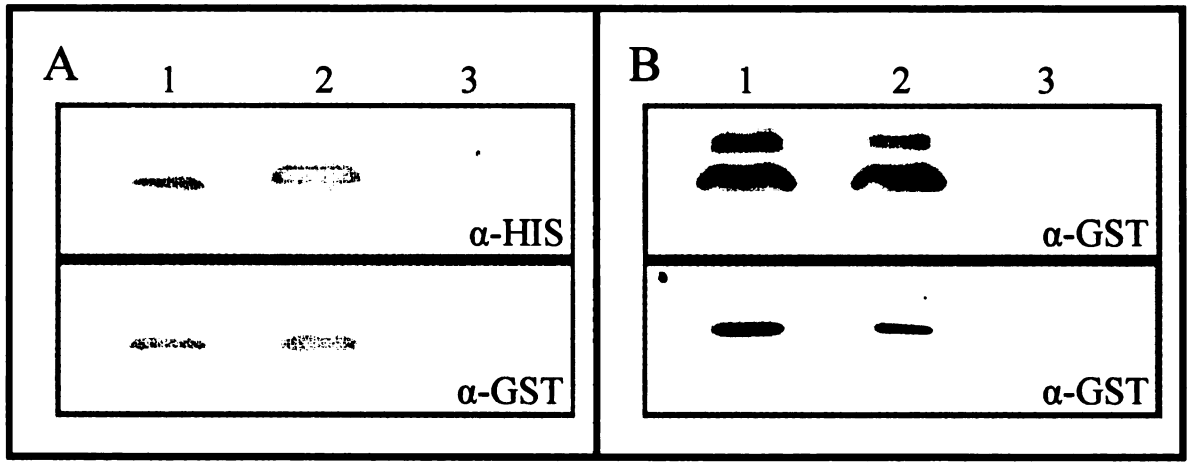

Figure 2.7. Pulldown of FtsZ2 by ARC6. (A) Anti-HIS immunoblot (upper panel) showing eluted bait protein and anti-GST (lower panel) showing eluted GST-FtsZ2$_{CT}$ fusions. Pulldown eluates from immobilized His$_8$-ARC6$_{ZBD}$ treated with GST-FtsZ2$_{CT}$ (lane 1); pulldown eluates from immobilized His$_8$-ARC6$_{ZBD(F442D)}$ treated with GST-FtsZ2$_{CT}$ (lane 2); and pulldown eluates from beads treated with GST-FtsZ2$_{CT}$ extract. (B) Anti-GST immunoblot showing eluted GST-FtsZ2$_{CT}$ fusions (upper panel) and input proteins (lower panel). Pulldown eluates from immobilized His$_8$-ARC6$_{ZBD}$ treated with GST-FtsZ2$_{CT}$ (upper panel, lane 1); pulldown eluates from His$_8$-ARC6$_{ZBD}$ treated with GST-FtsZ2$_{CT(F466A)}$ (upper panel, lane 2); and pulldown eluate from beads treated with only His$_8$-ARC6$_{ZBD}$ (upper panel, lane 3). Pulldown inputs (0.5 μg total protein/lane) for GST-FtsZ2$_{CT}$ (lower panel, lane 1); GST-FtsZ2$_{CT\ (F466A)}$ (lane 2); and His$_8$-ARC6$_{ZBD}$ (lower panel, lane 3). The molecular weight of the His$_8$-ARC6$_{ZBD}$ and His$_8$-ARC6$_{ZBD\ (F442D)}$ fusions are ~19 kD. The molecular weight of GST-FtsZ2$_{CT}$ and GST-FtsZ2$_{CT(F466A)}$ are ~28 kD.

transformation and transgenic individuals were selected using hygromycin. Once plants were approximately 5 weeks old, T_1 individuals and controls were examined for *ARC6* or *ARC6*$_{F442D}$ transgene expression by immunoblotting (Figure 2.8); only transformants from the SAIL_693_G04 background (*arc6*) were analyzed for ARC6 protein levels, as it would be impossible to differentiate the native and transgenic *ARC6* protein products using our polyclonal ARC6 antibody. Transformed (T_1) *arc6* individuals with *ARC6*$_{F442D}$ transgene expression near the range of expression yielding wild type chloroplast phenotypes were quantitatively assayed for chloroplast number and morphology (Figure 2.9), though all T_1 lines were subjected to microscopic examination. Consistent with pulldown results that hinted that ARC6$_{ZBD\ (F442D)}$ mutant proteins might be fully functional (Figure 2.7A), the *ARC6*$_{F442D}$ transgene was able to complement the *arc6* mutant (Figure 2.9D-E). Further, I observed very few defects in *Col-0* plants transformed with *ARC6*$_{F442D}$, (not shown) indicating that this transgene probably does not impart any dominant negative effect on chloroplast morphology, consistent with its ability to fully rescue an *arc6* mutant (Figure 2.9).

To determine if the *ARC6*$_{F442D}$-expressing lines have subtle defects in FtsZ assembly or disassembly, we examined Z-ring morphology within chloroplasts of juvenile leaves (Figure 2.10). Consistent with the ability of the *ARC6*$_{F442D}$ transgene to complement the chloroplast morphology defect of *arc6* mutants (Figure 2.9D-E), FtsZ

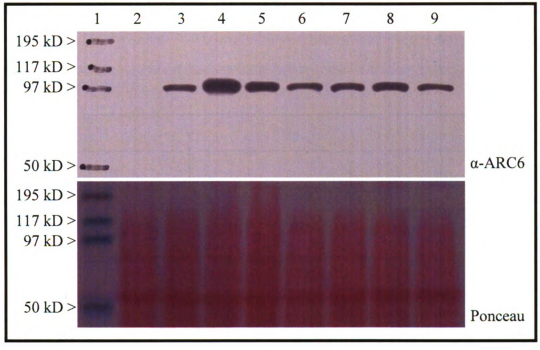

Figure 2.8. Demonstration of *ARC6* and *ARC6*$_{F442D}$ transgene expression in the *arc6* (SAIL_693_G04) background. Exposure from an anti-ARC6 immunoblot (top panel) and Ponceau stain of the corresponding membrane (lower panel). Whole cell extracts from controls and transformed *arc6* mutants: molecular weight marker (lane 1); untransformed SAIL_693_G04 (lane 2); untransformed *Col-0* (lane 3); *ARC6*$_{F442D}$-expressing transgenic line #1 (lane 4); *ARC6*$_{F442D}$-expressing transgenic line #2 (lane 5); *ARC6*-expressing transgenic line #1 (lane 6); *ARC6*-expressing transgenic line #2 (lane 7); *ARC6*-expressing transgenic line #3 (lane 8) ; and *ARC6*-expressing transgenic line #4 (lane 9). Two milligrams of whole-cell extract from flower buds are loaded in each lane.

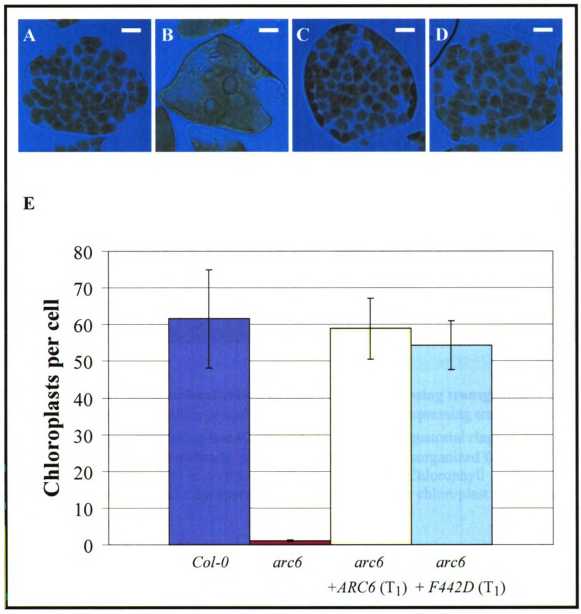

Figure 2.9. Quantitative analysis of chloroplast number in *ARC6*$_{F442D}$-expressing transgenics. Micrographs of mesophyll cells from: *Col-0* (A); *arc6* (B); *ARC6*-expressing transgenic line #3 (C); and *ARC6*$_{F442D}$-expressing line #2 (D). Scale bars = 10 μm. Quantitative analysis of chloroplast number within lines shown in A-D and Figure 2.8. Chloroplasts were counted using single-plane images from mesophyll cells with average areas of 3838 ± 713 μm^2. Ten cells were analyzed for each line using leaf tip samples from plants ~5 weeks post-germination. Error bars = standard deviation from the mean.

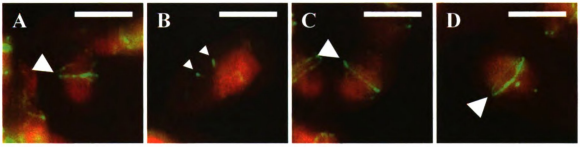

Figure 2.10. FtsZ immunolocalization in *ARC6*$_{F442D}$-expressing transgenics. FtsZ2-1 localization (green) in wild type *Col-0* (A); *arc6* (B); *ARC6*-expressing transgenic line #3 (C); *ARC6*$_{F442D}$-expressing line #2 (D). FtsZ localizes to equatorial rings in wild type chloroplasts (large arrowheads, panels A, C, and D) and disorganized fragments (small arrowheads, panel B) in *arc6* loss-of-function mutants. Chlorophyll autofluorescence (red) marks the approximate boundaries of the chloroplast. Scale bars = 5 μm.

morphology within the chloroplasts of $ARC6_{F442D}$-expressing lines (Figure 2.10D) was clearly different from that in untransformed *arc6* mutants (Figure 2.10B) and was indistinguishable from that in wild type *Col-0* (Figure 2.10A) and transgene-complemented *arc6* mutants (Figure 2.10C).

From these results, I conclude that $ARC6_{F442}$ is either not involved in mediating ARC6-FtsZ2 interaction *in vivo*, or is only one of several residues that stabilize ARC6-FtsZ2 interaction *in vivo*. These results are congruent with the comparable FtsZ2-binding abilities of both $ARC6_{ZBD}$ and $ARC6_{ZBD\ (F442D)}$ in pulldown assays (Figure 2.7). However, these results are inconclusive with regard to the function of $ARC6_{ZBD}$, as the prospective $ARC6_{F442D}$ transgene was fully functional and therefore did not provide further insight into the role of this proposed domain.

In vivo analysis of chloroplast targeted $ARC6_{ZBD}$.

As a secondary approach to elucidating the function of the FtsZ2-binding domain of ARC6, I generated a novel expression vector that targets the desired protein to the chloroplast stroma using the transit peptide of RecA (Kohler, Cao, *et al.* 1997). In addition to the N-terminal chloroplast transit peptide of RecA, the vector also encodes a C-terminal EYFP to verify protein expression and localization to the chloroplast. We placed the coding sequence of $ARC6_{ZBD}$ between that of the RecA transit peptide and EYFP; this transgene is expressed under control of the CaMV 35S promoter (Figure

2.11). The transgene was introduced into *Ws-2* and *arc6-1* backgrounds by *Agrobacterium*-mediated transformation. To assess localization of the $ARC6_{ZBD}$-EYFP fusion, I examined mesophyll cells from young leaves of several lines by fluorescence microscopy (Figure 2.12A-D). I observed EYFP signals that overlay with chlorophyll autofluorescence in transformed *Ws-2* and *arc6-1* backgrounds (Figures 2.12B and 2.12D), indicating that the $ARC6_{ZBD}$-EYFP was successfully imported into the chloroplast. Unlike ARC6, which forms a mid-plastid ring, I only observed plastid-targeted $ARC6_{ZBD}$-EYFP as a diffuse signal that was distributed throughout the chloroplast stroma (Figures 2.12B and 2.12D). Following examination by fluorescence microscopy, I verified transgene expression using an anti-YFP antibody. Protein extracts from some individuals within this T_1 population included a cross-reacting protein of ~47 kD (Figure 2.12E), which corresponds to the molecular weight of imported (processed) $ARC6_{ZBD}$-EYFP. To determine if the plastid-targeted $ARC6_{ZBD}$-EYFP expressing lines have defects in FtsZ assembly, I examined Z-ring morphology within dividing chloroplasts of juvenile leaves (Figure 2.13, insets). In each case, FtsZ morphology was similar to untransformed plants. To determine if the plastid-targeted $ARC6_{ZBD}$-EYFP had any gross effect upon chloroplast division, we examined fully expanded mesophyll cells from the same lines. Consistent with our observations of FtsZ morphology (Figure 2.13, insets), expression of $ARC6_{ZBD}$-EYFP had no effect upon chloroplast morphology in *Ws-2* nor *arc6-1* backgrounds (Figure 2.13A-D, large panels).

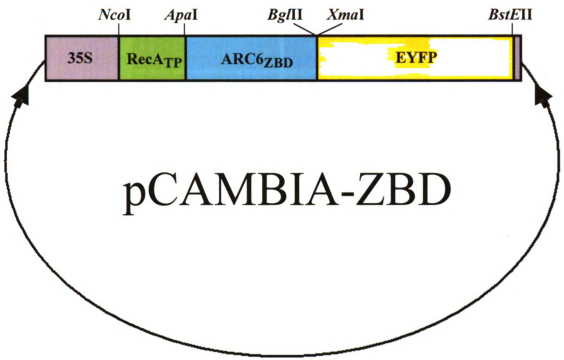

Figure 2.11. Schematic of plastid-targeting vector pCAMBIA-ZBD used for ARC6$_{ZBD}$ domain analysis. To gain insight into the role of the FtsZ2 binding domain of ARC6, the coding sequence for ARC6$_{ZBD}$ was cloned into a modified plant transformation vector derived from pCAMBIA-1302 (Hajdukiewicz, Svab, *et al.* 1994). Expression of the integrated transgene is driven by the CaMV 35S promoter (grey box, left side). The inserted coding sequence for the protein or domain of interest (light blue, ARC6$_{ZBD}$) is directed to the chloroplast by the transit peptide of *Arabidopsis* RecA (coding sequence shown in light green) (Kohler, Cao, *et al.* 1997). Protein expression and localization is confirmed by fusion to EYFP (coding sequence is shown in yellow). The nopaline synthase terminator sequence is used for transcriptional termination (grey box, right side). The left and right border sequences of the T-DNA are indicated by the large black arrowheads. Restriction sites are indicated above the schematic. Markers for selection of transformants are not shown. Drawing is not to scale.

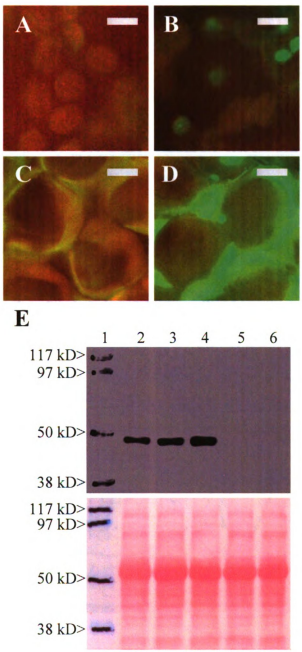

Figure 2.12. Demonstration of expression and targeting of ARC6$_{ZBD}$-EYFP. Merged fluorescence micrographs from young leaves of *Ws-2* (A); *Ws-2* expressing ARC6$_{ZBD}$-EYFP (B); *arc6-1* (C); and *arc6-1* expressing ARC6$_{ZBD}$-EYFP (D). Exposure times in all four panels are identical. (E) α-YFP immunoblot (upper panel) and Ponceau stain (lower panel) from *arc6* lines expressing pCAMBIA-ZBD-derived ARC6$_{ZBD}$-EYFP. Molecular weight marker (lane 1); protein extracts from three different transformant lines (lanes 2-4); *Ws-2* (lane 5); and *arc6-1* (lane 6). Extracts in lane 3 were taken from the transgenic individual shown in panel D. Scale bar = 5 μm.

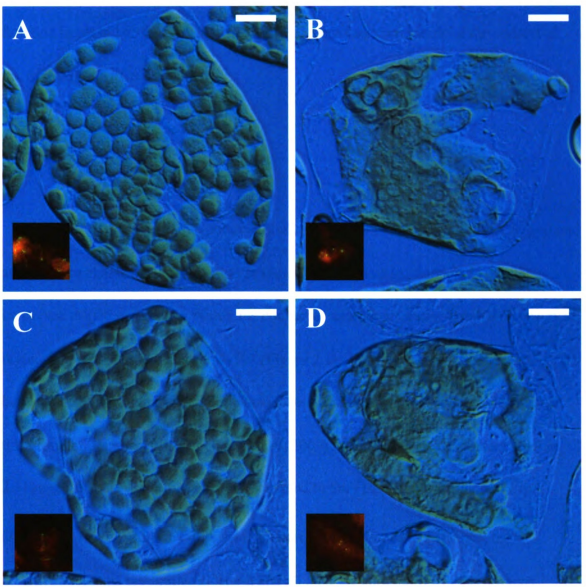

Figure 2.13. Chloroplast and FtsZ morphology in *ARC6$_{ZBD}$-EYFP* expressing lines. Terminal chloroplast phenotypes in expanded leaf cells from *Ws-2* (A); *arc6-1* (B); *Ws-2* expressing plastid-targeted ARC6$_{ZBD}$-EYFP (C); *arc6-1* expressing plastid-targeted ARC6$_{ZBD}$-EYFP (D). Insets in each panel show FtsZ2-1 localization (green) in chloroplasts (red) within young leaves of the same lines shown in the large panels of A-D. The inset micrographs are the same scale as the large panels. Scale bars = 10 μm.

Taken together, from these results I conclude that either $ARC6_{ZBD}$ does not function in plastid division or that $ARC6_{ZBD}$ cannot function outside of the context of the full-length ARC6 protein.

Discussion

Here I have identified a putative FtsZ2-binding domain of ARC6 ($ARC6_{ZBD}$) and attempted to characterize its function *in vivo*. From our results, I conclude that the conserved $ARC6_{ZBD}$ resides within the context of a larger stromally-localized conserved region, occupying amino acids 351-503 (Figure 2.1). Multiple sequence alignment between ARC6 orthologs of higher plants reveals that $ARC6_{ZBD}$ is conserved amongst this group of organisms (Glynn, Yang, *et al.* 2009) and our pairwise alignment (Figure 2.3) suggests that $ARC6_{ZBD}$ is distantly related to the FtsZ binding domain of ZipA ($ZipA_{ZBD}$) (Figure 2.3). Despite these differences in amino acid sequence, these divergent domains are similar in length and all bind the core motif of FtsZ proteins. Using sequence alignment software, a homology-modeling platform, and side-chain positioning algorithms, we generated a model of $ARC6_{ZBD}$ (Figure 2.4) based on the known crystal structure of $ZipA_{ZBD}$ (Mosyak, Zhang, *et al.* 2000). This model highlights the potential importance of at least 3 key residues within $ARC6_{ZBD}$ and provides a testable foundation for structural analysis of $ARC6_{ZBD}$ by crystallographic or

NMR-based methods. Similar to the ZipA-FtsZ interaction (Moreira, Fernandes, *et al.* 2006), site-directed mutagenesis of a conserved phenylalanine residue abolished $ARC6_{ZBD}$ interaction with FtsZ2 in yeast two-hybrid assays (Figure 2.6), suggesting that this residue of $ARC6_{ZBD}$ might secure the core motif of FtsZ2 within a hydrophobic pocket. To test this, I generated a site-directed mutation in recombinant $ARC6_{ZBD}$ protein, $ARC6_{ZBD(F442D)}$, that I predicted to be unable to bind FtsZ2 in pulldowns, but I could not validate two-hybrid results using this assay; both $ARC6_{ZBD}$ and $ARC6_{ZBD\ (F442D)}$ had similar affinity for FtsZ2 *in vitro* (Figure 2.7). This result conflicts with the structural model and hypothesis that $ARC6_{F442}$ is critical for ARC6 function *in vivo*. To determine the functional relevance of $ARC6_{F442}$ and to assess which of the interaction assays was yielding valid information, I made a construct that represents an $ARC6_{ZBD}$ loss-of-function mutant ($ARC6_{pro}$-$ARC6_{F442D}$), based on the two-hybrid results (Figure 2.6). $ARC6_{pro}$-$ARC6_{F442D}$ was able to fully complement an *arc6* T-DNA insertion mutation (Figure 2.9) and FtsZ ring morphology in complemented individuals was indistinguishable from that in wild type chloroplasts (Figure 2.10), suggesting that the two-hybrid tests between $ARC6_{ZBD\ (F442D)}$ and FtsZ2 may have yielded false negative results. However, the *in vivo* functionality of the $ARC6_{F442D}$ protein is completely consistent with our pulldown assays that show that $ARC6_{ZBD\ (F442D)}$ is able to coprecipitate the C-terminus of FtsZ2 (Figure 2.7). It is possible that site-directed

substitutions of ARC6 residues I362 and R422 (both individually and in combination with $ARC6_{F442}$ substitutions) might provide sufficient evidence to validate our structural model (Figure 2.4) if those substitutions significantly disrupt ARC6-FtsZ2 interaction both *in vitro* and *in vivo*. However, in the absence of these additional site-directed mutants and the lack of an experimentally-determined structure for $ARC6_{ZBD}$, our ZipA-based structural model should be considered preliminary.

While our work highlights a prospective functional domain within ARC6, the conflicting conclusions drawn from the two-hybrid and *in vivo* results does lead to some uncertainty regarding the structure and function of $ARC6_{ZBD}$. Our results here reiterate the previous findings of our colleagues (Maple, Aldridge, *et al.* 2005), who used yeast two-hybrid assays to identify the ARC6-FtsZ2 interaction. They claimed to confirm this two-hybrid result using BiFC between ARC6 and FtsZ2 in tobacco (Maple, Aldridge, *et al.* 2005, Maple and Moller 2006), using C-terminal BiFC tags for ARC6 and FtsZ2 to reconstitute YFP *in vivo*. The bitopic topology of ARC6 (Vitha, Froehlich, *et al.* 2003) and the stromal localization of FtsZ2 (McAndrew, Froehlich, *et al.* 2001) conflict with this result, because the C-terminus of ARC6 has been shown to reside within the intermembrane space; BiFC-based assays will not work across membrane boundaries, as the two halves of the fluorescent moiety cannot physically interact when separated by a membrane barrier (Bracha-Drori, Keren, *et al.* 2004). In this case, the topology of ARC6 in these assays was probably not the native topology (perhaps due to overexpression or the presence of the C-terminal tag) or some FtsZ2 was present within the intermembrane

space. We also analyzed a mutation in FtsZ2 ($FtsZ2_{F466A}$) that was shown to impede ARC6-FtsZ2 interaction by yeast two-hybrid (Maple, Aldridge, *et al.* 2005), but in our hands $FtsZ2_{F466A}$ was coprecipitated by $ARC6_{ZBD}$ (Figure 2.7), suggesting that previous results (Maple, Aldridge, *et al.* 2005) might be two-hybrid false negatives. Strangely, expression of plastid-targeted $ARC6_{ZBD}$ did not modify the chloroplast morphology of FtsZ immunolocalization patterns of wild type or *arc6* mutants (Figure 2.13), leading us to question the overall relevance of $ARC6_{ZBD}$ in the process of chloroplast division; perhaps the FtsZ2-binding domain of ARC6 has some other function *in vivo*. Further confounding the issue, another group has demonstrated that interaction between the cyanobacterial ortholog of ARC6 (Ftn2) and FtsZ requires the J-domain of Ftn2, suggesting that an interaction between ARC6 and FtsZ2 might occur directly through the putative J-domain of ARC6 — or may be indirect, perhaps occuring through a DnaK-like chaperone (Mazouni, Domain, *et al.* 2004). When combined with our negative results obtained using a prospective $ARC6_{ZBD}$ gain-of-function mutant (Figure 2.13), we believe more work is needed to show that $ARC6_{ZBD}$ directly binds FtsZ2 within the stroma and to identify the functional implications of that interaction, if it does, in fact, occur.

Regardless, the overall effect of ARC6 upon Z-ring formation is profound, as *arc6* mutants possess serious defects in Z-ring assembly (Vitha, Froehlich, *et al.* 2003). While recent data clearly provide evidence of a complex containing ARC6 and FtsZ2, it

does not resolve the issue of direct ARC6-FtsZ2 interaction (McAndrew, Olson, *et al.* 2008). Moreover, preliminary data suggest that ARC6 can immunoprecipitate FtsZ2-1, even in the absence of the FtsZ2-binding domain of ARC6, indicating that there may an indirect linkage between these two proteins *in vivo* (Figure 2.14). Further work will be required to sort out the details of the molecular arrangement within the ARC6-FtsZ2 complex and determine how ARC6 might modulate Z-ring formation *in vivo*.

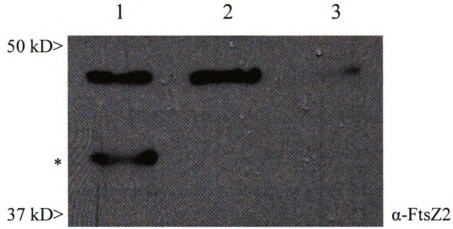

Figure 2.14. ARC6$_{AA\ 1\text{-}509}$-GFP and ARC6$_{AA\ 1\text{-}331}$-GFP can immunoprecipitate FtsZ2. Immunoblot showing eluates from immunoprecipitation reactions using an immobilized anti-GFP antibody incubated with whole-cell extracts from *arc6* lines expressing a *35S-ARC6$_{AA\ 1\text{-}509}$-GFP* transgene (lane 1); *35S-ARC6$_{AA\ 1\text{-}331}$-GFP* (lane 2); or *35S-GFP* (lane 3). Blot was probed with an FtsZ2-1-specific antibody. The molecular weight of processed FtsZ2-1 is predicted by ChloroP (Emanuelsson, Nielsen, *et al.* 1999) to be ~45.3 kD (upper band). The lower molecular weight band in lane 1 (*) is probably derived from FtsZ2-1, due to the high specificity of the FtsZ2-1 antibody. It is not clear if this lower molecular weight band represents an FtsZ2-1 breakdown product or if ARC6$_{AA\ 1\text{-}509}$ might somehow affect FtsZ2-1 translation or processing *in vivo*.

Materials and Methods

Yeast two-hybrid vector construction and reporter assays.

All GAL4-ARC6 fusion-encoding plasmids were generated by PCR using primers that correspond to the desired coding sequences, with NdeI and XmaI adapters to facilitate directional ligation. PCR products were generated using the ARC6 cDNA clone available from ABRC, cut, and ligated into NdeI-XmaI digested pGADT7 (Clontech). All GAL4-ARC6 site-directed mutants (F442A, F442D, F442K, and F442Y) were generated by SOE-PCR (Heckman and Pease 2007) and cloned into pGADT7 as described above. All GAL4-FtsZ2 fusions were generated using primers corresponding to the desired coding sequence, with NdeI and BamHI adapters to facilitate the desired directional ligation of the insert. PCR products were generated from an FtsZ2-1 clone, cut, and ligated into NdeI-BamHI digested pGBKT7 (Clontech). All clones were sequenced prior to transforming yeast to ensure that the inserts were free of coding errors. *HIS3* reporter assays were performed in line with the manufacturer's (Clontech) recommendations using an established protocol (Maple, Aldridge, *et al.* 2005). Relative interaction strengths were computed by comparison of the ratio of yeast growth on SD/-ULTH media to yeast growth on SD/-ULT media after ~48 hours of growth at 28-30 ^{o}C.

Multiple sequence alignments and homology model.

Multiple sequence alignments were performed using ClustalW (EBI) using the BLOSUM62 substitution matrix with all other parameters set to their default values. The alignment was formatted using ESPript (http://espript.ibcp.fr/ESPript/cgi-

bin/ESPript.cgi/). For homology modeling, a pairwise alignment between $ZipA_{AA\ 185\text{-}328}$ and $ARC6_{AA\ 351\text{-}503}$ was performed and used to make a primary homology model from PDB file 1F47 (Mosyak, Zhang, *et al.* 2000) (http://www.pdb.org/) with all identical residues from the ZipA-ARC6 pairwise alignment as anchor points using a homology modeling program (http://proteins.msu.edu/). We performed refinement of side chain positions using SCWRL3 (http://dunbrack.fccc.edu/SCWRL3.php). Cartoon representations of the homology model were generated using Pymol (http://pymol.sourceforge.net/).

In vitro pulldowns.

All fusion proteins were expressed in *E. coli* BL21 (DE3) Codon Plus cells (Stratagene) induced at OD_{600} = 0.8 with 2 mM IPTG for 2 hours at 37°C. 750 µg of protein from induced cell extract was used for each bait/prey combination. Pulldowns between His_8-$ARC6_{ZBD}$ and GST-$FtsZ2\text{-}1_{CT}$ or His_8-$ARC6_{ZBD\ (F442D)}$ and GST-$FtsZ2\text{-}1_{CT}$ were performed as in previous experiments (Glynn, Froehlich, *et al.* 2008), except Triton X-100 was present at 0.1% in all wash buffers to prevent clumping of the sepharose beads.

Analysis of chloroplast morphology and number.

Light micrographs depicting chloroplast morphology in expanded leaf cells were taken using DIC Optics on a Leica DMI3000B Inverted Microscope outfitted with a Leica DFC320 Camera. Samples for chloroplast morphology and quantitation were

prepared and analyzed using established protocols (Pyke and Leech 1991). Fluorescence micrographs were taken using a Leica DMRA2 using Q-Capture Camera Control Software (Q-Imaging) and the filter sets indicated (Leica) as previously described (Vitha, Froehlich, *et al.* 2003). Image analysis and RGB composites were made using ImageJ v1.37 (NIH) (Bearer 2003).

FtsZ immunofluorescence

Tissue preparation, fixation, and immunofluorescence analysis were carried out as described previously (Miyagishima, Froehlich, *et al.* 2006, Vitha, Froehlich, *et al.* 2003, Vitha, McAndrew, *et al.* 2001).

Construction of pCAMBIA-ZBD.

pCAMBIA-ZBD was constructed from pCAMBIA-1302 (Hajdukiewicz, Svab, *et al.* 1994) by removing an NcoI-BstEII fragment from pCAMBIA-1302 and performing a four-point ligation (see Figure 2.11) with: (1) NcoI/ApaI digested PCR products amplified from a RecA cDNA using primers TTTTTTCCATGGATTCACAGCTAGTCT TGTC and TTTTTTGGGCCCTCTGTCATCGAATTCAGAACTGATT; (2) ApaI/BglII digested PCR products amplified from an ARC6 cDNA using primers TTTTTTGGG CCCGAAGTTGCACTTGCTCTTGTGGCT and TTTTTTAGATCTAACTACCTCCA CTCTTTCCAAGT; and (3) BglII/BstEII digested PCR products amplified from an EYFP-coding plasmid (F. Brandizzi Laboratory, MSU DOE-PRL) using primers TTTTTTAGATCTCCCGGGATGGTGAGCAAGGGCGAGGAGCT and TTTTTTGGTTACCTTACTTGTACAGCTCGTCCATGCC. Following transformation,

clones were selected on LB plates containing kanamycin (50 μg/mL) and screened by PCR. Clones containing an insert of the expected size were miniprepped (Promega) and sequence-verified at the MSU-RTSF facility before transforming *Agrobacterium* and *Arabidopsis*.

Fluorescence microscopic analysis of $ARC6_{ZBD}$-EYFP expressing plants.

Fluorescence micrographs were taken using a Leica DMRA2 using Q-Capture Camera Control Software (Q-Imaging) and the filter sets indicated (Leica) as previously described (Vitha, Froehlich, *et al.* 2003). Image analysis and RGB composites were made using ImageJ v1.37 (NIH) (Bearer 2003).

Protein extraction and immunoblotting.

Proteins from whole-cell extracts (equivalent to ~2-3 mg liquid-nitrogen ground tissue) were prepared as previously described (Wiegel and Glazebrook 2002), separated by SDS-PAGE, and transferred to nitrocellulose. Anti-GFP Immunoblots were performed using Clontech JL-8 anti-GFP monoclonal antibody at 1:1000 in 5% nonfat dry milk in TBS-T, pH 7.4 (Miyagishima, Froehlich, *et al.* 2006).

Transgenic plant material and microscopic analyses.

Untagged *ARC6* and $ARC6_{F442D}$ transgenes were generated by SOE-PCR and ligated into a modified pCAMBIA-1302 (Hajdukiewicz, Svab, *et al.* 1994) using NcoI and BstEII; BstEII removes the mGFP tag from pCAMBIA-1302 and retains the *NOS* terminator sequence. All clones were sequence-verified and transformed into

Agrobacterium tumefaciens GV3101 by electroporation. Overnight cultures of *Agrobacterium* carrying the T-DNA construct were used to transform *Ws-2* and *arc6-1* plants (Clough and Bent 1998). Following hygromycin selection, putative transgenic T_1 plants were screened for transgene expression by Western blotting of whole-cell extracts from various individuals and probing with an anti-GFP antibody (BD-Biosciences JL-8 monoclonal antibody) and by fluorescence microscopy. Immunofluorescence analysis was carried out as previously described (Vitha, McAndrew, *et al.* 2001) using expanded leaf tissue.

Immunoprecipitation from Homogenized Arabidopsis Leaf Tissue.

Transgenic *arc6* plants expressing GFP-fusion proteins were grown in soil for 21 days. Approximately 150-200 mg of tissue was collected from whole leaves and ground to a powder in liquid nitrogen. Four (4) volumes of IP buffer (25 mM Tris, pH 7.50; 150 mM NaCl; 0.1% Triton X-100; and 1X Roche Protease Inhibitor Cocktail) were added to the frozen powder and gently mixed by pipeting on ice over several minutes. The homogenized slurry was spun through a Miracloth filter to remove large debris. 2.5 µg of BD Living Colors *A.v.* Peptide Antibody (Cat. # 632377) was gently mixed into to each filtered extract and incubated overnight. 50 µL of pre-conditioned protein A beads were added to each sample and incubated for 2 hours at room temperature with gentle mixing by inversion every 10 minutes. The beads were washed 4 times with 500 µL of IP buffer (each wash was 500 µL). Immune complexes were eluted from the beads using 100 µL of elution buffer (0.2M Glycine, pH 1.85) and then buffered with 20 µL of 1 M Tris, pH 8.5. 29 µL of 6X SDS-PAGE buffer were added to each buffered eluate, samples were

vortexed briefly, boiled, collected by centrifugation, and loaded for SDS-PAGE analysis. Transfer to nitrocellulose was performed using a GENIE Blotting Apparatus (Idea Scientific) according to the manufacturer's recommendations. Rabbit-derived anti-FtsZ2-1 antibodies were used as described previously (Vitha, McAndrew, *et al.* 2001).

Acknowledgements

I thank Bill Wedemeyer for instruction and assistance in generating the structural model of $ARC6_{ZBD}$ and for all the excellent structural analysis tools he has freely provided at his website.

Chapter 3

ARC6 Binds and Positions PDV2 During Plastid Fission in *Arabidopsis*.

Abstract

Chloroplasts arose from a free-living cyanobacterial endosymbiont and divide by binary fission. Division involves the assembly and constriction of the endosymbiont-derived, tubulin-like FtsZ ring on the stromal surface of the inner envelope membrane and the host-derived, dynamin-like ARC5 ring on the cytosolic surface of the outer envelope membrane. Despite identification of many proteins required for plastid division, the factors coordinating the internal and external division machineries are unknown. Here, we provide evidence that this coordination is mediated in *Arabidopsis* by an interaction between ARC6, an FtsZ-assembly factor spanning the inner envelope membrane, and PDV2, an ARC5 recruitment factor spanning the outer envelope membrane. ARC6 and PDV2 interact via their C-terminal domains within the intermembrane space of the chloroplast, consistent with their *in vivo* topologies. ARC6 acts upstream of PDV2 to localize PDV2 (and hence ARC5) to the division site. We present a model whereby ARC6 relays information on stromal FtsZ ring positioning through PDV2 to the chloroplast surface to specify the site of ARC5 recruitment. Because orthologs of ARC6 occur in land plants, green algae, and cyanobacteria whereas PDV2 occurs only in land plants, the connection between ARC6 and PDV2 represents the evolution of a plant-specific adaptation to coordinate the assembly and activity of the endosymbiont- and host-derived plastid division components.

Introduction

The plastids of plant cells arose from cyanobacteria by endosymbiosis and, like cyanobacteria, replicate by binary fission. This process requires the coordinated action of at least two macromolecular complexes, one composed of the tubulin-like cytoskeletal protein FtsZ and the other of the dynamin-related protein ARC5. These proteins assemble into mid-plastid ring-shaped structures on opposite sides of the two envelope membranes to mediate constriction of the organelle (Osteryoung and Nunnari 2003). Two nuclear-encoded plant FtsZ paralogs, FtsZ1 and FtsZ2, function within the chloroplast stroma. Both evolved from cyanobacterial FtsZ and have unique non-overlapping functions in plastid division (Schmitz, Glynn, *et al.* 2009, Stokes and Osteryoung 2003, Vitha, McAndrew, *et al.* 2001). Analogous to bacterial FtsZ (Bi and Lutkenhaus 1991, Goehring and Beckwith 2005), the plastidic FtsZ proteins assemble at an early step in division to form an equatorial ring, the Z-ring, on the stromal face of the inner envelope membrane (Vitha, McAndrew, *et al.* 2001). In bacteria and presumably in plastids, the Z-ring probably functions both as a scaffold for the recruitment of other division proteins and to provide the contractile force needed to pull the membrane inward during constriction (Ghosh and Sain 2008, Lan, Daniels, *et al.* 2009, Lan, Wolgemuth, *et al.* 2007, Osawa, Anderson, *et al.* 2008).

In contrast, ARC5 was a post-symbiotic adaptation of the eukaryotic host and functions outside the chloroplast (Gao, Kadirjan-Kalbach, *et al.* 2003, Miyagishima, Nishida, *et al.* 2003a). ARC5 is a member of the dynamin family of membrane

"pinchases," best characterized for their roles in endocytic vesicle-budding and mitochondrial fission in eukaryotes (Cerveny, Tamura, *et al.* 2007, Hoppins, Lackner, *et al.* 2007, McNiven 1998, Shaw and Nunnari 2002, Ungewickell and Hinrichsen 2007), though dynamins probably evolved from a prokaryotic ancestor (Low and Lowe 2006). ARC5 in *Arabidopsis* and its orthologue in the red alga *Cyaniodioschyzon merolae* function late in chloroplast division by assembling on the cytosolic surface of the outer envelope membrane, where they are thought to perform the final squeeze that aids partitioning of the two daughter organelles (Yoshida, Kuroiwa, *et al.* 2006). Both plastidic FtsZ and ARC5 arose early in the evolution of the chloroplast division machinery, as indicated by their occurrence in both the red and green lineages (Miyagishima 2005).

The assembly of the division machinery appears to occur in a linear order, with FtsZ assembly initiating the process and ARC5/dynamin mediating late-stage organelle constriction (Miyagishima, Nishida, *et al.* 2003a). However, the mechanisms coordinating these evolutionarily and compartmentally disparate events are unknown. Previous studies in *Arabidopsis* have implicated three plastid division proteins as candidate mediators of this coordination: ARC6, PDV1 and PDV2 (Miyagishima, Froehlich, *et al.* 2006, Vitha, Froehlich, *et al.* 2003). ARC6 is a bitopic transmembrane protein of the inner envelope membrane with its larger N-terminus protruding into the stroma and smaller C-terminus residing within the intermembrane space (IMS). ARC6 was inherited from the cyanobacterial endosymbiont and is localized to the mid-plastid division site. The chloroplasts of *Arabidopsis arc6* mutants, which have one or two

oversized chloroplasts per mesophyll cell (Pyke, Rutherford, *et al.* 1994), possess many short disorganized filaments, while *ARC6* overexpressors have excessively long FtsZ filaments (Vitha, Froehlich, *et al.* 2003). These findings, along with the fact that the N-terminus of ARC6 interacts specifically with FtsZ2 (Maple, Aldridge, *et al.* 2005), suggest that ARC6 facilitates FtsZ polymer assembly and regulates FtsZ ring dynamics through FtsZ2 (Maple, Aldridge, *et al.* 2005, McAndrew, Olson, *et al.* 2008, Vitha, Froehlich, *et al.* 2003). The function of the C-terminal IMS region of ARC6 is unknown, but it probably has a significant role in plastid replication based on the breadth of its conservation amongst plants, algae, and cyanobacteria (Glynn, Yang, *et al.* 2009, Vitha, Froehlich, *et al.* 2003). ARC6 is one of the few division proteins known to connect the stromal Z-ring to the IMS, suggesting it could play a critical role in coordinating the inner and outer subassemblies of the division machinery.

PDV1 and PDV2 are paralogous plastid division proteins identified based on the similarity of the *pdv1* mutant phenotype to that of *arc5*; in both mutants, chloroplasts are enlarged and dumbbell-shaped (Miyagishima, Froehlich, *et al.* 2006). PDV1 is a bitopic outer envelope membrane protein that localizes to the division site, with its N-terminus residing in the cytosol and its C-terminus extending into the IMS. *PDV1* and *PDV2* have partially redundant functions in recruiting ARC5 to the chloroplast. In *pdv1* and *pdv2* mutants, ARC5 localizes to the central constriction in the enlarged chloroplasts, but *pdv1 pdv2* double mutants fail to recruit ARC5 to the chloroplast (Miyagishima, Froehlich, *et al.* 2006). PDV1 and PDV2 proteins share some degree of sequence similarity and domain arrangement, though the localization and detailed function of PDV2 was not

determined previously (Miyagishima, Froehlich, *et al.* 2006). PDV1 and PDV2 have no significant sequence similarity to known proteins and are only evident in land plants, suggesting they represent an evolutionary development in the transition of plants to terrestrial habitats.

Here, we show that PDV2 has a localization and topology similar to that of PDV1 in the outer envelope membrane. However, PDV2 family members have a unique C-terminal extension in their IMS regions that is lacking in PDV1 proteins. We further show that the C-terminal IMS regions of ARC6 and PDV2 interact and that this interaction is required for full chloroplast division activity in *Arabidopsis*. Using genetic analysis, we demonstrate that ARC6 is required for positioning of PDV2 and ARC5, but PDV2 is not required for mid-plastid localization of ARC6. Our results establish a physical link across the envelope membranes at the division site and suggest that ARC6, through interaction with PDV2 within the IMS, coordinates Z-ring and ARC5 activity to synchronize scission of the envelope membranes. We present a model for the physical arrangement and interaction of these proteins in the chloroplast membranes.

Results

PDV2 localization and topology are similar to PDV1.

The similarity of PDV2 to PDV1 in sequence and domain arrangement (Figure 3.1) suggested its localization and topology might be similar to those of PDV1

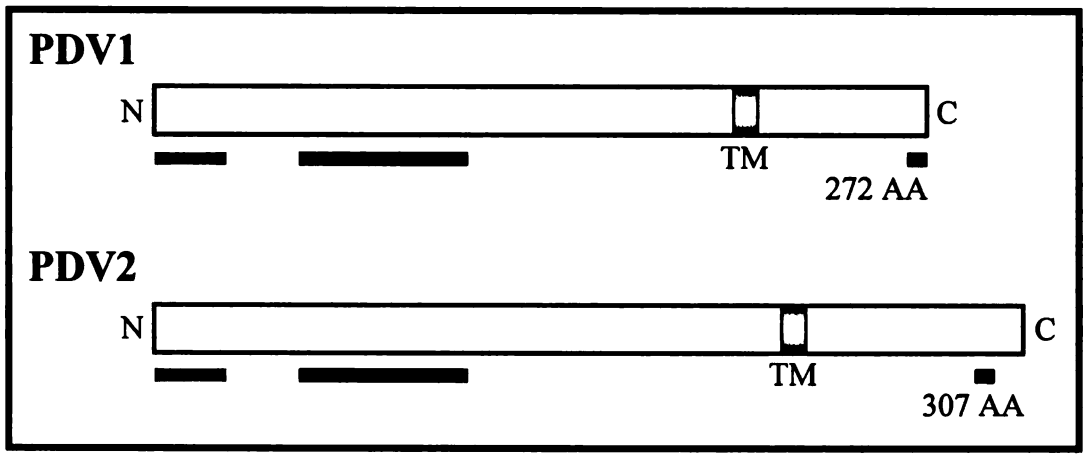

Figure 3.1. Schematic comparison of PDV1 and PDV2 proteins from *Arabidopsis*. Shaded lines below each protein indicate regions of high similarity between the two PDV paralogs. A comprehensive alignment and phylogeny of these two proteins that includes sequences from several plant species is published elsewhere (Glynn, Froehlich, *et al.* 2008). Amino terminus (N); carboxy terminus (C); transmembrane domain (TM); and amino acids (AA).

(Miyagishima, Froehlich, *et al.* 2006). To verify localization of PDV2 *in vivo*, we expressed a YFP-PDV2 fusion protein from the PDV2 promoter (*$PDV2_{pro}$-YFP-PDV2*) in wild-type *Arabidopsis* plants. Similar to PDV1, the YFP signal localized to the mid-plastid in young emerging leaves. The YFP-PDV2 signal appeared as a continuous ring (Figure 3.2) rather than as a series of equatorial spots as was previously noted for PDV1 (Miyagishima, Froehlich, *et al.* 2006). When YFP-PDV2 was co-expressed with an ARC6-CFP fusion protein, their fluorescence signals colocalized within mesophyll chloroplasts (Figure 3.3). To confirm the predicted topology of PDV2, we carried out *in vitro* chloroplast import and protease-protection assays (Figure 3.4, left panel). Following incubation with isolated pea chloroplasts, radiolabled PDV2 produced by *in vitro* translation (Figure 3.4, lane 1) was retained in the membrane fraction (Figure 3.4, lane 2). The protein was susceptible to degradation by thermolysin, consistent with outer envelope localization. However, a portion of PDV2, roughly corresponding to the size of the predicted C-terminal IMS domain (predicted size ~10 kD), was protected from thermolysin degradation (Figure 3.4, lane 4, arrowhead), but was sensitive to trypsin, which can penetrate the outer envelope membrane and enter the IMS (Jackson, Froehlich, *et al.* 1998, Tranel, Froehlich, *et al.* 1995). ARC6, used as an inner envelope control in these experiments (Figure 3.4, right panel), behaved as shown previously (Vitha, Froehlich, *et al.* 2003). Protease protection assays on wild type *Arabidopsis* chloroplasts using antibody-based detection of PDV2 showed the N-terminus of PDV2 to be susceptible to thermolysin and trypsin treatment (Ronit Knopf and Zach Adam, personal communication), consistent with *in vitro* assays. These results confirm that PDV2, like PDV1, is a mid-plastid-localized, bitopic protein of the chloroplast outer envelope

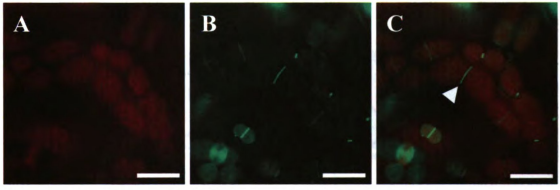

Figure 3.2. Localization of YFP-PDV2 in *Arabidopsis*. A *PDV2*$_{pro}$*-YFP-PDV2* transgene was expressed in *Arabidopsis Col-0* plants and tissue samples from emerging leaves were examined for YFP-PDV2 localization. Signals observed from: Chlorophyll autofluorescence (Chl, panel A); (B) Yellow Fluorescent Protein (YFP, panel B); and merged image (panel C). YFP-PDV2 was typically observed as a continuous ring at the mid-chloroplast (arrowhead, panel C). Scale bars = 10 μm.

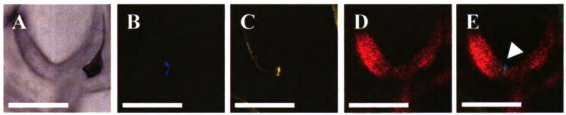

Figure 3.3. Colocalization of ARC6-CFP and YFP-PDV2 in *Arabidopsis*. ARC6-CFP and YFP-PDV2 were expressed under control of their native promoters and examined in emerging leaves. Micrographs from brightfield (A); CFP channel (B); YFP channel (C); chlorophyll autofluorescence (D); and a merged image from CFP, YFP and chlorophyll channels (E). Scale bar = 10 μm.

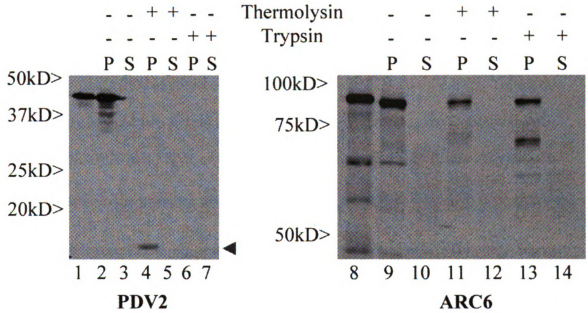

Figure 3.4. PDV2 fractionation and topology using isolated pea chloroplasts. *In vitro* chloroplast import of [^{3}H-leucine]-labeled PDV2 or [^{35}S-methionine]-labeled ARC6 and fractionation of chloroplasts following protease treatment and hypotonic lysis. *In vitro*-transcribed translation products are shown for PDV2 (lane 1) and ARC6 (lane 8). Pellet (P) fractions are shown in lanes 2, 4, 6, 9, 11, and 13. Supernatant (S) fractions are shown in lanes 3, 5, 7, 10, 12, and 14. The arrowhead points to the IMS-localized C-terminal fragment of PDV2 that remains following thermolysin treatment.

membrane, with its N-terminus exposed to the cytosol and its smaller C-terminus residing within the intermembrane space.

The IMS Regions of ARC6 and PDV2 Interact.

The localization of PDV1 (Miyagishima, Froehlich, *et al.* 2006), PDV2 (Figure 3.2) and ARC6 (Vitha, Froehlich, *et al.* 2003) at the division site, along with their demonstrated topological orientations in the envelope membranes, suggested the possibility that ARC6 might interact with PDV1 and/or PDV2 in the IMS. To test this, we carried out yeast two-hybrid assays with constructs encoding the C-terminal IMS domains of ARC6 and PDV1 or PDV2. PDV2 strongly and specifically activated the *HIS3* reporter in the presence of $ARC6_{IMS}$ (Figure 3.5A, third row). No interaction was observed between $PDV1_{IMS}$ and $ARC6_{IMS}$ using two hybrid assays (Figure 3.5A, first row). To confirm the $ARC6_{IMS}$-$PDV2_{IMS}$ interaction we carried out a pulldown assay (Figure 3.5B). A GST-$PDV2_{IMS}$ fusion protein was precipitated from crude *E. coli* extracts with Ni-Sepharose beads coated with His-$ARC6_{IMS}$ (Figure 3.5B, lane 1), but no pulldown of GST-$PDV2_{IMS}$ was observed using uncoated Ni-Sepharose beads (Figure 3.5B, lane 2). These results support an ARC6-PDV2 protein-protein interaction within the intermembrane space of dividing chloroplasts.

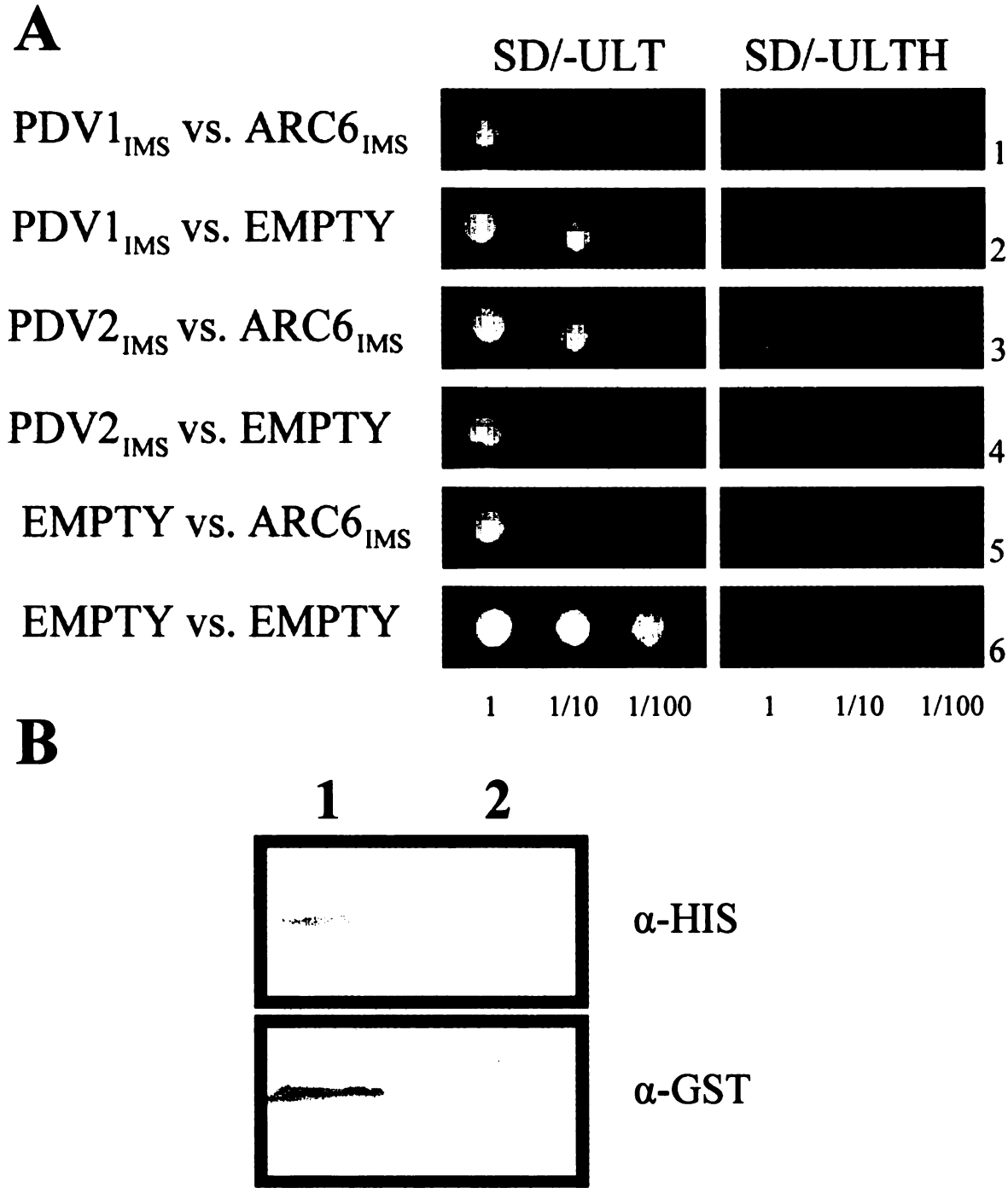

Figure 3.5. The IMS-localized regions of PDV2 and ARC6 interact. (A) Two-hybrid assays between PDV proteins and ARC6. The IMS regions of the proteins indicated were fused to either GAL4-BD (PDV1 and PDV2) or GAL4-AD (ARC6). Dilutions (indicated at bottom of panel) from a starting culture of OD_{600} = 1.0 are spotted onto synthetic dropout (SD) media containing (left) or lacking (right) histidine. (B) Immunoblots of eluates from pulldown assays using either immobilized His_8-$ARC6_{IMS}$ treated with GST-$PDV2_{IMS}$ (lane 1) or naked beads treated with GST-$PDV2_{IMS}$ (lane 2).

PDV2 Family Members Possess a Unique C-Terminal Domain.

To gain insight into features that distinguish the C-terminal IMS domains of PDV1 and PDV2 from one another and therefore might be important for the PDV2-specific interaction with ARC6, we generated sequence alignments between PDV1 and PDV2 proteins from several land plants using a CLUSTALW identity scoring matrix (Larkin, Blackshields, *et al.* 2007) to clearly define PDV1-specific and PDV2-specific features (Glynn, Froehlich, *et al.* 2008); the C-terminal segment of this alignment is shown in Figure 3.6. As noted previously, all PDV1 proteins have a conserved C-terminal glycine residue, and mutation of this residue impairs PDV1 function in *Arabidopsis* (Miyagishima, Froehlich, *et al.* 2006). A conserved terminal glycine is also found in all known PDV2 family members (Figure 3.6, red asterisk). However, PDV2 (294 ± 15 amino acids, n = 7 sequences) proteins are generally longer than PDV1 (261 ± 14 amino acids, n = 7 sequences); PDV2 family members harbor a conserved extension at their C-terminus. This C-terminal extension, which includes the terminal glycine residue, might be involved in mediating PDV2 interaction with ARC6.

The Conserved Terminal Glycine of PDV2 is Required for Interaction with ARC6 and PDV2 Function in vivo.

To ask whether the C-terminal glycine of PDV2 is important for the ARC6-PDV2 interaction, we engineered a missense mutation in the $PDV2_{IMS}$ two-hybrid plasmid that changes this glycine to aspartate. Following co-transformation of the resulting construct ($PDV2_{IMS(G307D)}$) and $ARC6_{IMS}$ into yeast and selection for both plasmids, we observed no growth on medium lacking histidine (Figure 3.7, row 3), indicating that

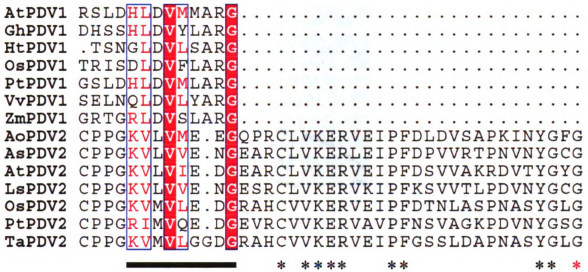

Figure 3.6. Alignment of C-termini of PDV1 and PDV2 family members. All PDV2 proteins possess a C-terminal extension that is not found in PDV1 family members. The dark line (bottom) corresponds to to the C-terminal conserved segment shown in Figure 3.1. Boxed regions indicate similarity between PDV1 and PDV2; boxed shaded regions represent identity between PDV1 and PDV2. Asterisks (*) represent identical residues within the C-terminal extension of all PDV2 family members. The red asterisk highlights the conserved glycine that ends all PDV2 proteins. *Arabidopsis thaliana* PDV1 (AtPDV1), *Gossypium hirsutum* PDV1 (GhPDV1), *Helianthus tuberosus* PDV1 (HtPDV1), *Oryza sativa* PDV1 (OsPDV1), *Populus trichocarpa* PDV1 (PtPDV1), *Vitis vinifera* PDV1 (VvPDV1), *Zea mays PDV1* (ZmPDV1), *Arabidopsis thaliana* PDV2 (AtPDV2), *Asparagus officinalis* PDV2 (AoPDV2), *Aquilegia species* PDV2 (AsPDV2), *Lactuca sativa* PDV2 (LsPDV2), *Oryza sativa* PDV2 (OsPDV2), *Populus trichocarpa* PDV2 (PtPDV2), and *Triticum aestivum* PDV2 (TaPDV2). The full-length alignment is published elsewhere (Glynn, Froehlich, *et al.* 2008).

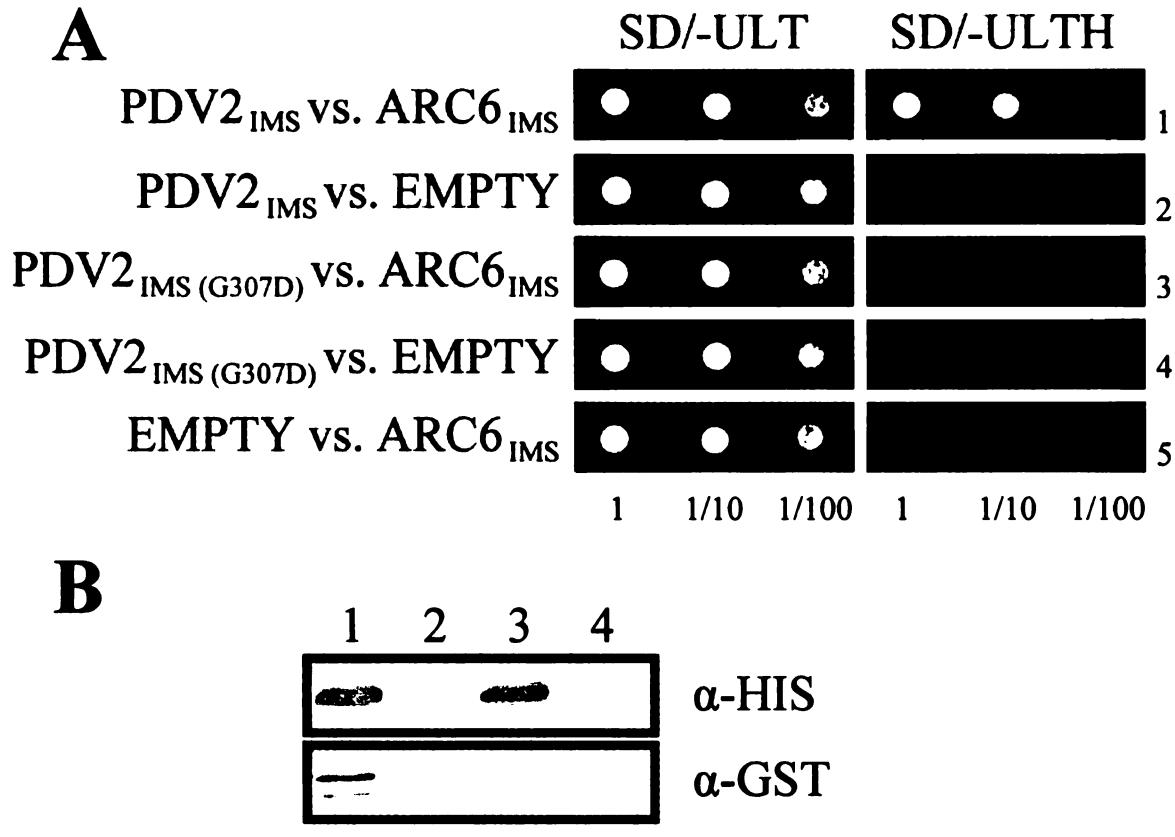

Figure 3.7. The terminal glycine of PDV2 is important for interaction with ARC6. (A) Yeast two-hybrid assays between PDV2 proteins and ARC6. The IMS regions of the proteins indicated were fused to either GAL4-BD (PDV2 and $PDV2_{G307D}$) or GAL4-AD (ARC6). Dilutions (indicated at bottom of panel) from a starting culture of OD_{600} = 1.0 are spotted onto synthetic dropout (SD) media containing (left) or lacking (right) histidine. (B) Immunoblots of eluates from pulldown assays using either immobilized His_8-$ARC6_{IMS}$ treated with GST-$PDV2_{IMS}$ (lane 1); naked beads treated with GST-$PDV2_{IMS}$ (lane 2); His_8-$ARC6_{IMS}$ treated with GST-$PDV2_{IMS\ (G307D)}$ (lane 3); or naked beads treated with GST-$PDV2_{IMS\ (G307D)}$ (lane 4).

mutation of the terminal glycine in PDV2 diminishes the $ARC6_{IMS}$-$PDV2_{IMS}$ interaction in yeast. We incorporated the same mutation into $PDV2_{IMS}$ to create GST-$PDV2_{IMS\ (G307D)}$ for use in pulldown assays and observed that the terminal G307D mutation reduced the affinity of $PDV2_{IMS}$ for $ARC6_{IMS}$ (Figure 3.7B, lane 3). The higher affinity of GST-$PDV2_{IMS}$ for His-$ARC6_{IMS}$ (Figure 3.7B, lane 1) was not a result of biased prey input into the reaction, as equal amounts of total protein were applied to each pulldown reaction and we verified equal input levels of GST-$PDV2_{IMS}$ and GST-$PDV2_{IMS\ (G307D)}$ in the reactions by anti-GST immunoblotting. We conclude from these results that the IMS-localized domains of ARC6 and PDV2 interact with each other and that the conserved terminal glycine of PDV2 is an important mediator of this interaction.

To assess the potential importance of the terminal missense mutation *in vivo*, we compared the relative abilities of $PDV2_{pro}$-*PDV2* and $PDV2_{pro}$-$PDV2_{G307D}$ transgenes encoding full-length proteins to complement *pdv2-1*, a line carrying a T-DNA insertion allele of *PDV2* in which chloroplasts are frequently constricted and larger than in wild type (Miyagishima, Froehlich, *et al.* 2006) (Figure 3.8B). We reasoned that a PDV2 protein incapable of interaction with ARC6 would not be able to rescue the *pdv2* phenotype. The wild type transgene fully complemented *pdv2* in the majority of selected lines (Figure 3.8C). In contrast, no modification of the *pdv2* phenotype occurred in lines transformed with $PDV2_{pro}$-$PDV2_{G307D}$ (Figure 3.8D) despite evidence based on

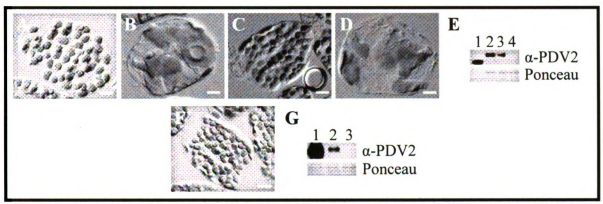

Figure 3.8. ***PDV2$_{G307D}$* is a loss-of function allele.** Chloroplast phenotypes from leaf cells of *Col-0* (A); *pdv2-1* (B); *pdv2-1* transformed with a *PDV2$_{pro}$-PDV2* transgene (C); and *pdv2-1* transformed with a *PDV2$_{pro}$-PDV2$_{G307D}$* transgene (D). An anti-PDV2 immunoblot is shown in (E) carrying recombinant PDV2 (lane 1); extract from plant expressing a *PDV2$_{pro}$-PDV2$_{G307D}$* transgene (lane 2); extract from *Col-0* (lane 3); and extract from *pdv2-1* (lane 4). Chloroplast phenotype from a plant expressing *35S-PDV2* (F). An immunoblot showing PDV2 expression levels is shown in (G) carrying extract from plant expressing *35S-PDV2* (lane 1); extract from *Col-0* (lane 2); and extract from *pdv2-1* (lane 3). Scale bars = 10 μm.

immunoblotting with a PDV2-specific antibody that $PDV2_{G307D}$ protein levels were equivalent to or greater than PDV2 levels in wild type (Figure 3.8E). Lack of complementation by $PDV2_{pro}$-$PDV2_{G307D}$ was not a consequence of overexpression, as overexpression of *PDV2* does not impede chloroplast division, but rather accelerates this process (Figure 3.8F-G) (Okazaki, Kabeya, *et al.* 2009).

To determine if the defect in $PDV2_{G307D}$ might be due to mislocalization or perhaps a loss in activity, we examined YFP-$PDV2_{G307D}$ localization in *Arabidopsis*. The YFP-$PDV2_{G307D}$ signal was observed as scattered fragments around the periphery of the chloroplast in the wild type background (Figure 3.9B), in contrast to the rings observed in YFP-PDV2 expressing lines (Figure 3.9A), likely due to the inability of $PDV2_{G307D}$ and ARC6 to interact with each other. While YFP-PDV2 was observed forming rings in the wild type plastids, we did not observe YFP-$PDV2_{G307D}$ associated with chloroplasts in the *pdv2-1* background, but it did localize to small epidermal plastids (compare Figures 3.9C-D); the significance of this observation is not yet clear.

We conclude that PDV2 interaction with ARC6 occurs through the conserved C-terminal glycine of PDV2 and that the major role of this protein-protein interaction is to localize PDV2 to the division site *in vivo*; loss of this interaction leads to a defect in plastid division that is reminiscent of *pdv2* and *arc5* loss-of-function mutants.

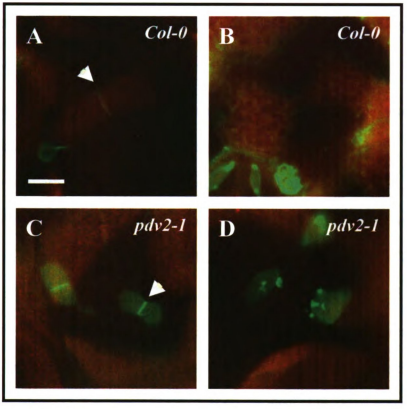

Figure 3.9. PDV2$_{G307D}$ localization in *Arabidopsis*. YFP-PDV2 and YFP-PDV2$_{G307D}$ were expressed under control of the native promoter in both *Col-0* (A, B) and *pdv2-1* (C, D) backgrounds. YFP-PDV2 localizes to continuous rings around plastids (arrowheads) in *Col-0* (A) and *pdv2-1* mutants (C). In contrast, YFP-PDV2$_{G307D}$ fails to localize to organized structures in either background (B, D). Scale in all images is identical. Scale bar = 2 μm.

The Complete IMS Region of ARC6 is not required for ARC6 Localization, but is required for Chloroplast Division Activity.

To determine if the C-terminal IMS-localized region of ARC6 is required for plastid division *in vivo*, as suggested by its interaction with PDV2, we expressed a truncated ARC6-GFP fusion protein lacking much of its C-terminal IMS region ($ARC6_{\Delta IMS}$-GFP) in the *arc6* background under control of the *ARC6* promoter (Figure 3.10A). A full-length ARC6-GFP protein, shown previously to complement the severe plastid division defect in *arc6* mutants (Vitha, Froehlich, *et al.* 2003, Vitha, Holzenburg, *et al.* 2005) was expressed as a control. Accumulation of the fusion proteins in transgenic individuals was confirmed by immunoblotting (Figure 3.10B), and chloroplast morphology was examined in fixed leaf cells. Similar to previous results (Vitha, Froehlich, *et al.* 2003), we observed rescue of the *arc6* phenotype (Figure 3.10D) in lines expressing full-length ARC6-GFP (Figure 3.10B), as indicated by the increase in number and decrease in size of the chloroplasts (25-60 cps/cell; Figure 3.10D) relative to those in the parent *arc6* plants (1-2 cps/cell; Figure 3.10C). A change in chloroplast number and size was also observed in lines expressing $ARC6_{\Delta IMS}$-GFP, but the extent to which the *arc6* mutation was complemented (4-10 cps/cell; Figure 3.10E) was less than observed in *arc6* lines expressing the full-length ARC6-GFP control. These results show that the IMS region of ARC6 is required for full plastid division activity *in vivo*. Moreover, *arc6* plants expressing either $ARC6_{pro}$-$ARC6_{\Delta IMS}$-*GFP* or $35S_{pro}$-$ARC6_{\Delta IMS}$-*GFP* exhibit GFP rings localized to sites of constriction in chloroplasts of young leaves (Figure 3.10F), indicating that the C-terminal region of ARC6 is not required for mid-plastid

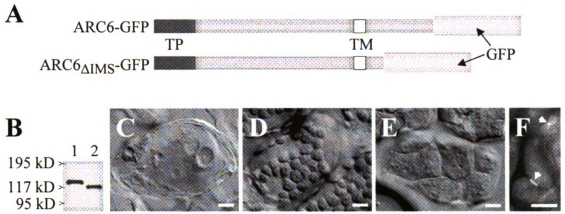

Figure 3.10. ARC6$_{\Delta IMS}$-GFP is partially functional and localizes to the division site. (A) Schematic of GFP fusions used for analysis. (B) Anti-YFP immunoblot showing expression of ARC6-GFP (lane 1) and ARC6$_{\Delta IMS}$-GFP (lane 2) in *Arabidopsis arc6* mutants. Chloroplast phenotypes of *arc6* (C); *arc6* complemented with *ARC6$_{pro}$-ARC6-GFP* (D); and *arc6* expressing *ARC6$_{pro}$-ARC6$_{\Delta IMS}$-GFP* (E) in leaf mesophyll cells. Localization of ARC6-GFP (arrowheads) in young leaf cells of an *arc6* mutant expressing *35S-ARC6$_{\Delta IMS}$-GFP* (F) suggests that only stromal components are required to localize ARC6 to sites of constriction. *ARC6$_{\Delta IMS}$-GFP* encodes amino acids 1-682 of ARC6 fused to GFP. Transit peptide (TP); transmembrane domain (TM); green fluorescent protein (GFP); kilodaltons (kD). Scale bars = 10 μm.

localization of ARC6 or for constriction of the plastid during division.

ARC6 acts upstream of PDV2 and is required for PDV2 activity.

Because $ARC6_{\Delta IMS}$-GFP localizes to constrictions at the plastid division site and *arc6* plants expressing $ARC6_{\Delta IMS}$-GFP phenocopy the terminal chloroplast number within mesophyll cells of *pdv2* mutants (Miyagishima, Froehlich, *et al.* 2006), we hypothesized that *ARC6* acts upstream of *PDV2*. Because the phenotypes of *arc6* (1-2 chloroplasts/cell) and *pdv2* (4-8 chloroplasts/cell) mutants are easily distinguished by microscopic observation (compare Figures 3.11C-D), we made reciprocal crosses to test for epistasis between the *arc6-1* and *pdv2-1* alleles. F_1 individuals were allowed to self-fertilize, and the chloroplast phenotypes in leaves of 105 F_2 individuals were examined (Figure 3.11). We observed all the expected phenotypes in the F_2 population, including individuals with wild-type (WT) phenotypes, intermediate (INT) phenotypes consistent with *PDV2/pdv2* heterozygotes (Miyagishima, Froehlich, *et al.* 2006), *pdv2*-like phenotypes, and *arc6*-like phenotypes in a ~9:3:4 ratio. Genotype analysis of individuals with *arc6*-like phenotypes confirmed the presence of *arc6 pdv2* double mutants within the F_2 population (Figure 3.11F). The overrepresentation of *arc6* mutant phenotypes in the F_2 population and the *arc6*-like phenotype of the *arc6 pdv2* double mutant are consistent with *ARC6* acting upstream of *PDV2*.

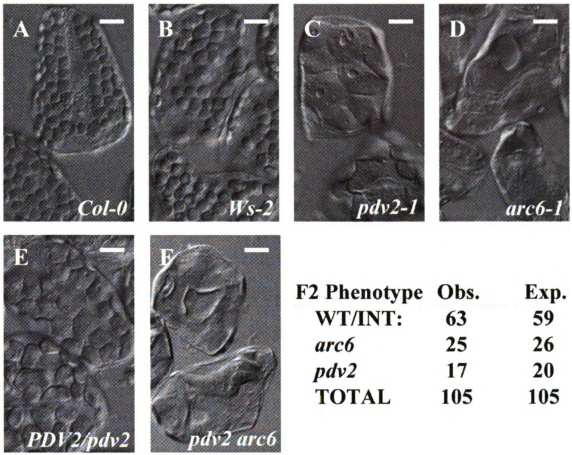

F2 Phenotype	Obs.	Exp.
WT/INT:	63	59
arc6	25	26
pdv2	17	20
TOTAL	105	105

Figure 3.11. ARC6 acts upstream of PDV2. Chloroplast phenotypes of *Col-0* (A); *Ws-2* (B); *pdv2-1* (C); *arc6-1* (D); *PDV2/pdv2* heterozygotes (E); and *pdv2 arc6* double mutants. Phenotypic distribution amongst an F_2 population originating from *arc6-1* x *pdv2-1* crosses (G) with observed (Obs.) phenotypes and expected (Exp.) values for *ARC6* acting upstream of *PDV2* ($\chi^2 \cong 0.7$; d.f. = 2; $P \geq 0.9$). Scale bars = 10 μm.

Interestingly, overexpression of *PDV2* alone leads to an increase in the rate of chloroplast division (Figure 3.8) (Okazaki, Kabeya, *et al.* 2009). Because *ARC6* acts upstream of *PDV2*, we suspected that PDV2 function might be fully dependent upon the presence of ARC6. To test this, we introduced a T-DNA carrying $35S_{pro}$-*PDV2* into the *arc6* mutant to ask whether overexpression of *PDV2* would abrogate the *arc6* phenotype. Following selection, we assayed T_1 individuals for PDV2 protein levels by immunoblotting and identified multiple lines with elevated PDV2 levels (Figure 3.12, lower right). In none of these *PDV2*-overexpressing lines did we observe significant modification of the *arc6* phenotype (Figure 3.12, upper right); mesophyll cells from all *PDV2*-overexpressors still contained only 1-2 oversized chloroplasts (Figure 3.12, lower left). This result indicates that *ARC6* is required for PDV2 function *in vivo*. Moreover, overexpression of *PDV2* in *pdv1* mutants (J.M. Glynn and K.W. Osteryoung, unpublished) does not bypass the division defect in the pdv1 background, consistent with non-overlapping functions for PDV2 and PDV1.

ARC6 is Required for Equatorial Positioning of PDV2, PDV1, and ARC5.

We showed that *ARC6* acts upstream of *PDV2* (Figure 3.11 and Figure 3.12) and that ARC6 is probably responsible for positioning PDV2 at the division site by binding the C-terminus of PDV2 (Figure 3.7, Figure 3.8, and Figure 3.9). To confirm this prediction, we introduced a transgene carrying $PDV2_{pro}$-*YFP-PDV2* into *Col-0* and into an *arc6* T-DNA insertion mutant (SAIL_693_G04) and examined YFP localization in young leaves

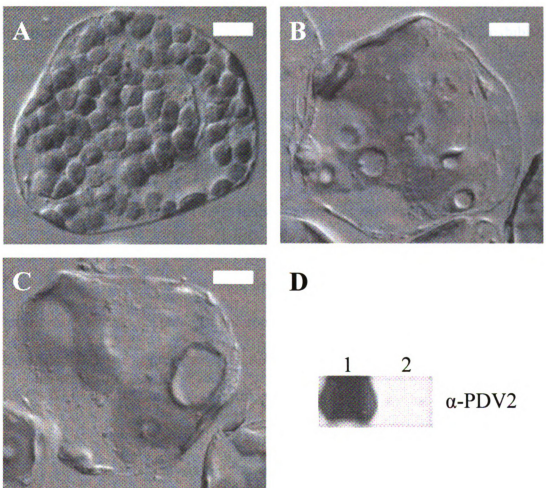

Figure 3.12. Overexpression of *PDV2* does not abrogate the *arc6* phenotype. Chloroplast phenotypes within leaf mesophyll cells of *Ws-2* (A); *arc6-1* (B); and *arc6-1* expressing a $35S_{pro}$-*PDV2* transgene (C). An anti-PDV2 immunoblot (D) demonstrating relative PDV2 in the *PDV2* overexpressor shown in panel C and the *arc6* mutant shown in panel B. Scale bar = 10 μm.

of T_1 individuals. In the wild type background, we observed equatorial rings of YFP-PDV2 in 34% of chloroplasts (Figure 3.13A; n = 200 chloroplasts from 20 independent T_1 individuals). In contrast, *arc6* lines expressing YFP-PDV2 exhibited diffuse YFP localization around the periphery of the chloroplasts, but no YFP-PDV2 rings were observed (Figure 3.13B; n = 200 chloroplasts from 16 T_1 individuals); this result is consistent with the diffuse localization of the dysfunctional YFP-PDV2$_{G307D}$ fusion around plastids (Figure 3.9). In the converse experiment, we examined ARC6-GFP localization in wild-type and *pdv2* backgrounds (Figure 3.14). In both cases, ARC6-GFP was observed in equatorial rings, indicating that PDV2 does not influence ARC6 localization, even in the enlarged chloroplasts of a *pdv2* mutant. We conclude that PDV2 is targeted to the outer envelope in an ARC6-independent manner, but absolutely requires ARC6 for its localization to the division site.

To extend this analysis and further elucidate the role of ARC6 in mediating dynamin recruitment through PDV1-PDV2, we examined GFP-ARC5 localization in wild-type cells and *arc6* mutants (Figure 3.15). In young wild-type leaf cells, GFP-ARC5 was frequently observed in a punctate pattern around the division site (Figure 3.15A). In contrast, we observed GFP-ARC5 in patches within the *arc6* mutant that do not appear to be associated with chloroplasts (Figure 3.15B), similar to reported GFP-ARC5 localization in the *pdv1 pdv2* double mutant; these patches are probably cytosolic (Miyagishima, Froehlich, *et al.* 2006). Because GFP-ARC5 still localizes to the division site in a *pdv2* mutant (Miyagishima, Froehlich, *et al.* 2006), we conclude that ARC6

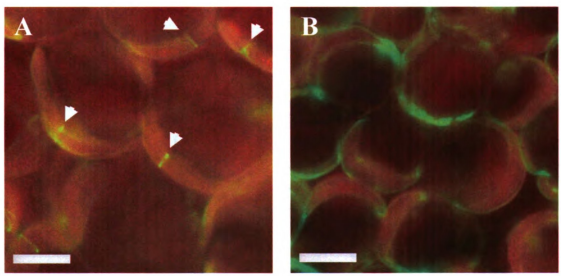

Figure 3.13. *ARC6* is required for localization of YFP-PDV2 to the division site. *YFP-PDV2* was expressed from its native promoter in *Col-0* (A) and *arc6* mutant (B) backgrounds. YFP-PDV2 localizes to central rings within chloroplasts of wild type cells (arrowheads), but exhibits diffuse localization around the periphery of the plastid in *arc6* mutants. A merged image showing signals from both chlorophyll autfluorescence (red) and YFP (green) is shown in each panel. Scale bars = 10 μm.

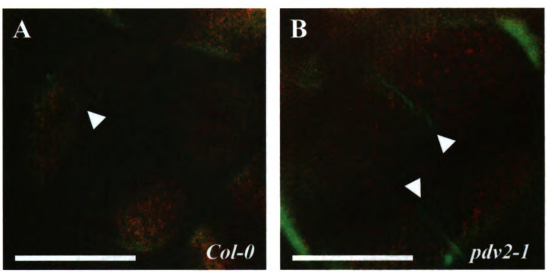

Figure 3.14. PDV2 is not required for ARC6-GFP localization to equatorial rings. *ARC6-GFP* was expressed from its native promoter in *Col-0* (A) and *pdv2-1* (B) backgrounds. ARC6-GFP localizes to central rings within chloroplasts of wild type cells and in *pdv2* mutants (arrowheads), suggesting that equatorial localization of ARC6 is independent of PDV2. A merged image showing signals from both chlorophyll autfluorescence (red) and GFP (green) is shown in each panel. Scale bars = 10 μm.

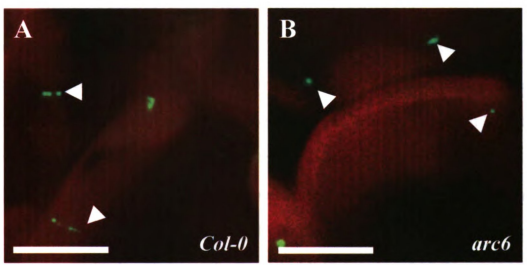

Figure 3.15. *ARC6* is required for localization of GFP-ARC5 to the division site. *GFP-ARC5* was expressed from its native promoter in *Col-0* (A) and *arc6* (B) backgrounds. GFP-ARC5 localizes to punctate equatorial rings within chloroplasts of wild type cells (arrowheads), but is only observed in cytosolic patches in *arc6* mutants. A merged image showing signals from both chlorophyll autofluorescence (red) and GFP (green) is shown in each panel. Scale bars = 10 μm.

mediates dynamin recruitment and patterning through both PDV1 and PDV2, but ARC6 might mediate PDV1 function through an indirect mechanism.

Discussion

Chloroplast division involves the consecutive formation and simultaneous constriction of the mid-plastid FtsZ and ARC5/dynamin rings on the stromal and cytosolic surfaces of the envelope membranes, respectively. ARC6 in the inner envelope interacts directly with FtsZ via its stroma-exposed N-terminus and is required for Z-ring assembly, while PDV2, shown here to be a transmembrane protein of the outer envelope, mediates recruitment of ARC5 to the chloroplast surface (Miyagishima, Froehlich, *et al.* 2006). Our results place ARC6 upstream of PDV2 in the chloroplast division process, identify a physical linkage between the C-terminal IMS domains of ARC6 and PDV2, and reveal that an important function of the $ARC6_{IMS}$ domain is to direct localization of PDV2 to the division site. These findings establish a role for a key inner envelope plastid division protein in organizing components of the outer envelope division machinery. Because the N-terminus of ARC6 plays a role in organizing FtsZ in the stroma (Vitha, Froehlich, *et al.* 2003), these findings suggest a model wherein interaction between ARC6 and PDV2 within the IMS links FtsZ assembly with ARC5 recruitment, thereby promoting coordinated fission of the two envelope membranes.

Our observation that ARC6 is able to localize to the division site without most of its IMS region (Figure 3.10) suggests that stromal factors are sufficient to organize ARC6

at the division site within chloroplasts. The FtsZ ring is a strong candidate as an ARC6-positioning factor. The recently demonstrated ability of recombinant *E. coli* FtsZ to assemble into rings inside liposomes suggests that FtsZ proteins, which are highly conserved across kingdoms, require only a membrane tether and GTP for ring assembly *in vivo* (Osawa, Anderson, *et al.* 2008). We suspect that self-assembly of the Z-ring at the mid-plastid division site in plants, controlled by MinD, MinE, and ARC3 (Colletti, Tattersall, *et al.* 2000, Fujiwara, Nakamura, *et al.* 2004, Glynn, Miyagishima, *et al.* 2007, Maple, Chua, *et al.* 2002, Maple, Vojta, *et al.* 2007, Reddy, Dinkins, *et al.* 2002), establishes the site for ARC6 localization, presumably via direct interaction with FtsZ2 (Maple, Aldridge, *et al.* 2005). From our results, we propose that ARC6 transduces positional information from the Z-ring to the intermembrane space and serves as a landmark for PDV2 and hence ARC5 recruitment (Figure 3.13 and Figure 3.15). Consistent with this idea, *arc6* plants expressing $ARC6_{\Delta IMS}$-GFP (Figure 3.10) phenocopy *pdv2* and *arc5* mutants with respect to their terminal chloroplast number (Gao, Kadirjan-Kalbach, *et al.* 2003, Miyagishima, Froehlich, *et al.* 2006), suggesting an equivalent block in the division process in these three genetically-distinct backgrounds. Additionally, the loss of PDV2 or ARC5 results in the formation of multiple adjacent Z-rings on the stromal side of the inner envelope membrane (Miyagishima, Froehlich, *et al.* 2006), suggesting that information may also travel inward from the outer envelope to the Z-ring through ARC6. Based on the collective data, we hypothesize that ARC6 has evolved to organize and coordinate the stromal and cytosolic components of the division complex and relay information about the status of each across compartment boundaries.

Though PDV1 and PDV2 have partially redundant functions in ARC5 recruitment (Miyagishima, Froehlich, *et al.* 2006), their exact functional relationship in the plastid division complex is not yet clear. In contrast to ARC6 and PDV2, we did not detect an interaction between ARC6 and PDV1 in yeast two-hybrid assays (Figure 3.5, row 1). However, preliminary experiments suggest that ARC6 is required for localization of PDV1 (Glynn, Froehlich, *et al.* 2008) and PDV2 (Figure 3.13), consistent with the lack of ARC5 recruitment in an *arc6* mutant (Figure 3.15). We do not believe that ARC6-dependent localization of PDV1 is mediated directly by PDV2 because GFP-ARC5 localizes properly in *pdv2-1* (Miyagishima, Froehlich, *et al.* 2006). Rather, the data suggest that another factor acts downstream of ARC6 to position PDV1, and hence ARC5, independently of PDV2 (Glynn, Yang, *et al.* 2009). In this context, it is interesting to note that PDV1 and PDV2 appear to have distinct localization patterns at the division site: GFP-PDV1 is observed in discrete foci (Miyagishima, Froehlich, *et al.* 2006, Yang, Glynn, *et al.* 2008), whereas YFP-PDV2 is observed as a continuous ring (Figure 3.2). The significance of this difference is unknown, but it could reflect their interactions with different positioning factors — ARC6 in the case of PDV2 and another factor in the case of PDV1.

The PDV2-interacting IMS region of ARC6 is mostly conserved with the corresponding region of the ARC6 cyanobacterial ortholog Ftn2, yet PDV2 is not found in cyanobacteria or green algae. Sequence alignments suggest the presence of land-plant-specific motifs within the IMS region of ARC6 that may have evolved in parallel with the emergence of PDV1 and PDV2 in land plants (Glynn, Yang, *et al.* 2009). Ftn2 is

localized to the division site in cyanobacteria (Mazouni, Domain, *et al.* 2004) and presumably has a topology similar to that of ARC6 (i.e. its C-terminus protrudes into the cyanobacterial periplasm). This leads us to ask: did PDV2 replace a periplasmic component of the cyanobacterial divisome (for example, a component of the peptidoglycan synthesis machinery or the murein layer itself) or does the ARC6-PDV2 interaction represent a completely new plant-specific function for ARC6? Identification of the precise boundaries of the PDV2-binding domain of ARC6 and rigorous sequence comparisons of ARC6 and Ftn2 family members will likely provide further insight into the evolution and operation of the plastid division machinery in land plants.

Materials and Methods

Plant transformation vectors and analysis

ARC6-GFP and $ARC6_{\Delta IMS}$-*GFP* were cloned into pCAMBIA-1302 (Hajdukiewicz, Svab, *et al.* 1994) or a derivative of pCAMBIA-1302 containing the ARC6 promoter region (Vitha, Froehlich, *et al.* 2003) using NcoI-BglII sites for insertion. $PDV2_{pro}$-*YFP-PDV2* was generated by removing the *35S* promoter and *mGFP-His* DNA sequences from pCAMBIA-1302 and replacing them with a fragment carrying the *PDV2* promoter region and *EYFP* (Clontech) fused to the *PDV2* coding sequence. For ARC6-CFP, *ARC6* was cloned into a derivative of pCAMBIA-1302 containing the ARC6 promoter region (Vitha, Froehlich, *et al.* 2003) and ECFP coding sequence (Clontech). Lines expressing proteins from both $PDV2_{pro}$-*YFP-PDV2* and $ARC6_{pro}$-*ARC6-CFP* were generated by crossing independently transformed T_1 lines (with demonstrated transgene expression) and selecting progeny with both YFP and CFP expression by epifluorescence microscopy. $PDV2_{pro}$-*PDV2* and $PDV2_{pro}$-$PDV2_{G307D}$ were generated by PCR and cloned into a derivative of pCAMBIA-1302 that lacks the *35S* promoter and *mGFP* coding sequence. All plant transformations were performed as previously described (Clough and Bent 1998) using *Agrobacterium tumefaciens* GV3101. Selection of T_1 individuals was performed on MS containing hygromycin (20-25ug/mL).

Microscopy and Image Analysis

Light micrographs depicting chloroplast morphology in expanded leaf cells were taken using DIC Optics on a Leica DMI3000B Inverted Microscope outfitted with a Leica DFC320 Camera. Samples for chloroplast morphology and quantitation were prepared and analyzed using established protocols (Pyke and Leech 1991). Fluorescence micrographs were taken using a Leica DMRA2 using Q-Capture Camera Control Software (Q-Imaging) and the filter sets indicated (Leica) as previously described (Vitha, Froehlich, *et al.* 2003). Image analysis and RGB composites were made using ImageJ v1.37 (NIH) (Bearer 2003).

Two-Hybrid Analysis

Yeast strain AH109 (Clontech) was cultured and transformed as recommended by the manufacturer using standard Synthetic Dropout (SD) Media (Clontech) as indicated. $ARC6_{AA\ 637\text{-}801}$ was cloned into pGADT7 using NdeI-XmaI and $PDV2_{AA233\text{-}307}$ was cloned into pGBKT7 using NdeI-XmaI sites. $PDV2_{AA\ 233\text{-}307\ (G307D)}$ was generated by PCR-based mutagenesis and cloned into pGBKT7 using NdeI-XmaI sites.

Pulldown Assays

Recombinant His-ARC6 (encoding $ARC6_{AA\ 637\text{-}801}$ with an N-terminal 8X His-tag) was generated in pHIS8-3 (Salk Institute, La Jolla, CA) and expressed in BL21 (DE3) Codon Plus Cells (Stratagene). 2mM IPTG was applied to the cells at OD600 ~ 0.8 and incubated for 4h to generate the His-$ARC6_{IMS}$ fusion protein. Total protein was

extracted from the induced cells by sonication in Buffer A (1X TBS, 40mM imidazole, and 1 Roche EDTA-free protease inhibitor cocktail tablet #11836170001 per 100 mL Buffer A) and treatment of the sonicated material with 0.5% Triton X-100 for 30 minutes at room temperature. Following centrifugation at 18000 x g, the supernatant was collected and analyzed by Bradford assay. 750 μg of total protein was applied to 50 μL of Ni-Sepharose beads equilibrated in Buffer A (Ni-Sepharose 6 Fast Flow, GE Healthcare, Uppsala, Sweden). Beads were washed 4 times in Buffer A to enrich for His-$ARC6_{IMS}$. Negative controls (beads only) were simply washed in Buffer A following equilibration. Production of crude GST-PDV2 (encoding $PDV2_{AA\ 233\text{-}307}$ with an N-terminal GST tag) and GST-G307D (encoding GST-$PDV2_{AA\ 233\text{-}307(G307D)}$) was performed using the methods described above, except pGEX-4T-2 (GE Healthcare) was used as the parent vector for cloning and expression of recombinant PDV2 proteins. The cell extracts containing the GST fusions were prepared by sonication and treatment with Triton X-100 and then centrifuged to yield a crudely purified sample. Total protein was measured by Bradford assay and 750 μg of total protein was applied to the naked Ni-Sepharose beads or Ni-Sepharose beads coated with His-$ARC6_{IMS}$. Following a 2.5 h incubation on a rocking platform, the samples were washed several times with Buffer A and then eluted into 250 μL Buffer B (Buffer A containing 1M imidazole). Approximately 240 μL of eluate was recovered following a brief spin and total eluted material was precipitated in acetone and reconstituted in 6X sample buffer prior to SDS-PAGE. Approximately 12.5% of the eluted material was applied in each lane for separation on 15% SDS-Polyacrylamide gels. Separated proteins were transferred to

nitrocellulose (GE Water and Process Technologies) and blotted with anti-His (Pierce, #15165) or anti-GST (Sigma, #G-1417) antibodies as recommended by the manufacturer and detected by standard chemilluminescence methods using the manufacturer's HRP-based detection protocol (Pierce).

Immunoblotting of Plant Material

Proteins from whole-cell extracts (equivalent to ~2-3 mg liquid-nitrogen ground tissue) were prepared as previously described (Wiegel and Glazebrook 2002), separated by SDS-PAGE, and transferred to nitrocellulose. Anti-GFP Immunoblots were performed using Clontech JL-8 anti-GFP monoclonal antibody at 1:1000 in 5% nonfat dry milk in TBS-T, pH 7.4 (Miyagishima, Froehlich, *et al.* 2006). Anti-PDV2 Immunoblots were performed using 1 mg/mL Protein-A purified IgG's from New Zealand White rabbit sera (CRP, Inc.) directed against $PDV2_{AA1-212}$ at 1:15000 in 5% nonfat dry milk in TBS-T, pH7.4. Recombinant PDV2 (rPDV2) used to generate the immunogen used for anti-PDV2 antibody production was generated by cloning the coding sequence for $PDV2_{AA\ 1-212}$ into pHIS8-3 (Salk Institute, La Jolla, CA), expressing in BL21 (DE3) Codon Plus Cells (Stratagene), and purifying the resulting fusion protein from cell extracts using Ni Sepharose 6 Fast Flow (GE Healthcare, Uppsala, Sweden) according to the manufacturer's recommendations.

Phylogenetic Analysis

ClustalW2 was used to generate a multiple sequence alignment using PDV1 and PDV2 sequences from the organisms shown. Scoring was based on an identity (ID)

matrix with default settings: Protein Gap Open Penalty = 10.0; Protein Gap Extension Penalty = 0.2; Protein ENDGAP = -1; Protein GAPDIST = 4. Phylogeny of the PDV proteins (Glynn, Froehlich, *et al.* 2008) was calculated using MEGA 4 (Tamura, Dudley, *et al.* 2007).

Chloroplast Import, Fractionation, and Protease Protection Assays

The cDNA for PDV2 was subcloned into pDEST14 (Invitrogen) according to the manufacturer's protocol prior to in vitro transcription translation. *In vitro*-produced protein was generated using a Promega TnT® Coupled Reticulocyte Lysate System (Promega, Madison, WI) according to the manufacturer's protocol using 3H-labeled leucine (Perkin-Elmer) as a marker for PDV2 and ^{35}S-labeled methionine (Perkin-Elmer) to track ARC6 protein. Pea chloroplasts were isolated, and import assays and fractionation were performed according to previously established protocols (Jackson, Froehlich, *et al.* 1998, Tranel, Froehlich, *et al.* 1995, Vitha, Froehlich, *et al.* 2003).

Accession Number

Genbank accession numbers used for multiple sequence alignments and phylogenetic analysis are as follows: *Arabidopsis thaliana* PDV1 (AAM64850), *Gossypium hirsutum* PDV1 (DW511385 and DW512027), *Helianthus tuberosus* PDV1 (EL464676), *Oryza sativa* PDV1 (NP_001042451), *Populus trichocarpa* PDV1 (ABK94742), *Vitis vinifera* PDV1 (CAO69353), *Zea mays* PDV1 (EE161990 and DR959634), *Arabidopsis thaliana* PDV2 (NP_028242), *Asparagus officinalis* PDV2 (CV287540), *Aquilegia species* PDV2 (DT728284 and DT749563), *Lactuca sativa* PDV2

(DY983634), *Oryza sativa* PDV2 (EAZ02618), *Populus trichocarpa* PDV2 (a GENSCAN based prediction (http://genes.mit.edu/GENSCAN.html) of *Populus trichocarpa* Scaffold LG_IX 3439000-3442500), and *Triticum aestivum* PDV2 (CK209373 and BJ311269).

Acknowledgements

I thank John Froehlich and Shin-ya Miyagishima for their advice during the early phases of this project. I thank John Froehlich for persevering through the difficulties we experienced in translating PDV2 *in vitro* and for his outstanding work that helped us confirm PDV2 topology in isolated chloroplasts. I also thank Ronit Knopf and Zach Adam of The Hebrew University in Israel for sharing data with us on native PDV2 topology in *Arabidopsis* prior to publication.

Most of this chapter and the figures therein are reproduced from (Glynn, Froehlich, *et al.* 2008) (http://www.plantcell.org/) and is Copyright American Society of Plant Biologists. ASPB grants to authors whose work has been published in The Plant Cell the royalty-free right to reuse images, portions of an article, or full articles in any book, book chapter, or journal article of which the author is the author or editor.

Chapter 4

Characterization of the PDV2 Binding Domain of ARC6.

Abstract

During plastid division, interaction between ARC6 and PDV2 is required to position PDV2 within the outer envelope membrane. PDV2 helps recruit the dynamin-like protein, ARC5, to the division site. Previously, we showed that a carboxy-terminal glycine of PDV2 resides within a conserved motif and is required for ARC6-PDV2 interaction and PDV2 function *in vivo*. However, the specific domains or motifs within ARC6 that contribute to PDV2 binding were not determined. Here, we isolate the PDV2-binding domain of ARC6 ($ARC6_{PBD}$) and perform comparative sequence and structural analysis of both $PDV2_{IMS}$ and $ARC6_{PBD}$. Multiple sequence alignments and structural models highlight a plant-specific serine residue within $ARC6_{PBD}$ whose modification might be important for controlling operation of the chloroplast divisome *in vivo*. Further, we show that single amino acid substitution at this conserved serine within ARC6 affects its ability to bind $PDV2_{IMS}$, leads to *arc5*-like chloroplast morphology, and upregulates Z-ring assembly within the stroma. Our results hint at a post-translational modification of ARC6 that fine-tunes coordination of the stromal and cytosolic plastid division machineries in land plants.

Introduction

The posttranslational modification of proteins can have profound consequences on their function (Huber and Hardin 2004). Several types of modification can occur in plants, including ubiquitylation (Dreher and Callis 2007), acetylation (He and Amasino 2005), methylation (Fischer, Hofmann, *et al.* 2006), lipoylation (Ewald, Kolukisaoglu, *et al.* 2007), and phosphorylation (Christie 2007). Amongst these types of modification, the phosphorylation and dephosphorylation of serine residues is a common theme amongst proteins involved in signal-transduction (Braun and Walker 1996, Michniewicz, Zago, *et al.* 2007, Sokolovski, Hills, *et al.* 2005).

Chloroplast division in plants and algae is mediated by two ring-like structures, both of which are composed of polymer-forming GTPases: (1) the FtsZ ring (Z-ring) on the stromal face of the inner envelope (McAndrew, Froehlich, *et al.* 2001, Vitha, McAndrew, *et al.* 2001) and (2) the ARC5 ring on the cytosolic face of the outer envelope membrane (Gao, Kadirjan-Kalbach, *et al.* 2003). The Z-ring is made up of two non-redundant FtsZ proteins, FtsZ1 and FtsZ2 (McAndrew, Froehlich, *et al.* 2001, Schmitz, Glynn, *et al.* 2009, Vitha, McAndrew, *et al.* 2001). ARC5 is a dynamin-like protein involved in the final squeeze that separates the two daughter organelles during plastid division (Gao, Kadirjan-Kalbach, *et al.* 2003, Miyagishima, Nishida, *et al.* 2003a, Yoshida, Kuroiwa, *et al.* 2006). In land plants, ARC5 is recruited to the surface of the plastid by the outer envelope proteins PDV1 and PDV2. While either PDV1 or PDV2

can recruit ARC5 to the surface of the plastid, both PDV1 and PDV2 are required for full ARC5 contractile activity *in vivo* (Miyagishima, Froehlich, *et al.* 2006).

ARC6 is a bitopic chloroplast inner membrane protein (Vitha, Froehlich, *et al.* 2003) that coordinates operation of the internal and external plastid division complexes (Glynn, Froehlich, *et al.* 2008). In the stroma, the N-terminus of ARC6 facilitates FtsZ ring (Z-ring) assembly (Vitha, Froehlich, *et al.* 2003); the Z-ring is a critical component of the division apparatus, acting as a scaffold for other division proteins and providing nominal contractile force during division (Erickson 2009, Osawa, Anderson, *et al.* 2008). The intermembrane space (IMS)-localized portion of ARC6 binds PDV2 directly and positions PDV2 at the division site; PDV2 is required for full dynamin (ARC5) activity during the final steps of chloroplast division (Glynn, Froehlich, *et al.* 2008, Miyagishima, Froehlich, *et al.* 2006).

Here, we characterize the PDV2 binding domain of ARC6 ($ARC6_{PBD}$) and identify a predicted serine phosphoacceptor within this domain that may modulate ARC6 activity in response to serine modification. We show that $ARC6_{PBD}$ occupies amino acids 636-759 and that serine 744 might play a critical role in both mediating ARC6-PDV2 interaction within the IMS and in regulating Z-ring assembly within the stroma. $ARC6_{S744}$ and the surrounding motif is found only in ARC6 orthologs from embryophytes, the lineage in which PDV2 first emerged (Glynn, Froehlich, *et al.* 2008, Miyagishima, Froehlich, *et al.* 2006). Phosphomimetic mutation of serine 744 (S744E)

weakens ARC6-PDV2 interaction, leads to *arc5*-like plastid division defects, and perturbs stromal Z-ring structure *in vivo* – but strangely, this mutation does not affect localization of PDV1, PDV2, or ARC5 at the division site. Our results suggest that persistent phosphorylation of $ARC6_{S744}$ slows recruitment of PDV2, but leads to profound upregulation of Z-ring assembly within the stroma. We propose that phosphorylation of $ARC6_{S744}$ is a regulatory feature that retards the recruitment of PDV2 until the Z-ring is fully established and ready for envelope constriction to occur.

Results

The PDV2-Binding Domain of ARC6 ($ARC6_{PBD}$) Occupies Amino Acids 636-759.

We previously showed that the C-terminal IMS-localized regions of ARC6 and PDV2 interact; this interaction serves to position PDV2 within the outer envelope membrane during division (Glynn, Froehlich, *et al.* 2008). While we showed that this interaction required the conserved terminal glycine residue of PDV2, the discrete domain within ARC6 that binds PDV2 was not defined. To gain further understanding of ARC6 function and its constitutive domains, we generated a series of two-hybrid deletion constructs for $ARC6_{IMS}$ (Figure 4.1). Following yeast transformation and selection on appropriate medium, we assayed for growth on dropout medium containing or lacking histidine; growth on medium lacking histidine is consistent with the presence of a protein-protein interaction between bait and prey leading to activation of the *HIS3* reporter gene. Based on the growth ratios, we observed that full interaction

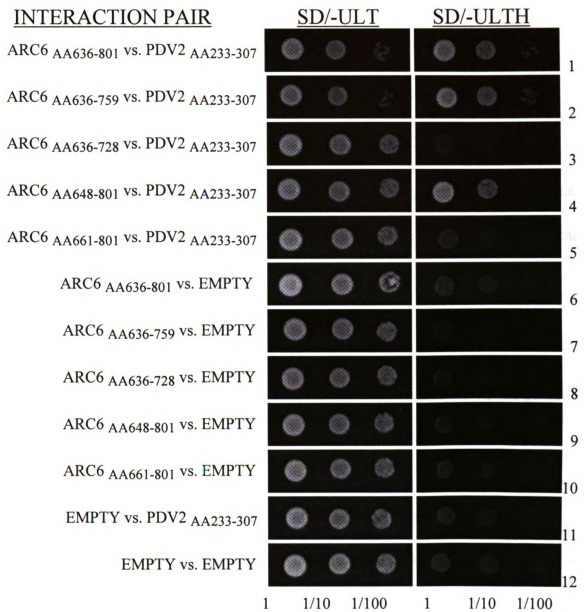

Figure 4.1. The PDV2 binding domain of ARC6 ($ARC6_{PBD}$) occupies AA 636-759. Yeast two-hybrid *HIS* reporter assays showing interaction strength between the IMS region of PDV2 (AA 233-307) and fragments of the IMS region of ARC6. Left hand column shows growth on synthetic dropout (SD) medium supplemented with histidine and right hand column shows growth on medium lacking histidine. For a schematic of the ARC6 protein, refer to Figure 1.4. Dilutions from a starting culture of $OD_{600} = 1.0$ are indicated at the bottom of panel. EMPTY = Empty vector control. AA = amino acids.

between ARC6 and PDV2 only requires $ARC6_{AA636-759}$ (Figure 4.1). We call this region of ARC6 the PDV2-binding domain ($ARC6_{PBD}$). The reporter activation of $ARC6_{PBD}$ is comparable to that observed for the full length C-terminus of ARC6, $ARC6_{AA636-801}$ (Figure 4.1). PDV2 does not interact with $ARC6_{AA661-801}$ nor $ARC6_{AA636-728}$, but weakly interacts with $ARC6_{AA648-801}$ (Figure 4.1), suggesting that the residues adjacent to the transmembrane domain of ARC6 are involved, but not critical for ARC6-PDV2 interaction.

Structural analysis of $ARC6_{PBD}$ and $PDV2_{IMS}$.

To gain additional insights into the interaction between ARC6-PDV2 and guide site-directed mutagenesis, we attempted to generate a model of $ARC6_{PBD}$. $ARC6_{PBD}$ was best-matched to the known structure of the Tim44 C-terminal domain (2CW9) using the meta-server at http://bioinfo.pl (Ginalski, Elofsson, *et al.* 2003). However, attempts to model $ARC6_{PDB}$ onto the structure of 2CW9 were unsuccessful, yielding several gaps between residues in the main chain of $ARC6_{PBD}$ (data not shown), suggesting that this is probably not a valid structural comparison. From this, we conclude that $ARC6_{PBD}$ probably has a structure unique from any of the structures currently present within the Protein Data Bank (http://www.pdb.org/).

We also attempted to generate a homology model for $PDV2_{IMS}$, hoping that it might reveal insights into both PDV2 and ARC6 function. Using the meta-server at http://bioinfo.pl/, we determined that the best structural match for $PDV2_{IMS}$ is 2J6Z (1W53), the N-terminal domain of a phosphoserine phosphatase that is involved in stress response in *Bacillus subtilis* and other gram-positive bacteria (Delumeau, Dutta, *et al.* 2004, Hardwick, Pane-Farre, *et al.* 2007). We made a pairwise comparison between $RsbU_{NT}$ and $PDV2_{IMS}$ (Figure 4.2) and used this alignment to generate a homology model of $PDV2_{IMS}$, using identical residues as anchor points for the $PDV2_{IMS}$ model.

The $PDV2_{IMS}$ sequence was highly similar to $RsbU_{NT}$ and was well-fit to 2J6Z (Figure 4.3, inset), suggesting that these two proteins might have similar functions. The N-terminus of RsbU is required for binding the RsbT stress response serine kinase (Dutta and Lewis 2003, Kang, Vijay, *et al.* 1998, Yang, Kang, *et al.* 1996), but $RsbU_{NT}$ does not appear to have kinase or phosphatase activity itself— this activity is thought to be exclusive to the C-terminal domain of RsbU (Delumeau, Dutta, *et al.* 2004, Kang, Vijay, *et al.* 1998). In this case, the C-terminus of ARC6 might be analogous to RsbT— perhaps even possessing a kinase or phosphatase activity itself. From this rudimentary structural analysis, we hypothesize that PDV2 may have a structure akin to a known protein phosphatase or may influence the activity of its binding partner through a simple protein-protein interaction, analogous to the RsbU-RsbT signal transduction cascade in

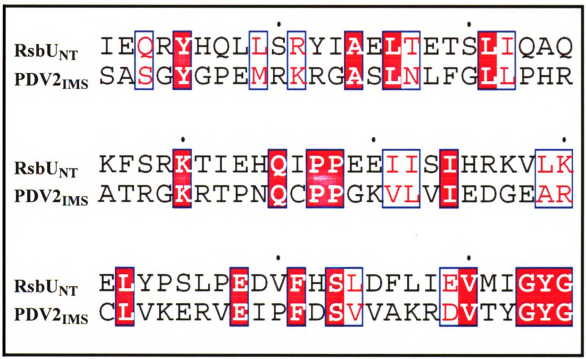

Figure 4.2. Pairwise alignment between the N-terminal domain of RsbU and the IMS region of PDV2. The N-terminal domain of RsbU used for crystal structure of 2J6Z (RsbU$_{NT}$, amino acids 7-81) and IMS region of PDV2 (PDV2$_{IMS}$, amino acids 233-307) are aligned using a BLOSUM62 scoring matrix. Boxed positions indicate sequence similarity and shaded positions highlight sequence identity.

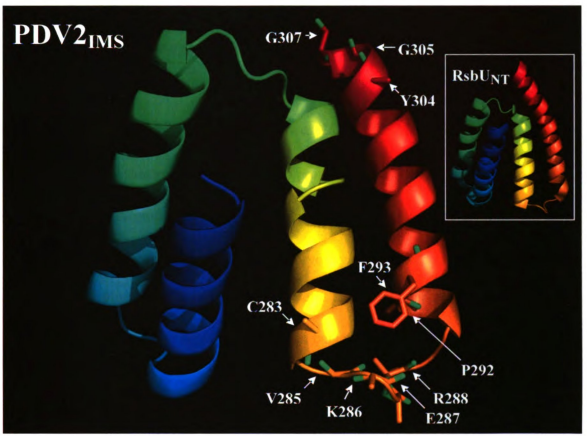

Figure 4.3. Structural model of $PDV2_{IMS}$. The IMS region of PDV2 (amino acids 233-307, main panel) was modeled using the known structure of $RsbU_{NT}$ (2J6Z/1W53, inset panel). Shown above are cartoon representations of the two structures. The side chains of conserved residues within the C-terminal extension of PDV2 proteins (see Figure 3.6) are highlighted in the $PDV2_{IMS}$ structural model.

some gram positive bacteria (Delumeau, Dutta, *et al.* 2004, Kang, Vijay, *et al.* 1998, Yang, Kang, *et al.* 1996). This IMS-localized interaction between ARC6 and PDV2 might modulate posttranslational modification of ARC6, thereby altering the activity of ARC6 within the IMS or chloroplast stroma.

A Conserved Serine within ARC6$_{PBD}$ Influences ARC6-PDV2 Interaction.

Because of the possible connection to protein kinase/phosphatase activity, we closely examined alignments between tracheophyte ARC6$_{PBD}$ and the corresponding region of cyanobacterial Ftn2 proteins for embryophyte-conserved residues that might act as phosphoacceptors (Figure 4.4), as PDV proteins are found only in land plants. We identified a plant-specific motif (Figure 4.4, red bar) within the ARC6$_{PBD}$ that was conserved amongst higher plants, but missing from or poorly aligned with algal ARC6 and cyanobacterial Ftn2 sequences; all ARC6 orthologs from higher plants possessed a serine near the middle of this motif (Figure 4.4, arrowhead indicates S744 in AtARC6); serine residues are common sites of posttranslational modification in eukaryotes. Because algae and cyanobacteria do not encode orthologs of PDV2, this embryophyte-specific serine residue (ARC6$_{S744}$), or other residues within the surrounding motif, might be targets of ARC6 posttranslational modification that have coevolved with emergence of PDV2 in land plants.

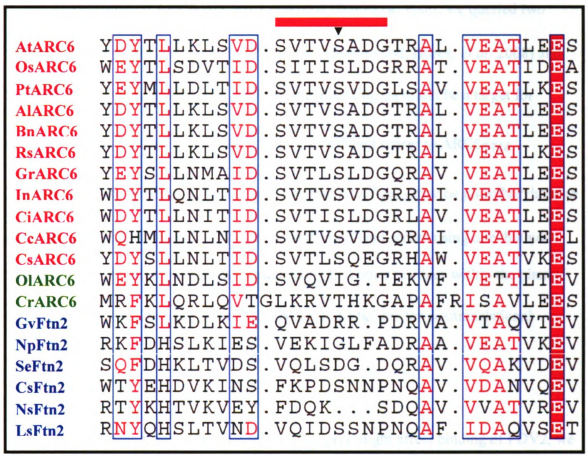

Figure 4.4. Identification of a plant-specific motif within the C-termini of ARC6/Ftn2 family members. A segment of a CLUSTALW alignment comparing the C-termini of ARC6 and Ftn2 family members is shown above and corresponds to *Arabidopsis thaliana* ARC6 amino acids 729-759. The red bar above the sequences indicates an amino acid motif unique to higher plants that may be involved in ARC6-PDV2 interaction, based on two hybrid results (Figure 4.1). The black arrowhead points to a serine (S744) predicted to be a phosphoacceptor (see text). *Arabidopsis thaliana* ARC6 (AtARC6); *Oryza sativa* cv. japonica (OsARC6); *Populus trichocarpa* ARC6 (PtARC6); *Arabidopsis lyrata* (AlARC6); *Brassica napus* ARC6 (BnARC6); *Raphanus sativus* (RsARC6); *Gossypium raimondii* (GrARC6); *Ipomoea nil* (InARC6); *Cichorium intybus* (CiARC6); *Coffea canephora* (CcARC6); *Citrus sinensis* (CsARC6); *Ostreococcus lucimarinus* CCE9901 (OlARC6); *Chlamydomonas reinhardtii* (CrARC6); *Gloeobacter violaceus* PCC7421 (GvFtn2); *Nostoc punctiforme* PCC 73102 (NpFtn2); *Synechococcus elongatus* PCC 6301 (SeFtn2); *Cyanothece sp.* CCY0110 (CsFtn2); *Nostoc sp.* PCC 7120 (NsFtn2); and *Lyngbya sp.* PCC 8106 (LsFtn2). Label colors in the lefthand column indicate groups of organisms: red = land plants, green = green algae, and blue = cyanobacteria. Boxed regions indicate sequence similarity in >70% of the lineages shown. Shaded regions indicate conserved residues.

To determine if $ARC6_{S744}$ was a potential phosphoacceptor, we queried two phosphorylation-prediction programs, PhosPhAt (Heazlewood, Durek, *et al.* 2008) and NetPhos (Blom, Gammeltoft, *et al.* 1999) to see if $ARC6_{S744}$ might be a target for phosphorylation. Both of these programs gave significant scores to $ARC6_{S744}$ (PhosPhAt, 0.496; NetPhos, 0.932), suggesting that $ARC6_{S744}$ may be phosphorylated *in vivo*. Notably, both S740 and T742 also yielded significant scores using one, but not both, of these prediction algorithms — suggesting that other residues within the plant-specific motif of $ARC6_{PBD}$ (Figure 4.4) might also be targets for posttranslational modification.

To determine if phosphorylation of $ARC6_{S744}$ might affect binding of PDV2, we generated site-directed mutants of $ARC6_{IMS}$, targeting the serine at position 744 in two-hybrid vectors. We named these mutant proteins $ARC6_{IMS\ (S744A)}$ and $ARC6_{IMS\ (S744E)}$, which mimic the unphosphorylatable (S744A) and constituitively phosphorylated (S744E) forms of the protein, respectively. Our results showed binding strengths consistent with PDV2 affinities as $ARC6_{IMS} > ARC6_{S744A} > ARC6_{S744E}$ (Figure 4.5A), indicating that PDV2 has low affinity for the phosphomimetic form of ARC6, $ARC6_{S744E}$. We validated this result using pulldown assays with recombinant His_8-$ARC6_{IMS}$ and GST-$PDV2_{IMS}$ proteins, which confirmed that $ARC6_{IMS\ (S744E)}$

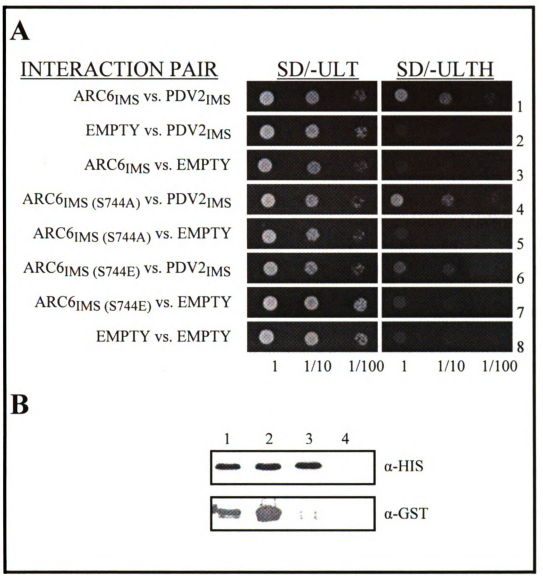

Figure 4.5. A phosphomimetic mutation in the IMS region of ARC6 ($ARC6_{S744E}$) decreases its affinity for PDV2. (A) Site-directed mutations in $ARC6_{IMS}$ were tested for their ability to interact with $PDV2_{IMS}$ by yeast two-hybrid. Interaction strengths are as follows: ARC6-PDV2 (0.64); $ARC6_{IMS\ (S744A)}$-PDV2 (0.54); $ARC6_{IMS\ (S744E)}$-PDV2 (0.14); all negative controls (≤ 0.01). Relative interaction strength was determined by ratio of growth on –HIS/+HIS synthetic dropout (SD) media. (B) Confirmation of two hybrid results by pulldown assay using immobilized ARC6 proteins treated with equal amounts of GST-$PDV2_{IMS}$. Immunoblots of eluates from pulldowns are shown: His_8-$ARC6_{IMS}$ (lane 1), His_8-$ARC6_{IMS\ (S744A)}$, His_8-$ARC6_{IMS\ (S744E)}$, or uncoated beads treated with GST-$PDV2_{IMS}$ (lane 4).

has significantly lower affinity for $PDV2_{IMS}$ than the wild type ($ARC6_{IMS}$) protein (Figure 4.5B). $ARC6_{IMS\ (S744A)}$ had slightly decreased affinity for $PDV2_{IMS}$ in two-hybrid assays and slightly increased affinity for $PDV2_{IMS}$ in pulldown assays, suggesting this mutation may not perturb ARC6 function.

A Phosphomimetic Mutation in $ARC6_{PBD}$ Causes Chloroplast Division Defects in vivo.

Because of the profound effect of our phoshphomimetic mutation ($ARC6_{S744E}$) on ARC6-PDV2 interaction, we wanted to know if this mutation was detrimental to the division process *in vivo*. Therefore, we generated a series of transgenes encoding wild type (*ARC6*), unphosphorylatable ($ARC6_{S744A}$), and phosphomimetic ($ARC6_{S744E}$) versions of ARC6; all of these were driven by the native *ARC6* promoter sequence. We transformed wild type (*Col-0*) and *arc6* (SAIL_693_G04) plants with each of these transgenes using *Agrobacterium* (Clough and Bent 1998) and selected T_1 individuals using hygromycin. We examined chloroplast morphology in independent T_1 lines that were expressing the transgene within the range that should complement the *arc6* mutant, based on the expression of the control (wild type) transgene (Figure 4.6). Both the wild type (ARC6) protein and the unphosphorylatable ($ARC6_{S744A}$) proteins were able to complement the *arc6* mutant when expressed at similar levels. However, $ARC6_{S744E}$ was unable to fully complement *arc6* mutants (Figure 4.6) and imposed a dominant-negative effect upon *Col-0* transformants (data not shown), suggesting that this transgene

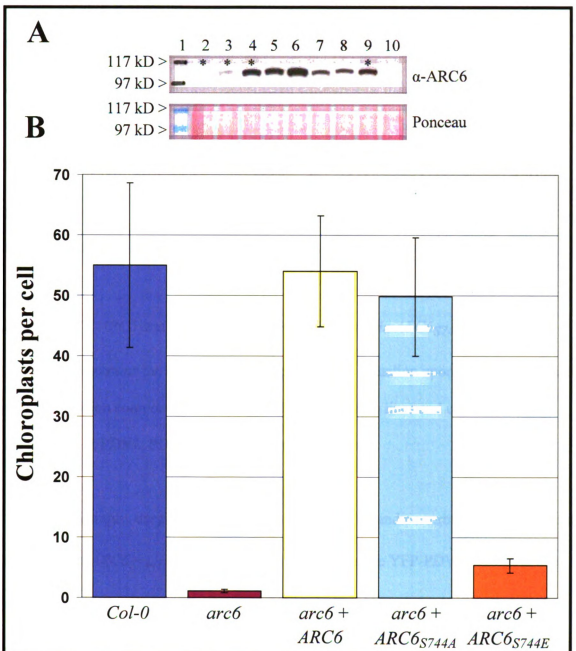

Figure 4.6. ARC6$_{S744E}$ is dysfunctional. (A) Sample of immunoblot data used to quantitate ARC6 protein levels in transformed *arc6* plants. Marker (lane 1); *arc6* (lane 2); *Col-0* (lane 3); four independent *arc6* T_1 transformants complemented by *ARC6* transgene (lanes 4-7); 3 independent *arc6* T_1 *ARC6$_{S744E}$* transformants (lanes 8-10). Protein levels in ARC6$_{S744A}$ lines were quantitated on a separate immunoblot (not shown). (B) Analysis of chloroplast number in expanded leaves of *Col-0*, *arc6*, and transgenic lines from 10 cells with average areas of 3109 ± 443 μm^2. Lines used for quantitative analysis in panel B are marked with asterisks (*) in panel A. Error bars = standard deviation.

was not functional *in vivo*, consistent with its low affinity for PDV2 in pulldowns and two-hybrid assays (Figure 4.5). Interestingly, many of the lines expressing $ARC6_{S744E}$ contained elongated and partially-constricted chloroplasts, indicative of a defect in PDV or ARC5 protein function (Figure 4.7E, arrowheads) (Gao, Kadirjan-Kalbach, *et al.* 2003, Miyagishima, Froehlich, *et al.* 2006). Taken together, we conclude that $ARC6_{S744}$ is probably important for the ARC6-PDV2 interaction *in vivo*, but cannot yet conclude that this residue is actually subject to post-translational modification *in vivo*.

PDV2, PDV1, ARC5 and FtsZ localize to the division site in $ARC6_{S744E}$ mutants.

To determine the effect of our phosphomimetic mutation upon the characteristics of other division components, we examined our transgenic lines and controls for localization of PDV2, PDV1, ARC5, and FtsZ proteins.

Surprsingly, despite their lower affinity for PDV2 and perturbation in chloroplast morphology, $ARC6_{S744E}$ mutants were still able to localize YFP-PDV2 to rings at sites of chloroplast constriction (Figure 4.8C). This conflicts with the reduced affinity of $ARC6_{S744E}$ for $PDV2_{IMS}$ in binding assays (Figure 4.5), but might reflect the ability of $ARC6_{S744E}$ to bind PDV2, albeit with less stringency than the wild type protein (Figure 4.5).

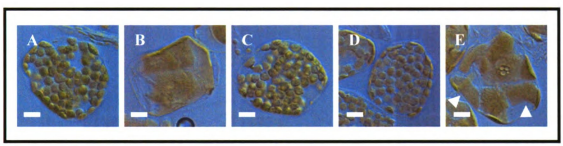

Figure 4.7. Phenotypes observed in lines expressing *ARC6*$_{S744A}$ and *ARC6*$_{S744E}$. Mesophyll cells from expanding leaves are shown for *Col-0* (A); *arc6* (B); *arc6* expressing transgenic *ARC6* (C); *arc6* expressing transgenic *ARC6*$_{S744A}$ (D); and *arc6* expressing transgenic *ARC6*$_{S744E}$ (E). Arrowheads in (E) indicate elongated and partially constricted chloroplasts. Scale bars = 10 μm.

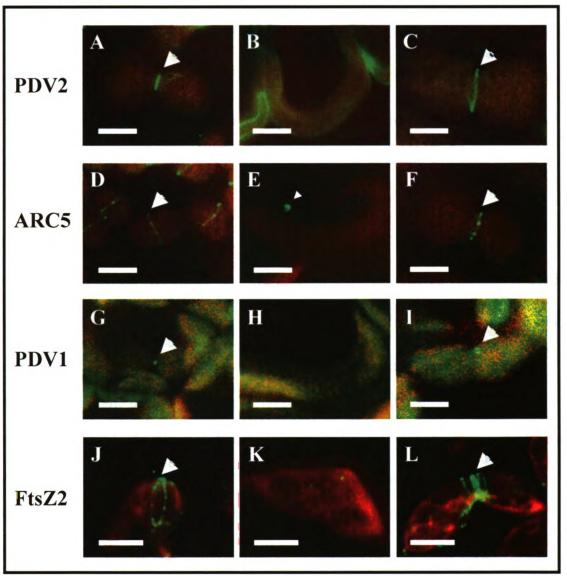

Figure 4.8. Localization of PDV2, ARC5, PDV1, and FtsZ in *ARC6*$_{S744E}$-expressing transgenics. All fluorescently-labeled proteins were expressed using their respective native promoters. Merged images showing chlorophyll autofluoresence (red) and the indicated fluorescent marker (green) are shown. YFP-PDV2 localization in *Col-0* (A); *arc6* (B); and *ARC6*$_{S744E}$ (C). GFP-ARC5 in *Col-0* (D); *arc6* (E); and *ARC6*$_{S744E}$ (F). GFP-PDV1 in *Col-0* (G); *arc6* (H); and *ARC6*$_{S744E}$ (I). Immunolabeling of FtsZ2-1 in *Col-0* (J); *arc6* (K); and *ARC6*$_{S744E}$ (L). Scale bars = 5 μm.

To determine if the division defect observed in *ARC6*$_{S744E}$ transgenics was a result of an indirect effect upon ARC5 or PDV1 localization, we examined GFP-ARC5 and GFP-PDV1 localization in lines *ARC6*$_{S744E}$ transgenics. Both GFP-ARC5 (Figure 4.8F) and GFP-PDV1 (Figure 4.8I) were localized to the division site, though GFP-PDV1 was not observed in a ring in lines expressing *ARC6*$_{S744E}$ as it is in wild-type plants (Miyagishima, Froehlich, *et al.* 2006).

Because Z-ring morphology is affected in the dumbbell-shaped plastids observed in *pdv1*, *pdv2*, and *arc5* mutants, we examined Z-ring morphology in *ARC6*$_{S744E}$ mutants using an FtsZ2-specific antibody (Figure 4.8L). In mutants with defects in dynamin activity, we typically observe multiple Z-rings at the division site, presumably as a feedback response to the defect in dynamin activity at the outer envelope (Gao, Kadirjan-Kalbach, *et al.* 2003, Miyagishima, Froehlich, *et al.* 2006, Yang, Glynn, *et al.* 2008). Consistent with a defect in dynamin activity (Gao, Kadirjan-Kalbach, *et al.* 2003, Miyagishima, Froehlich, *et al.* 2006), *ARC6*$_{S744E}$ mutants have multiple Z-rings at the division site (Figure 4.8L). Taken together, we conclude that ARC6$_{S744}$ is important for ARC6-PDV2 interaction, indirectly affecting dynamin (ARC5) pinchase activity at the outer envelope through PDV2, as ARC6$_{S744E}$ mutants have defects in chloroplast and FtsZ filament morphology similar to *pdv1*, *pdv2*, and *arc5* mutants (Gao, Kadirjan-Kalbach, *et al.* 2003, Miyagishima, Froehlich, *et al.* 2006).

Discussion

Here, we identify and characterize the PDV2-binding domain of ARC6 ($ARC6_{PBD}$). $ARC6_{PBD}$ occupies only a portion (AA 636-759) of the IMS-localized C-terminal region of ARC6. While our structural analysis of $ARC6_{PBD}$ was not insightful, the IMS-localized C-terminus of PDV2 ($PDV2_{IMS}$) modeled onto the known structure of RsbU (Delumeau, Dutta, *et al.* 2004, Hardwick, Pane-Farre, *et al.* 2007), a bacterial phosphoserine phosphatase (Delumeau, Dutta, *et al.* 2004, Hardwick, Pane-Farre, *et al.* 2007). Because of the structural similarity of $PDV2_{IMS}$ to RsbU and the prospect of posttranslational modification of ARC6, we examined alignments (Figure 4.4) within $ARC6_{PBD}$ for plant-specific motifs containing predicted phosphoacceptor sites. This analysis revealed that serine 744 ($ARC6_{S744}$) as a high-probability phosphoacceptor within a plant-specific motif of $ARC6_{PBD}$, based on NetPhos and PhosPhAt prediction programs. Our site-directed mutagenesis of this residue revealed that a phosphomimetic mutation ($ARC6_{S744E}$) causes reduced affinity for $PDV2_{IMS}$; this same mutation leads to chloroplast division defects (Figures 4.6-4.8) similar to those seen in mutants with defects in dynamin (ARC5) activity (Gao, Kadirjan-Kalbach, *et al.* 2003, Miyagishima, Froehlich, *et al.* 2006). However, despite the reduced affinity for $ARC6_{S744E}$ for PDV2, *arc6* mutants expressing an *$ARC6_{S744E}$* transgene still recruit YFP-PDV2 and other division factors to the division site (Figure 4.8).

Our identification of the rough boundaries of the PDV2-binding domain is a first step in understanding how ARC6 and PDV2 interact with each other and how this interaction might be regulated. Further work is required to identify the precise boundaries of $ARC6_{PBD}$, which might allow further refinement of the current structure-function model for this domain. While structural similarity to RsbU (2J6Z/1W53) is apparent, it is not yet clear if $PDV2_{IMS}$ possesses phosphatase or kinase activity and if $ARC6_{PBD}$ is truly a substrate for any posttranslational modification activity *in vivo*.

While $ARC6_{S744}$ might act as a phosphoacceptor *in vivo*, PDV2 itself probably does not modify this residue and likely uses $ARC6_{PBD}$ as a binding site, as the structural similarity to the RsbU phosphatase is limited to the RsbT-binding domain of RsbU. However, modification of the plant-specific motif within $ARC6_{PBD}$ clearly reduces affinity for PDV2, suggesting that a posttranslational modification at serine 744 might be a mechanism by which PDV2 recruitment to the division site is modulated. Alternatively, serine 744 of ARC6 might be required for structural intergrity of $ARC6_{PBD}$ and our mutant proteins are simply misfolded, leading to reduced affinity for PDV2. Either of these scenarios might explain the prevalence of dumbbell-shaped chloroplasts in lines expressing $ARC6_{S744E}$ (Figures 4.7-4.8). Curiously, we occasionally observed chloroplasts within petiole cells that possessed several constrictions along their length in $ARC6_{S744E}$-expressing lines (Figure 4.9), a phenotype

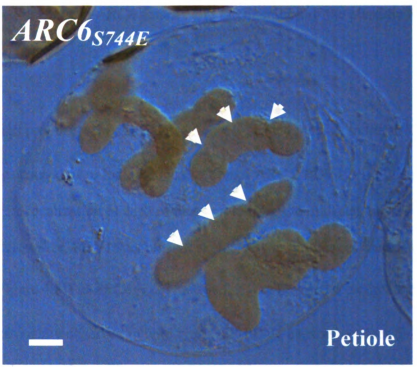

Figure 4.9. An unusual phenotype observed in *ARC6*$_{S744E}$ petioles phenocopies plastidic Min system defects. Multiple constrictions were observed along the length of elongated chloroplasts within large petiole cells of *ARC6*$_{S744E}$ transgenics. This phenotype has not been observed in *arc5* mutants and may reflect ARC6-mediated downregulation of AtMinD (Colletti, Tattersall, *et al.* 2000, Fujiwara, Nakamura, *et al.* 2004) and/or upregulation of AtMinE activity within the chloroplast (Fujiwara, Hashimoto, *et al.* 2008, Maple, Chua, *et al.* 2002). Scale bar = 10 μm.

that resembles both *atminD/arc11* loss-of-function mutants (Colletti, Tattersall, *et al.* 2000, Fujiwara, Nakamura, *et al.* 2004) and *AtMinE* overexpressors (Fujiwara, Hashimoto, *et al.* 2008, Maple, Chua, *et al.* 2002). The significance of this finding is not yet clear, nor is it understood why these phenotypes appear prominently in petiole cells, but the connection between ARC6 activity and the operation of the plastidic Min system is intriguing.

The high proportion of elongated dumbbell-shaped plastids in the $ARC6_{S744E}$ transgenic lines caused us to look the localization of ARC5, PDV1, PDV2, and FtsZ. Surprisingly, the localization of each of these proteins to the mid-plastid was mostly unperturbed. However, PDV1 was present exclusively as single foci associated with the chloroplast (Figure 4.8I) in $ARC6_{S744E}$ transgenics, but never as a complete punctate ring, as is occasionally observed in wild type GFP-PDV1 expressing lines (Miyagishima, Froehlich, *et al.* 2006, Yang, Glynn, *et al.* 2008). The reason for this is unclear, but the GFP-PDV1 punctate ring is the most uncommon PDV1 localization pattern observed; PDV1 is typically observed as a single spot in wild type cells and more observation of these transgenic lines may be required. Additionally, while FtsZ2 was localized to the mid-plastid in $ARC6_{S744E}$ lines, several adjacent Z-rings were observed (Figure 4.8L), reminiscent of the FtsZ2 localization pattern in *pdv1*, *pdv2*, and *arc5* (Gao, Kadirjan-Kalbach, *et al.* 2003, Miyagishima, Froehlich, *et al.* 2006); all these mutants have defects in dynamin activity, which presumably generates a signal leading to the formation of several central Z-rings (Yang, Glynn, *et al.* 2008). Based on the Z-ring morphology in

our *ARC6*$_{S744E}$ transgenics, we propose that this signal is transduced through ARC6. Because of this *arc5*-like Z-ring phenotype in ARC6$_{S744E}$ lines, we propose that the dumbbell-shape chloroplasts in these lines result from a decrease of dynamin pinchase activity at the outer envelope, perhaps resulting from a decrease in ARC6-PDV2 affinity due to the phosphomimetic mutation in ARC6. Alternatively, upregulation of stromal Z-ring assembly in *ARC6*$_{S744E}$ mutants (Figure 4.8L) might impede dynamin-mediated envelope constriction, as the Z-ring must presumably either constrict or disassemble to allow the division process to conclude.

How and why would ARC6$_{S744}$ phosphorylation within the IMS affect Z-ring assembly and/or dynamin activity? One highly speculative possibility is that S744 phosphorylation occurs to slow or regulate the division process. Perhaps ARC6$_{S744}$ is phosphorylated as the Z-ring is being assembled— this leads to controlled recruitment of PDV2 until the Z-ring is fully assembled within the stroma and ready to constrict. At this point, ARC6 molecules would then be progressively dephosphorylated at position 744, causing increased ARC6-PDV2 affinity and hence increased dynamin (ARC5) activity at the outer envelope with concurrent disassembly of the Z-ring in the stroma. If this is the case, it is unclear why we did not observe smaller chloroplasts in *ARC6*$_{S744A}$ lines; perhaps this phosphoregulatory mechanism may only be relevant when PDV2 is overexpressed, functions only under a particular set of growth conditions, or the modification of additional residues within the plant-specific motif of ARC6$_{PBD}$ (such as

S740 and/or T742) might also contribute to regulating ARC6-PDV2 interaction. Regardless, this hypothesis is in-line with observations that the rate of plastid division is affected by the amount of PDV2 protein: less PDV2 leads to a slower rate of division and more PDV2 leads to a faster rate of division (Okazaki, Kabeya, *et al.* 2009). ARC6 is absolutely required for PDV2 localization at the division site (Figure 4.8B) and ARC6 is absolutely required for PDV2-mediated division activity, as overexpression of PDV2 in the *arc6* background does not modify the number of chloroplasts observed within *arc6* mutants (Glynn, Froehlich, *et al.* 2008). Presumably, the amount of PDV2 present *at the division site* is a rate-limiting step, with regard to organelle constriction — and phosphorylation of $ARC6_{S744}$ might be a mechanism by which individual chloroplasts regulate PDV2 recruitment to the division site, providing a checkpoint for proper Z-ring assembly prior to dynamin-driven constriction of the organelle. Further work on this aspect of the division process might lead to the discovery of a novel auto-kinase/phosphatase activity for ARC6, or a separate novel kinase/phosphatase, that aids fine-tuning of the division process by controlling the recruitment of PDV2 to the division site.

Materials and Methods

Yeast two-hybrid analysis.

$ARC6_{AA\ 637\text{-}801}$ was cloned into pGADT7 using NdeI-XmaI and $PDV2_{AA233\text{-}307}$ was cloned into pGBKT7 using NdeI-XmaI sites. Site-directed alleles of ARC6 were made by SOE-PCR (Warrens, Jones, *et al.* 1997) and cloned into pGBKT7 using NdeI-XmaI sites. Yeast strain AH109 (Clontech) was cultured and transformed as recommended by the manufacturer using standard Synthetic Dropout (SD) Media (Clontech) as indicated. Growth assays were conducted using previously-established protocols.

Pulldown assays.

All fusion proteins were expressed in *E. coli* BL21 (DE3) Codon Plus cells (Stratagene) induced at OD_{600} = 0.8 with 2 mM IPTG for 2 hours at 37°C. 750 μg of protein from induced cell extract was used for each bait/prey combination. Pulldowns between His_8-$ARC6_{IMS}$ and GST-$PDV2_{IMS}$, $ARC6_{IMS\ (S744A)}$ and GST-$PDV2_{IMS}$, or $ARC6_{IMS\ (S744E)}$ and GST-$PDV2_{IMS}$ were performed as in previous experiments (Glynn, Froehlich, *et al.* 2008), except Triton X-100 was present at 0.1% in all wash buffers to prevent clumping of the sepharose beads.

Structural modeling.

A structural model of $PDV2_{IMS}$ was generated by comparison of $PDV2_{AA233-307}$ to all current PDB structures (http://www.pdb.org) using the MetaServer at http://bioinfo.pl. The best-matched protein (in terms of its secondary structure) was aligned with the relevant query protein using CLUSTALW (Larkin, Blackshields, *et al.* 2007) and a PDB file containing data for a three dimensional model was generated using the homology modeling server at http://proteins.msu.edu. The final images used in figures herein were rendered using PyMol 0.99rc6 (Delano Scientific).

Generation of transgenic lines.

$ARC6_{S744A}$ and $ARC6_{S744E}$ transgenes were generated using SOE-PCR and placed into a derivative of pCAMBIA-1302 containing the native ARC6 promoter using AvrII and BstEII restriction sites. Clones were sequence-verified and transformed into *Agrobacterium tumefaciens* GV3101 prior to transformation of *Arabidopsis* (Clough and Bent 1998). Trangenic lines were selected on Linsmaier-Skoog medium containing hygromycin (25 μg/mL). Only hygromycin-resistant individuals were transplanted to soil and used for further analysis.

Immunoblotting.

Plant extracts for determination of ARC6 protein level were taken from floral bud tissue. Flower buds were ground in liquid nitrogen and prepared for 10% SDS-PAGE using 6X sample buffer according to previously-established protocols (Wiegel and

Glazebrook 2002). 2.5 mg of homogenized tissue was loaded per lane. Immunoblotting of plant extracts was performed using an ARC6-specific antibody at 1:2500 in blocking buffer containing 5% nonfat dry milk (McAndrew, Olson, *et al.* 2008). The blot was washed several times in TBS-T before applying the secondary antibody. The anti-rabbit HRP-conjugated secondary was used at 1:5000 in TBS-T containing 5% nonfat dry milk and the blot was washed several times in TBS-T before applying the HRP chemilluminescent substrate (Thermo Scientific, Inc.) and exposing to film.

Quantitative analysis of chloroplast number.

Tissue preparation was carried out as described previously (Miyagishima, Froehlich, *et al.* 2006, Pyke and Leech 1991, Vitha, Froehlich, *et al.* 2003). Cell size and chloroplast number were measured using ImageJ v1.37 (NIH) (Bearer 2003). Quantitative analysis of phenotypes was performed using 10 cells of similar size.

Microscopy.

Light micrographs depicting chloroplast morphology in expanded leaf cells were taken using DIC Optics on a Leica DMI3000B Inverted Microscope outfitted with a Leica DFC320 Camera. Samples for chloroplast morphology and quantitation were prepared and analyzed using established protocols (Pyke and Leech 1991). Fluorescence micrographs were taken using a Leica DMRA2 using Q-Capture Camera Control Software (Q-Imaging) and the filter sets indicated (Leica) as previously described (Vitha, Froehlich, *et al.* 2003). Image analysis and RGB composites were made using ImageJ v1.37 (NIH) (Bearer 2003).

Acknowledgements

I thank Aaron Schmitz, Yue Yang, and Katherine Osteryoung for helpful discussions during the development and progression of this project.

Chapter 5

PARC6 Influences FtsZ Assembly and PDV1 Recruitment in *Arabidopsis*.

Abstract

Chloroplast division in plant cells is accomplished through the coordinated action of the tubulin-like FtsZ ring inside the organelle and the dynamin-like ARC5 ring outside the organelle. This coordination is facilitated by ARC6, an inner envelope protein required for both FtsZ assembly and ARC5 recruitment. Recently, we showed that ARC6 specifies the mid-plastid positioning of the outer envelope proteins PDV1 and PDV2, which have parallel functions in dynamin recruitment. PDV2 positioning involves direct ARC6-PDV2 interaction but PDV1 and ARC6 do not interact, indicating an additional factor functions downstream of ARC6 to position PDV1. Here, we show that PARC6 (Paralogue of ARC6), an ARC6-like protein unique to vascular plants, fulfills this role. Like ARC6, PARC6 is an inner envelope protein with its N-terminus exposed to the stroma and Arabidopsis *parc6* mutants exhibit chloroplast and FtsZ filament morphology defects. However, whereas ARC6 promotes FtsZ assembly, PARC6 appears to inhibit FtsZ assembly, suggesting ARC6 and PARC6 function as antagonistic regulators of FtsZ dynamics. The FtsZ inhibitory activity of PARC6 may involve its interaction with the FtsZ-positioning factor ARC3. A PARC6-GFP fusion protein localizes both to the mid-plastid and to a single spot at one pole, reminiscent of the localization of ARC3, PDV1 and ARC5. We show that PARC6 positions and binds PDV1, but PARC6 is not required for localization of PDV2 or ARC5. Our findings indicate that PARC6, like ARC6, plays a role in coordinating the internal and external components of the chloroplast division complex, but that PARC6 has evolved distinct functions in the division process.

Introduction

The chloroplasts of vascular plants replicate by binary fission, similar to their cyanobacterial relatives, but utilize a machinery that is a composite of cyanobacterial and host-derived components (Aldridge, Maple, *et al.* 2005, Gao, Kadirjan-Kalbach, *et al.* 2003, Kuroiwa, Kuroiwa, *et al.* 1998, Maple, Vojta, *et al.* 2007, Miyagishima, Takahara, *et al.* 2001, Miyagishima, Wolk, *et al.* 2005, Osteryoung 2001, Osteryoung and Nunnari 2003, Osteryoung and Vierling 1995). The proteins that make up this dynamic complex, all of which are nuclear-encoded, occupy the stroma, intermembrane space (IMS), and cytosol, with several key factors acting at or across the envelope membranes (Gao, Kadirjan-Kalbach, *et al.* 2003, Miyagishima, Froehlich, *et al.* 2006, Miyagishima, Nishida, *et al.* 2003a, Vitha, Froehlich, *et al.* 2003, Yang, Glynn, *et al.* 2008).

Within the stroma, two tubulin-like proteins, FtsZ1 and FtsZ2, both derived from cyanobacterial FtsZ via endosymbiosis (Osteryoung, Stokes, *et al.* 1998, Osteryoung and Vierling 1995, Stokes and Osteryoung 2003), are central players in the division process, comprising a mid-plastid contractile ring (Z-ring) (McAndrew, Froehlich, *et al.* 2001, Stokes, McAndrew, *et al.* 2000, Vitha, McAndrew, *et al.* 2001). In bacteria, the Z-ring marks the division site, acts as a scaffold for other division components, and may provide contractile force driving membrane constriction (Lan, Wolgemuth, *et al.* 2007, Li, Trimble, *et al.* 2007, Margolin 2005, Osawa, Anderson, *et al.* 2008). A third FtsZ-derived chloroplast division protein, ARC3, is a chimera of FtsZ and other host-derived functional domains (Shimada, Koizumi, *et al.* 2004). ARC3 has likely replaced MinC, an

inhibitor of FtsZ polymerization and a component of the Min system, which positions the Z-ring in bacteria (Glynn, Miyagishima, *et al.* 2007, Maple, Vojta, *et al.* 2007, Rothfield, Taghbalout, *et al.* 2005).

On the cytosolic surface of the chloroplast, factors of host origin mediate organelle constriction and separation (Gao, Kadirjan-Kalbach, *et al.* 2003, Glynn, Miyagishima, *et al.* 2007, Miyagishima, Froehlich, *et al.* 2006, Miyagishima, Nishida, *et al.* 2003a, Yang, Glynn, *et al.* 2008). ARC5 is a dynamin-like protein required for the late stages of division, acting as a pinchase (Gao, Kadirjan-Kalbach, *et al.* 2003, Miyagishima, Nishida, *et al.* 2003a, Yoshida, Kuroiwa, *et al.* 2006). Dynamins are best known for their roles in vesicle-budding and endocytosis in eukaryotes (Hinshaw 2000, Hinshaw and Schmid 1995, Praefcke and McMahon 2004, Wiejak and Wyroba 2002), though the origins of dynamins can be traced to prokaryotes (Low and Lowe 2006). ARC5 is recruited to the division site from cytosolic patches by PDV1 and PDV2, two coiled-coil transmembrane outer envelope proteins of host origin that are unique to land plants (Glynn, Froehlich, *et al.* 2008, Miyagishima, Froehlich, *et al.* 2006). The finding that ARC5 localizes to the division site in *pdv1* and *pdv2* mutants but not in the double mutant indicates that PDV1 and PDV2 function independently in recruiting ARC5 to the chloroplast, but both PDV proteins are required for full ARC5 contractile activity (Miyagishima, Froehlich, *et al.* 2006).

The stromal FtsZ and cytosolic dynamin complexes that drive division of the organelle must be coordinated across the two envelope membranes to ensure their

synchronous operation. A key factor coordinating these complexes is ARC6, a transmembrane protein of the inner envelope that evolved from the cyanobacterial cell division protein Ftn2 (Koksharova and Wolk 2002, Vitha, Froehlich, *et al.* 2003). The stromal region of ARC6 binds FtsZ2 (Maple, Aldridge, *et al.* 2005) and mediates Z-ring assembly (Vitha, Froehlich, *et al.* 2003), while the IMS region interacts with and positions PDV2 at the division site to facilitate ARC5 recruitment (Glynn, Froehlich, *et al.* 2008). ARC6 is also required for PDV1 positioning at the division site, but our finding that ARC6 and PDV1 do not interact suggested that an additional factor might function between ARC6 and PDV1 to localize PDV1 (Glynn, Froehlich, *et al.* 2008).

Here we show that PARC6, an ARC6-like protein unique to vascular plants, performs this function. Mutant analysis reveals that PARC6 is required for wild-type chloroplast replication and accumulation. Like ARC6, PARC6 resides in the inner envelope membrane (IEM) at the division site with its N-terminus facing the stroma. However, PARC6 acts downstream of ARC6 to mediate PDV1 localization, consistent with a previous model (Glynn, Froehlich, *et al.* 2008, Yang, Glynn, *et al.* 2008) and show that PARC6 interacts with the cytosolic domain of PDV1. In further contrast to ARC6, PARC6 localizes at one pole of some chloroplasts, similar to the localization patterns of PDV1 and ARC3 (Maple, Vojta, *et al.* 2007, Miyagishima, Froehlich, *et al.* 2006). Analysis of FtsZ filament morphology in *parc6* suggests that PARC6 inhibits FtsZ assembly, in contrast with ARC6, which promotes FtsZ assembly (Vitha, Froehlich, *et al.* 2003). We further show that PARC6 interacts with ARC3, and hypothesize that PARC6 inhibits FtsZ assembly via this interaction. Collectively, these findings suggest that

PARC6 and ARC6 may function as antagonistic regulators of Z-ring dynamics, and that PARC6 plays a role in coordinating Z-ring activity in the stroma with dynamin activity at the outer envelope. Additionally, the interaction of PARC6 with a component of the Min system and its localization pattern hint at the possibility that PARC6 may play a role in establishing polarity within newly divided chloroplasts.

Results

PARC6 Family Members are Distinct from ARC6 and are Unique to Vascular Plants.

We identified PARC6 by BLAST (Altschul, Madden, *et al.* 1997), shortly after the identification of ARC6 by a map-based approach (Vitha, Froehlich, *et al.* 2003). The *PARC6* locus (At3g19180) encodes a predicted protein product that shares ~21% identity with *Arabidopsis* ARC6 (Vitha, Froehlich, *et al.* 2003) and is predicted by ChloroP (Emanuelsson, Nielsen, *et al.* 1999) to bear a chloroplast transit peptide at its N-terminus (Figure 5.1). Consistent with this prediction, the N-terminus of PARC6 (amino acids (AA) 1-76) targets a YFP fusion to the chloroplast stroma in tobacco (Glynn, Yang, *et al.* 2009).

In contrast to ARC6, which contains one transmembrane helix that anchors it in the IEM (Vitha, Froehlich, *et al.* 2003), *Arabidopsis* PARC6 has two predicted transmembrane domains (Figure 5.1) based on output from Aramemnon (Schwacke, Schneider, *et al.* 2003). Multiple sequence alignment between PARC6, ARC6, and Ftn2 proteins from several organisms revealed two major regions of similarity, one near the N-

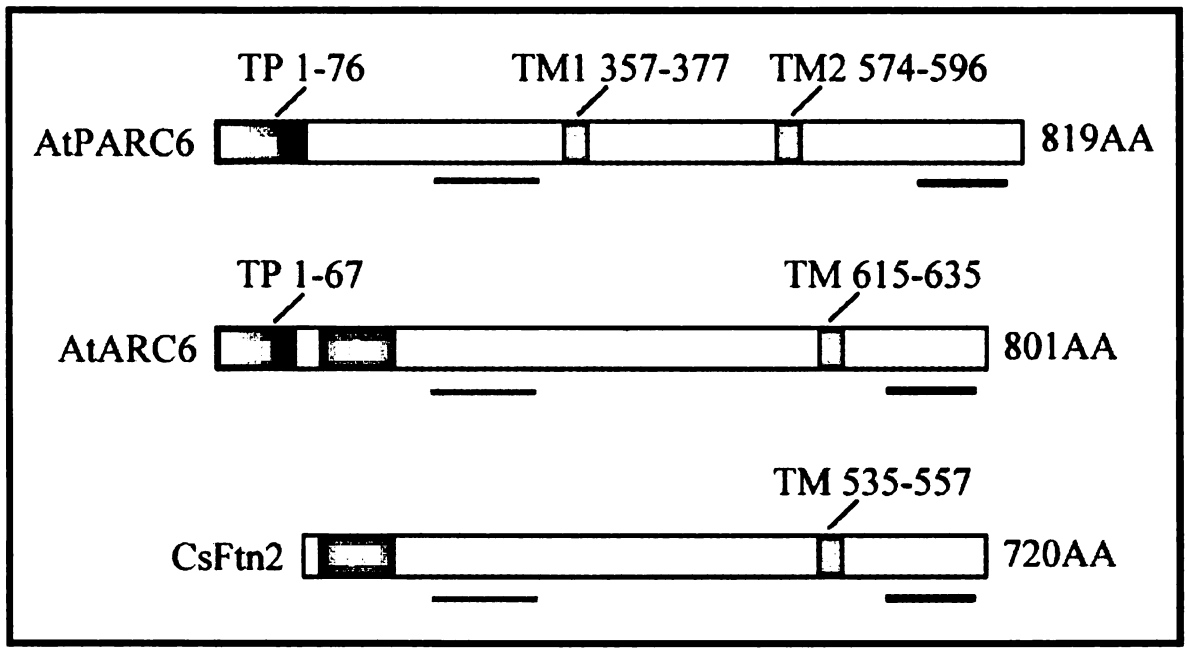

Figure 5.1. Summary of PARC6 protein features and similarity to related proteins. Lines under each diagram indicate regions of high similarity between all three proteins. A multiple sequence alignment comparing sequences of PARC6, ARC6, and Ftn2 from several species is shown elsewhere (Glynn, Yang, *et al.* 2009). Transit peptide (TP); transmembrane domain (TM); and amino acids (AA).

terminus and the other near the C-terminus (Figure 5.1), suggesting that these regions of PARC6, ARC6, and Ftn2 may have related functions. Several small regions conserved within, and unique to, PARC6 family members were also evident upon close examination of the alignment (Glynn, Yang, *et al.* 2009); these regions may harbor functions that are specific to PARC6 proteins. Notably, the conserved proline that resides within the central motif of the predicted J-domain of most ARC6/Ftn2 family members (Vitha, Froehlich, *et al.* 2003) is not evident in PARC6 sequences (Figure 5.1), suggesting that PARC6 does not function as a DnaJ-like co-chaperone.

While ARC6-like sequences are found in cyanobacteria, algae, and moss, PARC6 sequences were only detected in vascular plants (tracheophytes) suggesting that PARC6 emerged as a chloroplast division factor in this group of organisms. Consistent with this observation, phylogenetic analysis shows that PARC6 and ARC6 sequences from tracheophytes cluster into distinct clades and that both of these proteins may have diverged from a common ARC6-like ancestor (Figure 5.2). As postulated previously (Vitha, Froehlich, *et al.* 2003), ARC6 is more closely related to cyanobacterial Ftn2 than is PARC6 (Figure 5.2), suggesting that ARC6 and Ftn2 share greater functional similarity than PARC6 and Ftn2. These results, in combination with the sequence similarities and differences highlighted above, suggest that PARC6 arose as a result of gene duplication and divergence in primitive vascular plants and that it probably has evolved functions distinct from those of ARC6 within the tracheophyte lineage.

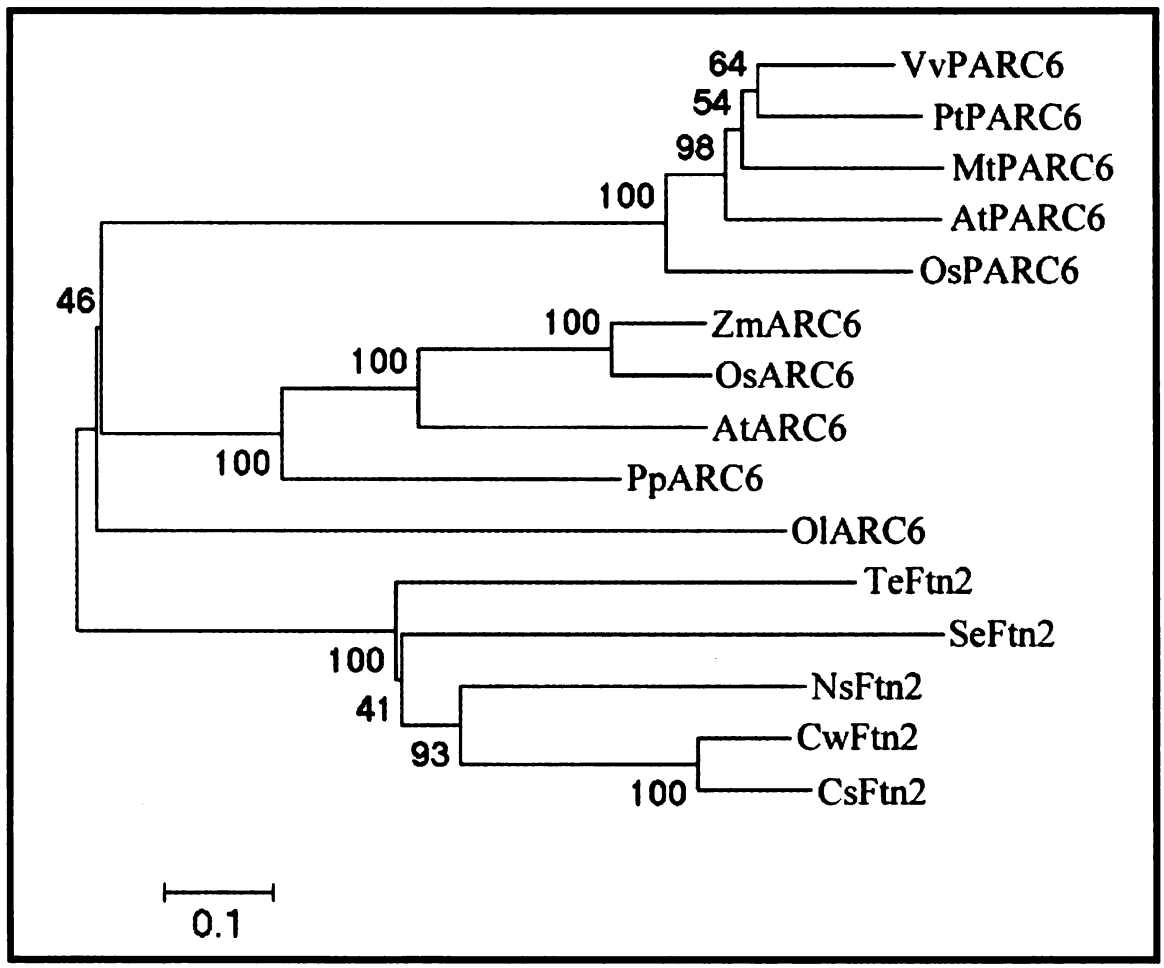

Figure 5.2. Phylogenetic analysis of PARC6, ARC6, and Ftn2 family members. Neighbor-joining tree showing the relationship between PARC6, ARC6, and Ftn2 family members from various species. Numbers at the nodes represent bootstrap values and scale bar corresponds to the number of amino acid substitutions per site. *Arabidopsis thaliana* (At); *Medicago truncatula* (Mt); *Oryza sativa* cv. japonica (Os); *Populus trichocarpa* (Pt); *Vitis vinifera* (Vv); *Ostreococcus lucimarinus* (Ol); *Physcomitrella patens* (Pp); *Zea mays* (Zm); *Thermosynechococcus elongatus* BP-1 (Te); *Synechococcus elongatus* PCC 7942 (Se); *Nostoc sp.* PCC 7120 (Ns); *Crocosphaera watsonii* WH 8501 (Cw); and *Cyanothece sp.* ATCC 51142 (Cs).

Mutations in PARC6 cause aberrations in chloroplast morphology and FtsZ filament morphology.

The similarity of PARC6 to ARC6 led us to investigate its role in plastid division. We identified a T-DNA insertion (SALK_100009) in the first exon of PARC6 (*parc6-1*, Figure 5.3A) and characterized homozygous lines for chloroplast morphology and number (Figure 5.3C).

parc6-1 mutants are less drastically impaired in chloroplast division than *arc6* mutants (compare Figure 5.3C and Figure 5.3F), but mesophyll cells in *parc6-1* mutants contain nearly 10-fold fewer chloroplasts (6.7 ± 2.4 chloroplasts per cell, n = 15 cells) than those in wild type (59.7 ± 11.2 chloroplasts per cell, n = 15 cells). *parc6-1* mesophyll cell chloroplasts possess characteristics of chloroplasts in both *arc3* and *arc5* mutants (Pyke and Leech 1994). Like *arc3* mutants, *parc6-1* mutants exhibit a heterogeneous mixture of chloroplast sizes within individual cells (Marrison, Rutherford, *et al.* 1999, Pyke and Leech 1992, Pyke and Leech 1994) (Figure 5.3C). Like *arc5* mutants, *parc6-1* mutants have some chloroplasts with prevalent constrictions (Figure 5.3C, arrowheads), suggesting a block in dynamin (ARC5) function (Gao, Kadirjan-Kalbach, *et al.* 2003, Miyagishima, Froehlich, *et al.* 2006). We also identified two additional alleles of *PARC6*, *parc6-2* and *parc6-3*, in a forward genetic screen (Figure 5.3D-E). These alleles confer phenotypes similar to those in *parc6-1*. *parc6-2* behaves as a dominant-negative mutation while *parc6-1* and *parc6-3* are recessive to the wild-type allele. These phenotypes lead us to conclude that PARC6 is a bona fide plastid

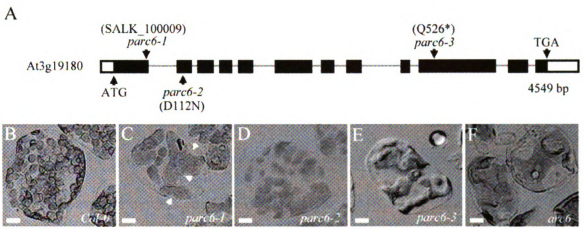

Figure 5.3. Diagram of the *PARC6* locus and phenotypic analysis of *parc6* mutants. (A) Gene structure and locations of characterized mutations in the *PARC6* locus. White boxes indicate untranslated regions. Black boxes indicate exons. Introns are denoted by thin grey lines. The transcribed region of At3g19180 is 4549 base pairs (bp). ATG, start codon; TGA, stop codon. (B-F) Chloroplast phenotypes in mesophyll cells of: *Col-0* (B); *parc6-1* (C); *parc6-2* (D); *parc6-3* (E); and *arc6-1* (F). Arrowheads denote sites of chloroplast constriction in the *parc6-1* mutant. Scale bar = 10 μm.

division protein and suggest that PARC6 could influence operation of the division machinery through ARC3, ARC5, or the ARC5 recruitment factors PDV1 and PDV2.

PARC6 is an inner envelope protein with localization similar to PDV1.

To examine the subcellular localization of PARC6, we generated a transgene encoding PARC6 fused to GFP expressed under control of the CaMV 35S promoter (*$35S_{pro}$:PARC6-GFP*). This transgene was capable of complementing the division defect in *parc6-1* mutants, indicating that it generates a functional protein product (Glynn, Yang, *et al.* 2009). Following selection of T_2 individuals, we examined epidermal cells in young leaves for expression of the fusion protein. PARC6-GFP localized to the middle of ovoid, partially constricted, and deeply constricted plastids (Figure 5.4), though whether it forms a complete ring during the early stages of division was not clear, as the GFP signal in these plastids was very weak. The GFP signal was most evident in deeply constricted plastids as single foci (Figure 5.4B), suggesting concentration of the fusion protein at the isthmus connecting plastids just prior to separation. In some plastids, PARC6-GFP was localized at the organelle surface in a single spot at one pole (Figure 5.4C), perhaps representing the persistence of the fusion protein at the pole following separation of the daughter plastids. A similar pattern of localization has been observed in *Arabidopsis* for both PDV1 and ARC5 (Miyagishima, Froehlich, *et al.* 2006), but not for ARC6 or PDV2 (Glynn, Froehlich, *et al.* 2008, Vitha, Froehlich, *et al.* 2003). In addition, we observed both polar and medial localization of PARC6-YFP at the

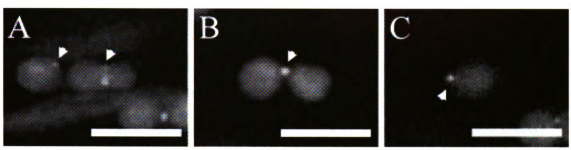

Figure 5.4. PARC6 is a plastid protein that localizes to the division site and to polar spots. PARC6-GFP localizes to mid-plastid puncta (A); mid-plastid spots (B); or polar spots (C) in *Arabidopsis*. Scale bar 5 μm.

chloroplast periphery in transiently transfected tobacco leaf cells (Glynn, Yang, *et al.* 2009), reminiscent of ARC3 localization under similar experimental conditions (Maple, Vojta, *et al.* 2007). In tobacco, the dual localization in the same plastid may be a consequence of overexpression as we did not observe both medial and polar localization in the same plastid in *Arabidopsis parc6-1* mutants complemented with the *PARC6-GFP* transgene (Figure 5.4). In both *Arabidopsis* and tobacco, PARC6-GFP was associated with the chloroplast periphery, suggesting it is localized in the envelope membrane.

To verify that PARC6 is an envelope membrane protein, we examined the fractionation of native PARC6 protein in isolated pea chloroplasts using an antibody generated against the region of *Arabidopsis* PARC6 residing between the transit peptide and the first predicted transmembrane domain (AA 77-356, Figure 5.1). The antibody detected a protein migrating at ~116 kD in whole-cell extracts from pea (Figure 5.5, lane 1) and a competition assay in which the antibody was preincubated with the immunizing antigen confirmed that this protein is native pea PARC6 (Glynn, Yang, *et al.* 2009). This protein was enriched in fractions containing isolated intact chloroplasts (Figure 5.5, lane 2) and chloroplast membrane fractions, (Figure 5.5, lane 3), suggesting that PARC6 is a chloroplast envelope protein. Preliminary analysis of PARC6 topology from pea chloroplast fractions indicates that the N-terminus of the protein resides in the stroma, but these experiments lacked controls and the orientation of the C-terminus of the protein remains unclear (Glynn, Yang, *et al.* 2009). Further work is needed to fully verify the topology of PARC6 *in vivo*.

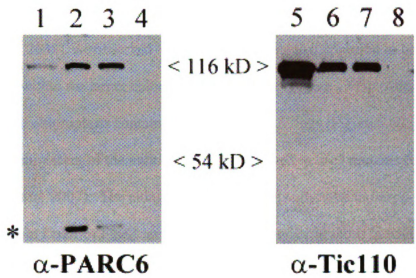

Figure 5.5. PARC6 is a chloroplast membrane protein. Whole-cell extract (lanes 1 and 5); isolated chloroplasts (lanes 2 and 6); chloroplast membrane fractions (lanes 3 and 7); and chloroplast soluble; fractions (lanes 4 and 8) were probed with an anti-PARC6 antibody (left) or an anti-Tic110 antibody (right) (Davila-Aponte, Inoue, *et al.* 2003). SDS-PAGE migration of PARC6 is slower than would be predicted based on its molecular weight, but we observed similar behavior with ARC6 (McAndrew, Olson, *et al.* 2008). Asterisk (*) indicates an unknown non-specific anti-PARC6 cross-reacting protein. Kilodaltons (kD).

PARC6 inhibits FtsZ assembly and interacts with ARC3.

Because ARC6 acts as a positive regulator of FtsZ assembly (Vitha, Froehlich, *et al.* 2003), we examined FtsZ organization in homozygous *parc6-1* mutants by immunostaining to determine if PARC6 also affects FtsZ assembly *in vivo*. In contrast to the short FtsZ filaments observed in the enlarged chloroplasts of *arc6* mutants (Vitha, Froehlich, *et al.* 2003), we observed long FtsZ1 filaments that appeared to be multiple rings or spirals within the larger chloroplasts of *parc6-1* (Figure 5.6B). Additionally, we observed tubular chloroplasts containing clusters of FtsZ rings (Figure 5.6C, arrowheads), reminiscent of the multiple Z-rings observed in *arc3* mutants (Glynn, Miyagishima, *et al.* 2007). The elongated FtsZ filaments observed in *parc6-1* were not due to a change in FtsZ1 or FtsZ2 levels, which were similar to those in wild type (Figure 5.6D). These results suggest that PARC6 might act as an antagonist of ARC6, with PARC6 inhibiting FtsZ assembly, and also implicate PARC6 in the functioning of the plastidic Min system (Fujiwara, Hashimoto, *et al.* 2008, Fujiwara, Nakamura, *et al.* 2004, Itoh, Fujiwara, *et al.* 2001, Maple and Moller 2007, Maple, Vojta, *et al.* 2007, Nakanishi, Suzuki, *et al.* 2009).

Arabidopsis ARC6 has been shown to interact with both FtsZ2 family members, but not FtsZ1 (Maple, Aldridge, *et al.* 2005, Schmitz, Glynn, *et al.* 2009). The profound effect of PARC6 depletion on Z-ring morphology led us to test for interaction between the putative N-terminal stromal region of PARC6 (AA 77-357) and both families of *Arabidopsis* FtsZ using two-hybrid assays. However, neither FtsZ1 nor FtsZ2 interacted

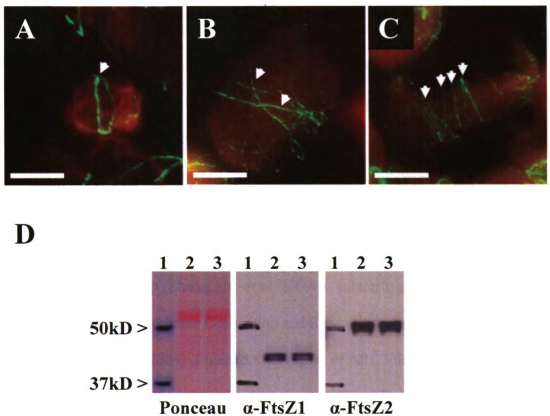

Figure 5.6. Analysis of FtsZ morphology and FtsZ protein levels in *parc6-1*. Immunolocalization of FtsZ1 in *Col-0* (A); and *parc6-1* mutants (B, C). Arrowheads point to structures formed by FtsZ. Chlorophyll autofluorescence (red) and FtsZ1 localization (green) is indicated. FtsZ2 filament morphology is also perturbed in *parc6*-1 mutants, as both FtsZ2-1 and FtsZ2-2 do not form regular rings, but instead form highly elongated filaments (Glynn, Yang, *et al.* 2009) that are unlike the short FtsZ filaments observed within the chloroplasts of *arc6* mutants (Vitha, Froehlich, *et al.* 2003). Immunoblots showing FtsZ levels are shown in panel (D). Ponceau stain of the membrane used for immunoblotting with FtsZ1 and FtsZ2-1 specific antibodies (left); FtsZ1 immunoblot (center); and FtsZ2-1 immunoblot (right). After Ponceau staining, blot was probed for FtsZ1, stripped, and then reprobed for FtsZ2-1. Molecular weight marker (lane 1); *Col-0* whole cell extract (lane 2); and *parc6-1* whole cell extract (lane 3). Scale bars = 5 μm.

with PARC6 (Figure 5.7). This result was somewhat surprising given the high affinity of ARC6 for FtsZ2 (Maple, Aldridge, *et al.* 2005).

Based on the chloroplast size heterogeneity in *parc6-1* (Figure 5.3) and *arc3* (Marrison, Rutherford, *et al.* 1999, Pyke and Leech 1992, Pyke and Leech 1994), the affect of PARC6 on FtsZ ring and filament morphology (Figure 5.6) and the ARC3-like localization of PARC6 in tobacco (Glynn, Yang, *et al.* 2009, Maple, Vojta, *et al.* 2007), we decided to test for interaction between PARC6 and ARC3 by two-hybrid. In contrast to ARC6 (Maple, Aldridge, *et al.* 2005), the N-terminus of PARC6 interacted strongly and specifically with the predicted mature ARC3 protein (Figure 5.8); these results were confirmed by another group (Zhang, Hu, *et al.* 2009b). Interestingly, the PARC6-ARC3 interaction requires the Membrane Occupation and Recognition Nexus (MORN) domain (Shimada, Koizumi, *et al.* 2004) (Figure 5.8), a region of ARC3 that was shown previously to inhibit a specific interaction between ARC3 and FtsZ1 (Maple, Vojta, *et al.* 2007).

PARC6 acts downstream of ARC6.

To investigate the functional relationship between ARC6 and PARC6, we generated *arc6 parc6* double mutants and compared their phenotypes with those of both parental mutants and wild-type plants (Figure 5.9A-D). *arc6 parc6* plants (Figure 5.9D) possess mesophyll chloroplast phenotypes that are more like those of *arc6* mutants (Figure 5.9C) than *parc6* mutants (Figure 5.9B), suggesting that *PARC6* acts downstream of *ARC6* during chloroplast division.

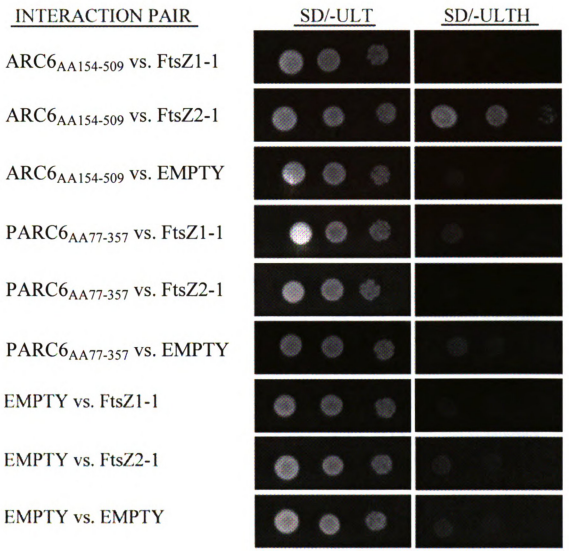

Figure 5.7. PARC6 does not interact with an FtsZ protein. Unlike ARC6, PARC6 does not interact with an FtsZ protein, as growth was not observed on synthetic dropout (SD) media lacking histidine (right column). Only constructs representing processed stromal portions of each protein were used to test for interaction. Dilutions at bottom of each column refer to dilution from a starting culture of $OD_{600} = 1.0$.

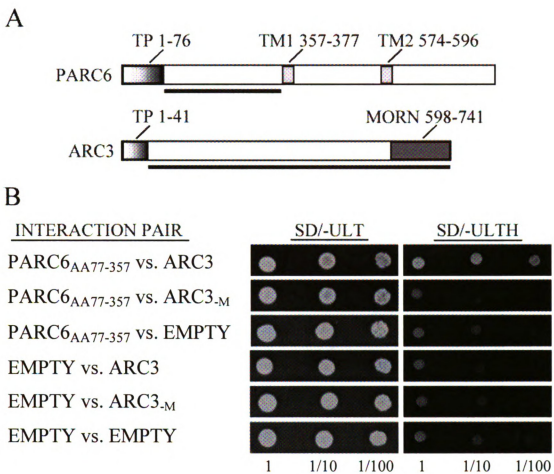

Figure 5.8. PARC6 interacts with ARC3. A schematic of the proteins used for interaction assays is shown in (A). The underline indicates the portion of the protein used for assay. Results of the two-hybrid assay are shown in (B). Dilutions at bottom of each column refer to dilution from a synthetic dropout (SD) starting culture of OD_{600} = 1.0. For interaction test between $PARC6_{AA77-357}$ and ARC3, a growth ratio of 0.67 was observed (growth on SD/-ULTH:growth on SD/-ULT) ~48h after spotting; all other interaction pairs had growth ratios of 0.07 or less. Transit peptide (TP); transmembrane domain (TM); $ARC3_{-MORN}$ ($ARC3_{-M}$).

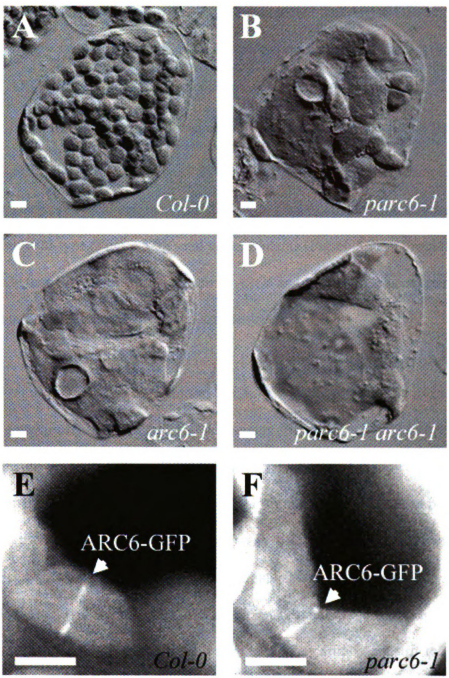

Figure 5.9. *PARC6* acts downstream of *ARC6*. Chloroplast phenotypes of *Col-0* (A); *parc6-1* (B); *arc6-1* (C); and a *parc6-1 arc6-1* double mutant are shown. ARC6-GFP localizes to mid-plastid rings in wild type *Col-0* (E) and *parc6-1* mutants (F), indicating that PARC6 is not required for ARC6 localization in *Arabidopsis*. Scale bar = 5 μm.

If PARC6 acts downstream of ARC6, we expected that ARC6-GFP should localize normally to chloroplast constriction sites in *parc6* mutants. To test this, we examined ARC6-GFP localization in *Col-0* and *parc6-1* mutants using an $ARC6_{pro}$:*ARC6-GFP* transgene that was used previously to examine ARC6 localization in *Arabidopsis* (Glynn, Froehlich, *et al.* 2008). Consistent with *ARC6* acting upstream of *PARC6*, we observed localization of ARC6-GFP to sites of constriction in young leaf cells of both wild-type (Figure 5.9E) and *parc6* mutants (Figure 5.9F). From these data, we conclude that *PARC6* acts downstream of *ARC6* and that PARC6 is not required for localization of *ARC6* to sites of chloroplast constriction.

PARC6 is required for PDV1 localization, but not for PDV2 or ARC5 localization.

We previously reported that ARC6 interacts directly with PDV2 and positions PDV2 at the division site (Glynn, Froehlich, *et al.* 2008). We also showed that ARC6 is required for equatorial positioning of GFP-PDV1, though direct interaction between ARC6 and PDV1 could not be confirmed by two-hybrid. At that time, we hypothesized the presence of at least one factor that acts as an intermediary between ARC6 and PDV1. Because PARC6 acts downstream of ARC6 and because *parc6* mutants (Figure 5.9B) possess a subpopulation of chloroplasts that resemble the partially-constructed chloroplasts observed in *pdv1* mutants (Miyagishima, Froehlich, *et al.* 2006), we hypothesized that PARC6 might be the factor that acts between ARC6 and PDV1. To test whether PARC6 is required for PDV1 localization, we examined GFP-PDV1 signals (Miyagishima, Froehlich, *et al.* 2006) in *Col-0* and *parc6-1* mutants (Figure 5.10). We

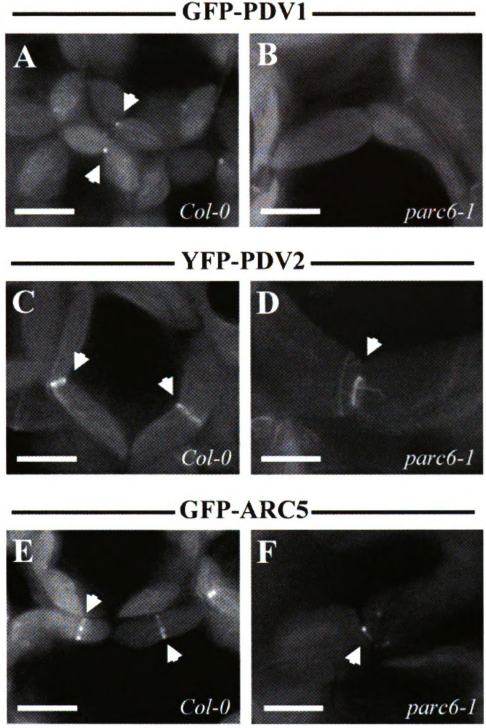

Figure 5.10. Localization of PDV1, PDV2, and ARC5 in *parc6* mutants. GFP-PDV1 localizes to mid-plastid constrictions in *Col-0* (A), but is unable to localize to the division site in *parc6-1* mutants (B). YFP-PDV2 (C, D) and GFP-ARC5 (E, F) localize to sites of constriction in *Col-0* (C, E) and *parc6-1* mutants (D, F). Scale bar = 5 μm.

were unable to observe any GFP-PDV1 signal at sites of chloroplast constriction in *parc6-1* mutants (Figure 5.10B), though GFP-PDV1 localized properly to dividing chloroplasts in wild-type (Figure 5.10A), was expressed in both wild type and *parc6-1* backgrounds based on immunoblotting (Glynn, Yang, *et al.* 2009), and can functionally complement the *pdv1* mutant (Miyagishima, Froehlich, *et al.* 2006). Taken together, the PDV1-like localization of PARC6 in *Arabidopsis* (Figure 5.4) and the loss of PDV1 localization in *parc6* mutants (Figure 5.10B) indicate a major role for PARC6 in positioning PDV1 at the division site.

Consistent with PARC6 acting downstream of ARC6 (Figure 5.9) and ARC6-dependent positioning of PDV2 (Glynn, Froehlich, *et al.* 2008), we observed YFP-PDV2 at sites of chloroplast constriction in *parc6-1* mutants as well as in wild type (Figure 5.10C-D). Further, in agreement with previous findingings that either PDV1 or PDV2 are capable of recruiting ARC5 to the division site (Miyagishima, Froehlich, *et al.* 2006), we also observed GFP-ARC5 positioned correctly in *parc6* mutants despite loss of PDV1 positioning (Figure 5.10E-F).

PARC6 binds the cytosolic domain of PDV1 in two-hybrid assays.

Because PARC6 is required for positioning PDV1 at the division site, we aimed to determine if PARC6 bound PDV1 in two hybrid assays. The C-terminus of PDV1 was previously shown to be localized to the IMS (Miyagishima, Froehlich, *et al.* 2006). We initially tested for interaction between the C-termini of PARC6 and PDV1, assuming that the C-terminus of PARC6 (AA 597-819, Figure 5.1) might reside within the

intermembrane space, with PARC6 having a topology similar to ARC6 (Vitha, Froehlich, *et al.* 2003). However, no interaction was detected between these two C-terminal domains, nor did the middle region of PARC6 (AA 378-573, Figure 1) interact with the C-terminus of PDV1 (M. Hemmes, J. Glynn, and K. Osteryoung, unpublished). Because PARC6 possesses two predicted transmembrane domains (Figure 1), possibly allowing it to span both envelope membranes (thereby placing the C-terminus (AA 597-819, Figure 5.1) in the cytosol), we also tested for interaction between the C-terminus of PARC6 and the cytosolic N-terminus of PDV1. To our surprise, a weak interaction between these two proteins was detected in yeast (Figure 5.11). This interaction is consistent with PARC6-dependent positioning of PDV1, but the precise topology of PARC6 remains to be determined. However, it must be seriously considered that PARC6 might have a more dynamic or complex topology relative to other division proteins.

PDV1 and PDV2 Independently Localize to the Division Site.

If PARC6 and ARC6 are responsible for positioning PDV1 and PDV2, at the division site, respectively, we predicted that PDV1 and PDV2 should localize independently of each other. To confirm this, we expressed GFP-PDV1 in *pdv2-1* mutants and YFP-PDV2 in *pdv1-1* mutants. GFP-PDV1 localized to the mid-plastid in the *pdv2-1* background (Figure 5.12B), indicating that PDV2 is not required for PDV1 localization. Similarly, YFP-PDV2 localized to the mid-plastid in the *pdv1-1* background (Figure 5.12D). We conclude that PDV1 and PDV2 localize to the division site independently of one another — PDV1 through PARC6 and PDV2 through ARC6 — though PARC6 localization and/or activity probably depends upon ARC6 (Figure 5.9).

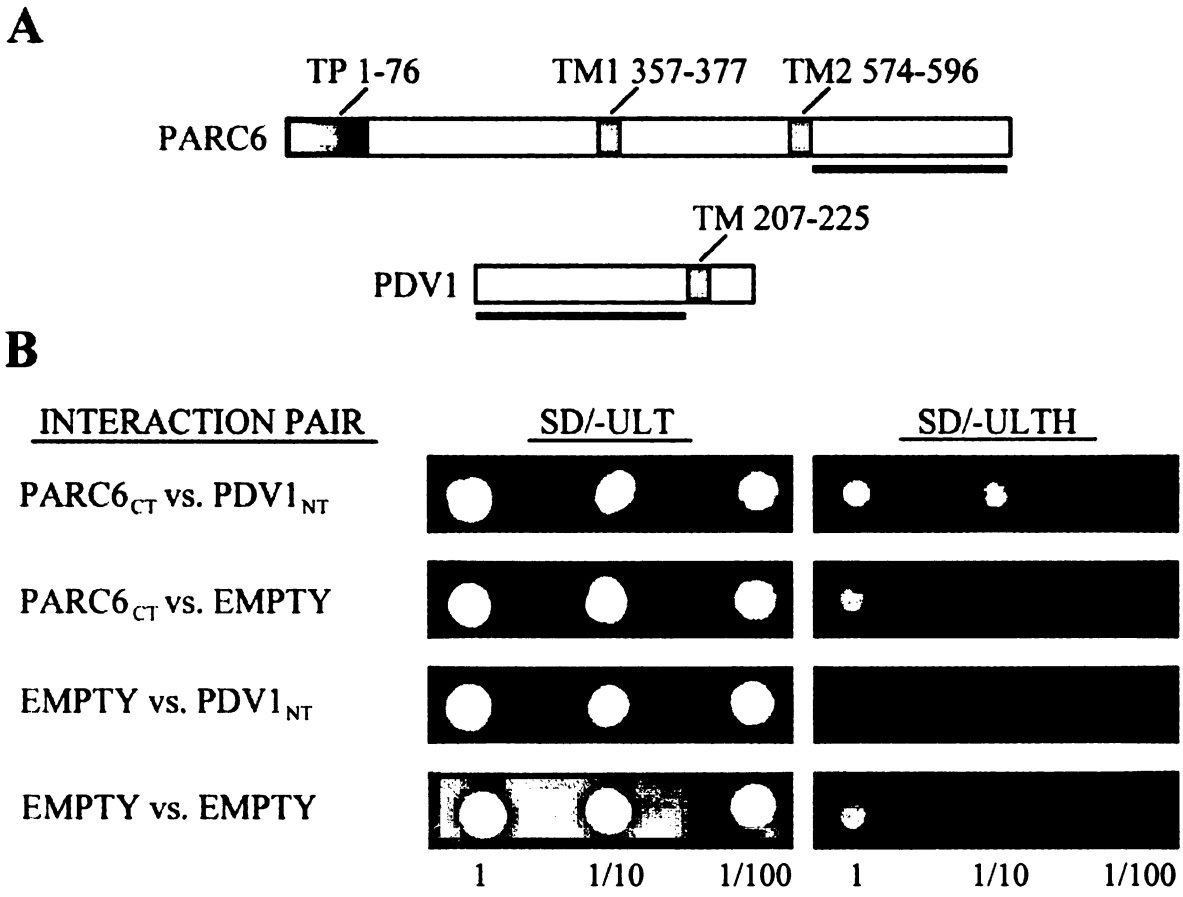

Figure 5.11. The C-terminus of PARC6 binds the cytosolic domain of PDV1. Schematic showing proteins tested in yeast two-hybrid interaction assays (A). The underline indicates the segment of each protein used in the interaction assays. Results of two-hybrid reporter assays on synthetic dropout (SD) media are shown in (B), showing growth on media supplemented with histidine (left panels) and media lacking histidine (right panels). Growth ratio (growth on SD/-ULTH: growth on SD/-ULT) for $PARC6_{CT}$ and $PDV1_{NT}$ was 0.37, while all other interactions tested were 0.1 or less. Dilutions at the bottom of each column indicate dilution from a starting culture of $OD_{600} = 1.0$.

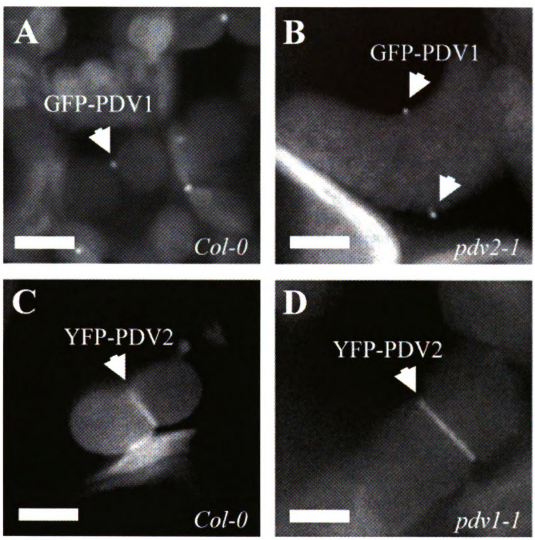

Figure 5.12. PDV1 and PDV2 localize independently of each other. GFP-PDV1 localization (A, B) and YFP-PDV2 localization (C, D) in *Col-0* (A, C), *pdv2-1* (B), and *pdv1-1* (D) mutants. PDV2 is not required for localization of PDV1 (B) nor is PDV1 required for localization of PDV2 (D). Scale bar = 5 μm.

Discussion

Here we characterize the new chloroplast division protein PARC6, a protein of tracheophyte origin that, like ARC6, is a multi-functional integral inner envelope protein that aids the coordination of the FtsZ and dynamin rings across the envelope membranes. However, our results show that PARC6 acts downstream of ARC6 in the division process and that its function differs significantly from that of ARC6: (1) PARC6 and ARC6 have distinct localization patterns in *Arabidopsis*. In incompletely constricted chloroplasts, ARC6 appears as a continuous ring at the division site (Glynn, Froehlich, *et al.* 2008, Vitha, Froehlich, *et al.* 2003, Yang, Glynn, *et al.* 2008) whereas PARC6 localizes to puncta. PARC6 also localizes to foci at the poles of some plastids, which has not been observed for ARC6. (2) PARC6 acts as an inhibitor of FtsZ assembly whereas ARC6 promotes FtsZ assembly. (3) ARC6 is required for recruitment of PDV1, PDV2, and ARC5 to the division site whereas PARC6 is required only for recruitment of PDV1. A working model depicting the roles of ARC6 and PARC6 in the coordination and activity of the FtsZ and dynamin rings at the division site is shown in a later chapter.

Despite the overall sequence identity between ARC6 and PARC6 (~21%), there are many differences that may contribute to their functional divergence. PARC6 lacks the J-like domain present in ARC6, suggesting it also lacks the co-chaperone activity hypothesized for ARC6 (Vitha, Froehlich, *et al.* 2003). Additionally in contrast with ARC6, which has one transmembrane domain, multiple PARC6 sequences bear two predicted transmembrane domains (Glynn, Yang, *et al.* 2009), one of which (TM1;

Figure 5.1) interrupts a segment conserved in ARC6 family members that resides in the stroma (Glynn, Yang, *et al.* 2009, Vitha, Froehlich, *et al.* 2003); the divergence in ARC6-PARC6 similarity in this region coincides with absence of the FtsZ2-binding domain ($ARC6_{AA\ 351-503}$) in PARC6 proteins (Figure 5.1). Preliminary protease protection assays in pea support the TM1 prediction (Glynn, Yang, *et al.* 2009) and, along with the interaction between $PARC6_{AA77-357}$ and ARC3 (Figure 5.8), are consistent with a topology placing the N-terminus of PARC6 in the stroma. Though the TM2 prediction remains to be confirmed, it is predicted in several PARC6 sequences and is aligned closely with the ARC6 transmembrane domain (Figure 5.1) (Glynn, Yang, *et al.* 2009). Moreover, we show here that the C-terminus of PARC6 interacts with the cytosolic domain of PDV1 (Figure 5.11), suggesting that PARC6 might traverse both envelope membranes. While preliminary protease protection assays indicate that PARC6 does not traverse the outer envelope (Glynn, Yang, *et al.* 2009), PARC6 may have a more complicated or dynamic topology *in vivo*. If such an orientation is validated, it is curious as to why the C-termini of ARC6 and PARC6 would be compartmentally separated, given the sequence similarity near their C-termini. Full topological analysis will be critical to confirm these results and for further dissection of PARC6 functional domains.

The long FtsZ filaments observed in the enlarged chloroplasts of *parc6-1* mutants (Figure 5.6) suggest that, *in vivo*, PARC6 inhibits FtsZ assembly. This activity may be indirect because PARC6 does not interact with FtsZ1 or FtsZ2 in two-hybrid assays (Figure 5.7). The inhibitory effect of PARC6 on FtsZ assembly may rather be a consequence of its interaction with ARC3 (Figure 5.8) (Zhang, Hu, *et al.* 2009b), because

ARC3 has been proposed as a functional replacement for MinC (Maple, Vojta, *et al.* 2007), a prokaryotic protein known to promote disassembly of bacterial FtsZ (Hu, Mukherjee, *et al.* 1999, Margolin 2003, Pichoff and Lutkenhaus 2001). The similar chloroplast and FtsZ morphologies in *parc6* (Figure 5.3 and Figure 5.6) and *arc3* mutants (Glynn, Miyagishima, *et al.* 2007, Marrison, Rutherford, *et al.* 1999, Pyke and Leech 1992, Pyke and Leech 1994), are consistent this hypothesis. The opposing activities of ARC6 and PARC6 in promoting and inhibiting FtsZ assembly, respectively, suggest that these two proteins may function as antagonistic regulators of Z-ring dynamics within the stroma. We do not yet know whether this or other activities of PARC6 involve direct interaction with ARC6, though preliminary data suggests that they may interact through their stromal domains (Y. Yang and K. Osteryoung, unpublished).

The requirement of the ARC3 MORN domain for PARC6-ARC3 interaction (Figure 5.8) contrasts with the finding that the MORN domain inhibits interaction between ARC3 and FtsZ1 (Maple, Vojta, *et al.* 2007). These observations suggest that FtsZ disassembly may be controlled, at least in part, by the availability of the ARC3 MORN domain. Interaction of ARC3 with PARC6 could sequester the MORN domain, allowing ARC3 to interact with FtsZ1 to promote FtsZ filament disassembly, perhaps through disruption of the FtsZ1-FtsZ2 heteropolymer. Dynamic interaction between ARC3 and PARC6 could thereby regulate FtsZ dynamics *in vivo*, though other factors, including MinD, MinE and MCD1, certainly contribute (Aldridge and Moller 2005, Colletti, Tattersall, *et al.* 2000, Fujiwara, Hashimoto, *et al.* 2008, Fujiwara, Nakamura, *et al.* 2004, Itoh, Fujiwara, *et al.* 2001, Maple, Chua, *et al.* 2002, Maple and Moller 2007,

Nakanishi, Suzuki, *et al.* 2009, Reddy, Dinkins, *et al.* 2002). Because MORN domains have been shown to be important for membrane association (Ma, Lou, *et al.* 2006), an alternative possibility for the MORN-mediated PARC6-ARC3 interaction is that it only occurs near the surface of a membrane. Removal of the MORN sequence from ARC3 could prevent its association with the IEM, thereby preventing interaction with PARC6.

PDV1 and PDV2 localization at the division site, though independent of one another (Figure 5.12), both require ARC6 (Glynn, Froehlich, *et al.* 2008). PDV2 localization is established by direct interaction with ARC6, but it was previously unclear how ARC6 directs PDV1 localization, as we did not detect interaction between ARC6 and PDV1 using two hybrid assays (Glynn, Froehlich, *et al.* 2008). Our current results show that PARC6 acts as an intermediary between ARC6 and PDV1, functioning to organize PDV1 at the division site (Figure 5.9 and Figure 5.10). PDV1 positioning by PARC6 may involve direct interaction with PDV1 within the cytosol, based on our two hybrid experiments (Figure 5.11). Beyond this question, the mid-plastid localization of either PDV1 or PDV2 is clearly sufficient for ARC5 recruitment, but our collective data indicate that localization of both PDV1 and PDV2 at the division site is required for full ARC5 contractile activity (Glynn, Froehlich, *et al.* 2008, Miyagishima, Froehlich, *et al.* 2006). This aspect of chloroplast division remains to be explored.

During division, PDV1 initially localizes to a medial punctate ring that becomes reduced to a single spot in deeply constricted chloroplasts. The PDV1 spot persists at the pole of one of the two daughter organelles following their separation. ARC5 behaves

similarly (Miyagishima, Froehlich, *et al.* 2006). Intriguingly, the localization patterns we observed for PARC6 (Figure 5.4) suggest that it also follows a PDV1-like progression during division, possibly being retained at the pole of a single daughter chloroplast. We speculate that the lingering PARC6 spot could play a role in establishing organelle polarity within the stroma, which might be important for defining the new division site prior to the next round of division. In *E. coli*, cell polarity and division-site positioning are established by the dynamic behavior of the Min system, which restricts FtsZ ring assembly to the midcell (Lutkenhaus 2007). The fact that ARC3 interacts with PARC6 and that ARC3 and PARC6 exhibit partial polar localization raises the possibility that PARC6, perhaps via interaction with ARC3 and/or other components of the plastidic Min system (Fujiwara, Hashimoto, *et al.* 2008, Fujiwara, Nakamura, *et al.* 2004, Itoh, Fujiwara, *et al.* 2001, Maple, Chua, *et al.* 2002, Maple and Moller 2007, Maple, Vojta, *et al.* 2007, Nakanishi, Suzuki, *et al.* 2009), could play a role in directing the orientation of the Min system within the stroma and hence in placing the new division site. Analysis of *parc6 arc3* double mutants, ARC3 localization in *parc6*, and PARC6 localization in *arc3* mutants will be critical to ordering these factors in a pathway and understanding how each of them impact division site selection.

The emergence of PARC6 in vascular plants follows the emergence of ARC3 in green algae (Yang, Glynn, *et al.* 2008) and PDV1/PDV2 in mosses (Miyagishima, Froehlich, *et al.* 2006), perhaps allowing for greater control of FtsZ dynamics and chloroplast morphology. Presumably, the dissimilar regions of ARC6 and PARC6 confer protein-specific functions and will provide clues to the individual domains responsible

for their unique functions. For example, the N-terminal stromal domain of PARC6 does not interact with Arabidopsis FtsZ2 (Figure 5.7), in contrast to that of ARC6 (Maple, Aldridge, *et al.* 2005), but has apparently evolved to interact with ARC3, perhaps via the ARC3 MORN domain. Similarly, while the C-termini of PARC6 and ARC6 share a high degree of sequence similarity (Figure 5.1) (Glynn, Yang, *et al.* 2009), subtle differences within this conserved region might mediate specific interactions with other proteins, though the precise location of the C-terminus of PARC6 remains to be determined.

The activities of the FtsZ and dynamin rings are presumably coordinated with those of the inner and outer plastid-dividing (PD) rings, electron-dense components of the plastid division machinery whose compositions are not yet known (Kuroiwa, Kuroiwa, *et al.* 1998, Miyagishima, Nishida, *et al.* 2003b, Yoshida, Kuroiwa, *et al.* 2006). It will be interesting to learn whether PARC6 and ARC6 interact with or otherwise influence the operation of the PD rings. Further studies to elucidate the functional and evolutionary relationship between PARC6 and other plastid division components should deepen our understanding of the mechanisms contributing to coordination of the internal and external division complexes.

Materials and Methods

Sequence and Phylogenetic Analysis.

These sequences were used for alignments and phylogeny: *Arabidopsis thaliana* (AtPARC6, NP_188549); *Medicago truncatula* (MtPARC6, IMGAG-annotated pseudomolecule AC157350_28.4); *Oryza sativa cv. japonica* (OsPARC6, NP_001054252); *Populus trichocarpa* (PtPARC6, a GENSCAN-based prediction (Burge and Karlin 1997) of *Populus trichocarpa* genome Scaffold_122 204390-215000); *Vitis vinifera* (VvPARC6, CAO48483); *Arabidopsis thaliana* (AtARC6, NP_199063); *Oryza sativa cv. japonica* (OsARC6, NP_001045726); *Ostreococcus lucimarinus* (OlARC6, XP_001421185); *Physcomitrella patens* (PpARC6, XP_001778770); *Zea mays* (ZmARC6, ACG29776); *Thermosynechococcus elongatus* BP-1 (TeFtn2, BAC08309); *Synechococcus elongatus* PCC 7942 (SeFtn2, ABB57973); *Nostoc* sp. PCC 7120 (NsFtn2, BAB74406); *Crocosphaera watsonii* WH 8501 (CwFtn2, EAM48783); and *Cyanothece* sp. ATCC 51142 (CsFtn2, ACB49642). Evolutionary history was inferred by Neighbor-Joining (Saitou and Nei 1987) following multiple sequence alignment with MEGA4 (Tamura, Dudley, *et al.* 2007) using an identity matrix. The bootstrap consensus-tree inferred from 1000 replicates represents the evolutionary history of the taxa analyzed (Felsenstein 1985). Branches corresponding to partitions reproduced in less than 50% bootstrap replicates are collapsed. The percentage of replicate trees in which the associated taxa clustered together in the bootstrap test (1000 replicates) are shown next to the branches (Felsenstein 1985). Tree is drawn to scale, with branch lengths in the same units as evolutionary distances used to infer the phylogenetic tree.

Evolutionary distances were computed using the Poisson correction method (Zuckerkandl and Pauling 1965) and are given as the number of amino acid substitutions per site. All positions containing gaps and missing data were eliminated from the dataset (Complete deletion option). There were 441 positions in the final dataset.

Analysis of Chloroplast Morphology.

Tissue preparation was carried out as described previously (Miyagishima, Froehlich, *et al.* 2006, Pyke and Leech 1991, Vitha, Froehlich, *et al.* 2003). Quantitative analysis of *Col-0* and *parc6-1* phenotypes was performed using the distal 3-4 mm of the largest leaf present on plants 30 days after sowing.

Analysis of Subcellular Localization of PARC6

$35S_{pro}$-*PARC6*$_{TP}$-*YFP* and $35S_{pro}$-*PARC6-YFP* constructs were made using the Gateway System (Invitrogen, http://www.invitrogen.com/). A *PARC6* cDNA was used as template for PCR. Analysis of PARC6 localization in tobacco and in *Arabidopsis* was performed as described (Glynn, Yang, *et al.* 2009).

Production of PARC6 antibody.

The coding sequence for the N-terminus of mature PARC6 ($PARC6_{AA\ 77\text{-}357}$) was cloned into pHIS9 (Yang, Xu, *et al.* 2008) and His-tagged protein was expressed in *E. coli* Rosetta DE3 (Novagen). The insoluble recombinant protein was solubilized with 6M urea and purified using Ni-agarose. Subsequent SDS-PAGE removed urea and purified the antigen. After brief coomassie-blue staining, antigen was excised from the

gel and rabbit antibodies for PARC6 were generated by Covance Research Products, Inc. Exsaguination serum was used at 1:5,000 for immunoblotting.

Analysis of PARC6 Fractionation and Topology.

Pea chloroplast isolation and fractionation into membrane and soluble fractions was performed as described previously (Bruce, Perry, *et al.* 1994); additional details can be found elsewhere (Glynn, Yang, *et al.* 2009).

Analysis of FtsZ Localization.

Tissue preparation, fixation, and immunofluorescence analysis were carried out as described previously (Miyagishima, Froehlich, *et al.* 2006, Vitha, Froehlich, *et al.* 2003, Vitha, McAndrew, *et al.* 2001).

Two-hybrid Analysis.

Clones for two hybrid analysis were made using methods as described (Glynn, Yang, *et al.* 2009). *HIS3* reporter assays were performed as described previously (Glynn, Froehlich, *et al.* 2008, Maple, Aldridge, *et al.* 2005).

Tests of Epistasis.

arc6-1 was crossed to *parc6-1* and *arc6 parc6* double mutants were identified by genotype. SALK genotyping primers were used as described (Alonso, Stepanova, *et al.* 2003) for identifying homozygous *parc6-1* plants. An NlaIII-containing dCAPS marker (Neff, Neff, *et al.* 1998) was used to identify the *arc6-1* mutation; the product generated

from these two primers harbors an additional NlaIII site when *arc6-1* genomic DNA is amplified. Lines homozygous for both mutations were used for double mutant analysis. All primers used for genotyping are described elsewhere (Glynn, Yang, *et al.* 2009).

Analysis of ARC6, PDV1, PDV2, and ARC5 Localization.

Transgenes for $ARC6_{pro}$-*ARC6-GFP*, $PDV1_{pro}$-*GFP-PDV1*, $PDV2_{pro}$-*YFP-PDV2*, and $ARC5_{pro}$-*GFP-ARC5* were introduced by *Agrobacterium*-mediated transformation (Clough and Bent 1998). Following selection of T_1 individuals, young leaves of transgenic plants were examined by fluorescence microscopy using a Leica DMRA2 microscope outfitted with a Retiga EXi camera.

Extract Preparation and Immunoblotting.

Whole-cell extracts for anti-FtsZ1-1 and anti-FtsZ2-1 immunoblots were prepared by grinding tissue from 11 day-old plate-grown plants in liquid nitrogen. The resulting powder was homogenized in 5 volumes of Extraction Buffer (25mM Tris, pH 7.4 containing 4mM dithiothreitol, 0.1% Triton X-100, and protease inhibitors). An equal amount of loading buffer was added to this homogenate before boiling. Four microliters of each sample was loaded for SDS-PAGE and transferred to nitrocellulose. The blot was probed with FtsZ1-1 or FtsZ2-1 antibodies at 1:15000 in 5% blocking buffer.

Acknowledgements

I thank Yue Yang for developing the PARC6 antibodies, determining preliminary topology of PARC6, providing localization of PARC6 in tobacco, and sharing data on ARC6-PARC6 interaction. I thank Stan Vitha for examining FtsZ localization in *parc6* mutants and determining localization of PARC6-GFP in *Arabidopsis*. I thank Aaron Schmitz (ARC3) and Mia Hemmes (PARC6) for generating the two hybrid clones used here. Finally, I thank Shin-ya Miyagishima for providing the *parc6*-2 and *parc6-3* alleles.

Most of this chapter and the figures therein are reproduced from (Glynn, Yang, *et al.* 2009) (http://www.wiley.com/bw/journal.asp?ref=0960-7412/) and is Copyright Blackwell Publishing. Blackwell Publishing allows the author to re-use your own article in another publication providing you are editor or co-editor (author or co-author) of the new publication.

Chapter 6

A Conserved Aspartate within ARC6 Influences Plastid Size and Z-ring Position.

Abstract

The systems controlling positioning and assembly of the complexes that mediate plastid division are likely to be integrated with each other to allow for efficient regulation of the division process. The site of bulk assembly of the FtsZ polymers within the stroma is restricted to the mid-plastid by the Min system, composed of ARC3, MinD, MinE, MCD1, and PARC6. However, ARC6 is absolutely required for Z-ring formation *in vivo*. It is unclear if or how the activities of ARC6 and the Min system are coordinated to ensure efficient assembly and operation of the plastidic Z-ring. Here, we perform preliminary characterization of a novel hypomorphic allele of *ARC6*, $arc6_{D205N}$. $arc6_{D205N}$ mutants possess subtle alterations in chloroplast size and morphology, relative to wild type, perhaps due to decreased amounts of ARC6 protein. Most intriguingly, $arc6_{D205N}$ mutants harbor misplaced and miniaturized Z-rings within the stroma, implicating ARC6 in the operation of the plastidic Min system. The conservation of $ARC6_{D205}$ amongst land plants, algae, and cyanobacteria suggests that this mechanism of crosstalk between factors that position and stabilize the Z-ring probably occurs in all ARC6- and Ftn2-encoding organisms.

Introduction

The FtsZ ring (Z-ring) is a central player in bacterial cell division and plastid fission, providing some small amount of contractile force and serving as a scaffold for other division proteins (Erickson 2009, Osawa, Anderson, *et al.* 2008, Rothfield, Taghbalout, *et al.* 2005). In most bacteria, a single FtsZ gene encodes a polymer-forming GTPase with structural similarity to eukaryotic tubulins (Erickson, Taylor, *et al.* 1996, Mukherjee, Dai, *et al.* 1993).

In bacteria, positioning of the Z-ring is critical to ensuring an equal distribution of cytoplasm and genetic material between new daughter cells. At least two systems provide input into the positioning of the Z-ring in *E. coli*: the *n*ucleoid *oc*clusion (Noc) system and the *min*icell (Min) system (Rothfield, Taghbalout, *et al.* 2005).

The Noc system prevents chromosomal scission during division by inhibiting Z-ring formation around the bacterial chromosome (Bernhardt and de Boer 2005). Uniquely, both plastids and cyanobacteria carry multiple chromosomal copies (Birky and Walsh 1992, Doolittle 1979, Falkow, Dworkin, *et al.* 2006, Schneider, Fuhrmann, *et al.* 2007) and do not utilize proteins with sequences similar to Noc proteins (Glynn, Miyagishima, *et al.* 2007). Moreover, it has been shown that Z-rings can form around the chromosome in the cyanobacterium *Synechococcus elongatus* (Miyagishima, Wolk, *et al.* 2005). Based on these and other observations, nucleoid occlusion is probably not a mechanism employed in these lineages; rather it is likely that chromosomal segregation

in the cyanobacteria is largely managed by maintaining multiple chromosomal copies (Bin, Guohua, *et al.* 2007). Because of its apparent lack of relevance to plastid division, we will limit our review of the nucleoid occlusion system and focus on the other Z-ring positioning input, the Min system.

The Min system in gram-negative bacteria is composed of three primary factors: MinC, MinD, and MinE (Lutkenhaus 2007). MinC binds FtsZ and inhibits Z-ring assembly by preventing lateral associations (Hu, Mukherjee, *et al.* 1999, Scheffers 2008, Shen and Lutkenhaus 2009). However, the FtsZ assembly-inhibiting activity of MinC is regulated by MinD, which is tethered to the membrane and promotes MinC activity only in the polar zones of the cell (Hu and Lutkenhaus 1999, Raskin and de Boer 1999a, Szeto, Rowland, *et al.* 2002). MinD is regulated by MinE through a mechanism in which MinE binds to MinD and causes it to be released from the membrane (Hu and Lutkenhaus 2001). The maximum concentration of MinE occurs near the midcell adjacent to the membrane, thereby causing the concentration of active MinC and MinD to be highest at the poles (Hale, Meinhardt, *et al.* 2001). While the determinants for MinE localization are unknown, the midcell zone created by MinE activity allows for FtsZ protofilament assembly along the inner leaflet of the plasma membrane at the midcell (Rothfield, Taghbalout, *et al.* 2005). In some bacteria that lack MinE, DivIVA tethers MinD at the cell poles and inhibits FtsZ polymerization within the polar zone by maintaining a higher concentration of active MinCD at the poles (Marston and Errington 1999).

The components of the plastidic Min system are the only known factors that are responsible for positioning the Z-ring within chloroplasts. The Min system is now known to be made up of at least five components in *Arabidopsis*: AtMinD (Colletti, Tattersall, *et al.* 2000), AtMinE (Maple, Chua, *et al.* 2002), ARC3 (Glynn, Miyagishima, *et al.* 2007, Maple, Vojta, *et al.* 2007), MCD1 (Nakanishi, Suzuki, *et al.* 2009), and PARC6 (Glynn, Yang, *et al.* 2009, Zhang, Hu, *et al.* 2009a). There is no MinC ortholog in any of the vascular plants sequenced to date (Yang, Glynn, *et al.* 2008), but ARC3 seems to fulfill a similar functional role *in vivo* (Glynn, Miyagishima, *et al.* 2007, Maple, Vojta, *et al.* 2007). On the basis of their sequence and phenotypic similarity, it was hypothesized that AtMinD and AtMinE might work similarly to *E. coli* MinD and MinE (Colletti, Tattersall, *et al.* 2000, Fujiwara, Nakamura, *et al.* 2004, Maple, Chua, *et al.* 2002). AtMinD exhibits both polar and equatorial localization in chloroplasts (Fujiwara, Nakamura, *et al.* 2004, Nakanishi, Suzuki, *et al.* 2009), suggesting that it may relocate or oscillate, similar to *E. coli* MinD (Raskin and de Boer 1999b), to regulate Z-ring position. AtMinE localizes to poles in tobacco chloroplasts (Maple, Chua, *et al.* 2002) in contrast to its mostly mid-zone localization in bacteria (Hale, Meinhardt, *et al.* 2001, Sun and Margolin 2001), though the localization pattern of functional AtMinE under native expression conditions in *Arabidopsis* has not yet been demonstrated. MCD1 is required for AtMinD function and binds AtMinD, but the inputs into this plant-specific division protein are not yet clear (Nakanishi, Suzuki, *et al.* 2009). Similarly, PARC6 appears to inhibit Z-ring assembly through its interaction with ARC3, but further work is required in order to fully determine how this protein is integrated into the plastidic Min system (Glynn, Yang, *et al.* 2009, Zhang, Hu, *et al.* 2009b).

ARC6 is a bitopic inner envelope protein of cyanobacterial origin and was shown to aid assembly and/or stabilization of the Z-ring (Vitha, Froehlich, *et al.* 2003). However, it was not clear if ARC6/Ftn2 has any role in positioning the Z-ring within chloroplasts or cyanobacteria. Here we characterize a novel allele of *ARC6*, $arc6_{D205N}$, that exhibits *min*-like defects in chloroplast morphology and Z-ring positioning. Consistent with its profound effect upon Z-ring placement, we show that $ARC6_{D205}$ is a conserved residue in all ARC6-like proteins. The effect of $arc6_{D205N}$ upon Z-ring placement probably does not occur through AtMinE, but we show here ARC6 ring formation requires both *FtsZ* and *AtMinE*. We conclude that ARC6 plays a role in influencing Z-ring placement and propose that ARC6 might affect division-site selection through PARC6 or another Min-system component.

Results

$arc6_{D205N}$ is a Hypomorphic Allele of ARC6 that is Associated with Defects in Chloroplast Morphology and Number.

To identify important functional domains within ARC6, we used TILLING (McCallum, Comai, *et al.* 2000) to identify novel alleles of *ARC6* that are associated with defects in chloroplast division. A major advantage of TILLING is that *in vivo* relevance for any new allele can be quickly determined by the same established assay(s) used to identify mutants in forward genetic screens (Henikoff, Till, *et al.* 2004). We targeted the two large conserved regions within ARC6 (see Figure 1.4) for TILLING (Vitha,

Froehlich, *et al.* 2003) and identified 14 novel mutations within the *ARC6* locus that lead to amino acid changes within the ARC6 protein: P85S, P87S, D205N, S250N, G293D, L309F, A328V, A592T, A621V, R677K, E705K, D708N, S763F, and T773I. We were able to isolate homozygous lines for each of these polymorphisms, with one exception (A328V), by screening with molecular markers (Neff, Neff, *et al.* 1998). Of these, only $arc6_{D205N}$ exhibited defects in chloroplast morphology and number. $arc6_{D205N}$ mutants have slightly enlarged chloroplasts and possess slightly fewer chloroplasts than the corresponding wild type TILLING parental line, Col-*er105* (Figure 6.1); the phenotype associated with $arc6_{D205N}$ is recessive to the wild type allele. In addition to the enlarged chloroplasts present within $arc6_{D205N}$, we occasionally observed mini-chloroplasts within this line (see later sections). These mini-chloroplasts could arise from asymmetric positioning of the Z-ring, in a process similar to the asymmetric division events that generate chloroplasts of varying sizes in *Arabidopsis min* mutants (Colletti, Tattersall, *et al.* 2000); however, the number and incidence of mini-chloroplasts in $arc6_{D205N}$ was highly variable. From these results, we conclude that $ARC6_{D205}$ is a functionally-important residue *in vivo* that could be involved in the operation of the plastidic Min system.

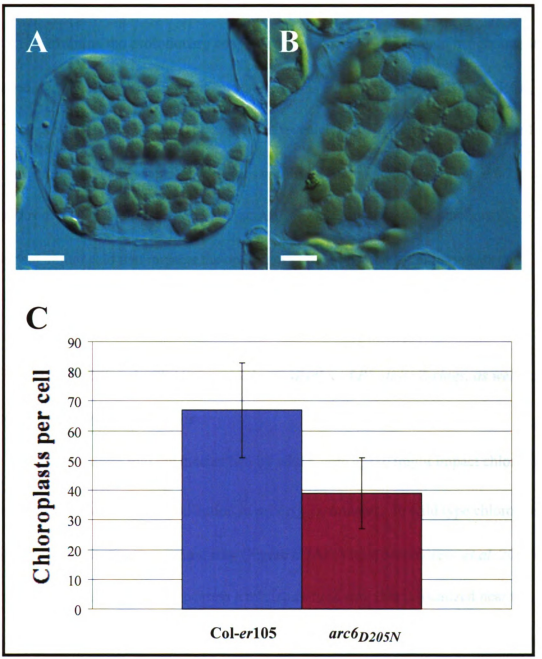

Figure 6.1. *arc6*$_{D205N}$ is associated with a defect in chloroplast size and number. Chloroplast phenotypes are shown from expanded leaf cells of Col-*er*105 (A) and *arc6*$_{D205N}$ (B). Scale bars = 10 μm. Quantitative analysis of chloroplast number is shown in panel (C). Error bars represent standard deviation from the mean; 25 cells were counted for each line; the average cell plan area was 3279 ± 467 μm^2.

$ARC6_{D205}$ is conserved in land plants, algae, and cyanobacteria.

To examine the evolutionary conservation of $ARC6_{D205}$ and gain insight into its function, we generated multiple sequence alignments between several ARC6, PARC6, and Ftn2 proteins (Figure 6.2). The alignment revealed that $ARC6_{D205}$ is a conserved residue (Figure 6.2, arrowhead) that resides within a 9 amino acid motif (Figure 6.2, line). From this analysis, we conclude that $ARC6_{D205}$ is likely to be a functionally-important amino acid that impacts the operation of the divisomes of chloroplasts and cyanobacteria by a similar mechanism.

$arc6_{D205N}$ is Associated with Miniaturized and Misplaced Plastidic Z-rings, as well as a Decrease in ARC6 Protein Levels .

To gain insight into the mechanism by which *$arc6_{D205N}$* might impact chloroplast division, we examined FtsZ localization in *$arc6_{D205N}$* mutants. In wild type chloroplasts, FtsZ proteins colocalize to a central ring (Figure 6.3A) (Vitha, McAndrew, *et al.* 2001). In contrast, *$arc6_{D205N}$* mutants possess a miniature FtsZ ring that is localized near the chloroplast periphery (Figure 6.3B). This FtsZ localization pattern suggests that ARC6 not only regulates FtsZ assembly within plastids (Vitha, Froehlich, *et al.* 2003), but may also influence the size and position of the Z-ring. Moreover, this peripheral Z-ring localization might be connected to the unusual mini-chloroplast phenotype observed in *$arc6_{D205N}$* plants (Figure 6.3C-D).

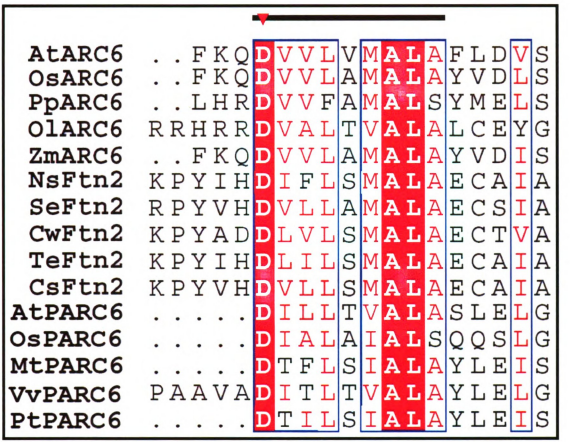

Figure 6.2. Multiple sequence alignment showing conservation of ARC6$_{D205}$. Boxed regions indicate sequence similarity and shaded regions indicate sequence identity. This portion of the alignment has been cropped from an alignment of the full-length proteins and is published elsewhere (Glynn, Yang, *et al.* 2009). Black line (top) indicates 9-mer amino acid motif and aspartate 205 of *Arabidopsis* ARC6 is indicated with a red arrowhead. *Arabidopsis thaliana* (At); *Medicago truncatula* (Mt); *Oryza sativa* cv. japonica (Os); *Populus trichocarpa* (Pt); *Vitis vinifera* (Vv); *Ostreococcus lucimarinus* (Ol); *Physcomitrella patens* (Pp); *Zea mays* (Zm); *Thermosynechococcus elongatus* BP-1 (Te); *Synechococcus elongatus* PCC 7942 (Se); *Nostoc sp.* PCC 7120 (Ns); *Crocosphaera watsonii* WH 8501 (Cw); and *Cyanothece sp.* ATCC 51142 (Cs).

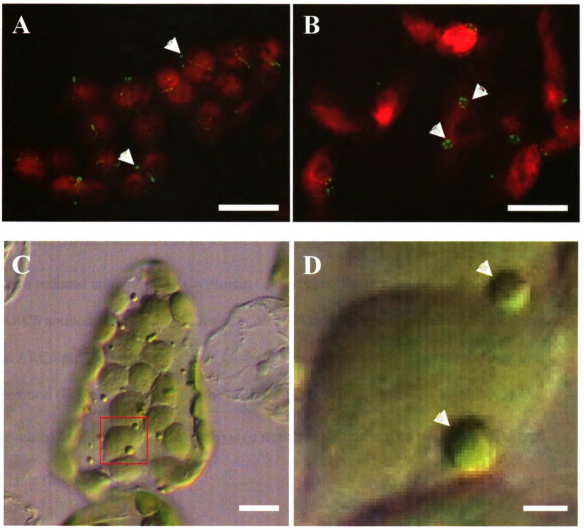

Figure 6.3. FtsZ localization and mini-chloroplasts in *arc6*$_{D205N}$.

Immunolocalization of FtsZ2-1 in young leaves of Col-*er*105 (A) and *arc6*$_{D250N}$ (B). Chlorophyll autofluorescence is indicated in red and FtsZ protein is shown in green; arrowheads point to Z-rings. Mini-chloroplast phenotype observed in *arc6*$_{D205N}$ is shown in (C), boxed region is magnified and shown in (D). Arrowheads point to mini-chloroplasts in (D). Scale bars in (A-C) are 10 μm. Scale bar in (D) is 2 μm.

To determine if ARC6 levels are affected in the *arc6$_{D205N}$* background, we examined the relative amounts of ARC6 and FtsZ protein in Col-*er105* and *arc6$_{D205N}$* flower buds using ARC6- and FtsZ-specific antibodies (McAndrew, Olson, *et al.* 2008, Vitha, McAndrew, *et al.* 2001). Consistent with a defect in ARC6 function, we observed less ARC6 protein in *arc6$_{D205N}$* lines than in wild type (Figure 6.4). While no ARC6 protein was detected in this background by immunoblotting, there must be a small amount of ARC6 protein present, as *arc6* null mutants have only one or two chloroplasts per cell (Glynn, Froehlich, *et al.* 2008, Vitha, Froehlich, *et al.* 2003); *arc6$_{D205N}$* likely has a reduced amount of ARC6 protein that is below the threshold of detection for our ARC6 antibody (McAndrew, Olson, *et al.* 2008). However, it is unclear if this decrease in ARC6 protein level is the basis for the defect observed in Z-ring morphology and position (Figure 6.3B). Unlike the *arc6-1* mutant (Vitha, Froehlich, *et al.* 2003), the levels of FtsZ1 and FtsZ2 in *arc6$_{D205N}$* were mostly unchanged relative to wild type plants (Figure 6.4).

AtMinE-YFP has a unique localization pattern in Arabidopsis and ARC6$_{D205}$ mutants do not interact with AtMinE.

It was previously noted that both *arc6-1* mutants and *arc12* (*atminE*) mutants have very similar phenotypes with respect to chloroplast morphology, as the leaf cells within both of these mutants typically contain only one or two large chloroplasts (Glynn, Miyagishima, *et al.* 2007, Pyke, Rutherford, *et al.* 1994, Rutherford 1996). Interestingly,

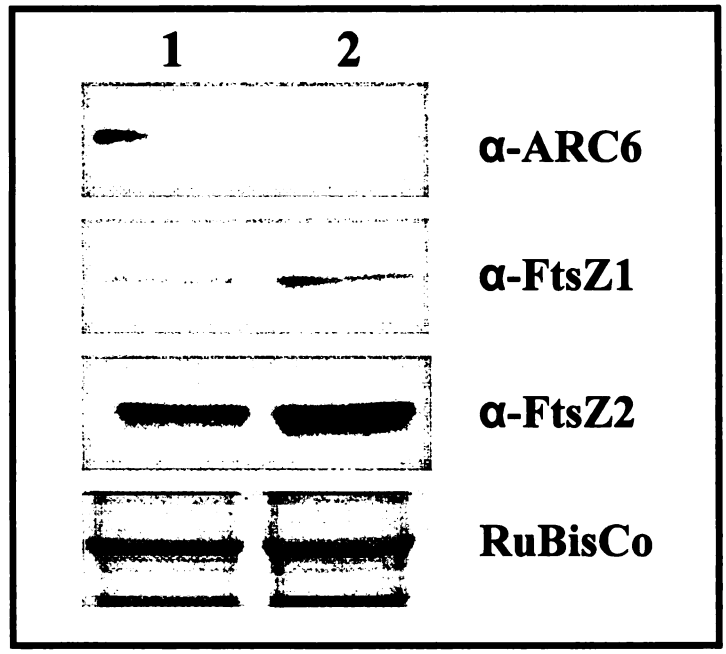

Figure 6.4. Preliminary analysis of ARC6, FtsZ1, and FtsZ2 levels in *arc6$_{D205N}$*. ARC6 protein levels (top panel) in *arc6$_{D205N}$* (lane 2) are diminished relative to wild type (lane 1), while FtsZ1 and FtsZ2-1 levels (center panels) are mostly unchanged. An estimate of relative loading is indicated by the Coomassie stain showing RuBisCo levels in each lane; based on this, there is slightly more protein in the lane carrying extract from an *arc6$_{D205N}$* plant, probably explaining the higher FtsZ1 and FtsZ2-1 signals in the mutant.

not only are their chloroplast morphologies similar, but FtsZ immunolocalization patterns observed within *arc6* and *arc12* are indistinguishable from one another (Glynn, Miyagishima, *et al.* 2007), suggesting that the functions of the two proteins might be connected. Because previous studies have shown that ARC6 and AtMinE have similar phenotypes, we aimed to determine if AtMinE localizes to equatorial rings in *Arabidopsis*, similar to ARC6 (Vitha, Froehlich, *et al.* 2003). Curiously, previous studies have shown that AtMinE localizes to polar spots within plastids of tobacco leaf cells (Maple, Chua, *et al.* 2002), in contrast to its largely mid-zone localization in bacteria (Hale, Meinhardt, *et al.* 2001, Sun and Margolin 2001). However, these localization results for AtMinE are disputed, as they are observed in terminally-differentiated leaf cells with very high levels of *35S-AtMinE* expression — *AtMinE* expression in *Arabidopsis* is highest in regions surrounding and including the apical meristem in vegetative tissues (Itoh, Fujiwara, *et al.* 2001). Other studies have shown that polar localization of *Arabidopsis* Min proteins within tobacco may not be representative of their native localization in *Arabidopsis*, as AtMinD localizes to a polar spot when transiently overexpressed in tobacco (Fujiwara, Nakamura, *et al.* 2004), but also localizes to a ring-like structure in *Arabidopsis* chloroplasts (Nakanishi, Suzuki, *et al.* 2009). To clarify the precise localization pattern for AtMinE in *Arabidopsis*, we introduced an $AtMinE_{pro}$-*MinE-YFP* transgene into *Col-0* and *arc12* mutants; *arc12* is an *AtMinE* loss-of-function allele (Glynn, Miyagishima, *et al.* 2007). We examined emerging leaves for a YFP signal using epifluorescence microscopy. To our surprise, we saw neither AtMinE-YFP spots nor rings in these samples; AtMinE-YFP was localized to a diffuse pattern within very small plastids (Figure 6.5D), suggesting that AtMinE may only have a

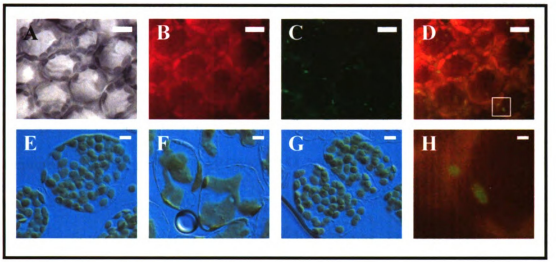

Figure 6.5. Localization of AtMinE-YFP in *Arabidopsis*. Micrographs from a young emerging leaf expressing AtMinE-YFP in the *arc12* background is shown in the upper panels: bightfield (A); chlorophyll autofluorescence (B); AtMinE-YFP fluorescence (C); and a merged image of chlorophyll and YFP fluorescence (D). In the lower panels, verification of functional complementation the plastid division defect in the *arc12* (*atminE*) mutant using an $AtMinE_{pro}$-*AtMinE-YFP* transgene is shown: *Col-0* (E); *arc12* (F); *arc12* rescued with the $AtMinE_{pro}$-*AtMinE-YFP* transgene. The boxed region in (D) is magnified and shown in (H). Scale bars in (A-G) = 10 μm. Scale bar in (H) = 1 μm.

significant impact upon proplastid division rather than chloroplast division, consistent with its high level of expression within the apical meristem (Itoh, Fujiwara, *et al.* 2001). We did not observe any AtMinE-YFP signal within plastids of older, expanded leaves (not shown). Our *AtMinE*$_{pro}$*-MinE-YFP* transgene was fully functional, as most *arc12* lines carrying this transgene possessed wild type chloroplasts in fully expanded leaf cells (Figure 6.5G). Further work is required to determine if AtMinE-YFP exhibits aberrant localization in the *arc6*$_{D205N}$ background.

Because of their similar phenotypes and expression patterns, we aimed to determine if a stromal portion of ARC6 (AA154-340) interacts with processed AtMinE (AA34-229) using yeast two hybrid assays; this region of ARC6 (AA154-340) has no defined function, but is conserved in all ARC6-like proteins. Previous work showed no interaction between these two proteins, but because of the defect in ARC6 function observed in *arc6*$_{D205N}$ mutants and the prospect of aspartate phosphorylation in cyanobacteria and chloroplast response regulators (Jacobs, Connell, *et al.* 1999, Li and Kehoe 2005, Maeda, Sugita, *et al.* 2006, Ruiz, Salinas, *et al.* 2008), we hypothesized that perhaps ARC6 might conditionally interact with AtMinE as a result of posttranslational modification. We generated site-directed mutants of ARC6$_{AA154-340}$, coding for D205A and D205E amino acid changes. In no instance did ARC6 interact with AtMinE$_{AA34-229}$ using two hybrid assays (not shown), suggesting that these proteins probably do not interact in *Arabidopsis*, despite their similar mutant chloroplast and FtsZ morphology

phenotypes (Glynn, Miyagishima, *et al.* 2007, Itoh, Fujiwara, *et al.* 2001, Pyke, Rutherford, *et al.* 1994, Rutherford 1996, Vitha, Froehlich, *et al.* 2003). Taken together, we conclude that the mispositioned Z-rings observed in the $arc6_{D205N}$ background occur through a MinE-independent mechanism, but the localization of all of the Min system components needs to be examined in the $arc6_{D205N}$ background.

ARC6 probably functions downstream of FtsZ1/FtsZ2 assembly and downstream of AtMinE.

Despite its lack of ARC6 interaction with AtMinE, our FtsZ immunolocalization data for $arc6_{D205N}$ still suggest that ARC6 might be somehow connected to the plastidic Min system, as $arc6_{D205N}$ mutants clearly possess mispositioned Z-rings (Figure 6.3B). To confirm where ARC6 functions within the pathway of plastidic Z-ring formation, we introduced an ARC6-GFP transgene (Glynn, Froehlich, *et al.* 2008) into *ftsZ2* mutants (Schmitz, Glynn, *et al.* 2009) and *arc12/atminE* (Glynn, Miyagishima, *et al.* 2007) to examine its localization in these backgrounds; we cannot use traditional tests of epistasis in this case because the *arc6*, *arc12*, and *ftsZ2* phenotypes are not easily distinguished from one another. In both cases, we were unable to observe ARC6-GFP localization to organized structures (Figure 6.6), though we were able to confirm expression of the fusion protein in all cases by immunoblotting (data not shown). The absence of ARC6-GFP rings was probably not a consequence of plastid size, as the enlarged plastids

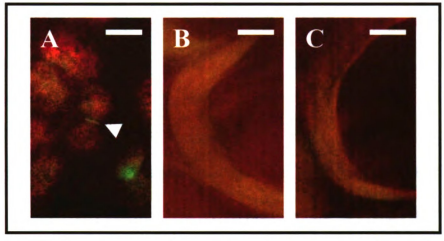

Figure 6.6. ARC6-GFP does not localize to rings in *ftsZ2* or *arc12* mutants. Shown is preliminary ARC6-GFP localization in *Col-0* (A); an *ftsZ2* mutant; and (C) an *arc12* (*atminE*) mutant. The background of the mutants shown above is *Col-0*. The *ftsZ2* mutant carries homozygous T-DNA insertions in the loci for *FtsZ2-1* and *FtsZ2-2* (Schmitz, Glynn, *et al.* 2009). Scale bar = 5 μm.

of *pdv2* mutants still form ARC6-GFP rings (Glynn, Froehlich, *et al.* 2008). These results indicate that at least some degree of FtsZ assembly is required for localization of ARC6 to mid-plastid rings *in vivo*; when FtsZ is either depleted (as in *ftsZ2* mutants) or filament assembly is constituitively inhibited (as in *atminE/arc12* mutants), ARC6 does not form a ring. From these results, we conclude that the plastidic Min system, or at least AtMinE, functions upstream of ARC6 and that some degree of FtsZ assembly is required for ARC6 localization to a ring *in vivo*.

Discussion

Here we perform preliminary characterization of a novel allele of *ARC6*, $arc6_{D205N}$, that possesses defects in chloroplast morphology and Z-ring placement that appear somewhat similar to *Arabidopsis min* mutants. The precise connection to the Min system was initially unclear, so we looked for interaction with a Min system component, AtMinE, whose mutant phenotype is strinkingly similar to *arc6* mutants. While we were unable to detect any interaction between ARC6 and AtMinE, nor provide further indication of the basis for the $arc6_{D205N}$ phenotype, our preliminary results do shed light on a frequently-encountered question relating to plastid division: does FtsZ ring formation precede ARC6 localization or does ARC6 localize independently of the Z-ring? Our observations of ARC6-GFP in an *ftsZ2* depletion mutant show that FtsZ is absolutely required for ARC6 localization to the division site. Further, our examination of ARC6-GFP localization in *arc12* (an *AtMinE* loss-of-function allele) shows that the presence of FtsZ protein within the plastid is insufficient for ARC6 localization;

chloroplast polarity and probably some degree of FtsZ polymerization are required for ARC6 localization to the mid-plastid.

While the connection of ARC6 to the plastidic Min system does not appear to occur through AtMinE, it is possible that another Min system component interfaces ARC6 with the Min system. In three very recent studies, novel components or novel localization patterns of known components have come to light. Similar to ARC6, native AtMinD protein was shown to localize to mid-plastid rings in *Arabidopsis* (Nakanishi, Suzuki, *et al.* 2009), in contrast to the polar localization of AtMinD when overexpressed in mature tobacco leaf cells (Maple, Chua, *et al.* 2002). It is possible that ARC6 conditionally interacts with AtMinD, but previous work suggests that it does not (Maple, Aldridge, *et al.* 2005) and the plastid phenotypes of *arc6* and *atminD* loss-of-function mutants are quite different (Fujiwara, Hashimoto, *et al.* 2008, Fujiwara, Nakamura, *et al.* 2004, Vitha, Froehlich, *et al.* 2003). A novel division protein, MCD1, was recently shown to be a modifier of the plastidic Min-system and possesses partial equatorial localization within the plastid (Nakanishi, Suzuki, *et al.* 2009), similar to ARC6 (Vitha, Froehlich, *et al.* 2003). However, the precise topology and function of MCD1 is still unclear, making its involvement with the Min system (and possibly ARC6) difficult to address. Most recently, PARC6 (a Paralog of ARC6) was shown to play a role in inhibiting Z-ring assembly and positioning, possibly through another Min system component, ARC3 (Glynn, Yang, *et al.* 2009, Zhang, Hu, *et al.* 2009b). Like ARC6, PARC6 localizes to a ring during plastid division (Glynn, Yang, *et al.* 2009) and $PARC6_{AA77-356}$ interacts with $ARC6_{AA154-340}$, possibly through the conserved motifs

(Figure 6.2) harboring $PARC6_{D211}/ARC6_{D205}$ (Y. Yang and K. Osteryoung, unpublished). Consistent with this, both ARC6 (Maple, Aldridge, *et al.* 2005) and PARC6 (Zhang, Hu, *et al.* 2009b) have been shown to be capable of self-interaction. Furthermore, a recent study has shown that Cdv3, a cyanobacterial protein with some sequence similarity to a portion of the stromal domain of PARC6, binds the cytosolic region of Ftn2/ARC6 in bacterial two hybrid assays (Marbouty, Saguez, *et al.* 2009). These observations indicate that the $arc6_{D205N}$ mutant may lead to a change in affinity between ARC6 and PARC6 (a component of the plastidic Min system), possibly explaining the mislocalization of the Z-ring observed in $arc6_{D205N}$ mutants (Figure 6.3). Alternatively, the irregular position of the Z-ring in $arc6_{D205N}$ mutants may somehow be a side-effect of low ARC6 protein levels (Figure 6.4). Regardless, further work that analyzes the ARC6-PARC6 interaction and the impact of site-directed mutations at or near $ARC6_{D205}$ might provide insights into the intriguing division defects observed in the $arc6_{D205N}$ mutant.

In the course of this work, we also analyzed the localization of AtMinE-YFP in *Arabidopsis*. The $AtMinE_{pro}$-*AtMinE-YFP* transgene was able to complement *arc12*, an *AtMinE* loss-of-function mutant (Glynn, Miyagishima, *et al.* 2007), suggesting that the transgene is functional and the localization pattern observed is relevant. Unlike the polar spot localization of AtMinE-YFP observed in mature tobacco leaf cells (Fujiwara, Nakamura, *et al.* 2004), we observed no YFP signals that colocalized with chlorophyll

autofluorescence and no obvious expression of AtMinE-YFP in expanded *Arabidopsis* leaf tissue. Instead, we observed a diffuse AtMinE-YFP signal associated with very small plastids within juvenile leaves of *Arabidopsis*, consistent with the expression of *AtMinE* within and proximal to the shoot apical meristem (Itoh, Fujiwara, *et al.* 2001). From our analysis (Figure 6.5), it was not possible to determine if this localization pattern was associated with the inner envelope membrane or if it was randomly distributed throughout the stroma. From these results, we conclude that the native localization pattern of AtMinE is diffuse within the plastid, and not polar, being more similar to the localization of *E. coli* MinE to a broad zone within the cell (Hale, Meinhardt, *et al.* 2001, Sun and Margolin 2001) rather than to polar spots observed during transient overexpression assays in tobacco leaf cells (Itoh, Fujiwara, *et al.* 2001). Regardless, analysis of the localization of Min system components (ARC3, MinD, MinE, MCD1, PARC6, and ARC6) in the $arc6_{D205N}$ background is still required. In a related line of investigation, we showed that ARC6-GFP fails to localize to a ring in *ftsZ2* or *arc12* (*atminE*) mutants, suggesting some basal level of FtsZ assembly must occur for ARC6 to localize to a ring; this presumably means that ARC6 acts downstream of the plastidic Min system. Further analysis of the interactions and localization patterns of proteins that make up the plastidic Min system will be critical to understanding the how the site for Z-ring assembly is selected and what conditions trigger bulk FtsZ assembly at any particular site.

Materials and Methods

Identification of EMS-induced polymorphisms in ARC6 and genotypic analysis.

Single nucleotide polymorphisms (SNPs) that cause missense mutations were identified as described previously through the *Arabidopsis* TILLING Project: http://tilling.fhcrc.org/ (Till, Colbert, *et al.* 2006). Progeny of mutagenized lines that harbored the mutation indicated were sown on Linsmaier-Skoog medium and screened by CAPs or dCAPs-based genotyping (Neff, Neff, *et al.* 1998). Primers used for screening the mutant pool for mutations in the ARC6 amino terminus were: CCTCCGATTCCTCC TCCTCCTCCT (left) and GACAACCCCTGCCAACCAGGTTTC (right). Primers used for screening the mutant pool for mutations in the ARC6 amino terminus were: GGCAGGGGTTGTCTTTCCTAGGTTCAG (left) and GATCAAGGAAAAGGGTG TGCCAAGAAC (right). The polymorphisms in each line are as follows (nucleotide positions are indicated relative to the primer start position for each TILLING screen: P85S (C96T); P87L (C103T); D205N (G538R); S250N (G761A); G293D (G890R); L309F (C937T); A328V (C995Y); A592T (G377A); A621V (C465T); R677K (G922A); E705K (G1005A); D708N (G1105A); S763F (C1271T); and T773I (C1301T). None of the seeds from the line harboring the A328V mutation could be germinated, but this may be due to a background mutation.

Phenotypic analysis of plants carrying TILLING-derived missense alleles of ARC6.

Individuals that were shown to be homozygous for the indicated mutation were examined for chloroplast morphology and compared to the parental TILLING line (Col-

*er*105), using established fixation and analysis protocols (Miyagishima, Froehlich, *et al.* 2006, Pyke and Leech 1991, Vitha, Froehlich, *et al.* 2003).

Multiple sequence alignment.

These sequences were used for multiple sequence alignment: *Arabidopsis thaliana* (AtPARC6, NP_188549); *Medicago truncatula* (MtPARC6, IMGAG-annotated pseudomolecule AC157350_28.4); *Oryza sativa cv. japonica* (OsPARC6, NP_001054252); *Populus trichocarpa* (PtPARC6, a GENSCAN-based prediction (Burge and Karlin 1997) of *Populus trichocarpa* genome Scaffold_122 204390-215000); *Vitis vinifera* (VvPARC6, CAO48483); *Arabidopsis thaliana* (AtARC6, NP_199063); *Oryza sativa cv. japonica* (OsARC6, NP_001045726); *Ostreococcus lucimarinus* (OlARC6, XP_001421185); *Physcomitrella patens* (PpARC6, XP_001778770); *Zea mays* (ZmARC6, ACG29776); *Thermosynechococcus elongatus* BP-1 (TeFtn2, BAC08309); *Synechococcus elongatus* PCC 7942 (SeFtn2, ABB57973); *Nostoc* sp. PCC 7120 (NsFtn2, BAB74406); *Crocosphaera watsonii* WH 8501 (CwFtn2, EAM48783); and *Cyanothece* sp. ATCC 51142 (CsFtn2, ACB49642). Multiple sequence alignment was performed with MEGA4 (Tamura, Dudley, *et al.* 2007) using an identity matrix.

FtsZ immunolocalization.

Tissue preparation, fixation, and immunofluorescence analysis were carried out as described previously (Miyagishima, Froehlich, *et al.* 2006, Vitha, Froehlich, *et al.* 2003, Vitha, McAndrew, *et al.* 2001).

Immunoblotting.

Plant extracts for determination of FtsZ and ARC6 protein levels were taken from floral bud tissue. Flower buds were ground in liquid nitrogen and prepared for 10% SDS-PAGE using 6X sample buffer according to previously-established protocols (Wiegel and Glazebrook 2002). Immunoblotting for FtsZ1 and FtsZ2-1 protein was performed as described previously (Stokes, McAndrew, *et al.* 2000). Immunoblotting of plant extracts was performed using an ARC6-specific antibody at 1:2500 in TBS-T containing 5% nonfat dry milk. The blot was washed several times in TBS-T before applying the secondary antibody. The anti-rabbit HRP-conjugated secondary was used at 1:5000 in TBS-T containing 5% nonfat dry milk and the blot was washed several times in TBS-T before applying the HRP chemilluminescent substrate (Thermo Scientific, Inc.) and exposing to film.

Yeast two hybrid analysis.

ARC6 and AtMinE clones for two hybrid analysis were made by PCR and cloned into pGADT7 and pGBKT7, respectively. Mutations causing the missense mutations D205A and D205E in ARC6 were generated by SOE-PCR and cloned into pGADT7. Growth assays (*HIS3* reporter assays) were performed according to methods as described previously (Glynn, Froehlich, *et al.* 2008, Maple, Aldridge, *et al.* 2005).

Generation of $AtMinE_{pro}$-AtMinE-YFP, transformation, selection, and microscopy.

Analysis of ARC6-GFP localization.

The *$AtMinE_{pro}$-AtMinE-YFP* transgene was generated by amplifying the promoter and coding regions of the *AtMinE* locus with primers TTTTTTTCTGCAGACTTGTTT CAAAACGACTGTGTTTTTTG and CCAGAGAGATCTCTCTGGAACATAAAAATC GAACCTGACATC by PCR. This fragment was cloned into a derivative of pCAMBIA-1302 (Hajdukiewicz, Svab, *et al.* 1994) carrying C-terminal EYFP coding sequence by digesting the vector and PCR products with PstI and BglII; digestion with PstI and BglII removes the 35S promoter from the plant transformation vector. Clone was sequenced and shown to be free of coding errors prior to transformation of *Agrobacterium* and *Arabidopsis*. Plants were transformed as described previously (Clough and Bent 1998). Selection of transgenic individuals was performed on Linsmaier-Skoog media containing hygromycin (25 μg/mL). Hygromycin-resistant lines were transplanted to soil and allowed to recover for several days prior to analysis. Analysis of ARC6-GFP localization in *arc12* and *ftsZ2-1 ftsZ2-2* double mutants was conducted using GFP fusion vectors as previously described (Glynn, Froehlich, *et al.* 2008, Vitha, Froehlich, *et al.* 2003) and selecting on Linsmaier-Skoog media containing hygromycin (25 μg/mL). Hygromycin-resistant lines were transplanted to soil and allowed to recover for several days prior to microscopic analysis.

Acknowledgements

I thank Mia Hemmes for backcrossing the *arc6*$_{D205N}$ TILLING mutant, Joyce Bower for assisting with quantitative analysis of the *arc6*$_{D205N}$ phenotype, and Deena Kadirjan-Kalbach for continuing technical assistance with this project.

Chapter 7

Conclusions and Future Directions

Summary of ARC6 and PARC6 Functional Analysis and Future Directions.

In Figure 7.1, I show a schematic detailing the functional domains we have characterized within ARC6 and PARC6, in addition to previously annotated features.

ARC6-FtsZ2 Interaction

Our body of work here identifies a prospective domain within ARC6 that binds the C-terminus of FtsZ2 family members (Figure 7.1, ZBD) and might have structural similarity to *E. coli* ZipA. While our pulldown assays and *in vivo* analysis of $ARC6_{F442D}$ site-directed mutants negates the criticality of the core hydrophobic phenylalanine (F442) of $ARC6_{ZBD}$ we had hypothesized based on two-hybrid results, rigorous structural analysis is still required to fully refute the proposed ZipA-like structure we show in Chapter 2. While an X-ray crystal structure or NMR-based solution structure of $ARC6_{ZBD}$ is highly preferred, a comparison between circular dichroism (CD) spectra from $ARC6_{ZBD}$ and $ZipA_{ZBD}$ may be sufficient for a preliminary test of the model we show in Figure 2.4 (Greenfield 2006, Whitmore and Wallace 2008). If $ARC6_{ZBD}$ and $ZipA_{ZBD}$ have similar CD profiles, it is reasonable to assume that their structures are probably similar. However, if their CD profiles are different, it would suggest that $ARC6_{ZBD}$ has a structure distinct from that of $ZipA_{ZBD}$; this result would be consistent with secondary structure predictions of $ARC6_{ZBD}$ (Figure 2.5) and *in vivo* analysis of $ARC6_{ZBD}$ in *Arabidopsis* (Figure 2.9 and Figure 2.13). However, we still

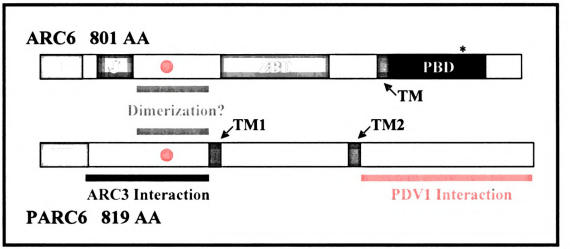

Figure 7.1. Domain Architecture of ARC6 and PARC6 Proteins. ARC6 (top) has a transit peptide (TP, AA 1-67); a predicted J-domain (J, AA 89-153); a hypothesized dimerization domain (AA 154-340) containing a conserved aspartate at position 205 (red dot); an FtsZ2-binding domain (ZBD, AA 351-503); a transmembrane domain (TM, AA 615-635); and a PDV2-binding domain (PBD, AA 636-759) containing a serine residue at position 744 that influences ARC6-PDV2 interaction and is predicted to be a phosphoacceptor site (asterisk, *). $ARC6_{AA68-614}$ resides in the chloroplast stroma and $ARC_{AA636-801}$ resides within the intermembrane space. PARC6 (bottom) has a transit peptide (TP, AA 1-76); an ARC3-interacting region (AA 77-357); a hypothesized dimerization domain (AA 169-335) containing a conserved aspartate at position 211 (red dot); two predicted transmembrane domains (TM1, AA 357-377; TM2, AA 574-596); and a PDV1-interacting region (AA 575-819). $PARC6_{AA77-356}$ is stromal, but the C-terminus of the protein has yet-undefined topology within the chloroplast.

emphasize that outside of its affinity for the C-terminus of FtsZ2 proteins, the precise function of $ARC6_{ZBD}$ remains undefined, but hypothesize that this domain is somehow involved in assembly or stabilization of FtsZ polymers within the chloroplast. To determine if $ARC6_{ZBD}$ has a direct effect upon the polymerization of FtsZ1 and FtsZ2, analysis of FtsZ copolymer assembly in the presence of $ARC6_{ZBD}$ could be conducted. The effect of $ARC6_{ZBD}$ upon FtsZ assembly could be analyzed using light scattering assays and electron microscopy following treatment of FtsZ assembly reactions (containing FtsZ1 and FtsZ2) with recombinant $ARC6_{ZBD}$ protein according to previously established protocols (Lu and Erickson 1998, Olson 2008).

ARC6-PDV2 Interaction

We have shown that ARC6 is responsible for positioning PDV2 at the division site within dividing chloroplasts and that PDV2-positioning activity occurs within the intermembrane space of the chloroplast (Glynn, Froehlich, *et al.* 2008). In Chapters 3 and 4 we showed that the ARC6-PDV2 interaction only requires a small domain contained within the IMS-localized portion of the ARC6 protein (Figure 7.1, PBD). While we were unable to generate a contiguous structural model of this domain within ARC6, the structural similarity of the IMS-localized region of PDV2 to the RsbU phosphoprotein phosphatase (Figure 4.3) (Delumeau, Dutta, *et al.* 2004, Dutta and Lewis 2003, Hardwick, Pane-Farre, *et al.* 2007) led us to hypothesize that interaction between ARC6 and PDV2 might be controlled by differential phosphorylation of ARC6. Using multiple sequence comparison of ARC6/Ftn2 proteins and phosphorylation prediction

algorithms, we identified one high-confidence phosphoacceptor site (S744) and two lower-confidence phosphoacceptor sites (S740 and T742) within $ARC6_{PBD}$. Phosphomimetic mutations at one of these sites ($ARC6_{S744E}$) disrupts the ARC6-PDV2 interaction (Figure 4.5) and impedes chloroplast division (Figure 4.6 and Figure 4.7), but does not grossly alter PDV2 localization to the division site (Figure 4.8). The presence of dumbbell-shaped plastids and multiple Z-rings at the division site within chloroplasts of *$ARC6_{S744E}$*-expressing lines are strikingly similar to those reported for both *pdv2* and *arc5* mutants (Gao, Kadirjan-Kalbach, *et al.* 2003, Miyagishima, Froehlich, *et al.* 2006). In other words, the *$ARC6_{S744E}$* phosphomimetic mutation generates two effects: (1) decreased dynamin activity at the outer envelope membrane and (2) an increase in Z-ring assembly within the stroma. While it is unclear if the *$ARC6_{S744E}$* mutation simply impedes dynamin activity by altering ARC6-PDV2 interaction affinity or by upregulating Z-ring assembly within the stroma (thus creating a rigid physical barrier that blocks constriction of the plastid membranes), the change of a single residue within the IMS-localized portion of ARC6 certainly leads to upregulation of Z-ring assembly within the stroma. However, it remains to be seen whether ARC6 residues S740, T742, or S744 are actually subject to posttranslational modification *in vivo*. There is no evidence of phosphorylation of any of these residues based on current phosphoproteomic data provided in the PhosPhAt database (http://phosphat.mpimp-golm.mpg.de/) (Heazlewood, Durek, *et al.* 2008), but this might reflect the transient nature of phosphorylation of the ARC6 protein *in vivo* — perhaps only a small fraction of ARC6 molecules are phosphorylated at these sites at any one time or are only phosphorylated under certain

environmental or developmental conditions. To address this potential mechanism further, it is suggested that *in vitro* assays are conducted in which radiolabeled phosphate is used to detect phosphorylation and/or dephosphorylation of $ARC6_{S744}$ following treatment of recombinant $ARC6_{PBD}$ with plant cell or chloroplast extracts. If $ARC6_{PBD}$ is a substrate for a phosphatase and/or kinase, a change in the amount of radioactivity should be observable following treatment of recombinant proteins with plant cell extracts; the amount of radiolabel carried by S740A, T742A, and/or S744A site-directed mutants could be compared to that of the wild type recombinant protein to demonstrate that these residues are actually the target of a phosphatase and/or kinase enzyme contained within cell extracts. Similar methods have been utilized for other proteins (Ben-Nissan, Cui, *et al.* 2008, Xu, Wong, *et al.* 2008) and may provide insight into the validity of the hypothesis that ARC6 activity is controlled through phosphomodification of $ARC6_{PBD}$.

PARC6-ARC3 Interaction.

In Chapter 5, we introduced *PARC6*, a novel chloroplast division gene that probably arose as a result of *ARC6* duplication in the tracheophyte lineage. While ARC6 and PARC6 do share some degree of sequence similarity, they vary significantly in function. Unlike ARC6, which promotes Z-ring assembly (Vitha, Froehlich, *et al.* 2003), PARC6 appears to inhibit FtsZ assembly within the stroma (Figure 5.6) and does not directly interact with FtsZ1 or FtsZ2 (Figure 5.7). However, we showed that PARC6 interacts with ARC3, a protein with functional similarity to bacterial MinC and that this interaction requires the MORN region of ARC3 (Figure 5.8) — the MORN region of

ARC3 inhibits its interaction with FtsZ1 proteins (Maple, Vojta, *et al.* 2007). Based on these data, I hypothesize that PARC6 inhibits FtsZ assembly through ARC3: when PARC6 is present, it sequesters the MORN region of ARC3, allowing ARC3 to bind FtsZ1 and disrupt the FtsZ1/FtsZ2 copolymer that makes up the Z-ring; in the absence of PARC6, the MORN region of ARC3 is exposed and inhibits ARC3 interaction with FtsZ1, allowing for assembly of the FtsZ1/FtsZ2 copolymer. Furthermore, because of the high PARC6-YFP signal intensity at the isthmus connecting the dividing plastid during the late stages of division (Figure 5.4) and because *parc6* mutants commonly have chloroplasts that are dumbbell-shaped (Figure 5.3 and Figure 5.9), I hypothesize that PARC6 functions to aid disassembly of the Z-ring during the late stages of division. The plastid morphology phenotypes in *parc6* mutants could result from disorganized or inefficient Z-ring disassembly in the absence of PARC6, causing hyperstabilized Z-ring(s) to block the final stages of plastid division. To determine whether this model is correct, *in vitro* assays could be conducted using purified recombinant proteins to monitor the assembly of the FtsZ1/FtsZ2 copolymer (Lu and Erickson 1998, Olson 2008) in the presence of various domains of ARC3 and PARC6. For this example, I hypothesize that recombinant ARC3 lacking its transit peptide and MORN region would be capable of inhibiting assembly of the FtsZ1/FtsZ2 copolymer. In contrast, a recombinant form of ARC3 protein lacking only its transit peptide would have no effect on FtsZ1/FtsZ2 copolymer assembly due to the presence of the MORN region of ARC3, as this region of ARC3 inhibits interaction between ARC3 and FtsZ1 (Maple, Vojta, *et al.* 2007). The addition of the N-terminal stromal region of PARC6 to assembly assays containing FtsZ1/FtsZ2 and mature recombinant ARC3 protein would lead to

sequestration of the MORN region of ARC3, thereby allowing ARC3 to bind FtsZ1 and inhibit assembly (or perhaps promote disassembly) of the FtsZ1/FtsZ2 copolymer, as bulk FtsZ polymer assembly only occurs in the presence of both FtsZ1 and FtsZ2 protein (Olson 2008). The use of complex, multiprotein mixtures in assembly assays will be critical for determining how plastidic FtsZ assembly is regulated *in vivo*.

PARC6-PDV1 Interaction.

Another possible explanation for the common observation of dumbbell-shaped plastids in *parc6* mutants might be a defect in dynamin (ARC5) activity at the outer envelope. Previously, PDV1 was shown to be critical for full ARC5 pinchase activity at the outer envelope (Miyagishima, Froehlich, *et al.* 2006). In Chapter 5, we demonstrated that PARC6 is required for PDV1 localization to sites of constriction (Figure 5.10) and that PARC6 interacts with PDV1 in two-hybrid assays (Figure 5.11), suggesting that PARC6 might directly position PDV1 during plastid division, thereby influencing ARC5 pinchase activity by directly recruiting PDV1 to the division site. However, this hypothesis is somewhat cursory due to the lack of knowledge regarding the topology of PARC6. Our preliminary analysis indicated that PARC6 may only traverse the inner envelope membrane (Glynn, Yang, *et al.* 2009), but this experiment was preliminary and may not possess the sensitivity to detect multiple or transient topological orientations of PARC6 within the envelope membrane(s) in dividing chloroplasts; a complete diagnostic of PARC6 topology needs to be examined using protease protection assays to determine the validity and/or plausibility of an interaction between PARC6 and PDV1.

Furthermore, we also observed the persistence of a PARC6 spot at one pole of the chloroplast (Figure 5.4), presumably representing its localization following separation of the two daughter plastids. Similar localization patterns have been observed for PDV1 and ARC5, but not for PDV2 or ARC6. We suspect that the similarity of PARC6, PDV1, and ARC5 at this stage represents a multiprotein complex that is retained on one pole of the chloroplast, possibly serving as a marker or reference point to aid division-site selection during the next round of division, perhaps analogous to the way some yeast species maintain cell polarity following cell division (Amberg, Zahner, *et al.* 1997, Drubin 1991, Glynn, Lustig, *et al.* 2001, Minc, Bratman, *et al.* 2009). Isolation of this putative polarity-determining complex from chloroplasts using affinity chromatography of affinity-tag-labeled PARC6 folowed by LC-MS/MS might allow for the identification of the factors composing this complex and provide insights into how polarity might be established within daughter plastids following division.

ARC6 is a Component of the Plastidic Min System.

Historically, I had thought of the plastidic Min system and ARC6 as two separate entities with little or no connection between their apparent functional roles. However, as a result of two major observations, I now believe ARC6 function is integrated into the plastidic Min system that functions to position the Z-ring at the division site: (1) expression of $ARC6_{S744E}$ *in vivo* results in the production of elongated chloroplasts containing multiple sites of constriction within petiole cells (Figure 4.9), similar to phenotypes observed in petiole cells of *Arabidopsis atminD/arc11* loss-of-function mutants (Fujiwara, Hashimoto, *et al.* 2008, Fujiwara, Nakamura, *et al.* 2004) and *35S-*

AtMinE overexpressing plants (Reddy, Dinkins, *et al.* 2002); and (2) the *min*icelling-like phenotype and aberrant Z-ring position in $arc6_{D205N}$ mutants (Figure 6.3) is consistent with a role for ARC6 in promoting equatorial positioning of the Z-ring prior to chloroplast division. To further examine this phenomenon, it is suggested that the localization patterns of other Min system proteins (AtMinD, AtMinE, ARC3, and PARC6) are examined in these mutant backgrounds to determine if the D205N or S744E mutations somehow impact function of the plastidic Min system. Additionally, preliminary data shows that a conserved segment of the stromal regions of ARC6 and PARC6 family members (Figure 5.1, grey underline) is important for homo- or hetero-dimerization between these proteins (Y. Yang and K. Osteryoung, unpublished). The conserved aspartate residues within these segments of ARC6 ($ARC6_{D205}$) and PARC6 ($PARC6_{D211}$) might be critical for their ability to dimerize within the chloroplast stroma (Maple, Aldridge, *et al.* 2005, Zhang, Hu, *et al.* 2009a) and/or mediate their communication with other components of the plastidic Min system. Interestingly, the cyanobacterial Cdv3/DivIVA division protein (Marbouty, Saguez, *et al.* 2009, Miyagishima, Wolk, *et al.* 2005) also shares some degree of sequence similarity with PARC6 (J.M. Glynn and K. Osteryoung, unpublished) and like both *parc6* and $arc6_{D205N}$ mutants, Cdv3-deficient cyanobacteria possess ectopic Z-rings (Marbouty, Saguez, *et al.* 2009), suggesting that dimerization of ARC6 with PARC6 (or Ftn2 with Cdv3 in the case of cyanobacteria) serves to interface ARC6/Ftn2 with the Min system. Consistent with this idea, the loss of Cdv3/DivIVA from the plastid divisome during the evolution of land plants (J.M. Glynn and K. Osteryoung, unpublished) loosely

corresponds with the acquisition of PARC6 in vascular plants (Glynn, Yang, *et al.* 2009). Further analysis of the interaction properties and localization of site-directed mutants of $ARC6_{D205}$ and $PARC6_{D211}$ may provide key insights into the coordination of Z-ring placement with organized Z-ring assembly and disassembly in chloroplasts.

Unanswered Questions, Additional Observations, and New Hypotheses.

Does ARC6 function as a DnaJ-like cochaperone?

While shown to have sequence and probable structural similarity to DnaJ-like cochaperones (Vitha, Froehlich, *et al.* 2003), it remains to be seen whether the predicted J-domain of ARC6 actually stimulates the chaperone activity of a DnaK-like protein. Moreover, it is unclear as to what function this chaperone activity serves within the chloroplast.

One possibility is that ARC6 is required for efficient import and/or refolding of FtsZ following import into the chloroplast stroma. Two points support this hypothesis: DnaJ/DnaK type chaperone systems have been shown to be important for protein import into eukaryotic organelles (Ivey and Bruce 2000, Zhang, Elofsson, *et al.* 1999); and intraplastidic FtsZ protein levels are significantly diminished in *arc6* mutants (Figure 1.3) (Vitha, Froehlich, *et al.* 2003). It is reasonable to suggest that comparative import experiments might highlight such an activity; perhaps higher efficiency FtsZ protein import would be observed in the presence of increasing amounts of ARC6 protein if ARC6 contributes to FtsZ import and/or folding.

A second possibility is that the J-domain activity is important for chaperoning the assembly or disassembly of FtsZ proteins into ordered structures within the stroma. Bacterial *dnaK* and *dnaJ* mutations affect cell division (Clarke, Jacq, *et al.* 1996, McCarty and Walker 1994), FtsZ dynamics (Uehara, Matsuzawa, *et al.* 2001), and overexpression of FtsZ has been shown to complement the cell division defects observed in a *dnaK* mutant (Bukau and Walker 1989). Furthermore, a recent study has suggested that DnaK chaperone activity is important for proper localization of the Z-ring in *E. coli* (Sugimoto, Saruwatari, *et al.* 2008). Presumably, the role of chaperones in Z-ring assembly and cell division in bacteria is conserved in plastids. Unfortunately, the analysis of plastidic *hsp70* T-DNA mutants has revealed partial redundancy between the two *Arabidopsis* chloroplast Hsp70 proteins and implicated them in chloroplast biogenesis *in vivo*; mutants that lack both plastidic Hsp70 proteins are non-viable (Su and Li 2008) and as a result are probably uninformative with regard to the role of these proteins in FtsZ import or assembly *in vivo*. However, the analysis of J-domain mutants of ARC6 is currently underway (Y. Yang and K. Osteryoung, unpublished) and may provide some exciting insights into this aspect of ARC6 function.

Is ARC6 localized to thylakoid membranes?

Interestingly, analysis of proteomic data from plastid membrane fractions suggests that the localization and topology of ARC6 might be more complex or more dynamic than import and fractionation assays suggest. The initial analysis of ARC6 fractionation and topology was performed using an *in vitro* approach with isolated pea

chloroplasts; this work placed ARC6 within the inner envelope membrane (Vitha, Froehlich, *et al.* 2003). However, more recent work indicates that ARC6 is present within the inner envelope and also the thylakoid membrane system, as multiple ARC6 peptide fragments are found in isolated thylakoid membrane fractions (http://ppdb.tc.cornell.edu/) (Sun, Zybailov, *et al.* 2009). While it is possible that these ARC6-derived peptides simply represent contamination of the thylakoid membrane fraction, this experimentally-determined thylakoid fractionation of ARC6 might represent a novel function for ARC6 during the early stages of division, or perhaps occurs as a result of the process of membrane breakage and resealing during the final stage of daughter plastid separation. It is unclear as to whether the thylakoid membrane is extricated from the division furrow prior to the final pinch, or if portions of the thylakoid membrane fuse with the inner envelope. Such a fusion event could lead to temporary relocation of ARC6 from the inner envelope to the thylakoid membrane, but the fate and/or purpose of these thylakoid-localized ARC6 molecules is unclear.

How is dynamin (ARC5) recruited to the division site?

While the roles of ARC6 and PARC6 in recruiting the PDV proteins to the division site are becoming more transparent, it is still unclear how the PDV proteins might recruit dynamin (ARC5) to the division site. Interestingly, *pdv1 pdv2* double mutants are blocked in their ability to recruit ARC5 from cytosolic patches, but *pdv1* and *pdv2* mutants can localize ARC5 at the division site (Miyagishima, Froehlich, *et al.* 2006). Similarly, *arc6* mutants are defective in their ability to recruit ARC5 patches from the cytosol (Glynn, Froehlich, *et al.* 2008) and phenocopy *pdv1 pdv2* mutants in this

regard (Miyagishima, Froehlich, *et al.* 2006). While PDV1 and PDV2 localize to the chloroplast periphery in *arc6* mutants, neither of the PDV proteins localize to a central ring in the *arc6* background (Glynn, Froehlich, *et al.* 2008); this suggests that PDV1 and/or PDV2 must be concentrated at a single site within the outer envelope to facilitate dynamin recruitment to the dividing chloroplast. Curiously, neither PDV1 (Miyagishima, Froehlich, *et al.* 2006) nor PDV2 (M. Hemmes and J.M. Glynn, unpublished) interact with ARC5 in yeast two-hybrid assays. I have also constructed novel N-terminal BiFC vectors to test for identify interaction between PDV1-ARC5, PDV2-ARC5, PDV1-PDV2, PDV1-PDV1, PDV2-PDV2, and ARC5-ARC5 – but these experiments have yet to be performed. Collectively, these data hint at a factor (or factors) that bridge PDV proteins to ARC5, and aid ARC5 patch recruitment from the cytosol.

The N-terminal domains of PDV1 and PDV2 are both localized in the cytosol, exhibit some low-level sequence similarity with each other, and have coiled-coil regions, indicating that they might have related functions (Glynn, Froehlich, *et al.* 2008, Miyagishima, Froehlich, *et al.* 2006). Unfortunately, the PDV proteins of land plants share little sequence similarity to any other proteins (Miyagishima, Froehlich, *et al.* 2006). To gain further insight into the proteins or entities that might bridge the PDV proteins with ARC5 recruitment, I performed comparative structural analysis of the N-terminal domains of PDV1 (AA 1-206) and PDV2 (AA 1-213) to all extant PDB structures using the MetaServer at http://bioinfo.pl (Ginalski, Elofsson, *et al.* 2003).

The best match for $PDV1_{AA1-206}$ was a crystal structure of the C-terminus of human EB1 (1YIB), a protein domain with homodimeric fold comprised of a coiled-coil and four-helix bundle (Slep, Rogers, *et al.* 2005). EB1 belongs to a conserved protein family that localizes to microtubule plus ends and recruits cell polarity and signaling molecules to growing microtubule tips (Askham, Moncur, *et al.* 2000, Bu and Su 2003, Nakamura, Zhou, *et al.* 2001, Slep and Vale 2007, Wen, Eng, *et al.* 2004). The N-terminus of EB1 is required for binding microtubles (Barth, Siemers, *et al.* 2002, Hayashi and Ikura 2003), while the C-terminus (i.e. the portion of EB1 with structural similarity to $PDV1_{AA1-206}$) has been shown to be a cargo-recognition domain. The C-terminus of EB1 family proteins bind several cargo proteins that regulate microtubule dynamics, including APC in mammals (Su, Burrell, *et al.* 1995), Kar9p in yeast (Miller, Cheng, *et al.* 2000), and may be involved in crosslinking the microtubule and actin cytoskeletons through spectraplakin-like proteins (Slep, Rogers, *et al.* 2005).

The best match for $PDV2_{AA1-213}$ was a crystal structure of the repetitive elements of fruit fly spectrin (2SPC). Spectrin is a cytoskeletal protein descended from an α-actinin-like ancestor (Dixson, Forstner, *et al.* 2003). Spectrins enhance the mechanical stability of membranes and promote the assembly of specialized membrane domains (Broderick and Winder 2005, Kordeli 2000). Spectrin functions as a tetramer (Liu and Palek 1980) that cross-links transmembrane proteins, membrane lipids, and actin; this cross-linking activity occurs directly (Brenner and Korn 1979) or through

adaptor proteins such as ankyrin and 4.1 (Bennett and Baines 2001, Goodman, Krebs, *et al.* 1988).

Dynamins do not generally interact directly with actin, but are typically associated with membrane structures (Wiejak and Wyroba 2002). My preliminary structural analysis of the PDV proteins point toward a mechanism where PDV1 (and possibly PDV2) might reorganize the actin and/or microtubule cytoskeleton to facilitate trafficking of dynamin (ARC5) patches to the cytosolic side of the chloroplast outer envelope through microtubule and/or actin-anchored motor proteins. Consistent with this hypothesis, at least two kinesin-like proteins, At5g10470 and At4g38950, have PDV1-like mRNA expression profiles (J.M. Glynn, unpublished) based on analysis using Expression Angler (http://bbc.botany.utoronto.ca/) (Toufighi, Brady, *et al.* 2005). Furthermore, the membrane remodeling properties of spectrin-like proteins, perhaps including PDV2, could create lipid microdomains that may be necessary (Lemmon 2004) for attracting the pleckstrin homology domain of ARC5 (Gao, Kadirjan-Kalbach, *et al.* 2003, Hong, Bednarek, *et al.* 2003), distributing ARC5 around the organelle surface, and/or facilitating stimulation of ARC5 pinchase activity at the division site (Yoshida, Kuroiwa, *et al.* 2006).

Working Model of the Coordination of the Chloroplast Divisome in Tracheophytes.

In Figure 7.2, I show a rudimentary model that reflects our current understanding of the roles of ARC6 and PARC6 in coordinating the assembly and operation of the plastid divisome. The plastid PD rings (Kuroiwa, Kuroiwa, *et al.* 1998) are omitted from this model, as their constituents are yet unknown and uncharacterized. This schematic reiterates the complexity of the process of plastid division and hints at several new hypotheses regarding the operation and regulation of some of the components that make up the plastid divisome. Firstly, while ARC6 certainly plays a role in the assembly and/or stabilization of the Z-ring, the mechanism by which it does so remains enigmatic. Our attempt to identify the discrete region of ARC6 that binds FtsZ2 family members within plant chloroplasts was a necessary step, but indicates that this issue may be more complicated than previously thought. Beyond its role in regulating FtsZ assembly within the stroma, we showed that ARC6 also mediates the activity of division factors that act upon the outer envelope. ARC6 is required to position PDV1 and PDV2 within the outer envelope membrane. ARC6 positions PDV2 by direct interaction, but only influences PDV1 localization indirectly through its paralog, PARC6. Our genetic and cytological analyses suggest that ARC6 is probably required for PARC6 localization and/or activity during division. It remains to be seen if ARC6 interacts directly with PARC6 *in vivo* or if other proteins bridge these two division factors. Furthermore, the precise topology of PARC6 is still rather murky, making it difficult to determine the validity of PARC6-PDV1 interaction data. The interaction between PARC6-ARC3 and the similarity of

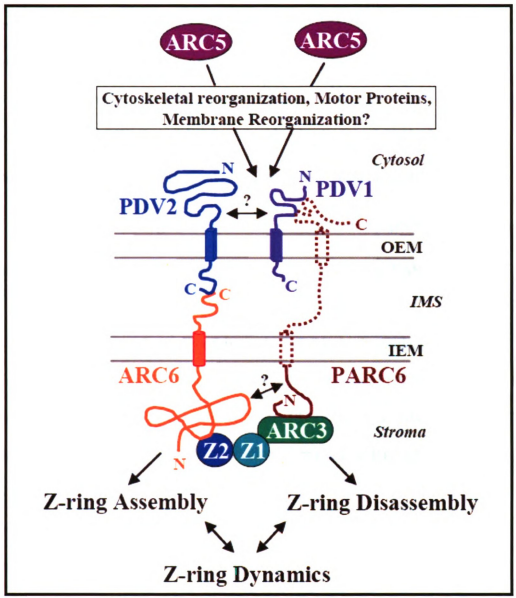

Figure 7.2. Coordination of Z-ring Dynamics and ARC5 Recruitment through ARC6 and PARC6. PD rings are omitted from this model for simplicity. Division is initiated by FtsZ assembly at the division site, which is determined by the Min system (not shown). ARC6 may influence Z-ring positioning and stabilize the Z-ring at the division site through its interaction with FtsZ2. PARC6 is a Min system component hypothesized to inhibit Z-ring assembly through ARC3. ARC6 and PARC6 form homodimers; ARC6 and PARC6 may (?) form heterodimers within the stroma. PDV2 is positioned in the outer envelope by interacting with ARC6 in the IMS. ARC6 indirectly positions PDV1 in the outer envelope, but does so through PARC6. Preliminary data suggests that PARC6 binds PDV1 in the cytosol. It is unknown (?) if PDV1 and PDV2 form hetero- or homodimers *in vivo*. The recruitment of ARC5 may occur through cytoskeletal reorganization, kinesin-driven directed movement, and/or membrane lipid reorganization by the PDV proteins. Not all detail is shown. See text for details.

their respective mutant phenotypes indicate that these two proteins might work together to inhibit FtsZ assembly, perhaps contributing to Z-ring disassembly during the final stages of division and/or aiding division-site selection along with other components of the plastidic Min system. While previously thought to be distinct from the Min system, ARC6 may also contribute to positioning of the Z-ring, based on analysis of $ARC6_{S744E}$ and $arc6_{D205N}$ alleles. Though the exact connection is unclear, ARC6 may interface with the Min system through heterodimerization with its paralog, PARC6.

The recruitment and activity of dynamin (ARC5), both regulated by the PDV proteins, remains a complicated matter. While both PDV1 and PDV2 are presumed to be required for full ARC5 contractile activity, either PDV protein is sufficient for ARC5 recruitment to the division site. ARC5 recruitment may occur through reorganization of the cytoskeleton, directing the dynamin-like protein to the division site through a vesicular transport mechanism that utilizes microtubule and/or actin-tracking motor proteins like kinesins (microtubules) or myosins (actin). Further work on this aspect of the division process may not only prove useful for improving our understanding of plastid replication, but may provide novel insights into general aspects of dynamin recruitment and activity within other types of eukaryotes as well.

APPENDIX

Appendix A

NExT and CIENA: Pipelines for Identification of Plastid Division Genes.

Summary

Reverse genetic screens for plastid division factors have relied heavily upon gene identification and characterization of division factors in other systems; when a new division component is identified in *E. coli* or another prokaryote, a researcher typically performs a BLAST query against finished plant genomes to determine if similar factors might contribute to organelle division. Several plastid division genes have been identified using this approach, including: FtsZ (Osteryoung, Stokes, *et al.* 1998, Osteryoung and Vierling 1995), GC1 (Maple, Fujiwara, *et al.* 2004), AtMinD (Colletti, Tattersall, *et al.* 2000), and AtMinE (Itoh, Fujiwara, *et al.* 2001). However, this mode of gene identification is limiting and novel approaches are required to determine the complete inventory of genes involved in organelle division. Here we highlight two platforms that we tested in an attempt to identify new plastid division factors. These platforms utilize genomic context and/or transcriptional profiling to identify new candidate genes and assign them priority.

NExT: A Platform for Identification of Candidate Genes by Genome Neighborhood Analysis and Priority Ranking Based on Gene Expression and Intracellular Targeting.

To start our search for new plastid division genes, we utilized The Seed gene neighborhood analysis tool (http://www.theseed.org/wiki/Main_Page) (Overbeek, Begley, *et al.* 2005). In prokaryotes, conserved gene proximity can be indicative of

related functions, as genes linked to a similar cellular process are often clustered together on the bacterial chromosome. Prokaryotic gene operons are a popular example of gene clustering (Overbeek, Fonstein, *et al.* 1999), and gene-gene association approaches have been used successfully to define the function of several genes of unknown function (de Crecy-Lagard 2007, de Crecy-Lagard and Hanson 2007). We pinned known prokaryotic cell division genes (Miyagishima, Wolk, *et al.* 2005) and then examined the surrounding genomic sequence amongst several bacterial species for coding loci that frequently reside within proximity (< 5000 bases) to a query gene. We identified approximately 80 candidates that commonly co-occur with our set of query genes. Within this set, 55 of these had orthologous sequences in *Arabidopsis* using BLAST-based queries (Altschul, Madden, *et al.* 1997).

We then used Genevestigator (https://www.genevestigator.com/) (Zimmermann, Hirsch-Hoffmann, *et al.* 2004) to prioritize our panel of ~55 candidates. Genevestigator is a gene expression analysis tool that allows the user to compare the degree of correlative expression between any two genes in *Arabidopsis*; we used *ARC6* (At5g42480) as a reference gene, as it is likely to be a critical regulator of plastid division *in vivo* (Marrison, Rutherford, *et al.* 1999, Pyke, Rutherford, *et al.* 1994, Vitha, Froehlich, *et al.* 2003), and arranged our candidates in order, based on the degree of expression profile similarity to *ARC6*.

To further prioritize candidates coming out of the pipeline described above, we used the TargetP (http://www.cbs.dtu.dk/services/TargetP/) intracellular prediction

targeting algorithm (Emanuelsson, Nielsen, *et al.* 2000) to identify genes encoding proteins bearing chloroplast transit peptides, as we guessed that chloroplast division genes might be more likely to be inside the chloroplast stroma. We referred to this complete pipeline as the NExT (*N*eighborhood Analysis, *Ex*pression Analysis, and *T*argeting Analysis) Functional Identification Platform. For our pilot screen, we elected to examine chloroplast phenotypes in the 12 loci that had the highest-priority ranking. We obtained T-DNA insertion lines for this set of 12 *Arabidopsis* candidate genes and analyzed chloroplast morphology in each of these lines: At5g19850 (SALK_026840); At5g40500 (SALK_029848); At3g25470 (SALK_043556); At5g10720 (SALK_051629); At3g07430 (SALK_056049); At5g53920 (SALK_070621); At3g04870 (SALK_079674); At4g01900 (SALK_095650); At1g53120 (SALK_099429); At1g08530 (SALK_101302); At5g14800 (SALK_127043); and At1g32440 (SALK_142845). Unfortunately, we were unable to identify homozygous insertions in a few of these lines (SALK_026840, SALK_029848, SALK_101302, and SALK_142845) and we did not observe any lines in this candidate set with noticeable defects in chloroplast morphology. From these results, we conclude that these genes probably do not encode plastid division factors and that our NExT-based approach will need further refinement if it is to be a successful platform for identifying gene function.

CIENA: Identification of Candidate Division Genes by Gene Network Analysis.

Because we were unable to identify any new division genes using NExT, we aimed to identify new candidate division genes based on their siliarity of expression to

known plastid division genes using publicly available *Arabidopsis* microarray data. This screen for new candidates is arguably less biased than NeXT, as it relies solely upon expression data and may more easily allow for the identification of factors that were not inherited from the cyanobacterial endosymbiont. Recently, more advanced expression-clustering algorithms have become widely accessible and their power will continue to improve as more genome-wide expression data becomes available (Kinoshita and Obayashi 2009). We used the ATTED-II database (http://atted.jp) (Obayashi, Hayashi, *et al.* 2009) to identify *Arabidopsis* genes that reside in gene expression networks with known plastid division genes. This approach was termed CIENA (*C*andidate *I*dentification by *E*xpression *N*etwork *A*nalysis). As proof of concept, we examined the gene expression network surrounding *ARC6* and found two of its three nearest-neighbors to be *FtsZ1-1* and *FtsZ2-1* (Table A.1). We performed this same query for 21 genes known to affect plastid morphology (Table A.1). We compared network members arising from this analysis and found 3 candidates that appear in more than one network: At3g28760, At4g19710, and At4g28210 (Table A.1). At4g28210 is annotated as embryo-defective (Tzafrir, Pena-Muralla, *et al.* 2004). At4g19710 has already been characterized as a bifunctional aspartate kinase/homoserine dehydrogenase (Paris, Wessel, *et al.* 2002) and is already present within the Plastid 2010 (http://plastid.msu.edu/) (Lu, Savage, *et al.* 2008) chloroplast morphology pipeline. As such, we chose not to analyze T-DNA alleles within At4g28210 or At4g19710. However, At3g28760 is a gene of unknown function and was not present within the Plastid 2010 pipeline, so we analyzed homozygous T-DNA insertions within an exon of

Table A.1. Known Plastid Division Genes and their Network Members.

Division Gene	ATTED-II Network Members
ARC1 (At4g23940)	At5g49030, At3g04340,**At3g28760**, **At4g19710**, At5g50110
ARC2 (At2g28000)	At5g20720, At3g13470, At2g04030, At4g24280
ARC3 (At1g75010)	At1g80480, At2g39930, At3g57430
ARC5 (At3g19720)	At5g06060, **At4g19710**, At5g58550, At2g28100
ARC6 (At5g42480)	At2g36250, At2g39670, At5g55280
BR04 (At1g55490)	At5g63310, At2g44650, At1g56050
CRF2 (At4g23750)	At1g74890, At1g69040, At1g68400
CRL (At5g51020)	At3g52230, At1g68660, At5g44000, At1g21065, At4g36530, At1g70580, At2g34310
CYO1 (At3g19220)	**At4g28210**, At2g39080, At3g04550
FtsZ1-1 (At5g55280)	At1g69200, At5g42480, At3g54090, At2g29690
FtsZ2-1 (At2g36250)	At5g42480, At1g09795, At1g13270
FtsZ2-2 (At3g52750)	At1g63610, At2g32500, At2g47590, At3g10940, **At3g28760**, At4g20760, At3g01510
GC1 (At2g21280)	At4g34190, At3g63140, At1g31800, At1g80030, At4g13670, At3g05350
AtMinD (At5g24020)	At2g33430, **At4g28210**, At3g46740
AtMinE (At1g69390)	At1g65260, At1g12410, At2g04700
MSL2 (At5g10490)	At1g56560, At1g77800, At4g37320
MSL3 (At1g58200)	At5g53050, At3g62010, At5g54170, At4g01026, At3g06500, At1g75960
OR (At5g61670)	At4g34350, At5g64840, At5g43850, At5g44190
PARC6 (At3g19180)	Affymetrix data not available.
PDV1 (At5g53280)	At1g78580, At4g04870, At5g09250
PDV2 (At2g16070)	At4g37460, At4g32770, At2g21320, At3g45900

Network members that appear in more than one network and have undefined roles in plastid division are indicated in **bold** text.

the At3g28760 locus (SALK_083209). We observed no difference in chloroplast morphology between SALK_083209 homozygotes and *Col-0*. It remains to be seen if At4g19710 has a role in plastid fission, but based on our analysis thus far we must conclude that At3g28760 is not involved in chloroplast division. It would be worth the effort to examine lines carrying T-DNA insertions (if available) within the other loci that appear Table A.1., even if they only appear in one network, but it is certainly worth establishing priority amongst this large number of candidate genes to make analysis more efficient. Alternatively, TILLING or RNAi-based approaches may be used to gain perspective on gene function if analysis of T-DNA insertion mutants proves unfruitful. If the remaining candidates turn out to be involved in plastid division, further refinement of this approach will be required.

Acknowledgements

I thank Dean Dellapenna for introducing me to gene neighborhood analysis and Ross Overbeek and Sveta Gerdes for their instruction on using the SEED database. I thank the horde of rotation students and undergraduate helpers that assisted with this project: Wei-ning Huang, Christine Shyu, Mia Hemmes, James Morgan, and John Sherbeck genotyped and phenotyped most of the T-DNA insertion lines analyzed in the NExT and CIENA pipelines.

Appendix B

Mapping Novel Alleles of Plastid Division Genes

Summary

Forward and reverse genetic approaches have identified slightly more than 20 genes in *Arabidopsis* that affect plastid division. About half of these can be directly traced to a cyanobacterial gene and the others are inventions of the host organism, arising after stable endosymbiosis was established. It is presumed that several more factors are involved in plastid division in land plants, because: (1) a number of cyanobacterial division genes have been lost, and presumably were replaced by other factors, during chloroplast evolution; (2) the components of the plastid dividing (PD) rings of higher plants remain unknown; (3) some molecules must exist to link certain division components to one another; (4) the scope of control mechanisms, including metabolites and transcription factors, that act as inputs and outputs of plastid division have yet to be determined. Despite the predicted near-saturation of forward genetic screens for division mutants, we attempted to identify novel factors by examining the chloroplasts in M_2 individuals derived from EMS-mutagenized *Col-0* lines. This analysis has yielded 13 new division mutants. Some of these have been shown to be novel alleles of known loci and several are yet unidentified. Additionally, we provide rough mapping data for the *ARC9* mutation, which was previously obtained from a T-DNA mutant screen for chloroplast division mutants.

New Plastid Division Alleles Discovered within an EMS-mutagenized Population.

To identify new plastid division genes we grew pools of M_2 progeny of EMS-mutagenized *Col-0* individuals (Lehle Seeds) on Linsmaier-Skoog medium. This M_2

population is part of the same batch that yielded two mutant alleles of *PDV1* (Miyagishima, Froehlich, *et al.* 2006). At 15-25 days post-germination, we examined the largest leaves for defects in chloroplast morphology by light microscopy. We identified 22 plants with aberrations in chloroplast morphology from a pool of ~14,000 M_2 individuals. We confirmed the chloroplast morphology in fresh tissue samples and then transplanted plants to soil. Out of the original 22 plants, 13 survived transplantation and were fertile. We termed these lines *c*hloroplast *a*ltered *n*umber (*can*) mutants. We prioritized the mutants based on their division phenotype and plant vigor; the mutants with more interesting phenotypes were given higher priority and amongst these, the healthier plants were given the highest priority to facilitate quick identification of the causative mutation (Table B.1).

We crossed each of our high-priority candidates (*can2*, *CAN3*, *can4*, *can5*, and *can8*) to known division mutants with similar chloroplast phenotypes to test for allelism. In parallel, we outcrossed each of our high-priority candidates to L*er*-0 to generate a mapping population for each of these mutants. We verified F_1 hybrids by genotypic analysis, examined their chloroplast morphology phenotypes, and allowed these individuals to self-fertilize to generate an F_2 mapping population. We quickly identified *can2* and *can4* as recessive alleles of *arc5* and *ftsZ1*, respectively, based on crosses to previously characterized mutants (Gao, Kadirjan-Kalbach, *et al.* 2003, Yoder, Kadirjan-Kalbach, *et al.* 2007). The relevant loci were then sequenced to identify the causative mutation. The remaining three alleles (*CAN3*, *can5*, and *can8*) were rough-mapped to a

Table B.1. A Summary of the *Arabidopsis can* Mutants.

Mutant	Phenotypes and inheritance pattern	Status
can1	*arc1*-like chloroplasts. Plant is severely stunted and pale, requiring more than 40 days to produce flowers. Unknown inheritance pattern.	Causitive mutation unknown. Check for allelism with *arc1*. Mapping population needed
can2	*arc5*-like chloroplasts. Recessive inheritance pattern.	***ARC5* codon 564 GAG to AAG (E564K).**
CAN3	Unique chloroplast phenotype. Dominant inheritance pattern.	***FTSZ2-1* codon 319 GAT to AAT (D319N).**
can4	*ftsZ1*-like chloroplasts. Recessive inheritance pattern.	***FTSZ1* codon 275 GAT to AAT (D275N).**
can5	Unique chloroplast phenotype. Recessive inheritance pattern.	***ARC3* codon 106 TGG to TGA (W106*). Mutation occurs at splice acceptor site.**
can6	Unique chloroplast phenotype. Unknown inheritance pattern.	Causitive mutation unknown. Mapping population needed.
can7	Unique chloroplast phenotype. Unknown inheritance pattern.	Causitive mutation unknown. Mapping population needed.
can8	Unique chloroplast phenotype. Plant flowers earlier than wild type. Recessive inheritance.	**Linked to right arm of chr 5 near *FTSZ1* locus; non-allelic with *ftsZ1* and *arc6* mutants.**
can9	Unique chloroplast phenotype. Unknown inheritance pattern.	Causitive mutation unknown. Mapping population needed.
can10	Unique chloroplast phenotype. Unknown inheritance pattern.	Causitive mutation unknown. Mapping population needed.
can12	*crl*-like plant and chloroplast phenotypes. Unknown inheritance pattern.	Causitive mutation unknown. Mapping population needed.
can13	*ftsZ1*-like chloroplast phenotype. Unknown inheritance pattern.	Causitive mutation unknown. Mapping population needed.
can16	Unique chloroplast phenotype. Plant produced less than 20 seeds. Unknown inheritance pattern.	Causitive mutation unknown. Mapping population needed.

specific *Arabidopsis* chromosome using molecular markers on a small F_2 population of 20-30 plants and then identified based on their proximity to known plastid division genes.

***ARC9* is an allele of *PDV2*.**

The original *arc9* mutant was originally isolated from a population of T-DNA-mutagenized *Ws* individuals and previously annotated as a recessive mutation (Aldridge, Maple, *et al.* 2005, Rutherford 1996). We received seeds from the *arc9* line (CS283) from the *Arabidopsis* Biological Resource Center (ABRC), with the hope of identifying the mutation which causes the chloroplast morphology defect within this line. We quickly noted two populations of plants emerging from this single seed stock, one with wild-type chloroplasts (~90%) and the others with aberrant chloroplast morphology that we presumed to be *arc9* mutants (~10%) (Figure B.1), indicating that the seed stock may have been contaminated or segregating during propagation at ABRC. We selected one of the individuals with abnormal chloroplasts for propagation and again noticed two populations occurring within ~50 offspring from this single plant. One population (~40%) possessed wild-type chloroplasts and the other (~60%) harbored chloroplasts similar to the parental plant. We hypothesized that the mutation in CS283 was dominant and that a background mutation might be contributing to the skewed phenotypic ratio observed within the progeny, as the expected phenotypic ratios observed in the progeny from an individual carrying a heterozygous dominant mutation should be 3:1. Consistent with this hypothesis, we examined embryos within developing siliques of a heterozygous plant and observed that ~30% of the embryos were stunted and/or undeveloped.

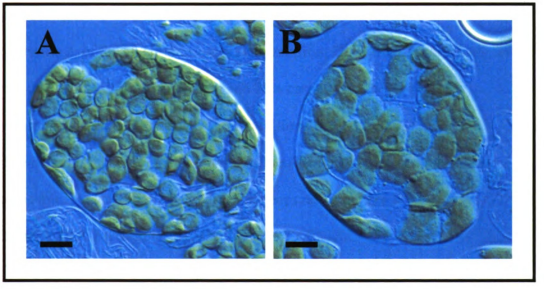

Figure B.1. Chloroplast phenotype observed in *ARC9/arc9* (CS283) plants. DIC images showing mesophyll cells from from *Ws-2* (A) and and *ARC9/arc9* heterozygote. Scale bar = 10 μm.

To identify the causative mutation in *ARC9*, we crossed an *ARC9/arc9* plant to *Col-0* and allowed the mutant F_1 individuals to self-fertilize to produce an F_2 generation for rough mapping. From a population of 80 F_2 individuals, we identified 30 with wild type chloroplast morphology and collected genomic DNA from these plants for genotypic analysis. Using 10 polymorphic PCR markers that allow for the differentiation of *Ws* and *Col-0* backgrounds by agarose gel electrophoresis, we observed the highest degree of linkage between the wild type phenotype and two molecular markers, both located on chromosome 2; of the 56 chromosomes analyzed from 28 wild type individuals, 79% carried the *Col-0* RGA polymorphism and 71% carried the *Col-0* NGA168 polymorphism (Bell and Ecker 1994); both of these polymorphisms reside on *Arabidopsis* chromosome 2, suggesting that the *ARC9* locus also resides on this chromosome. At least four plastid division genes reside on this chromosome: *PDV2* (At2g16070), *GC1* (At2g21280), *ARC2* (At2g28000), and *FtsZ2-1* (At2g36250).

Notably, the *PDV2* locus resides in the center of the interval bounded by the RGA and NGA168 markers; and the *ARC9/arc9* chloroplast morphology phenotype is remarkably similar to *PDV2/pdv2* (Glynn, Froehlich, *et al.* 2008, Miyagishima, Froehlich, *et al.* 2006). Furthermore, like *ARC9*, the two characterized mutations in *PDV2* are dominant-negative (Glynn, Froehlich, *et al.* 2008, Miyagishima, Froehlich, *et al.* 2006) due to gene dosage effects (J.M. Glynn and K. Osteryoung, unpublished) (Okazaki, Kabeya, *et al.* 2009). Therefore, we wanted to determine if *ARC9* might be an allele of *PDV2*. To do this we crossed a PDV2-deficient heterozygous T-DNA line (SAIL_875E10) to an *ARC9/arc9* heterozygote, using the *ARC9/arc9* plant as a pollen

donor. We genotyped F_1 individuals from this cross to verify that they were *Col/Ws* hybrids using the ATPase molecular genetic marker, which easily distinguishes *Ws* and *Col* accessions. Out of 11 marker-verified *Col/Ws* F_1 hybrids resulting from the *ARC9/arc9* x SAIL_875E10 (heterozygous) cross, 3 (27%) had severe chloroplast morphology phenotypes similar to lines lacking any PDV2 protein (Glynn, Froehlich, *et al.* 2008, Miyagishima, Froehlich, *et al.* 2006). These results suggest that either *ARC9* is an allele of *PDV2* or that the aggregated effect of these two dominant mutations (*ARC9* and *PDV2*) results in a severe chloroplast morphology phenotype. To determine if the severe phenotype observed in the cross progeny were due to a lack of PDV2 protein, we examined PDV2 protein levels in cell extracts from a wild-type plant, three cross progeny with *PDV2/pdv2* heterzoygote-like phenotypes, and the three cross progeny with severe phenotypes (Figure B.2). Consistent with *ARC9* and *PDV2* allelism, we observed that all three progeny with severe phenotypes contained no detectable PDV2 protein (Figure B.2, lanes 6-8). From this we conclude that the dominant mutation that leads to the chloroplast morphology phenotype in *ARC9/arc9* plants is likely due to PDV2 haploinsufficiency (Okazaki, Kabeya, *et al.* 2009) resulting from a T-DNA insertion in the *PDV2* locus; the cause of the embryo lethality observed in this line is still unknown, but is probably due to a background mutation since neither *pdv2-1* nor *pdv2-2* alleles exhibit embryo lethality defects (Miyagishima, Froehlich, *et al.* 2006). Further work would be required to identify the precise borders of the T-DNA insertion in *ARC9/arc9* plants, if necessary.

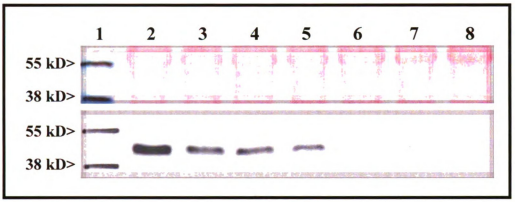

Figure B.2. *ARC9* is associated with a decrease in PDV2 protein level. Molecular weight marker (lane 1); extract from the eighth leaf of a wild-type plant (lane 2); *ARC9/arc9* x *PDV2/pdv2* cross progeny (F_1) with *PDV2/pdv2* heterozygote-like phenotypes (lanes 3-5); and *ARC9/arc9* x *PDV2/pdv2* cross progeny (F_1) with severe chloroplast morphology phenotypes (lanes 6-8). Approximately 2 mg of whole cell extract is loaded in each lane; extracts were made from 30-day old plants. kD = kiloDaltons.

Acknowledgments

Afiqah Ahmadhisham and John Sherbeck screened the bulk of the EMS-mutagenized *Col-0* population. Afiqah Ahmadhisham performed rough mapping of *can8* and did so with great care and efficiency. I am very much appreciative of John and Afiqah's efforts and for being such hard-working, flexible, and cheerful members of the Osteryoung lab over the past few years. I thank Joyce Bower for providing seeds from the ABRC *ARC9* mutant stock and Kathy Osteryoung for allowing me to identify *ARC9*.

REFERENCES

REFERENCES

Aldridge, C., Maple, J. and Moller, S.G. (2005) The molecular biology of plastid division in higher plants. *J. Exp. Bot.*, **56**, 1061-1077.

Aldridge, C. and Moller, S.G. (2005) The Plastid Division Protein AtMinD1 Is a Ca2+-ATPase Stimulated by AtMinE1. *J. Biol. Chem.*, **280**, 31673-31678.

Alonso, J.M., Stepanova, A.N., Leisse, T.J., Kim, C.J., Chen, H., Shinn, P., Stevenson, D.K., Zimmerman, J., Barajas, P., Cheuk, R., Gadrinab, C., Heller, C., Jeske, A., Koesema, E., Meyers, C.C., Parker, H., Prednis, L., Ansari, Y., Choy, N., Deen, H., Geralt, M., Hazari, N., Hom, E., Karnes, M., Mulholland, C., Ndubaku, R., Schmidt, I., Guzman, P., Aguilar-Henonin, L., Schmid, M., Weigel, D., Carter, D.E., Marchand, T., Risseeuw, E., Brogden, D., Zeko, A., Crosby, W.L., Berry, C.C. and Ecker, J.R. (2003) Genome-wide insertional mutagenesis of Arabidopsis thaliana. *Science*, **301**, 653-657.

Altschul, S.F., Madden, T.L., Schaffer, A.A., Zhang, J., Zhang, Z., Miller, W. and Lipman, D.J. (1997) Gapped BLAST and PSI-BLAST: a new generation of protein database search programs. *Nucleic Acids Res*, **25**, 3389-3402.

Amberg, D.C., Zahner, J.E., Mulholland, J.W., Pringle, J.R. and Botstein, D. (1997) Aip3p/Bud6p, a yeast actin-interacting protein that is involved in morphogenesis and the selection of bipolar budding sites. *Mol Biol Cell*, **8**, 729-753.

Askham, J.M., Moncur, P., Markham, A.F. and Morrison, E.E. (2000) Regulation and function of the interaction between the APC tumour suppressor protein and EB1. *Oncogene*, **19**, 1950-1958.

Austin II, J. and Webber, A.N. (2005) Photosynthesis in Arabidopsis thaliana mutants with reduced chloroplast number. *Photosynth Res*, **85**, 373-384.

Barth, A.I., Siemers, K.A. and Nelson, W.J. (2002) Dissecting interactions between EB1, microtubules and APC in cortical clusters at the plasma membrane. *J Cell Sci*, **115**, 1583-1590.

Baskin, T.I., Cork, A., Williamson, R.E. and Gorst, J.R. (1995) STUNTED PLANT 1, A Gene Required for Expansion in Rapidly Elongating but Not in Dividing Cells and Mediating Root Growth Responses to Applied Cytokinin. *Plant Physiol*, **107**, 233-243.

Bearer, E.L. (2003) Overview of image analysis, image importing, and image processing using freeware. *Curr Protoc Mol Biol*, **Chapter**, Unit 14.15.

Beemster, G.T. and Baskin, T.I. (2000) Stunted plant 1 mediates effects of cytokinin, but not of auxin, on cell division and expansion in the root of Arabidopsis. *Plant Physiol*, **124**, 1718-1727.

Bell, C.J. and Ecker, J.R. (1994) Assignment of 30 microsatellite loci to the linkage map of Arabidopsis. *Genomics*, **19**, 137-144.

Ben-Nissan, G., Cui, W., Kim, D.J., Yang, Y., Yoo, B.C. and Lee, J.Y. (2008) Arabidopsis casein kinase 1-like 6 contains a microtubule-binding domain and affects the organization of cortical microtubules. *Plant Physiol*, **148**, 1897-1907.

Bennett, V. and Baines, A.J. (2001) Spectrin and ankyrin-based pathways: metazoan inventions for integrating cells into tissues. *Physiol Rev*, **81**, 1353-1392.

Bernhardt, T.G. and de Boer, P.A. (2005) SlmA, a nucleoid-associated, FtsZ binding protein required for blocking septal ring assembly over Chromosomes in E. coli. *Mol Cell*, **18**, 555-564.

Bi, E.F. and Lutkenhaus, J. (1991) FtsZ ring structure associated with division in Escherichia coli. *Nature*, **354**, 161-164.

Bin, H., Guohua, Y., Weixing, Z., Yingjiao, Z. and Jindong, Z. (2007) MreB is important for cell shape but not for chromosome segregation of the filamentous cyanobacterium *Anabaena* sp. PCC 7120. *Molecular Microbiology*, **63**, 1640-1652.

Birky, C.W., Jr. and Walsh, J.B. (1992) Biased gene conversion, copy number, and apparent mutation rate differences within chloroplast and bacterial genomes. *Genetics*, **130**, 677-683.

Blom, N., Gammeltoft, S. and Brunak, S. (1999) Sequence and structure-based prediction of eukaryotic protein phosphorylation sites. *J Mol Biol*, **294**, 1351-1362.

Boffey, S.A. and Lloyd, D. (1988) *Division and Segregation of Organelles.* Cambridge, UK: Cambridge University Press.

Bracha-Drori, K., Keren, S., Aviva, K., Moran, O., Ruthie, A., Shaul, Y. and Nir, O. (2004) Detection of protein-protein interactions in plants using bimolecular fluorescence complementation. *The Plant Journal*, **40**, 419-427.

Braun, D.M. and Walker, J.C. (1996) Plant transmembrane receptors: new pieces in the signaling puzzle. *Trends Biochem Sci*, **21**, 70-73.

Brenner, S.L. and Korn, E.D. (1979) Spectrin-actin interaction. Phosphorylated and dephosphorylated spectrin tetramer cross-link F-actin. *J Biol Chem*, **254**, 8620-8627.

Broderick, M.J. and Winder, S.J. (2005) Spectrin, alpha-actinin, and dystrophin. *Adv Protein Chem*, **70**, 203-246.

Bruce, B.D., Perry, S., Froehlich, J. and Keegstra, K. (1994) *In vitro Import of Protein into Chloroplasts.* Boston: Kluwer Academic Publishers.

Bu, W. and Su, L.K. (2003) Characterization of functional domains of human EB1 family proteins. *J Biol Chem*, **278**, 49721-49731.

Bukau, B. and Walker, G.C. (1989) Cellular defects caused by deletion of the Escherichia coli dnaK gene indicate roles for heat shock protein in normal metabolism. *J Bacteriol*, **171**, 2337-2346.

Burge, C. and Karlin, S. (1997) Prediction of complete gene structures in human genomic DNA. *J Mol Biol*, **268**, 78-94.

Castellano, M.d.M., Boniotti, M.B., Caro, E., Schnittger, A. and Gutierrez, C. (2004) DNA Replication Licensing Affects Cell Proliferation or Endoreplication in a Cell Type-Specific Manner. *Plant Cell*, **16**, 2380-2393.

Cavalier-Smith, T. (2000) Membrane heredity and early chloroplast evolution. *Trends in Plant Science*, **5**, 174.

Cerveny, K.L., Tamura, Y., Zhang, Z., Jensen, R.E. and Sesaki, H. (2007) Regulation of mitochondrial fusion and division. *Trends Cell Biol*, **17**, 563-569.

Chen, J.G., Shimomura, S., Sitbon, F., Sandberg, G. and Jones, A.M. (2001) The role of auxin-binding protein 1 in the expansion of tobacco leaf cells. *Plant J*, **28**, 607-617.

Chen, Y., Asano, T., Fujiwara, M.T., Yoshida, S., Machida, Y. and Yoshioka, Y. (2009) Plant cells without detectable plastids are generated in the crumpled leaf mutant of Arabidopsis thaliana. *Plant Cell Physiol*, **50**, 956-969.

Christie, J.M. (2007) Phototropin blue-light receptors. *Annu Rev Plant Biol*, **58**, 21-45.

Clarke, D.J., Jacq, A. and Holland, I.B. (1996) A novel DnaJ-like protein in Escherichia coli inserts into the cytoplasmic membrane with a type III topology. *Mol Microbiol*, **20**, 1273-1286.

Clough, S.J. and Bent, A.F. (1998) Floral dip: a simplified method for Agrobacterium-mediated transformation of Arabidopsis thaliana. *Plant J*, **16**, 735-743.

Colletti, K.S., Tattersall, E.A., Pyke, K.A., Froelich, J.E., Stokes, K.D. and Osteryoung, K.W. (2000) A homologue of the bacterial cell division site-determining factor MinD mediates placement of the chloroplast division apparatus. *Current Biology*, **10**, 507.

Cordell, S.C., Robinson, E.J. and Lowe, J. (2003) Crystal structure of the SOS cell division inhibitor SulA and in complex with FtsZ. *Proc Natl Acad Sci U S A*, **100**, 7889-7894.

Cramer, W.A., Engelman, D.M., Von Heijne, G. and Rees, D.C. (1992) Forces involved in the assembly and stabilization of membrane proteins. *FASEB J*, **6**, 3397-3402.

Cui, L., Veeraraghavan, N., Richter, A., Wall, K., Jansen, R.K., Leebens-Mack, J., Makalowska, I. and dePamphilis, C.W. (2006) ChloroplastDB: the Chloroplast Genome Database. *Nucleic Acids Res*, **34**, D692-696.

Davila-Aponte, J.A., Inoue, K. and Keegstra, K. (2003) Two chloroplastic protein translocation components, Tic110 and Toc75, are conserved in different plastid types from multiple plant species. *Plant Mol Biol*, **51**, 175-181.

de Crecy-Lagard, V. (2007) Identification of genes encoding tRNA modification enzymes by comparative genomics. *Methods Enzymol*, **425**, 153-183.

de Crecy-Lagard, V. and Hanson, A.D. (2007) Finding novel metabolic genes through plant-prokaryote phylogenomics. *Trends Microbiol*, **15**, 563-570.

de Souza, S.J., Long, M., Schoenbach, L., Roy, S.W. and Gilbert, W. (1996) Intron positions correlate with module boundaries in ancient proteins. *Proc Natl Acad Sci U S A*, **93**, 14632-14636.

Delumeau, O., Dutta, S., Brigulla, M., Kuhnke, G., Hardwick, S.W., Volker, U., Yudkin, M.D. and Lewis, R.J. (2004) Functional and structural characterization of RsbU, a stress signaling protein phosphatase 2C. *J Biol Chem*, **279**, 40927-40937.

DePamphilis, M.L. (2003) The 'ORC cycle': a novel pathway for regulating eukaryotic DNA replication. *Gene*, **310**, 1-15.

Dixson, J.D., Forstner, M.J. and Garcia, D.M. (2003) The alpha-actinin gene family: a revised classification. *J Mol Evol*, **56**, 1-10.

Dobson, C.M. (2003) Protein folding and misfolding. *Nature*, **426**, 884.

Doolittle, W.F. (1979) The cyanobacterial genome, its expression, and the control of that expression. *Adv Microb Physiol*, **20**, 1-102.

Dreher, K. and Callis, J. (2007) Ubiquitin, hormones and biotic stress in plants. *Ann Bot (Lond)*, **99**, 787-822.

Drubin, D.G. (1991) Development of cell polarity in budding yeast. *Cell*, **65**, 1093-1096.

Dutta, S. and Lewis, R.J. (2003) Crystallization and preliminary crystallographic analysis of the kinase-recruitment domain of the PP2C-type phosphatase RsbU. *Acta Crystallogr D Biol Crystallogr*, **59**, 191-193.

Dyall, S.D., Brown, M.T. and Johnson, P.J. (2004) Ancient Invasions: From Endosymbionts to Organelles. *Science*, **304**, 253-257.

Emanuelsson, O., Nielsen, H., Brunak, S. and von Heijne, G. (2000) Predicting subcellular localization of proteins based on their N-terminal amino acid sequence. *J Mol Biol*, **300**, 1005-1016.

Emanuelsson, O., Nielsen, H. and von Heijne, G. (1999) ChloroP, a neural network-based method for predicting chloroplast transit peptides and their cleavage sites. *Protein Sci*, **8**, 978-984.

Erickson, H.P. (2009) Modeling the physics of FtsZ assembly and force generation. *Proc Natl Acad Sci U S A*, **106**, 9238-9243.

Erickson, H.P., Taylor, D.W., Taylor, K.A. and Bramhill, D. (1996) Bacterial cell division protein FtsZ assembles into protofilament sheets and minirings, structural homologs of tubulin polymers. *Proc Natl Acad Sci U S A*, **93**, 519-523.

Ewald, R., Kolukisaoglu, U., Bauwe, U., Mikkat, S. and Bauwe, H. (2007) Mitochondrial protein lipoylation does not exclusively depend on the mtKAS pathway of de novo fatty acid synthesis in Arabidopsis. *Plant Physiol*, **145**, 41-48.

Falkow, S., Dworkin, M., Rosenburg, E., Schleifer, K.-H. and Stackebrandt, E. (2006) *The Prokaryotes: Firmicutes, Cyanobacteria* 3rd edn. New York: Springer Science and Business Media.

Felsenstein, J. (1985) Confidence Limits on Phylogenies: An Approach Using the Bootstrap. *Evolution*, **39**, 783-791.

Fischer, A., Hofmann, I., Naumann, K. and Reuter, G. (2006) Heterochromatin proteins and the control of heterochromatic gene silencing in Arabidopsis. *J Plant Physiol*, **163**, 358-368.

Fodor, A.A. and Aldrich, R.W. (2009) Convergent Evolution of Alternative Splices at Domain Boundaries of the BK Channel. *Annual Review of Physiology*, **71**, 19-36.

Forth, D. and Pyke, K.A. (2006) The suffulta mutation in tomato reveals a novel method of plastid replication during fruit ripening. *J. Exp. Bot.*, **57**, 1971-1979.

Fujiwara, M.T., Hashimoto, H., Kazama, Y., Abe, T., Yoshida, S., Sato, N. and Itoh, R.D. (2008) The assembly of the FtsZ ring at the mid-chloroplast division site depends on a balance between the activities of AtMinE1 and ARC11/AtMinD1. *Plant Cell Physiol*, **49**, 345-361.

Fujiwara, M.T., Nakamura, A., Itoh, R., Shimada, Y., Yoshida, S. and Moller, S.G. (2004) Chloroplast division site placement requires dimerization of the ARC11/AtMinD1 protein in Arabidopsis. *J Cell Sci*, **117**, 2399-2410.

Gao, H., Kadirjan-Kalbach, D., Froehlich, J.E. and Osteryoung, K.W. (2003) ARC5, a cytosolic dynamin-like protein from plants, is part of the chloroplast division machinery. *PNAS*, **100**, 4328-4333.

Gao, H., Sage, T.L. and Osteryoung, K.W. (2006) FZL, an FZO-like protein in plants, is a determinant of thylakoid and chloroplast morphology. *PNAS*, **103**, 6759-6764.

Geissler, B., Elraheb, D. and Margolin, W. (2003) A gain-of-function mutation in ftsA bypasses the requirement for the essential cell division gene zipA in Escherichia coli. *Proc Natl Acad Sci U S A*, **100**, 4197-4202.

Ghosh, B. and Sain, A. (2008) Origin of contractile force during cell division of bacteria. *Phys Rev Lett*, **101**, 178.

Ginalski, K., Elofsson, A., Fischer, D. and Rychlewski, L. (2003) 3D-Jury: a simple approach to improve protein structure predictions. *Bioinformatics*, **19**, 1015-1018.

Glynn, J.M., Froehlich, J.E. and Osteryoung, K.W. (2008) Arabidopsis ARC6 coordinates the division machineries of the inner and outer chloroplast membranes through interaction with PDV2 in the intermembrane space. *Plant Cell*, **20**, 2460-2470.

Glynn, J.M., Lustig, R.J., Berlin, A. and Chang, F. (2001) Role of bud6p and tea1p in the interaction between actin and microtubules for the establishment of cell polarity in fission yeast. *Curr Biol*, **11**, 836-845.

Glynn, J.M., Miyagishima, S.Y., Yoder, D.W., Osteryoung, K.W. and Vitha, S. (2007) Chloroplast division. *Traffic*, **8**, 451-461.

Glynn, J.M., Yang, Y., Vitha, S., Schmitz, A.J., Hemmes, M., Miyagishima, S. and Osteryoung, K.W. (2009) PARC6, a novel chloroplast division factor, influences FtsZ assembly and is required for recruitment of PDV1 during chloroplast division in Arabidopsis. *Plant J*, **59**, 700-711.

Goehring, N.W. and Beckwith, J. (2005) Diverse paths to midcell: assembly of the bacterial cell division machinery. *Curr Biol*, **15**, R514-526.

Goodman, S.R., Krebs, K.E., Whitfield, C.F., Riederer, B.M. and Zagon, I.S. (1988) Spectrin and related molecules. *CRC Crit Rev Biochem*, **23**, 171-234.

Greenfield, N.J. (2006) Using circular dichroism spectra to estimate protein secondary structure. *Nat Protoc*, **1**, 2876-2890.

Hajdukiewicz, P., Svab, Z. and Maliga, P. (1994) The small, versatile pPZP family of Agrobacterium binary vectors for plant transformation. *Plant Mol Biol*, **25**, 989-994.

Hale, C.A., Meinhardt, H. and de Boer, P.A. (2001) Dynamic localization cycle of the cell division regulator MinE in Escherichia coli. *EMBO J*, **20**, 1563-1572.

Hale, C.A., Rhee, A.C. and de Boer, P.A. (2000) ZipA-induced bundling of FtsZ polymers mediated by an interaction between C-terminal domains. *J Bacteriol*, **182**, 5153-5166.

Hales, K.G. and Fuller, M.T. (1997) Developmentally Regulated Mitochondrial Fusion Mediated by a Conserved, Novel, Predicted GTPase. *Cell*, **90**, 121.

Hardwick, S.W., Pane-Farre, J., Delumeau, O., Marles-Wright, J., Murray, J.W., Hecker, M. and Lewis, R.J. (2007) Structural and functional characterization of partner switching regulating the environmental stress response in Bacillus subtilis. *J Biol Chem*, **282**, 11562-11572.

Haswell, E.S. and Meyerowitz, E.M. (2006) MscS-like Proteins Control Plastid Size and Shape in Arabidopsis thaliana. *Current Biology*, **16**, 1-11.

Hayashi, I. and Ikura, M. (2003) Crystal structure of the amino-terminal microtubule-binding domain of end-binding protein 1 (EB1). *J Biol Chem*, **278**, 36430-36434.

He, Y. and Amasino, R.M. (2005) Role of chromatin modification in flowering-time control. *Trends Plant Sci*, **10**, 30-35.

Heazlewood, J.L., Durek, P., Hummel, J., Selbig, J., Weckwerth, W., Walther, D. and Schulze, W.X. (2008) PhosPhAt: a database of phosphorylation sites in Arabidopsis thaliana and a plant-specific phosphorylation site predictor. *Nucleic Acids Res*, **36**, D1015-1021.

Heckman, K.L. and Pease, L.R. (2007) Gene splicing and mutagenesis by PCR-driven overlap extension. *Nat Protoc*, **2**, 924-932.

Henikoff, S., Till, B.J. and Comai, L. (2004) TILLING. Traditional mutagenesis meets functional genomics. *Plant Physiol*, **135**, 630-636.

Hinshaw, J.E. (2000) Dynamin and its role in Membrane Fission. *Annual Review of Cell and Developmental Biology*, **16**, 483-519.

Hinshaw, J.E. and Schmid, S.L. (1995) Dynamin self-assembles into rings suggesting a mechanism for coated vesicle budding. *Nature*, **374**, 190-192.

Holzinger, A., Kwok, E.Y. and Hanson, M.R. (2008) Effects of arc3, arc5 and arc6 mutations on plastid morphology and stromule formation in green and nongreen tissues of Arabidopsis thaliana. *Photochem Photobiol*, **84**, 1324-1335.

Hong, Z., Bednarek, S.Y., Blumwald, E., Hwang, I., Jurgens, G., Menzel, D., Osteryoung, K.W., Raikhel, N.V., Shinozaki, K., Tsutsumi, N. and Verma, D.P. (2003) A unified nomenclature for Arabidopsis dynamin-related large GTPases based on homology and possible functions. *Plant Mol Biol*, **53**, 261-265.

Hoppins, S., Lackner, L. and Nunnari, J. (2007) The machines that divide and fuse mitochondria. *Annu Rev Biochem*, **76**, 751-780.

Hu, Y., Poh, H.M. and Chua, N.H. (2006) The Arabidopsis ARGOS-LIKE gene regulates cell expansion during organ growth. *Plant J*, **47**, 1-9.

Hu, Z. and Lutkenhaus, J. (1999) Topological regulation of cell division in Escherichia coli involves rapid pole to pole oscillation of the division inhibitor MinC under the control of MinD and MinE. *Mol Microbiol*, **34**, 82-90.

Hu, Z. and Lutkenhaus, J. (2001) Topological regulation of cell division in *E. coli* spatiotemporal oscillation of MinD requires stimulation of its ATPase by MinE and phospholipid. *Mol Cell*, **7**, 1337-1343.

Hu, Z., Mukherjee, A., Pichoff, S. and Lutkenhaus, J. (1999) The MinC component of the division site selection system in Escherichia coli interacts with FtsZ to prevent polymerization. *PNAS*, **96**, 14819-14824.

Huber, S.C. and Hardin, S.C. (2004) Numerous posttranslational modifications provide opportunities for the intricate regulation of metabolic enzymes at multiple levels. *Curr Opin Plant Biol*, **7**, 318-322.

Huisman, O., D'Ari, R. and Gottesman, S. (1984) Cell-division control in Escherichia coli: specific induction of the SOS function SfiA protein is sufficient to block septation. *Proceedings of the National Academy of Sciences of the United States of America*, **81**, 4490-4494.

Itoh, R., Fujiwara, M., Nagata, N. and Yoshida, S. (2001) A Chloroplast Protein Homologous to the Eubacterial Topological Specificity Factor MinE Plays a Role in Chloroplast Division. *Plant Physiol.*, **127**, 1644-1655.

Ivey, R.A., 3rd and Bruce, B.D. (2000) In vivo and in vitro interaction of DnaK and a chloroplast transit peptide. *Cell Stress Chaperones*, **5**, 62-71.

Jackson, D.T., Froehlich, J.E. and Keegstra, K. (1998) The hydrophilic domain of Tic110, an inner envelope membrane component of the chloroplastic protein translocation apparatus, faces the stromal compartment. *J Biol Chem*, **273**, 16583-16588.

Jacobs, M.A., Connell, L. and Cattolico, R.A. (1999) A conserved His-Asp signal response regulator-like gene in Heterosigma akashiwo chloroplasts. *Plant Mol Biol*, **41**, 645-655.

Jander, G., Norris, S.R., Rounsley, S.D., Bush, D.F., Levin, I.M. and Last, R.L. (2002) Arabidopsis map-based cloning in the post-genome era. *Plant Physiol*, **129**, 440-450.

Jensen, S.O., Thompson, L.S. and Harry, E.J. (2005) Cell division in Bacillus subtilis: FtsZ and FtsA association is Z-ring independent, and FtsA is required for efficient midcell Z-Ring assembly. *J Bacteriol*, **187**, 6536-6544.

Jeong, W.J., Park, Y.-I., Suh, K., Raven, J.A., Yoo, O.J. and Liu, J.R. (2002) A Large Population of Small Chloroplasts in Tobacco Leaf Cells Allows More Effective Chloroplast Movement Than a Few Enlarged Chloroplasts. *Plant Physiol.*, **129**, 112-121.

Jones, A.M., Im, K.H., Savka, M.A., Wu, M.J., DeWitt, N.G., Shillito, R. and Binns, A.N. (1998) Auxin-dependent cell expansion mediated by overexpressed auxin-binding protein 1. *Science*, **282**, 1114-1117.

Kang, C.M., Vijay, K. and Price, C.W. (1998) Serine kinase activity of a Bacillus subtilis switch protein is required to transduce environmental stress signals but not to activate its target PP2C phosphatase. *Mol Microbiol*, **30**, 189-196.

Kasahara, M., Kagawa, T., Oikawa, K., Suetsugu, N., Miyao, M. and Wada, M. (2002) Chloroplast avoidance movement reduces photodamage in plants. *Nature*, **420**, 829-832.

Kinoshita, K. and Obayashi, T. (2009) Multi-dimensional correlations for gene coexpression and application to the large-scale data of Arabidopsis. *Bioinformatics*, **25**, 2677-2684.

Kohler, R.H., Cao, J., Zipfel, W.R., Webb, W.W. and Hanson, M.R. (1997) Exchange of protein molecules through connections between higher plant plastids. *Science*, **276**, 2039-2042.

Koksharova, O.A. and Wolk, C.P. (2002) A Novel Gene That Bears a DnaJ Motif Influences Cyanobacterial Cell Division. *J. Bacteriol.*, **184**, 5524-5528.

Kordeli, E. (2000) The spectrin-based skeleton at the postsynaptic membrane of the neuromuscular junction. *Microsc Res Tech*, **49**, 101-107.

Kuroiwa, T., Kuroiwa, H., Sakai, A., Takahashi, H., Toda, K. and Itoh, R. (1998) The division apparatus of plastids and mitochondria. *Int Rev Cytol*, **181**, 1-41.

Lan, G., Daniels, B.R., Dobrowsky, T.M., Wirtz, D. and Sun, S.X. (2009) Condensation of FtsZ filaments can drive bacterial cell division. *Proc Natl Acad Sci U S A*, **106**, 121-126.

Lan, G., Wolgemuth, C.W. and Sun, S.X. (2007) Z-ring force and cell shape during division in rod-like bacteria. *Proc Natl Acad Sci U S A*, **104**, 16110-16115.

Larkin, M.A., Blackshields, G., Brown, N.P., Chenna, R., McGettigan, P.A., McWilliam, H., Valentin, F., Wallace, I.M., Wilm, A., Lopez, R., Thompson, J.D., Gibson, T.J. and Higgins, D.G. (2007) Clustal W and Clustal X version 2.0. *Bioinformatics*, **23**, 2947-2948.

Leech, R.M., Thomson, W.W. and Platt-Aloia, K.A. (1981) Observations on the mechanism of chloroplast division in higher plants. *New Phytologist*, **87**, 1-9.

Lemmon, M.A. (2004) Pleckstrin homology domains: not just for phosphoinositides. *Biochem Soc Trans*, **32**, 707-711.

Levin, P.A., Shim, J.J. and Grossman, A.D. (1998) Effect of minCD on FtsZ ring position and polar septation in Bacillus subtilis. *J Bacteriol*, **180**, 6048-6051.

Li, L. and Kehoe, D.M. (2005) In vivo analysis of the roles of conserved aspartate and histidine residues within a complex response regulator. *Mol Microbiol*, **55**, 1538-1552.

Li, Z., Trimble, M.J., Brun, Y.V. and Jensen, G.J. (2007) The structure of FtsZ filaments in vivo suggests a force-generating role in cell division. *EMBO J*, **26**, 4694-4708.

Liu, S.C. and Palek, J. (1980) Spectrin tetramer-dimer equilibrium and the stability of erythrocyte membrane skeletons. *Nature*, **285**, 586-588.

Low, H.H. and Lowe, J. (2006) A bacterial dynamin-like protein. *Nature*, **444**, 766-769.

Low, H.H., Moncrieffe, M.C. and Lowe, J. (2004) The crystal structure of ZapA and its modulation of FtsZ polymerisation. *J Mol Biol*, **341**, 839-852.

Lu, C. and Erickson, H.P. (1998) Purification and assembly of FtsZ. *Methods Enzymol*, **298**, 305-313.

Lu, C., Reedy, M. and Erickson, H.P. (2000) Straight and Curved Conformations of FtsZ Are Regulated by GTP Hydrolysis. *J. Bacteriol.*, **182**, 164-170.

Lu, Y., Savage, L.J., Ajjawi, I., Imre, K.M., Yoder, D.W., Benning, C., Dellapenna, D., Ohlrogge, J.B., Osteryoung, K.W., Weber, A.P., Wilkerson, C.G. and Last, R.L. (2008) New connections across pathways and cellular processes: industrialized mutant screening reveals novel associations between diverse phenotypes in Arabidopsis. *Plant Physiol*, **146**, 1482-1500.

Lutkenhaus, J. (2007) Assembly dynamics of the bacterial MinCDE system and spatial regulation of the Z ring. *Annu Rev Biochem*, **76**, 539-562.

Ma, H., Lou, Y., Lin, W.H. and Xue, H.W. (2006) MORN motifs in plant PIPKs are involved in the regulation of subcellular localization and phospholipid binding. *Cell Res*, **16**, 466-478.

Ma, X. and Margolin, W. (1999) Genetic and Functional Analyses of the Conserved C-Terminal Core Domain of Escherichia coli FtsZ. *J. Bacteriol.*, **181**, 7531-7544.

Maeda, S., Sugita, C., Sugita, M. and Omata, T. (2006) A new class of signal transducer in His-Asp phosphorelay systems. *J Biol Chem*, **281**, 37868-37876.

Maple, J., Aldridge, C. and Moller, S.G. (2005) Plastid division is mediated by combinatorial assembly of plastid division proteins. *The Plant Journal*, **43**, 811-823.

Maple, J., Chua, N.H. and Moller, S.G. (2002) The topological specificity factor AtMinE1 is essential for correct plastid division site placement in Arabidopsis. *Plant J*, **31**, 269-277.

Maple, J., Fujiwara, M.T., Kitahata, N., Lawson, T., Baker, N.R., Yoshida, S. and Moller, S.G. (2004) GIANT CHLOROPLAST 1 Is Essential for Correct Plastid Division in Arabidopsis. *Current Biology*, **14**, 776-781.

Maple, J. and Moller, S.G. (2006) Plastid Division: Evolution, Mechanism and Complexity. *Ann Bot (Lond)*.

Maple, J. and Moller, S.G. (2007) Interdependency of formation and localisation of the Min complex controls symmetric plastid division. *J Cell Sci*, **120**, 3446-3456.

Maple, J., Vojta, L., Soll, J. and Moller, S.G. (2007) ARC3 is a stromal Z-ring accessory protein essential for plastid division. *EMBO Rep*, **8**, 293-299.

Marbouty, M., Saguez, C., Cassier-Chauvat, C. and Chauvat, F. (2009) ZipN, an FtsA-like orchestrator of divisome assembly in the model cyanobacterium Synechocystis PCC6803. *Molecular Microbiology*.

Margolin, W. (2003) Bacterial division: the fellowship of the ring. *Curr Biol*, **13**, R16-18.

Margolin, W. (2005) FtsZ and the division of prokaryotic cells and organelles. *Nat Rev Mol Cell Biol*, **6**, 862-871.

Marrison, J.L., Rutherford, S.M., Robertson, E.J., Lister, C., Dean, C. and Leech, R.M. (1999) The distinctive roles of five different ARC genes in the chloroplast division process in Arabidopsis. *Plant J*, **18**, 651-662.

Marston, A.L. and Errington, J. (1999) Selection of the midcell division site in Bacillus subtilis through MinD-dependent polar localization and activation of MinC. *Mol Microbiol*, **33**, 84-96.

Masuda, H.P., Ramos, G.B., de Almeida-Engler, J., Cabral, L.M., Coqueiro, V.M., Macrini, C.M., Ferreira, P.C. and Hemerly, A.S. (2004) Genome based identification and analysis of the pre-replicative complex of Arabidopsis thaliana. *FEBS Lett*, **574**, 192-202.

Mazouni, K., Domain, F., Cassier-Chauvat, C. and Chauvat, F. (2004) Molecular analysis of the key cytokinetic components of cyanobacteria: FtsZ, ZipN and MinCDE. *Molecular Microbiology*, **52**, 1145-1158.

McAndrew, R.S., Froehlich, J.E., Vitha, S., Stokes, K.D. and Osteryoung, K.W. (2001) Colocalization of plastid division proteins in the chloroplast stromal compartment establishes a new functional relationship between FtsZ1 and FtsZ2 in higher plants. *Plant Physiol*, **127**, 1656-1666.

McAndrew, R.S., Olson, B.J.S.C., Kadirjan-Kalbach, D., Chi-Ham, C.L., Vitha, S., Froehlich, J.E. and Osteryoung, K.W. (2008) In vivo quantitative relationship between plastid division proteins FtsZ1 and FtsZ2 and identification of ARC6 and ARC3 in a native FtsZ complex. *Biochem J*, **412**, 367-378.

McCallum, C.M., Comai, L., Greene, E.A. and Henikoff, S. (2000) Targeted screening for induced mutations. *Nat Biotechnol*, **18**, 455-457.

McCarty, J.S. and Walker, G.C. (1994) DnaK mutants defective in ATPase activity are defective in negative regulation of the heat shock response: expression of mutant DnaK proteins results in filamentation. *J Bacteriol*, **176**, 764-780.

McDonald, M.S. (2003) *Photobiology of Higher Plants.* West Sussex, England: Wiley.

McNiven, M.A. (1998) Dynamin: a molecular motor with pinchase action. *Cell*, **94**, 151-154.

Michniewicz, M., Zago, M.K., Abas, L., Weijers, D., Schweighofer, A., Meskiene, I., Heisler, M.G., Ohno, C., Zhang, J., Huang, F., Schwab, R., Weigel, D., Meyerowitz, E.M., Luschnig, C., Offringa, R. and Friml, J. (2007) Antagonistic regulation of PIN phosphorylation by PP2A and PINOID directs auxin flux. *Cell*, **130**, 1044-1056.

Miller, R.K., Cheng, S.C. and Rose, M.D. (2000) Bim1p/Yeb1p mediates the Kar9p-dependent cortical attachment of cytoplasmic microtubules. *Mol Biol Cell*, **11**, 2949-2959.

Minc, N., Bratman, S.V., Basu, R. and Chang, F. (2009) Establishing new sites of polarization by microtubules. *Curr Biol*, **19**, 83-94.

Miyagishima, S.-y. (2005) Origin and evolution of the chloroplast division machinery. *Journal of Plant Research*, **118**, 295.

Miyagishima, S.-y., Froehlich, J.E. and Osteryoung, K.W. (2006) PDV1 and PDV2 Mediate Recruitment of the Dynamin-Related Protein ARC5 to the Plastid Division Site. *Plant Cell*, **18**, 2517-2530.

Miyagishima, S.-y., Kuroiwa, H. and Kuroiwa, T. (2001) The timing and manner of disassembly of the apparatuses for chloroplast and mitochondrial division in the red alga *Cyanidioschyzon merolae*. *Planta*, **V212**, 517-528.

Miyagishima, S.-y., Nishida, K., Mori, T., Matsuzaki, M., Higashiyama, T., Kuroiwa, H. and Kuroiwa, T. (2003a) A Plant-Specific Dynamin-Related Protein Forms a Ring at the Chloroplast Division Site. *Plant Cell*, **15**, 655-665.

Miyagishima, S.-y., Takahara, M., Mori, T., Kuroiwa, H., Higashiyama, T. and Kuroiwa, T. (2001) Plastid Division Is Driven by a Complex Mechanism That Involves Differential Transition of the Bacterial and Eukaryotic Division Rings. *Plant Cell*, **13**, 2257-2268.

Miyagishima, S.-y., Wolk, C.P. and Osteryoung, K.W. (2005) Identification of cyanobacterial cell division genes by comparative and mutational analyses. *Molecular Microbiology*, **56**, 126-143.

Miyagishima, S.Y., Nishida, K. and Kuroiwa, T. (2003b) An evolutionary puzzle: chloroplast and mitochondrial division rings. *Trends Plant Sci*, **8**, 432-438.

Miyagishima, S.Y., Nozaki, H., Nishida, K., Nishida, K., Matsuzaki, M. and Kuroiwa, T. (2004) Two types of FtsZ proteins in mitochondria and red-lineage chloroplasts: the duplication of FtsZ is implicated in endosymbiosis. *J Mol Evol*, **58**, 291-303.

Moreira, I.S., Fernandes, P.A. and Ramos, M.J. (2006) Detailed Microscopic Study of the Full ZipA:FtsZ Interface. *Proteins*, **63**, 811-821.

Mosyak, L., Zhang, Y., Glasfeld, E., Haney, S., Stahl, M., Seehra, J. and Somers, W.S. (2000) The bacterial cell-division protein ZipA and its interaction with an FtsZ fragment revealed by X-ray crystallography. *EMBO J*, **19**, 3179-3191.

Mukherjee, A., Dai, K. and Lutkenhaus, J. (1993) Escherichia coli cell division protein FtsZ is a guanine nucleotide binding protein. *Proc Natl Acad Sci U S A*, **90**, 1053-1057.

Nakamura, M., Zhou, X.Z. and Lu, K.P. (2001) Critical role for the EB1 and APC interaction in the regulation of microtubule polymerization. *Curr Biol*, **11**, 1062-1067.

Nakanishi, H., Suzuki, K., Kabeya, Y. and Miyagishima, S.Y. (2009) Plant-specific protein MCD1 determines the site of chloroplast division in concert with bacteria-derived MinD. *Curr Biol*, **19**, 151-156.

Nakaya, M., Tsukaya, H., Murakami, N. and Kato, M. (2002) Brassinosteroids control the proliferation of leaf cells of Arabidopsis thaliana. *Plant Cell Physiol*, **43**, 239-244.

Neff, M.M., Neff, J.D., Chory, J. and Pepper, A.E. (1998) dCAPS, a simple technique for the genetic analysis of single nucleotide polymorphisms: experimental applications in Arabidopsis thaliana genetics. *Plant J*, **14**, 387-392.

Obayashi, T., Hayashi, S., Saeki, M., Ohta, H. and Kinoshita, K. (2009) ATTED-II provides coexpressed gene networks for Arabidopsis. *Nucleic Acids Res*, **37**, D987-991.

Okazaki, K., Kabeya, Y., Suzuki, K., Mori, T., Ichikawa, T., Matsui, M., Nakanishi, H. and Miyagishima, S.-y. (2009) The PLASTID DIVISION1 and 2 Components of the Chloroplast Division Machinery Determine the Rate of Chloroplast Division in Land Plant Cell Differentiation. *Plant Cell*, **21**, 1769-1780.

Olson, B.J.S.C. (2008) Biochemical Analysis of the Chloroplast Division Proteins FtsZ1 and FtsZ2. In *Department of Biochemistry and Molecular Biology*. East Lansing: Michigan State University.

Osawa, M., Anderson, D.E. and Erickson, H.P. (2008) Reconstitution of contractile FtsZ rings in liposomes. *Science*, **320**, 792-794.

Osteryoung, K.W. (2001) Organelle Fission in Eukaryotes. *Curr Opin Microbiol*, **4**, 639-646.

Osteryoung, K.W. and Nunnari, J. (2003) The division of endosymbiotic organelles. *Science*, **302**, 1698-1704.

Osteryoung, K.W., Stokes, K.D., Rutherford, S.M., Percival, A.L. and Lee, W.Y. (1998) Chloroplast division in higher plants requires members of two functionally divergent gene families with homology to bacterial ftsZ. *Plant Cell*, **10**, 1991-2004.

Osteryoung, K.W. and Vierling, E. (1995) Conserved cell and organelle division. *Nature*, **376**, 473.

Overbeek, R., Begley, T., Butler, R.M., Choudhuri, J.V., Chuang, H.Y., Cohoon, M., de Crecy-Lagard, V., Diaz, N., Disz, T., Edwards, R., Fonstein, M., Frank, E.D., Gerdes, S., Glass, E.M., Goesmann, A., Hanson, A., Iwata-Reuyl, D., Jensen, R., Jamshidi, N., Krause, L., Kubal, M., Larsen, N., Linke, B., McHardy, A.C., Meyer, F., Neuweger, H., Olsen, G., Olson, R., Osterman, A., Portnoy, V., Pusch, G.D., Rodionov, D.A., Ruckert, C., Steiner, J., Stevens, R., Thiele, I., Vassieva, O., Ye, Y., Zagnitko, O. and Vonstein, V. (2005) The subsystems approach to genome annotation and its use in the project to annotate 1000 genomes. *Nucleic Acids Res*, **33**, 5691-5702.

Overbeek, R., Fonstein, M., D'Souza, M., Pusch, G.D. and Maltsev, N. (1999) Use of contiguity on the chromosome to predict functional coupling. *In Silico Biol*, **1**, 93-108.

Pagel, K. and Koksch, B. (2008) Following polypeptide folding and assembly with conformational switches. *Curr Opin Chem Biol*, **12**, 730-739. Epub 2008 Oct 2007.

Paris, S., Wessel, P.M. and Dumas, R. (2002) Overproduction, purification, and characterization of recombinant bifunctional threonine-sensitive aspartate kinase-homoserine dehydrogenase from Arabidopsis thaliana. *Protein Expr Purif*, **24**, 105-110.

Paves, H. and Truve, E. (2007) Myosin inhibitors block accumulation movement of chloroplasts in Arabidopsis thaliana leaf cells. *Protoplasma*, **230**, 165-169.

Pichoff, S. and Lutkenhaus, J. (2001) Escherichia coli division inhibitor MinCD blocks septation by preventing Z-ring formation. *J Bacteriol*, **183**, 6630-6635.

Pichoff, S. and Lutkenhaus, J. (2002) Unique and overlapping roles for ZipA and FtsA in septal ring assembly in Escherichia coli. *EMBO J*, **21**, 685-693.

Pichoff, S. and Lutkenhaus, J. (2005) Tethering the Z ring to the membrane through a conserved membrane targeting sequence in FtsA. *Mol Microbiol*, **55**, 1722-1734.

Pichoff, S. and Lutkenhaus, J. (2007) Identification of a region of FtsA required for interaction with FtsZ. *Mol Microbiol*, **64**, 1129-1138.

Possingham, J.V. and Lawrence, M.E. (1983) Controls to plastid division. *International Review of Cytology*, **84**, 1-56.

Praefcke, G.J. and McMahon, H.T. (2004) The dynamin superfamily: universal membrane tubulation and fission molecules? *Nat Rev Mol Cell Biol*, **5**, 133-147.

Pyke, K. (1998) Plastid Division: The Origin of Replication. *Plant Cell*, **10**, 1971-1972.

Pyke, K. (2006) Plastid Division: The Squeezing Gets Tense. *Current Biology*, **16**, R60.

Pyke, K.A. (1999) Plastid Division and Development. *Plant Cell*, **11**, 549-556.

Pyke, K.A. (2009) *Plastid Biology* 1st edn. Cambridge: Cambridge University Press.

Pyke, K.A. and Leech, R.M. (1991) Rapid Image Analysis Screening Procedure for Identifying Chloroplast Number Mutants in Mesophyll Cells of Arabidopsis thaliana (L.) Heynh. *Plant Physiol*, **96**, 1193-1195.

Pyke, K.A. and Leech, R.M. (1992) Chloroplast Division and Expansion Is Radically Altered by Nuclear Mutations in Arabidopsis thaliana. *Plant Physiol*, **99**, 1005-1008.

Pyke, K.A. and Leech, R.M. (1994) A Genetic Analysis of Chloroplast Division and Expansion in Arabidopsis thaliana. *Plant Physiol.*, **104**, 201-207.

Pyke, K.A., Rutherford, S.M., Robertson, E.J. and Leech, R.M. (1994) arc6, A Fertile Arabidopsis Mutant with Only Two Mesophyll Cell Chloroplasts. *Plant Physiol.*, **106**, 1169-1177.

Raskin, D.M. and de Boer, P.A. (1999a) MinDE-dependent pole-to-pole oscillation of division inhibitor MinC in Escherichia coli. *J Bacteriol*, **181**, 6419-6424.

Raskin, D.M. and de Boer, P.A. (1999b) Rapid pole-to-pole oscillation of a protein required for directing division to the middle of Escherichia coli. *Proc Natl Acad Sci U S A*, **96**, 4971-4976.

RayChaudhuri, D. (1999) ZipA is a MAP-Tau homolog and is essential for structural integrity of the cytokinetic FtsZ ring during bacterial cell division. *EMBO J*, **18**, 2372-2383.

Raynaud, C., Cassier-Chauvat, C., Perennes, C. and Bergounioux, C. (2004) An Arabidopsis homolog of the bacterial cell division inhibitor SulA is involved in plastid division. *Plant Cell*, **16**, 1801-1811.

Raynaud, C., Perennes, C., Reuzeau, C., Catrice, O., Brown, S. and Bergounioux, C. (2005) Cell and plastid division are coordinated through the prereplication factor AtCDT1. *PNAS*, **102**, 8216-8221.

Reddy, M.S., Dinkins, R. and Collins, G.B. (2002) Overexpression of the Arabidopsis thaliana MinE1 bacterial division inhibitor homologue gene alters chloroplast size and morphology in transgenic Arabidopsis and tobacco plants. *Planta*, **215**, 167-176.

Reski, R., Wehe, M., Hadeler, B., Marienfield, J.R. and Abel, W.O. (1991) Cytokinin and light quality interact at the molecular level in the chloroplast mutant PC22 of the moss Physcomitrella. *J. Plant Physiol.*, **138**, 236-243.

Ricard, M. and Hirota, Y. (1973) Process of cellular division in Escherichia coli: physiological study on thermosensitive mutants defective in cell division. *J Bacteriol*, **116**, 314-322.

Robertson, E.J., Pyke, K.A. and Leech, R.M. (1995) arc6, an extreme chloroplast division mutant of Arabidopsis also alters proplastid proliferation and morphology in shoot and root apices. *J Cell Sci*, **108**, 2937-2944.

Rost, B. and Eyrich, V.A. (2001) EVA: large-scale analysis of secondary structure prediction. *Proteins*, **Suppl**, 192-199.

Rothfield, L., Taghbalout, A. and Shih, Y.L. (2005) Spatial control of bacterial division-site placement. *Nat Rev Microbiol*, **3**, 959-968.

Ruiz, D., Salinas, P., Lopez-Redondo, M.L., Cayuela, M.L., Marina, A. and Contreras, A. (2008) Phosphorylation-independent activation of the atypical response regulator NblR. *Microbiology*, **154**, 3002-3015.

Rutherford, S.M. (1996) The genetic and physical analysis of mutants of chloroplast number and size in Arabidopsis thaliana.: University of York, UK.

Saitou, N. and Nei, M. (1987) The neighbor-joining method: a new method for reconstructing phylogenetic trees. *Mol Biol Evol*, **4**, 406-425.

Sakr, S., Jeanjean, R., Zhang, C.-C. and Arcondeguy, T. (2006) Inhibition of Cell Division Suppresses Heterocyst Development in Anabaena sp. Strain PCC 7120. *J. Bacteriol.*, **188**, 1396-1404.

Scheffers, D.J. (2008) The effect of MinC on FtsZ polymerization is pH dependent and can be counteracted by ZapA. *FEBS Lett*, **582**, 2601-2608.

Schimper, A. (1883) Über die Entwicklung der Chlorophyllkörner und Farbkörper. *Bot Zeit*, **41**, 105-112.

Schmidt von Braun, S. and Schleiff, E. (2008) The chloroplast outer membrane protein CHUP1 interacts with actin and profilin. *Planta*, **227**, 1151-1159.

Schmitz, A.J., Glynn, J.M., Olson, B.J.S.C., Stokes, K.D. and Osteryoung, K.W. (2009) Arabidopsis FtsZ2-1 and FtsZ2-2 are Functionally Redundant, but FtsZ-based Plastid Division is Not Essential for Chloroplast Partitioning or Plant Growth and Development. *Molecular Plant*, **2**, 1211-1222.

Schneider, D., Fuhrmann, E., Scholz, I., Hess, W.R. and Graumann, P.L. (2007) Fluorescence staining of live cyanobacterial cells suggest non-stringent chromosome segregation and absence of a connection between cytoplasmic and thylakoid membranes. *BMC Cell Biol*, **8**, 39.

Schwacke, R., Schneider, A., van der Graaff, E., Fischer, K., Catoni, E., Desimone, M., Frommer, W.B., Flugge, U.I. and Kunze, R. (2003) ARAMEMNON, a novel database for Arabidopsis integral membrane proteins. *Plant Physiol*, **131**, 16-26.

Scott, N.S. and Possingham, J.V. (1980) Chloroplast DNA in Expanding Spinach Leaves. *J. Exp. Bot.*, **31**, 1081-1092.

Shaw, J.M. and Nunnari, J. (2002) Mitochondrial dynamics and division in budding yeast. *Trends Cell Biol*, **12**, 178-184.

Shen, B. and Lutkenhaus, J. (2009) The conserved C-terminal tail of FtsZ is required for the septal localization and division inhibitory activity of MinC(C)/MinD. *Mol Microbiol*, **72**, 410-424.

Shimada, H., Koizumi, M., Kuroki, K., Mochizuki, M., Fujimoto, H., Ohta, H., Masuda, T. and Takamiya, K.-i. (2004) ARC3, a Chloroplast Division Factor, is a Chimera of Prokaryotic FtsZ and Part of Eukaryotic Phosphatidylinositol-4-phosphate 5-kinase. *Plant Cell Physiol.*, **45**, 960-967.

Singh, J.K., Makde, R.D., Kumar, V. and Panda, D. (2007) A membrane protein, EzrA, regulates assembly dynamics of FtsZ by interacting with the C-terminal tail of FtsZ. *Biochemistry*, **46**, 11013-11022.

Slep, K.C., Rogers, S.L., Elliott, S.L., Ohkura, H., Kolodziej, P.A. and Vale, R.D. (2005) Structural determinants for EB1-mediated recruitment of APC and spectraplakins to the microtubule plus end. *J Cell Biol*, **168**, 587-598.

Slep, K.C. and Vale, R.D. (2007) Structural basis of microtubule plus end tracking by XMAP215, CLIP-170, and EB1. *Mol Cell*, **27**, 976-991.

Sokolovski, S., Hills, A., Gay, R., Garcia-Mata, C., Lamattina, L. and Blatt, M.R. (2005) Protein phosphorylation is a prerequisite for intracellular Ca2+ release and ion channel control by nitric oxide and abscisic acid in guard cells. *Plant J*, **43**, 520-529.

Stokes, K.D., McAndrew, R.S., Figueroa, R., Vitha, S. and Osteryoung, K.W. (2000) Chloroplast division and morphology are differentially affected by overexpression of FtsZ1 and FtsZ2 genes in Arabidopsis. *Plant Physiol*, **124**, 1668-1677.

Stokes, K.D. and Osteryoung, K.W. (2003) Early divergence of the FtsZ1 and FtsZ2 plastid division gene families in photosynthetic eukaryotes. *Gene*, **320**, 97.

Strepp, R., Scholz, S., Kruse, S., Speth, V. and Reski, R. (1998) Plant nuclear gene knockout reveals a role in plastid division for the homolog of the bacterial cell division protein FtsZ, an ancestral tubulin. *Proc Natl Acad Sci U S A*, **95**, 4368-4373.

Su, L.K., Burrell, M., Hill, D.E., Gyuris, J., Brent, R., Wiltshire, R., Trent, J., Vogelstein, B. and Kinzler, K.W. (1995) APC binds to the novel protein EB1. *Cancer Res*, **55**, 2972-2977.

Su, P.H. and Li, H.M. (2008) Arabidopsis stromal 70-kD heat shock proteins are essential for plant development and important for thermotolerance of germinating seeds. *Plant Physiol*, **146**, 1231-1241.

Suetsugu, N. and Wada, M. (2007) Chloroplast photorelocation movement mediated by phototropin family proteins in green plants. *Biol Chem*, **388**, 927-935.

Sugimoto, S., Saruwatari, K., Higashi, C. and Sonomoto, K. (2008) The proper ratio of GrpE to DnaK is important for protein quality control by the DnaK-DnaJ-GrpE chaperone system and for cell division. *Microbiology*, **154**, 1876-1885.

Sun, Q. and Margolin, W. (2001) Influence of the nucleoid on placement of FtsZ and MinE rings in Escherichia coli. *J Bacteriol*, **183**, 1413-1422.

Sun, Q., Zybailov, B., Majeran, W., Friso, G., Olinares, P.D.B. and van Wijk, K.J. (2009) PPDB, the Plant Proteomics Database at Cornell. *Nucl. Acids Res.*, **37**, D969-974.

Szeto, T.H., Rowland, S.L., Rothfield, L.I. and King, G.F. (2002) Membrane localization of MinD is mediated by a C-terminal motif that is conserved across eubacteria, archaea, and chloroplasts. *PNAS*, **99**, 15693-15698.

Tamura, K., Dudley, J., Nei, M. and Kumar, S. (2007) MEGA4: Molecular Evolutionary Genetics Analysis (MEGA) software version 4.0. *Mol Biol Evol*, **24**, 1596-1599.

Thomer, M., May, N.R., Aggarwal, B.D., Kwok, G. and Calvi, B.R. (2004) Drosophila double-parked is sufficient to induce re-replication during development and is regulated by cyclin E/CDK2. *Development*, **131**, 4807-4818.

Till, B.J., Colbert, T., Codomo, C., Enns, L., Johnson, J., Reynolds, S.H., Henikoff, J.G., Greene, E.A., Steine, M.N., Comai, L. and Henikoff, S. (2006) High-throughput TILLING for Arabidopsis. *Methods Mol Biol*, **323**, 127-135.

Toufighi, K., Brady, S.M., Austin, R., Ly, E. and Provart, N.J. (2005) The Botany Array Resource: e-Northerns, Expression Angling, and promoter analyses. *Plant J*, **43**, 153-163.

Tranel, P.J., Froehlich, J., Goyal, A. and Keegstra, K. (1995) A component of the chloroplastic protein import apparatus is targeted to the outer envelope membrane via a novel pathway. *EMBO J*, **14**, 2436-2446.

Trusca, D., Scott, S., Thompson, C. and Bramhill, D. (1998) Bacterial SOS Checkpoint Protein SulA Inhibits Polymerization of Purified FtsZ Cell Division Protein. *J. Bacteriol.*, **180**, 3946-3953.

Tzafrir, I., Pena-Muralla, R., Dickerman, A., Berg, M., Rogers, R., Hutchens, S., Sweeney, T.C., McElver, J., Aux, G., Patton, D. and Meinke, D. (2004) Identification of genes required for embryo development in Arabidopsis. *Plant Physiol*, **135**, 1206-1220.

Uehara, T., Matsuzawa, H. and Nishimura, A. (2001) HscA is involved in the dynamics of FtsZ-ring formation in Escherichia coli K12. *Genes Cells*, **6**, 803-814.

Ungewickell, E.J. and Hinrichsen, L. (2007) Endocytosis: clathrin-mediated membrane budding. *Curr Opin Cell Biol*, **19**, 417-425.

van den Ent, F. and Lowe, J. (2000) Crystal structure of the cell division protein FtsA from Thermotoga maritima. *EMBO J*, **19**, 5300-5307.

Vitha, S., Froehlich, J.E., Koksharova, O., Pyke, K.A., van Erp, H. and Osteryoung, K.W. (2003) ARC6 Is a J-Domain Plastid Division Protein and an Evolutionary

Descendant of the Cyanobacterial Cell Division Protein Ftn2. *Plant Cell*, **15**, 1918-1933.

Vitha, S., Holzenburg, A. and Osteryoung, K.W. (2005) Assembly Dynamics of FtsZ and ARC6 Plastid-Dividing Proteins. *Microsc Microanal*, **11**, 1154-1155.

Vitha, S., McAndrew, R.S. and Osteryoung, K.W. (2001) FtsZ Ring Formation at the Chloroplast Division Site in Plants. *The Journal of Cell Biology*, **153**, 111-119.

Wada, M., Kagawa, T. and Sato, Y. (2003) Chloroplast movement. *Annu Rev Plant Biol*, **54**, 455-468.

Wang, Q., Canutescu, A.A. and Dunbrack, R.L., Jr. (2008) SCWRL and MolIDE: computer programs for side-chain conformation prediction and homology modeling. *Nat Protoc*, **3**, 1832-1847.

Warrens, A.N., Jones, M.D. and Lechler, R.I. (1997) Splicing by overlap extension by PCR using asymmetric amplification: an improved technique for the generation of hybrid proteins of immunological interest. *Gene*, **186**, 29-35.

Wen, Y., Eng, C.H., Schmoranzer, J., Cabrera-Poch, N., Morris, E.J., Chen, M., Wallar, B.J., Alberts, A.S. and Gundersen, G.G. (2004) EB1 and APC bind to mDia to stabilize microtubules downstream of Rho and promote cell migration. *Nat Cell Biol*, **6**, 820-830.

Whitmore, L. and Wallace, B.A. (2008) Protein secondary structure analyses from circular dichroism spectroscopy: methods and reference databases. *Biopolymers*, **89**, 392-400.

Wiegel, D. and Glazebrook, J. (2002) *Arabidopsis: A Laboratory Manual.* New York: Cold Spring Harbor Press.

Wiejak, J. and Wyroba, E. (2002) Dynamin: characteristics, mechanism of action and function. *Cell Mol Biol Lett*, **7**, 1073-1080.

Xu, C., Fan, J., Cornish, A.J. and Benning, C. (2008) Lipid trafficking between the endoplasmic reticulum and the plastid in Arabidopsis requires the extraplastidic TGD4 protein. *Plant Cell*, **20**, 2190-2204.

Xu, S., Wong, C.C., Tong, E.H., Chung, S.S., Yates, J.R., 3rd, Yin, Y. and Ko, B.C. (2008) Phosphorylation by casein kinase 1 regulates tonicity-induced osmotic response element-binding protein/tonicity enhancer-binding protein nucleocytoplasmic trafficking. *J Biol Chem*, **283**, 17624-17634. Epub 12008 Apr 17614.

Yang, X., Kang, C.M., Brody, M.S. and Price, C.W. (1996) Opposing pairs of serine protein kinases and phosphatases transmit signals of environmental stress to activate a bacterial transcription factor. *Genes Dev*, **10**, 2265-2275.

Yang, Y., Glynn, J.M., Olson, B.J.S.C., Schmitz, A.J. and Osteryoung, K.W. (2008) Plastid division: across time and space. *Curr Opin Plant Biol*, **11**, 577-584.

Yang, Y., Xu, R., Ma, C.J., Vlot, A.C., Klessig, D.F. and Pichersky, E. (2008) Inactive methyl indole-3-acetic acid ester can be hydrolyzed and activated by several esterases belonging to the AtMES esterase family of Arabidopsis. *Plant Physiol*, **147**, 1034-1045.

Yoder, D.W., Kadirjan-Kalbach, D., Olson, B.J.S.C., Miyagishima, S.Y., Deblasio, S.L., Hangarter, R.P. and Osteryoung, K.W. (2007) Effects of mutations in Arabidopsis FtsZ1 on plastid division, FtsZ ring formation and positioning, and FtsZ filament morphology in vivo. *Plant Cell Physiol*, **48**, 775-791.

Yoon, H.S., Hackett, J.D., Ciniglia, C., Pinto, G. and Bhattacharya, D. (2004) A molecular timeline for the origin of photosynthetic eukaryotes. *Mol Biol Evol*, **21**, 809-818.

Yoshida, Y., Kuroiwa, H., Misumi, O., Nishida, K., Yagisawa, F., Fujiwara, T., Nanamiya, H., Kawamura, F. and Kuroiwa, T. (2006) Isolated Chloroplast Division Machinery Can Actively Constrict After Stretching. *Science*, **313**, 1435-1438.

Zhang, M., Hu, Y., Jia, J., Gao, H. and He, Y. (2009a) A plant MinD homologue rescues Escherichia coli HL1 mutant (DeltaMinDE) in the absence of MinE. *BMC Microbiol*, **9**, 101.

Zhang, M., Hu, Y., Jia, J., Li, D., Zhang, R., Gao, H. and He, Y. (2009b) CDP1, a novel component of chloroplast division site positioning system in Arabidopsis. *Cell Res*, **19**, 877-886.

Zhang, X.P., Elofsson, A., Andreu, D. and Glaser, E. (1999) Interaction of mitochondrial presequences with DnaK and mitochondrial hsp70. *J Mol Biol*, **288**, 177-190.

Zimmermann, P., Hirsch-Hoffmann, M., Hennig, L. and Gruissem, W. (2004) GENEVESTIGATOR. Arabidopsis Microarray Database and Analysis Toolbox. *Plant Physiol.*, **136**, 2621-2632.

Zuckerkandl, E. and Pauling, L. (1965) Molecules as documents of evolutionary history. *J Theor Biol*, **8**, 357-366.